The Type Ia supernovae rate with Subaru/XMM-Newton Deep Survey(Dissertation_全文)

AUTHOR(S):

Okumura, Jun Ernesto

CITATION:

Okumura, Jun Ernesto. The Type Ia supernovae rate with Subaru/XMM-Newton Deep Survey. 京都大学, 2014, 博士(理学)

ISSUE DATE:

2014-03-24

URL:

https://doi.org/10.14989/doctor.k18079

The Type Ia supernovae rate with Subaru/XMM-Newton Deep Survey

すばる/XMM-ニュートン・ディープサーベイを用いた Ia型超新星発生頻度の研究

A dissertation submitted in partial satisfaction of the requirement for the degree of

Doctor of Philosophy

in

Astronomy

by

Jun Ernesto Okumura

奥村 純

Department of Astronomy, Graduate School of Science
Kyoto University

Jan 2014

Abstract

The Type Ia supernovae rate with Subaru/XMM-Newton Deep Survey

Jun E. Okumura

Type Ia supernova (SN Ia) is an explosion of a white dwarf (WD) which exceeded the Chandrasekhar mass through accumulating material from a companion star in a binary system. From early time, SN Ia has been well-known for its homogenious brigtness and light curve shape. Particurally, the relation between a light curve width and a peak brightness provides an opportunity to use SN Ia as a distance indicator, which enable us to investigate the expansion history of the Universe. Besides its usage as a cosmological tool, SN Ia is also important as a producer of iron-peak elements, a kinetic-energy sources in galaxy evolution, and an endpoint of binary evolution. Although its importance in astrophysics, the progenitor systems of SN Ia are yet solved. Two major scenarios are proposed: single-degenerate model, which a single WD accretes material from non-degenerated companion through Roch-lobe overflow, and double-degenerate model, which two WDs which form a binary merge. Although many recent studies have been constraining progenitor systems for individual objects, the needs for statistical studies (delay time distribution, environmental dependence) is increasing to link observation and theoretical understanding on the binary evolution and the explosion. In this context, high-redshift supernova survey is one of the key issue for investigating young population and the evolution of SN Ia.

This thesis presents measurements of the rates of high-redshift Type Ia supernovae using data from the Subaru/XMM-Newton Deep Survey (SXDS). We use the data from repeat deep imaging observations with Suprime-Cam on the Subaru Telescope, and detected 1040 variable objects over 0.918 deg^2 in the Subaru/XMM-Newton Deep Field. Then 141 supernova candidates are selected by requiring variability timescale less than one year, and at least two epochs showing $5\sigma_b$ variability. To construct a SN Ia sample from SN candidates, SN II like objects are discriminated first, through light curve fitting in i'-band. The second component of sample refinement is the removal of SN Ib/c contamination. The author used a portion of sample whose color information is available to estimate possibe contamination from SNe Ib/c. Finally, out of the 1040 variable objects, 39 objects over the redshift range $0.2 < z < 1.4$ are classified as SNe Ia. Since the sample refinement is crucial factor for estimating the rates, the properties of SN Ia sample and possible contamination of other transients such like core-collapse SNe and AGNs are carefully examined.

To convert observed number of SN Ia to occurence rates, one needs to estimate the control time (i.e., effective visibility time). The control time depends both on the observation parameters (cadence, limiting flux) and on the supernova modeling (birightness distribution, evolution modeling, dust effect). In this phase, the uncertainty caused by dust extinction and possible evolution of SN Ia parameters are estimated.

Finally, the volometric rates of SN Ia are calculated as following equation:

$$\widehat{r}_v(z_1 < z < z_2) = \frac{N_{Ia}(z_1 < z < z_2)}{\int_{z_1}^{z_2} \frac{CT(z)}{1+z} \frac{\Theta}{4\pi} V(z) dz},$$

where N_{Ia} is the number of SN Ia, CT is the control time, and Θ is the survey area. The resulted rates are $0.262^{+0.229+0.144}_{-0.133-0.120}$, $0.839^{+0.230+0.423}_{-0.185-0.120}$, and $0.705^{+0.239+0.366}_{-0.183-0.103}$ (stasistical error, followed by systematic error) in the unit of $10^{-4}\mathrm{yr}^{-1}\mathrm{Mpc}^{-3}$ at $< z >= 0.44$, 0.80, and 1.14. We find that the SN Ia rate continues to increase up to $z \sim 0.8$ and may then flatten at higher redshift. The rates can be fitted by a simple power law, $r_V(z) = r_0(1+z)^{\alpha}$ with $r_0 = 0.20^{+0.52}_{-0.16}(\mathrm{stat.})^{+0.26}_{-0.07}(\mathrm{syst.})\times 10^{-4}\mathrm{yr}^{-1}\mathrm{Mpc}^{-3}$, and $\alpha = 2.04^{+1.84}_{-1.96}(\mathrm{stat.})^{+2.11}_{-0.86}(\mathrm{syst.})$. These results are consistent with measurements by other authours, and are among the most distant SN Ia rate measurements to date.

As to the uncertainty, the statistical error dominates in the lowest redshift bin ($0.2 \leq z < 0.4$) due to the small number statistics. In addition, the number of SN Ia in this range is easily affected by core-collapse SNe contaminations, which results in large error. In the middle redshift bin, the rich sample in the range leads to the precise measurement of rate. The effect of systematics is samaller compared with other two bins. In the highest redshift bin, the effect of evolution and dust are large since the control time is sensitive in higher redshift. Nevertheless many uncertainties are included in the rate calculation, the resulted rate is precise comparable with other measurements using different instruments and techniques. Note that this result is derived from single-band light curve fitting and small number of color sample.

The significance of this thesis is that the rates approache to the high redshift regime ($z > 1.0$) and showed that the technique introduced in this work is effective in the survey such as SXDS. Second, this work will be useful for upcoming large systematic transient survey in the next decade. In particular, Hyper Suprime-Cam (HSC) Survey in Subaru Telescope, is expected to detect about 300 SNe Ia with good quality in the redshift range of $0.2 < z < 1.8$. Coupled with analysis used in this work, HSC survey will produce one of the most precise measurement of SN Ia rates up to $z \sim 2$. This thesis will contribute to the future statistical SN studies.

Keywords:
supernovae, stellar evolution, rate, SXDS

Acknowledgments

First of all, I would like to thank Tomonori Totani for leading me to the fields in astronomy, in particular high-energy astrophysics and observational cosmology, and initiating my researches in these fields. I have spend an additional year in the bachelor course to join his research group, but that was not a wrong choise. The exact guides and kind advices of Prof. Totani always have been helped my researches. In addition, I thank him for providing a lot of opportunities to study abroad. It was a fortunate situation that I could introduce my works in a number of international conferences and workshopes from early stage. I have learned much from Prof. Totani during my doctoral course and honestly, appreciate for five-years successful collaboration. I also would like to thank to Yutaka Ihara and Prof. Mamoru Doi. This work is based on their initial analysis. In particular, Prof. Doi has introduced me to the Supernova Cosmology Project (SCP) group and his international connections was quite helpful for me. Many results obteined in this thesis were never obtained without the invaluable assistance of the Subaru Telescope staff and the support from Tomoki Morokuma and Naoki Yasuda, who provided me the photometry data of SXDS. They taught me the procedure of image analsys and had many discussion regarding photometric calibration.

This work has been completed due to the international collaboration with SCP group. In particular, Greg Aldering and Chris Lidman have supported me in completing this thesis. Most of the scientific discussion were done with them and I would like to thank them for lots of useful comments and kind considerations. I also appreciate Saul Perlmutter and Anthony Spadafora for accepting me to stay in the Lawrence Berkeley National Laboratory (LBNL) many times. These visits were unforgettable experiences for me. I could have discussions with many top-class scientists and it was also grateful for me that I could spend time with my families living in San Fransisco. In addition, I was honorable for me to work with Prof. Saul Perlmutter. I heard the news of his recieving Nobel Prize in Physics 2011 just before visiting the LBNL, and I remember the discussions we had during the stay very well. I would like to thank the SCP collaboration members, Kyle Barbary, Gerson Goldhaber, Eric Hsiao, Nao Suzuki, Lifan Wang, Kyle Dawson, Reynald Pain, Naohiro Takanashi, and Isobel Hook, for the successful collaboration. During my research in LBNL, David Rubin, Josh Meyers, Yakob Nordin, Clare Saunders, Xiaosheng Huang, Hannah Kakhouri were so kind to me. We had many discussions and chats everyday in the same office.

Regarding studing supernovae as my field, I have been helped from supernova researchers in Japan. I had many useful discussions with Masaomi Tanaka, Nozomu Tominaga, Keiichi Maeda, Takashi Moriya, Masayuki Yamanaka, Takaya Nozawa, Kohki Konishi, Hanindyo Kuncarayakti, Yasuomi Kamiya, Koh Takahashi in weekly seminar. In particular, discussions with Masaomi Tanaka was fruitful for me. I remember that he gave me lots of advices when I was feeling anxious in proceeding to the doctoral course. I would like to express my gratitude to my friend Takashi Moriya. Being in the same grade, I really enjoyed studing supernovae with him. In terms of international conferences, I was happy to spend time with researchers all over the world. I met with Or Graur, Steve Rodney, Nicki Mennekens, Ashley Ruiter, Silvia Toonen, Joke Claeys, Alex Chiotellis, Jelle de Plaa, Wolfgang Kerzendorf, Mikkel Nielsen, Maria Pruzhinskaya, and Timothy Brandt, who are my good friends. I also would like to thank Prof. Ken'ichi Nomoto for useful comments and Prof. Dan Maoz for inviting me to

the workshop at the Lorentz Center.

During five years of research life as a doctoral student, I had many nice colleagues to work with. I thank group members of Prof. Totani: Ken'ichiro Nakazato, Norita Kawanaka, Takeshi Oda, Masakazu Kobayashi, Yuu Niino, Yoshiyuki Inoue, Masanao Sumiyoshi, Ryu Makiya, Takashi Ishikawa, Motonari Tonegawa, Hiroyuki Okada. Especially, I enjoyed talking with Yoshiyuki Inoue about many topics and his adivices were quite helpful. I spent most of my graduate school days at Kyoto University. I thank Kazuo Hiroi, Shun Takeuchi, Shota Furumagi, Tatsuhito Yoshikawa, Takaya Tamura, Akimasa Kataoka, Junpei Tanaka, Yuki Hashimoto, Kohei Ichikawa, Megumi Shidatsu, Andrew Hillier, Kazuya Matsubayashi, Tetsu Anan, Jin Matsumoto, Kiyoto Yabe, Yuuki Moritani, Kaori Kawate, Hiroko Watanabe, and Hiroaki Isobe for a fun time. I also thank the seminar members in the AP seminar, namely, Yudai Suwa, Makoto Takamoto, Kazumi Kashiyama, Kohei Inayoshi, Kenta Hotokezaka, Soichiro Isoyama, Koutarou Kyutoku, and Kazuyuki Sugimura for giving me opportunities to introduce my research to groups in other department. I would like to show my gratitude to Keiko Ohara for her crucial support to my research activities. I spent my last year as a graduate student in the University of Tokyo. During the stay in Tokyo, Shin Mineshige was supporting my research as teaching advisor in Kyoto University. I could spend fun time in Tokyo thanks to Kazuhiro Maeda, Mélanie Godart, Kei Fukue, Takafumi Sonori, Shinogo Shinogi, Goto Ryosuke, Hamid Hamidani, and Ryou Ohsawa.

I had joined many activities during my student life. These activities, though they are not directly related to the science, made my life enjoyable and motivated me to keep working on science. I would like to appreciate my friends in Kyoto University Student Orchestra, Kumon Kokusai Gakuen Blassband Club, Contenporary Art Studies, and Kyoto International Student Film & Video Festival. I also thank to the member of Kansai Cluster: Takuya Kuratsu, Shohei Kobayashi, Hiromi Suzuki, Akihiro Ohta, Yoshihiro Tanigawa, Tomoyasu Okada, and Takuya Kitagawa. We had a variety of studing seminar ragarding Philosophy, Architecture, Art, Infosocionomics Society, and many other fields. I am confident that these activities gave me diversified perspectives and ways of thinking, which were useful in Astrophysics as well.

I would like to express my sincere gratitude to my parents, Koichi Okumura and Martha Lidia Zeleyandía Cisneros. My interest in the Universe was originated from my young days with my parents. My father brought me to Germany to observe the solar eclipse in 1999, and my mother always has been showing understanding to study Astrophysics. They also gave me a healthy body and finacial supports which are crucial for doing research. I thank to my diligent sister, Akemi. I am proud to be a brother of you. My family in San Fransisco were supportive to me when I was visiting LBNL. Thank you very much Gregorio Zelayandía, Reina, Sonia, Jorge, Daniel, Lucie, and Xochitl. In addition, I appreciate Yoko Marisol Shinohara, for being so kind to me and making me feel positive. I sincerely thank to my soulmates, whose kindness and affectionate words have always encouraged me. I feel so grateful that I could have such magnificent relationships, nice family, friends, and many others who have supported my life.

Finally, I would like to express my sincere appreciation to Aoba Uematsu for being with me throughout my tough years in the doctoral course. She has always cheering me up in spite of her busy bussiness as an illustrator. This thesis has never been accomplished without her support and smile.

This work was supported in part with scientific research grants from the Ministry of Education, Science, Culture, and Sports, Science and Technology (MEXT) of Japan,and by the grant-in-aid for the Global COE Program "The Next Generation of Physics, Spun from Universality and Emergenc" from MEXT. The author has been financially supported by the Japan Society for the Promotion of Science (JSPS) through the JSPS Research Fellowship. This work was also supported in part by the Director, Office of Science, Office of High Energy and Nuclear Physics and the Office of Advanced Scientific Computing Research, of the U.S. Department of Energy (DOE) under Contract Nos. DE-FG02-92ER40704, DE-AC02-05CH11231, DE-FG02-06ER06-04, and DE-AC02-05CH11231.

Contents

The Type Ia supernovae rate with Subaru/XMM-Newton Deep Survey

I never could have done what I have done without the habits of punctuality, order, and diligence, without the determination to concentrate myself on one subject at a time.

Charles Dickens (1812 - 1870)

1 Introduction

1.1 Supernovae

A supernova (SN) is an extremely luminous explosion of the star, witch appears suddenly in the celestial sphere. This event has been recorded from ancient history. For example, chinese astronomers has described an appearance of a "guest star" occured in 185 A.D., which is though to be indeed a SN event (Stephenson & Green 2002, Zhao et al. 2006). Tycho Brahe and Johannes Kepler are the remarkable figures for their throughout naked-eye observation; they observed SN 1572 and SN 1604, respectively, and left the most accurate and complete sets of measurement before the telescope era (Brahe 1573, Kepler 1606). In the early 20th century, it become apparent that a supernova is extremely brighter event compared with a *common nova*, a sudden brightening of a star (Baade & Zwicky 1934).

SNe are classified into some subclasses according to their observational feature (e.g. spectrum, light curve shape). The overview of the classification scheme is shown in Figure 1.1 (see also Filippenko 1997 for a detailed review). First, SNe are divided into two categolies from the presense of hydrogen in the optical spectra (first remarks has done by Minkowski 1941). "Type II SNe" (SNe II) are defined by the presense of hydrogen and they show a wide variety of photometric and spectroscopic properties. "Type I SNe" (SNe I) are characterised by hidrogen-deficient and rather homogenious spectra. Among SNe I, three subclasses are known: those whose spectra show strong Si II (Type Ia), prominnent He I (Type Ib), or neither Si II nor He I (Type Ic). SNe II, despite a wide variety of properties, are roughly devided into two groups: those with linearly decaying light curve, SNe II-L, and those showing long-lasting (a few months) plateau, SNe II-P (Minkowski 1964, Barbon et al. 1979, Doggett & Branch 1985). Furthermore, SNe II showing relatively narrow emission lines are called SNe IIn, which indicate a presense of dense circumstellar materials (Figure 2.2). It is also known that there are some SNe which are classified as a SN II and later resembles rather a SN Ib, showing links between SNe II and

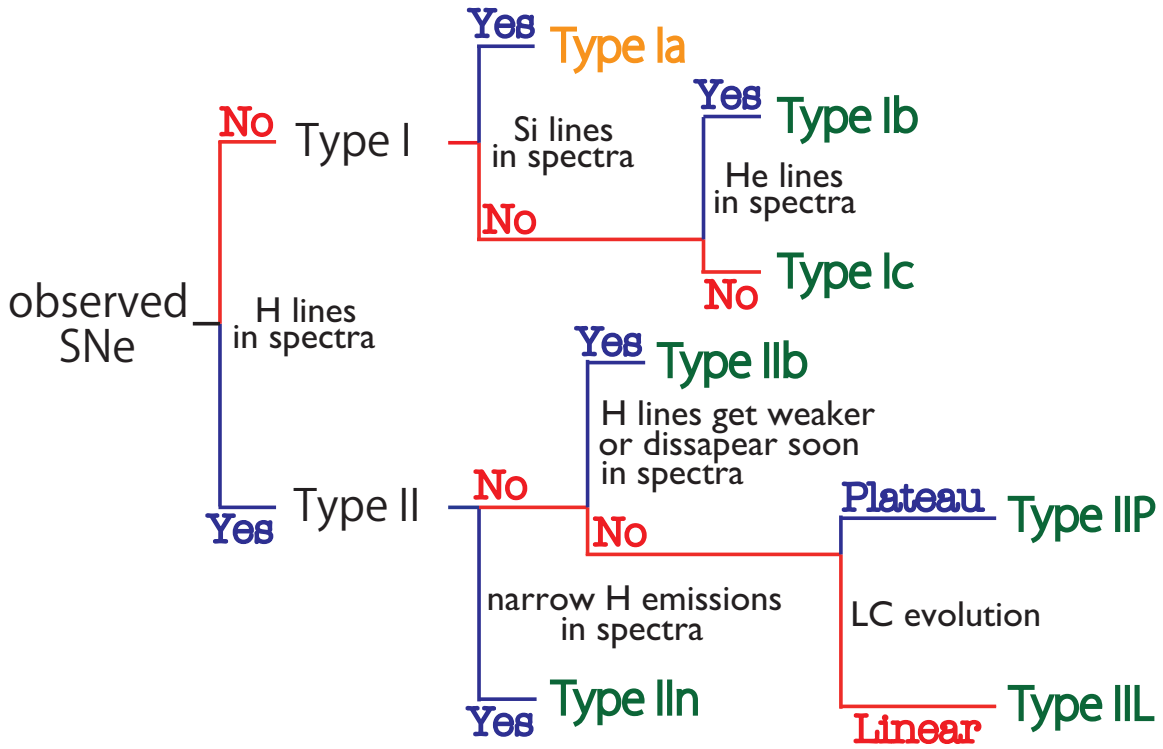

Figure 1.1: Observational classification scheme of SNe (from Moriya 2013). SNe Ia (orange) are thermonuclear explosions (see Section 2.2) of WDs and SNe of the other types (green) are explosions of massive stars (see Section 2.1). 'Linear' LC evolution used in Type IIL means the linear evolution in time-magnitude plane (Figure 2.2).

SNe Ib/c. This subclass was first proposed by Woosley et al. 1987 from the similar preliminary model for SN 1987A, and later, throghout studies on an unusual supernova SN 1993 revealed that this object is actually classified as SN IIb.

1.2 Type Ia Supernova

Among many subclasses of SNe, SN Ia plays important roles in Astrophysics. They are remarkable objects as cosomological distance indicators, having provided the first direct evidence of the accelarating cosmic expansion (see section 2.2.5). This cosmic acceleration was first reported by two independent supernova observation teams: the Supernova Cosmology Project (SCP) (Perlmutter et al. 1999) and the High-Z SN Search Team (Riess et al. 1998). Since then, many large SN surveys have been carried out to measure the cosmological parameters accurately (e.g., Knop et al. 2003, Tonry et al. 2003, Astier et al. 2006, Riess et al. 2007, Wood-Vasey et al. 2007, Kowalski et al. 2008, Hicken et al. 2009, Amanullah et al. 2010, Sullivan et al. 2011, Suzuki et al. 2012).

Although SNe Ia are effective as standard candles, their progenitors are yet to be conclusively identified (see section 2.3). It is widely believed that the progenitor of a SN Ia is a binary system containing a C+O white dwarf (WD), and recently the compact nature of the exploding star has been confirmed (Nugent et al. 2011, Bloom et al. 2012; see also 2.2.1). There are two widely discussed scenarios for the progenitor, the single degenerate (SD) scenario and the double degenerate (DD) scenario. In the SD scenario, a C+O WD accretes gas from a companion star in a binary system (see section 2.2.3.1). Its mass increases up to the Chandrasekhar limit where it explodes as an SN Ia (e.g., Nomoto 1982, Hachisu et al. 1996, Nomoto et al. 1997). If SNe Ia from the SD scenario exist, the companion star survives in the supernova remnant after the SN Ia explosion. Various methods have been used to search for such companion stars, but to date no clear detection has been made (e.g., Ruiz-Lapuente et al. 2004, Ihara et al. 2007, González Hernández et al. 2012, Kerzendorf et al. 2009, Schaefer & Pagnotta 2012, Nugent et al. 2011, Bloom et al. 2012, Brown et al. 2012, Chomiuk et al. 2012, Margutti et al. 2012). Other constraints on the SD scenario had been obtained from X-ray and radio observations, which showed no clear evidence of an interaction between the ejecta and the circumstellar material (CSM) surrounding the SNe (e.g. Panagia et al. 2006, Hancock et al. 2011, Chomiuk et al. 2012). Though these observations disfavor non-degenerate donors, some SN Ia spectra show narrow time varying and/or blue-shifted Na I D absorption features possibly associated with a SD donor star (e.g. Patat et al. 2007, Simon et al. 2009, Blondin et al. 2009, Stritzinger et al. 2010, Sternberg et al. 2011, Maguire et al. 2013). These features are also investigated in the context of DD scenario (Shen et al. 2013, Raskin & Kasen 2013).

In the DD scenario, a merger of two C+O WDs with a combined mass exceeding the Chandrasekhar mass leads to an SN Ia explosion (e.g., Iben & Tutukov 1984, Webbink 1984; see section 2.2.3.2). Searches have been carried out to detect DD binaries that could be SN Ia progenitors, but strong limits have not yet been reached due to small number statistics (e.g., Koester et al. 2005, Geier et al. 2007).

1.3 Delay time distribution

One promissing way to test the detailed progenitor components is "delay time distribution (DTD)". SNe Ia explode with a "delay time" between binary system formation and subsequent SN explosion. This delay time is one of the primary methods for understanding the progenitor scenario of SNe Ia. If we compare theoretical and observational DTDs, this provide opportunities to investigate the components of SN Ia progenitors.

1.3.1 theoretical DTDs

Theoretical DTDs are predicted through binaly population synthesis (BPS) simulation, which is Monte Carlo simulation based on parametrised binary evolution models. As shown in Figure 1.3, derived DTDs from SD and DD models differ in many points. In DD model, the dilay time is essentially determined by the separation of binary, especially in the long delay time range above $\sim$ 1Gyr. Since two WDs merge through angular momentum loss by gravitational-wave radiation, the timescale of merger is proportional to the separation (a) to the 4th power (see Equation 2.7). If the separation distribution is fiven by $f_{sep}(a) \propto a^{\alpha}$, the DTD ($f_{sep}(t)$) should be expressed as

$$f_{DTD}(t) = \frac{dN}{dt} \propto f_{sep}(a)\frac{da}{dt} \propto t^{-(3-\alpha)/4}. \tag{1.1}$$

For the separation distribution, it iw a good aproximation to assume $\alpha \sim -1$ for WDs binaries (e.g. Toonen et al. 2012). As a consequence, the DTD for DD model perform as $f_{DTD} \propto t^{-1}$. All the BPS calculation agrees with a t^{-1} DTD for DD channel, ranging from short delay time to Hubble time (see Figure 1.3).

In the other hand, SD models varies according to authors. This is caused due to the complicated treatment and various parametrization of binary evolution physics (especially, the common envelope phase). Since the timescale of final mass-accretion phase ($\sim 1-10$Myr, assuming typical accretion rate $\dot{M} \sim 3 \times 10^{-7} M_{\odot}$ yr^{-1}), is much smaller than the evolution timescale of the secondary ($\sim$ 1Gyr), the lifetime of the secondary is the dominat factor in the DTD. Taking the small mass range of the secondary for successfull SD system into the account, the resulted DTD will concentrate between a few-hundred Myr and 1-2Gyr. In the larger delay time ($\leq$ 10Gyr), corresponding to a low-mass secondary system, SD channel fails to produce enough SNe Ia due to the low-efficient mass-transfer from non-degenerate donor. In addition, since parametrazations of binary evolution such as mass transfer and common envelope are complicated, BPS calculation produce various DTD shapes.

1.3.2 observational DTDs

From observational side, it has been generally known that more star-forming, or more massive galaxies host more SN Ia (Cappellaro et al. 1999, Mannucci et al. 2005, Mannucci et al. 2006, Sullivan et al. 2006). These results suggest that more SNe Ia arise from younger stellar population (i.e., decreasing DTD function). In the observational point of view, one can recover DTD from SN Ia rates and star-formation histories (SFHs). For example, if the galaxy with age t have a SFH as $\psi(t)$, current SN Ia rate of the galaxy can

be expressed as summation of contributions from different time t' (Figure 1.2):

$$R_{Ia}(t) = \int_0^t \psi(t') f_{DTD}(t - t') dt'. \tag{1.2}$$

Hence, DTD recovery can be archieved by estimating SN Ia rate and assuming SFH. The pioneering result was Totani et al. 2008. They measured the DTD based on the stellar age estimate of each galaxy in a sample of passively evolving galaxies from Subaru/XMM-Newton Deep Survey (SXDS[1]), finding that the time distribution could be described by a featureless power law going as $f_{DTD}(t) \propto t^{-1.08\pm0.15}$ over $t = 0.1-10$ Gyr. Other studies using different methods also show consistency with a t^{-1} trend (see Maoz & Mannucci 2012, for a review).

The comparison between observation and theoretical prediction of DTDs are shown in Figure 1.3. As noted, t^{-1} DTDs strongly suggest DD models. SD models concentrate in certain range, and fail to explain a power-law function for wide delay time range (but also see Hachisu et al. 2008 for an attempt to explain observed DTDs in SD channels). However, in spite of good agreements with DD models, observed DTDs tend to be higher than predicted. The absolute values of DTDs varies in a facter of $3-10$ among observations and still needs further investigations. The normalization problem may come from the dependence of IMF on galaxy mass, or the assumption of BPS calculations that total masses of WDs should be larger than the Chandrasekhar limit, $M_{\rm ch}$. Actually, if all double WDs binaries become SN Ia, time-integrated rate of $\sim 0.8 \times 10^{-3} M_\odot^{-1}$ matches with observational SN Ia production efficiency, $10^{-3} M_\odot^{-1}$ (Toonen et al. 2012).

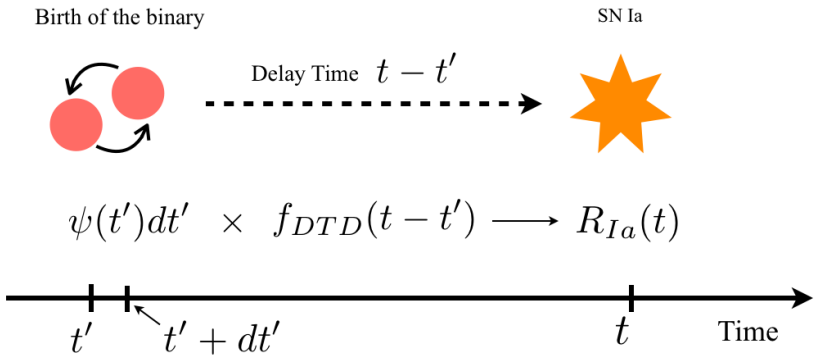

Figure 1.2: Schematic picture of SN Ia rate and DTD.

1.4 High-z SN Ia rate

Though more detailed investigations are expected in both DTD observations and theoretical BPS calculations, the approach from SN Ia rates is shedding light on progenitor populations. Besides the progenitor issues, SN Ia rates is also important in the contexts of Fe production history, kinetic-energy sources in galaxy evolution, and endpoints of stellar binary evolution.

[1] http://www.naoj.org/Science/SubaruProject/SDS/

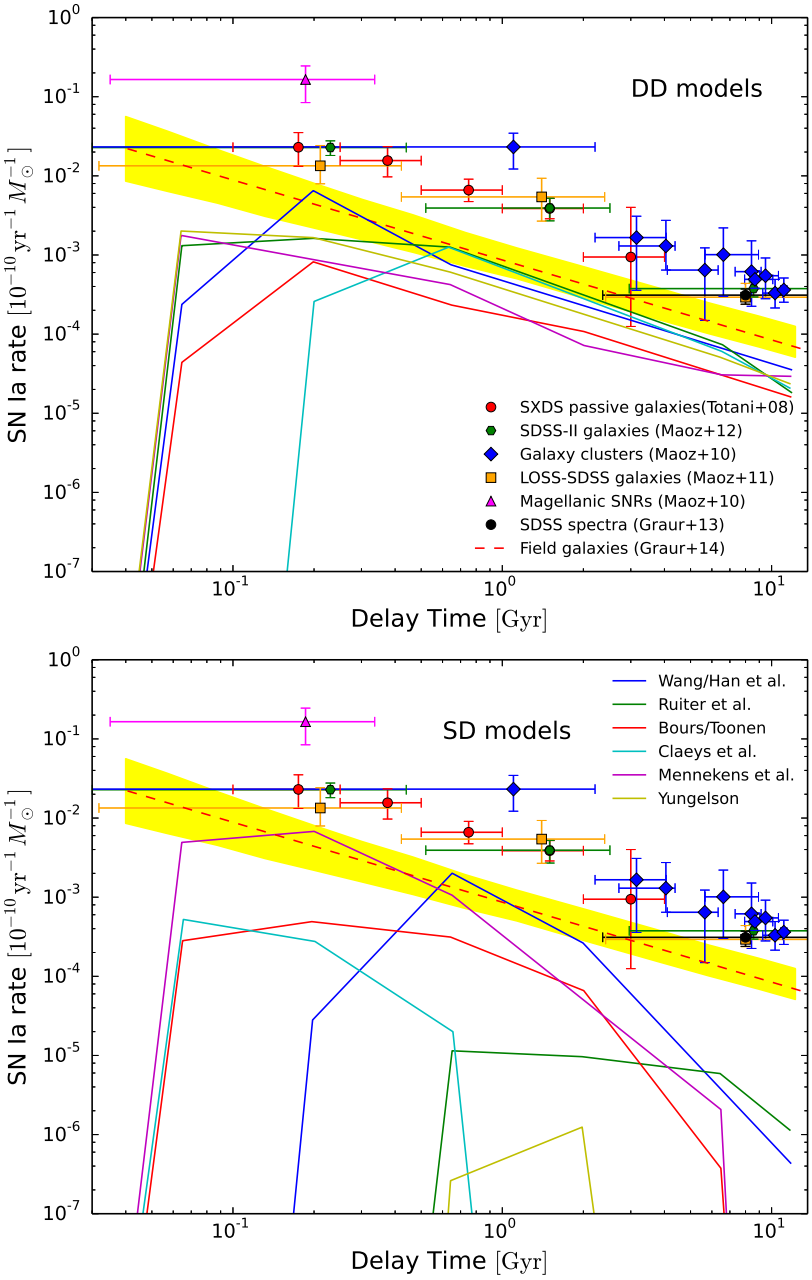

Figure 1.3: Comparison of observed DTD and theoretical BPS simulations. Upper panel show the results of DD models and lower panel shows SD models. Solid lines represents theoretical DTDs summarized by Nelemans et al. 2013, which all models have the same physical parameters. Several observed DTDs are plotted in both panels: *red points* by Totani et al. 2008, *green points* by Maoz et al. 2012b, *blue diamonds* by Maoz & Badenes 2010, *orange square* by Maoz et al. 2011, *magenta triangle* by Maoz & Badenes 2010, and *black point* by Graur & Maoz 2013. The *red dashed line* is the power-law fit derived by field SN Ia rates, and *yellow hashed region* represents corresponding 1σ error (Graur et al. 2013). All observed DTDs suggest t^{-1} power-law, which coincide with theoretical DD models in shapes (but also show somewhat offset), whereas theoretical SD predictions concentrate in certain delay time.

SN Ia rate is one of the cutting edge issues, and several systematic surveys such as SDSS Supernova Survey[2] (Frieman et al. 2008, Sako et al. 2008) or Supernova Legacy Survey (SNLS[3]) are unveiling the nature of SN Ia rates. Recently, Perrett et al. 2012 has measured the SN Ia rate over the redshift range $0.1 \leq z \leq 1.1$ using 286 spectroscopically confirmed and $\gtrsim 400$ photometrically identified SNe Ia from SNLS, which is one of the most precise estimation of SN Ia rate in $z \leq 1$. Figure 1.4 shows the compilation of recent studies. Nevertheless good number of SNe Ia are studied in $z \leq 1$, high-z rates are highly unclear due to the magnitude limit of transient surveys. Since the depth to reach high-z and the area to increase sample number is a tradeoff factor, high-z studies always face the small number statistics.

High-z SN Ia rates have been measured in several surveys. Dahlen et al. 2008 obtained the first SN Ia rate measurement beyond z of 1, based on the Great Observatories Origins Deep Survey (GOODS) survey. They used 56 high-redshift SNe Ia, the majority of which were spectroscopically confirmed. Interestingly, they find that the SN Ia rate decreases beyond $z \sim 1.6$, contradicting the expectation from the delay time distribution measurements of Totani et al. 2008. However, the rate in the highest redshift bin ($z \gtrsim 1.4$) has a large uncertainty due to small number statistics. The detection efficiency at $z > 1.4$ rapidly decreases with redshift as the observed bands shift farther into the rest-frame UV. Other high-z rate measurements have been reported in the literature. Graur et al. 2011 derived the SN Ia rate up to $z \sim 2.0$ using 150 SNe from a SN survey in the Subaru Deep Field (SDF), and found that the SN Ia rate levels off at $1.0 < z < 2.0$. Their SN classification method is based on a single epoch in the R, i',and z' bands, provided in Poznanski et al. 2007b. Barbary et al. 2012 derived the SN Ia rate up to $z \sim 1.6$ using ~ 20 SNe Ia from the *Hubble Space Telescope* Cluster Supernova Survey, finding a rate that is broadly consistent with previous measurements but with large uncertainties. The behavior of SN Ia rates at high redshifts is not clear yet and is a key issue in SN Ia studies.

In this context, high-z SN Ia rates ($z > 1$) play an important role in investigating the DTD, especially for the short delay time regime. If SNe Ia with short delay times dominate SN Ia populations, the cosmic SN Ia rate evolution should closely trace that of the cosmic star formation, and thus high-z SN Ia rates provide information about the short delay time population.

[2] http://www.sdss.org/supernova/aboutsprnova.html
[3] http://cfht.hawaii.edu/SNLS/

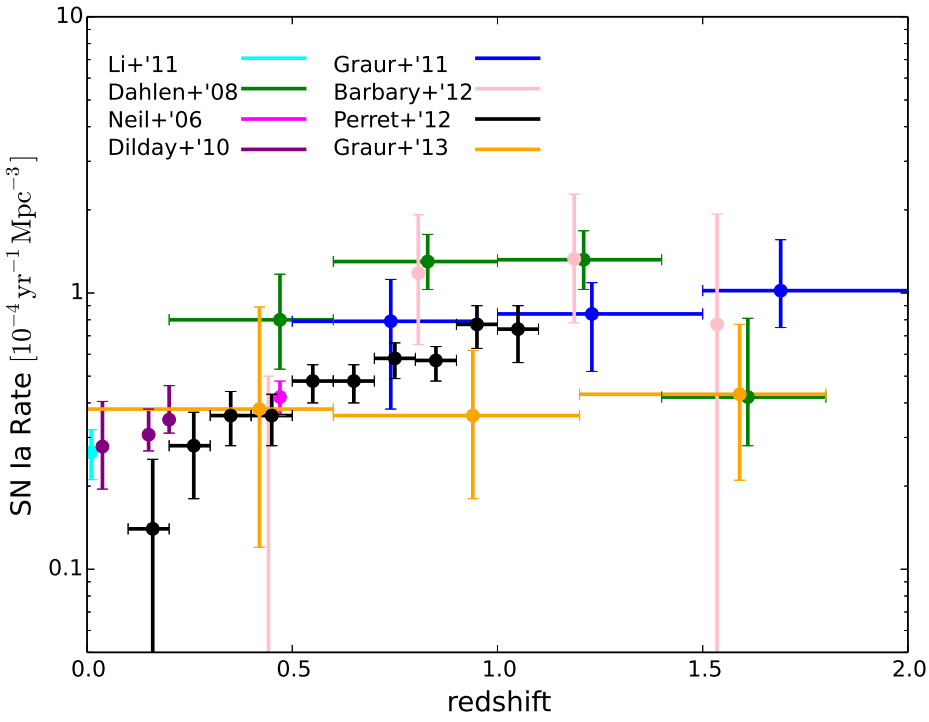

Figure 1.4: The recent measurements of SN Ia rates. Above $z \sim 1$, the behavior of rates are still unclear.

1.5 The Purpose of This Thesis

SNe Ia have been played important rool in astrophysics; especially, the role as "standard candle" is remarkable. However, some misteries, in particular progenitor models of SNe Ia still remain as a controversial problem. One promissing aproach to study the progenitor is the SN Ia rates as a function of the delay time (i.e., delay time distribution). Compared with binary population synthesis calculations, observational DTD provide us an opportunity to estimate the evolution history and the fraction of each progenitor models. Thus, SN Ia rates at high-redshift is considered important to investigate DTD, especially for the short delay time. In addition, high-redshift SNe Ia provide lots of information on the evolution and enviromental dependence of SN Ia, which is not clear yet. In the next decade, the significance of investigating high-redshift SNe will keep growing.

In this thesis, we report the mesurement of SN Ia rate to high redshift using the Subaru/XMM-Newton Deep Survey (SXDS) data set. The survey area is large ($\sim$1 deg^2) enough to obtain many SNe Ia. With the repeat imaging observations we are able to construct high-quality SN light curves. 39 SNe Ia have been obtained in the range $0.2 \lesssim z \lesssim 1.4$ using a classification method that relies primarily on light-curve fitting and photometric redshifts. Spectroscopic identifications, source colors, host galaxy redshifts, and X-ray data are used when available to remove contamination or to improve statistical contamination corrections.

The thesis is organized as follows. In chapter 2, a review on supernovae, in particular recent discussions on the progenitor of SN Ia, is summarized. Then the detailed observation used for this study is introduced in chapter 3. In chapter 4 and chapter 5, sample refinements and rate calculation are described. The base analysis of the thesis is done in these two chapter. In chapter 6, the uncertainties in rate measurements are examined carefully, and discussion follows in chapter 7. Finally, this work is summarized in chapter 8.

Throughout the thesis, we adopt the cosmological parameters $H_0 = 70$ km s^{-1} Mpc^{-1}, $\Omega_M = 0.3$, $\Omega_\Lambda = 0.7$.

Principles for the Development of a Complete Mind:
Study the science of art. Study the art of science.
Develop your senses — especially learn how to see.
Realize that everything connects to everything else.

Leonardo da Vinci (1452 - 1519)

2

Review on Supernovae

In this chapter, discussions on SNe are briefly summarized. In section 2.1 and section 2.2, the details of core-collapse supernova and Type Ia supernova are introduced. In particular, section 2.2 is comprised of seven subsections, summarizing current understanding on SN Ia (homogeneity, evolution pathway, progenitors, explosion mechanism, application to the cosmology). Since the progenitor problem is the most interest here, it is separately introduced in section 2.3.

2.1 Core-Collapse Supernova

Superenova related to the explosion of the massive star are grouped as core-collapse Supernova (CC SN). This class includes SN IIP, IIL, IIb, IIn, Ib, and Ic. Though the explosion machanism and the evolution pathway to these SNe are not fully understood, there is a general picture of core-collapse explosions. When a star evolves, H is converted into He through nuclear burning. If He core exceed a critical mass ($0.3M_{\odot}$), He is gnited and C and O are created. In the same way, the core continues its nuclear fusion creating heavier elements. The star with its zero age main sequence (ZAMS) mass greater than $\sim 8M_{\odot}$ but not heavy enough to make Fe ($\lesssim 10M_{\odot}$), electron capture occurs after the density of the core become around 4×10^9g cm^{-3} (e.g. Nomoto 1987). Since the star at this sage is supported by degeneracy pressure of the core, sudden decrease of electrons lead to the collapse of the core. This may cause an electron-capture SN (ECSN) event. If ZAMS mass is heavier than $\sim 10M_{\odot}$, nuclear fusion continues until Fe production. As Fe is the most stable nuclei, Fe is accumulated in the core without further burning and the temperature continues to increase. Consequently, at the critical temperature, Fe core is photodisintegrated.

$$^{56}\mathrm{Fe} \longrightarrow 13\,^{4}\mathrm{He} + 4\mathrm{n} - 124.4[\mathrm{MeV}] \tag{2.1}$$

$$^{4}\mathrm{He} \longrightarrow 2\mathrm{p} + 2\mathrm{n} - 28.3[\mathrm{MeV}] \tag{2.2}$$

This collapse occurs at a star with $10M_{\odot} \lesssim M_{ZAMS} \lesssim 130M_{\odot}$. Difference among CC SN subclasses is determined by the structure of the star at the explosion point. If outer layer contain enough H, the explosion is observed as SN II. The difference between SN IIL and SN IIP is controversial. Generally, the amount of H layer is thought to determine the two distinct type of SN II. More massive star will experience mass loss due to its large luminosity, blowing away the H layer. This kind of star will explode as SN Ib, and if the remaining He layer is swept away, such a star will explode as SN Ic (see Figure 2.1). As to the mass loss, binarity may contribute to the strip of H emvelope (e.g. Yoon et al. 2010). SN IIn is a subtype of SN II which shows strong narrow emission (Figure 2.2). This emission is thought to come from the existence of cirmumstellar media (CSM).

2.2 Type Ia Supernova (Thermonuclear Supernova)

2.2.1 Progenitor

From the observational point of view, SN Ia is characterized by its absence of hydrogen emission lines and the presence of a blueshifted Si II absorption line (λ6355 near-maximum lignt). The first feature means that the atmosphere of the explosing star contains at most $0.1M_{\odot}$ hydrogen, and the second feature indicate that some nuclear processes take place, whose products are ejected in the explosion. Combining the fact that peak velocities exceed 20,000 km s^{-1}, it is feasible that the explosion is the fusion about $1M_{\odot}$ carbon and oxgen into Fe group elemets and intermediate mass elements (IMEs) such as Si and Ca. This insight follows the first discovery by Hoyle & Fowler 1960 that an electron-degenerate stellar core might trigger an explosion, and the idea that produced radioactive ^{56}Ni may power light curves of SNe (Truran et al. 1967, Colgate & McKee 1969). ^{56}Ni decay to ^{56}Co with a half time of 6.075 days and then decays further to ^{56}Fe with a half-time of 77.23 days, which naturally explain the decline rate of lightcurve of SN Ia.

$$^{56}\mathrm{Ni} \xrightarrow{6.075d} {}^{56}\mathrm{Co} \xrightarrow{77.23d} {}^{56}\mathrm{Fe} \tag{2.3}$$

We can also connect the peak luminosity and the amount of ^{56}Ni (M_{Ni}), by simple calculation known as the Arnett law (Arnett 1982, Arnett et al. 1985, Branch & Tammann 1992):

$$L_{\max} = (6.45e^{\frac{-t_r}{8.8\mathrm{d}}} + 1.45e^{\frac{-t_r}{111.3\mathrm{d}}}) \left(\frac{M_{\mathrm{Ni}}}{M_{\odot}}\right) \times 10^{43}\mathrm{erg\,s^{-1}} \tag{2.4}$$

where t_r is the rise time of the bolometric light curve. The dominance of Fe II lines after about 2 week from the maximum also supports this progenitor model. For these reasons, there is wide consensus that SN Ia is a thrmonuclear explosion of a Chandrasekhar-mass C+O white dwarf. A white dwarf (WD) is a compact stellar remnant composed mostly of electron-degenerate matter, which is formed at the final evolutionary phase of stars whose mass is not high enought to become a neutron star. A WD, since it is a degenerate star, has the maximum mass that can support itself by electron generacy pressure. This limit is called the Chandrasekhar limit after Subramanyan Chandrasekhar, who carried out the accurate

[4] http://www.cfa.harvard.edu/supernova/SNarchive.html

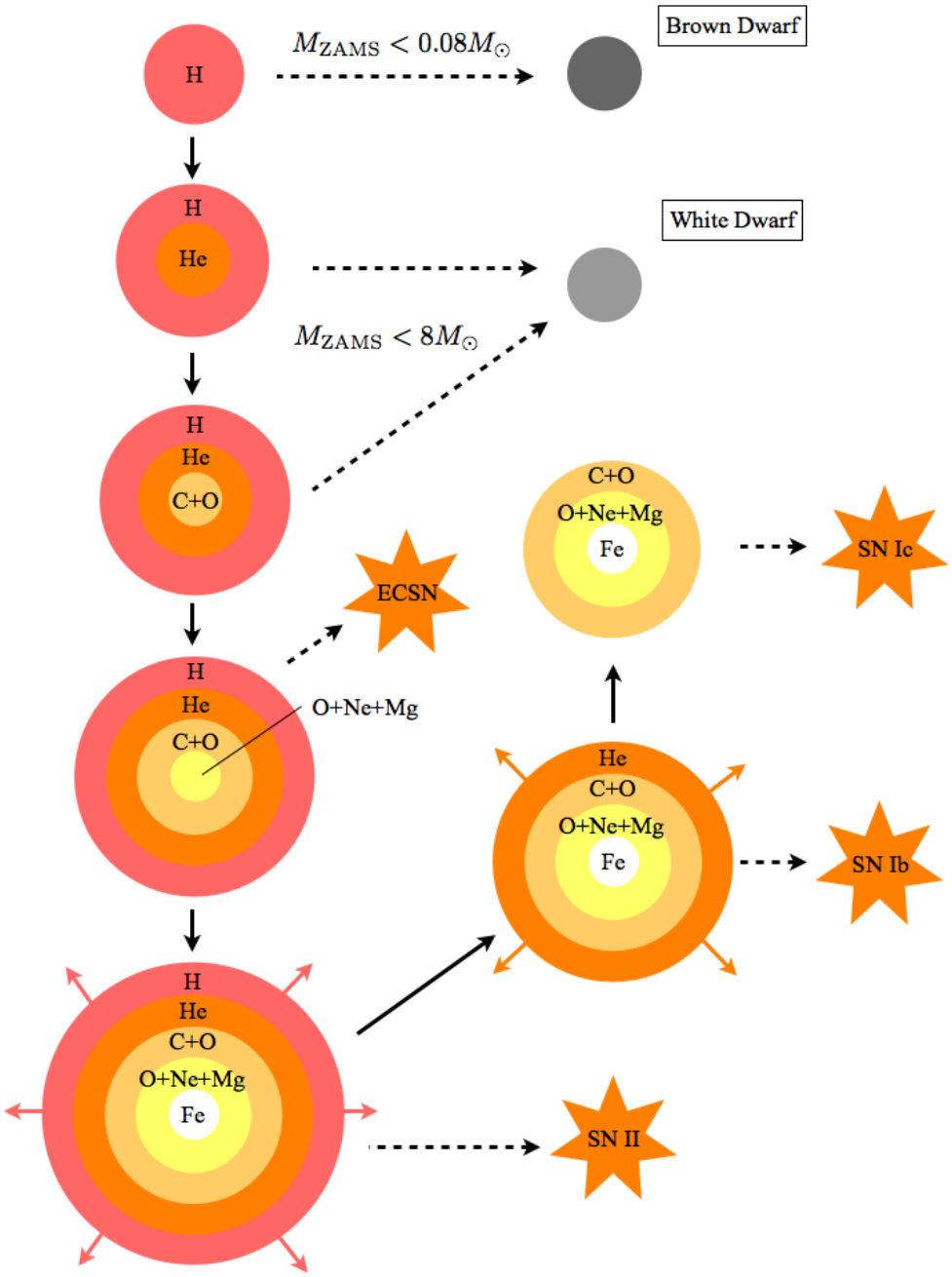

Figure 2.1: Evolutionary pathway to CC SN.

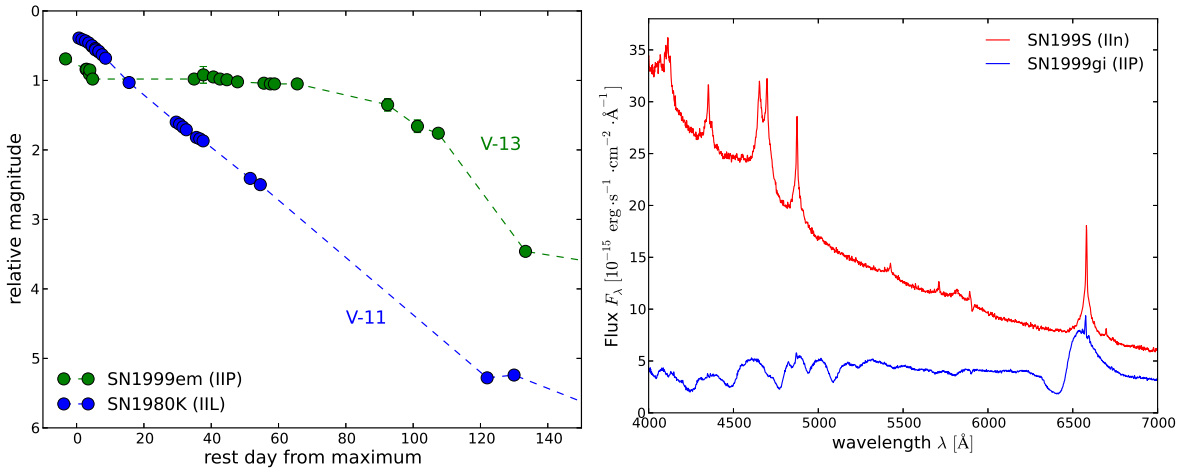

Figure 2.2: *Left:* The comparison of light curves of SN IIP and SN IIL. The green data is the photometry of SN 1999em from Elmhamdi et al. 2003, and the blue data is that of SN 1980K from Buta 1982. *Right:*The comparison between spectra of normal SN II, SN 1999gi (Leonard et al. 2002), and typical SN IIn, SN 1998S (Lentz et al. 2001, Fransson et al. 2005). The figure was constructed from The CfA Supernova Data Archive[4].

calculation of the limit (Chandrasekhar 1931). It is about $1.4M_\odot$ for a C+O WD. If we stand for this simple progenitor model, the homogenious observational features of SN Ia are quite naturally explained. Recently, remarkable conclusion was made by Nugent et al. 2011, Bloom et al. 2012. They analysed very early time observation of SN 2011fe, which occured at nearby galaxy M101 (6.4 Mpc), and concluded that this SN Ia is acutually an explosion of compact star with radius smaller than $0.1R_\odot$. Using the similar technique, Zheng et al. 2013 derived a constraint of $R_0 < 0.25R_\odot$ for nearby SN 2013dy at NGC 7250 (13.7 Mpc).

2.2.2 Homogeneity and Diversity

SN Ia is known for its homogenious properties such as peak magnitudes, spectra, and light curve shapes, but exhibiting only small differences (Branch 1998). Until early 1990s, it was believed that approximately 85% of SNe Ia belong to "normal" (or "Branch normal") SNe Ia according to the classification by Branch et al. 1993. Generally, SNe Ia rise to its maximum with small dispersion:

$$M_B \sim -19.05 \pm 0.38 + 5\log(H_0/65), \tag{2.5}$$

where H_0 is the Hubble constant in the unit of [km s^{-1}Mpc^{-1}] (Hamuy et al. 1996).

Furthermore, SNe Ia are known to have a prominent relation between their decline rates and brightness, indicating that the brightness of SNe Ia is arrangeable in a one-parameter sequence. Fainter explosions are redder and have a faster decline light curve, whereas Brighter events have a slower decline light curve. This correlation, known as "Phillips relation" (Figure 2.3), have two major method of parametrization: the decline rate in magnitude from maximum light to 15 days after (Δm_{15}: Phillips 1993, Hamuy et al. 1996) and the simple stretch of light curves (stretch factor, s: Perlmutter et al. 1997). This is what SN Ia makes a

good "standard candle", the astrophysical object whose luminosity can be calibrated. Thanks to the Phillips relation, the dispersion of peak brightness is reduced significantly.

However, recent observations also shows that peculiar subtypes, very luminous or subluminous SNe Ia, can hold ∼30% of all SNe Ia (Li et al. 2011b). Here we sammarize current understanding of those subtypes and peculiarities.

Branch normal SN Ia:
This class was first defined as SNe Ia whose optical spectra resemble those of SNe 1981B, 1989B, 1992A and 1972E rather than those of the peculiar SNe 1991T or 1991bg (Branch et al. 1993). More specifically, conspicuous absorption features near λ6150 (Si II) and near λ3750 (Ca II) are seen around maximum light with some other IMEs features, and a few weeks later Fe II features become apparent around $\lambda\lambda$4000-5000. The majority of SN Ia belong to this class.

91bg-like SN Ia:
Some SNe Ia such like SN 1991bg, 1992K, 1999by, and 2005bl form a subluminous class of SN Ia which some of them may violate the Phillips relation (Figure 2.3). B-band peak absolute magnitudes are around $M_B \sim -17$, roughly one magnitude fainter than "normal" SNe Ia. Light curves of 91bg-like object decline unusually quickly, also showing no second maximum in I-band, which is common feature of normal SN Ia light curve. As to spectra, the most striking peculiarity of SN 1991bg is the presence of a broad absorption feature around $\lambda\lambda$4150-4400 produced by a blend of Ti II, accompanied by a deep absorption near λ5000. The abundance of IMEs is higher than normal group, also showing low expansion velocities. In addition, little iron and the evidence for unburnt C and O are characteristics for these SNe Ia. Inferred amount of ^{56}Ni is very low (e.g. $\sim 0.07 M_\odot$ for SN 1991bg). According to Li et al. 2011b, these subluminous class accounts for about 15% of all SNe Ia.

02cx-like SN Ia (Iax):
These unusually subluminous object, grouped as "SNe Iax", have recently garnered considerable interest within the community (see Foley et al. 2013 and reference therein). SNe Iax is spectroscopicaly calacterized by their lower maximum-light velocities ($2000 \leq |v| \leq 8000 \mathrm{km\ s^{-1}}$; even lower than 91bg-like object). Maximum light spectra resemble those of the luminous SN Ia 1991T (see the next paragraph), with blue continua and absorption from higher-ionization species consistent with a hot photosphere. At late-time, spectra are dominated by narrow permitted Fe II lines. Interestingly, this class favors late-type galaxies and no SNe Iax is discovered in elliptical galaxies, indicative of a preference of their environments. In addition, this class harbor some extreme members. SN 2008ha and SN 2010ae are unusually faint objects (~ -14 mag) and the estimated amounts of ^{56}Ni are about $0.001 - 0.01 M_\odot$. In SN 2008ha case, it is suggest that the most plausible explanation was a failed deflagration of a WD (Foley et al. 2009, Foley et al. 2010). Li et al. 2011b estimated that SNe Iax contribute $\sim 5\%$ of all SNe Ia, however, with their underluminous nature, it is suspected that the volumetric fraction of SNe Iax can even reach $30^{+21}_{-15}\%$ (Foley et al. 2013).

91T-like SN Ia:

SN 1991T is a well-known prototype of luminous SNe Ia. At near maximum light of pectrum of SN 1991T is strikingly peculiar in having unusually weak lines of Si II, S II, and Ca II. Also prominent features of Fe III can be seen. One week later, this object has developed all the usuall Si II, S II, and Ca II features. Three weeks after the maximum, spectra become almost normal. This class contributes $\sim 9\%$ of all SNe Ia (Li et al. 2011b).

superluminous SN Ia:
Recently, some superluminous SNe Ia have reported, putting them well above the Phillips relation. With their maximum luminosity (brighter than ~ -20 mag), these events have brought a mystely about their progenitor. For example, SN 2009dc is the brightest SN Ia so far, which reached $M_V = -19.9$ even assuming null extinction in the host galaxy (Yamanaka et al. 2009). Combined with the fact that the explosion is nearly spherically symmetric (small polarization $< 0.3\%$ was estimated by Tanaka et al. 2010), SN 2009dc requires $1.6 \pm 0.4 M_\odot$ of ^{56}Ni (assuming $A_V = 0.29$ mag), challenging the Chandrasekhar mass WD explosion model. SN 2009dc can be a result of the explosion of two WDs whose total mass exceeds Chandrasekhar limit, but alternative scenario by Hachinger et al. 2012 suggests that an rapid rotating $2M_\odot$ WD can explain the observation. Explosion models of these superluminous (super-Chandrasekhar) explosions are still under controversial discussions.

2.2.3 Evolutional path to SN Ia: Single-Degenerate or Double-Degenerate

Although there is a concensus that SN Ia is an explosion of a Chandrasekhar-mass WD, the evolution path to the explosion is yet unsolved. Even more, some alternative theoretical models suggest that a WD can explode with sub-Chandrasekhar masses or super-Chandrasekhar masses. We also have to explain how these subclasses of SN Ia are formed. So far, the explanation of these deviation can be made from both binary evolution theory and explosion mechanisms. Here we briefly summarize known evolutional paths to SN Ia explosion.

First of all, since single WD cannot reach a critical mass alone, mass accretion from other star, witch form binary system together, is needed. Current understang is that a companion star is a non-degenerated star such like red giant (RG) and main-sequence (MS) star, or degenerated WD. The former process is called "single degenerated (SD) senario" and the latter is called "double degenerated (DD) senario" (see the schematic figure in Figure 2.4).

2.2.3.1 Single Degenerate Model

Hydrogen-burning donors:
SD model were thought to be the most promising SN Ia progenitor model in the past, since these system accutually exist in the Nature, observed as reccurent novae. If a binary composed of two stars with different masses is created, the heavier star evolve faster than the other, and finally evolve to a C+O WD when the $M_{\rm ZAMS}$ is within a certain mass range. This range can be infered from the mass enough to fuse helium in the core of the star, but not heavier than the mass which carbon fusion occurs (i.e. $0.5 M_\odot \lesssim M_{\rm ZAMS} \lesssim 8 M_\odot$). This stage is also known for unstable mass trasfer to the secondary (lighter star). When the primary become

[5] http://www.cfa.harvard.edu/supernova/CfA3/

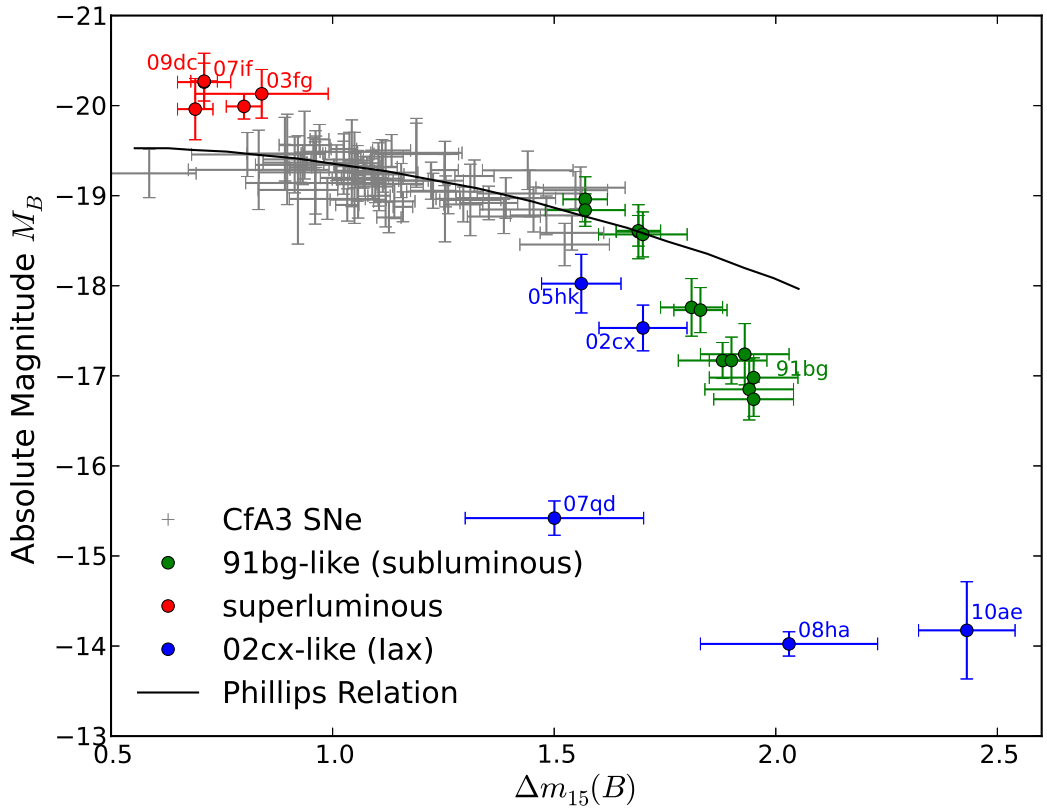

Figure 2.3: Absolute magnitude M_B vs. decline rate Δm_{15} diagram for SNe Ia. Gray data are from a subsample of the CfA3 SNe Ia[5] (Hicken et al. 2009). For peculiar subtypes, green data represent "subluminous (SN1991bg-like)" SNe Ia (Taubenberger et al. 2008), red data represent "superluminous" SNe Ia (Taubenberger et al. 2011), and SNe Iax (SN 2010ae: Stritzinger et al. 2013, SN 2005hk: Phillips et al. 2007, SN 2002cx: Li et al. 2003, Phillips et al. 2007, SN 2007qd: McClelland et al. 2010, and SN 2008ha: Foley et al. 2009). Black line shows a correlation for normal SNe Ia. All magnitudes are corrected to $H_0 = 70$ km s^{-1} Mpc^{-1} cosmology, and Δm_{15} of CfA3 sample are derived using conversion eqution from SALT2 fitter parameter (x_1, equivalent with stretch factor) as $\Delta m_{15} = 1.09 - 0.161 x_1 + 0.013 x_1^2 - 0.0013 x_1^3$ (Guy et al. 2007).

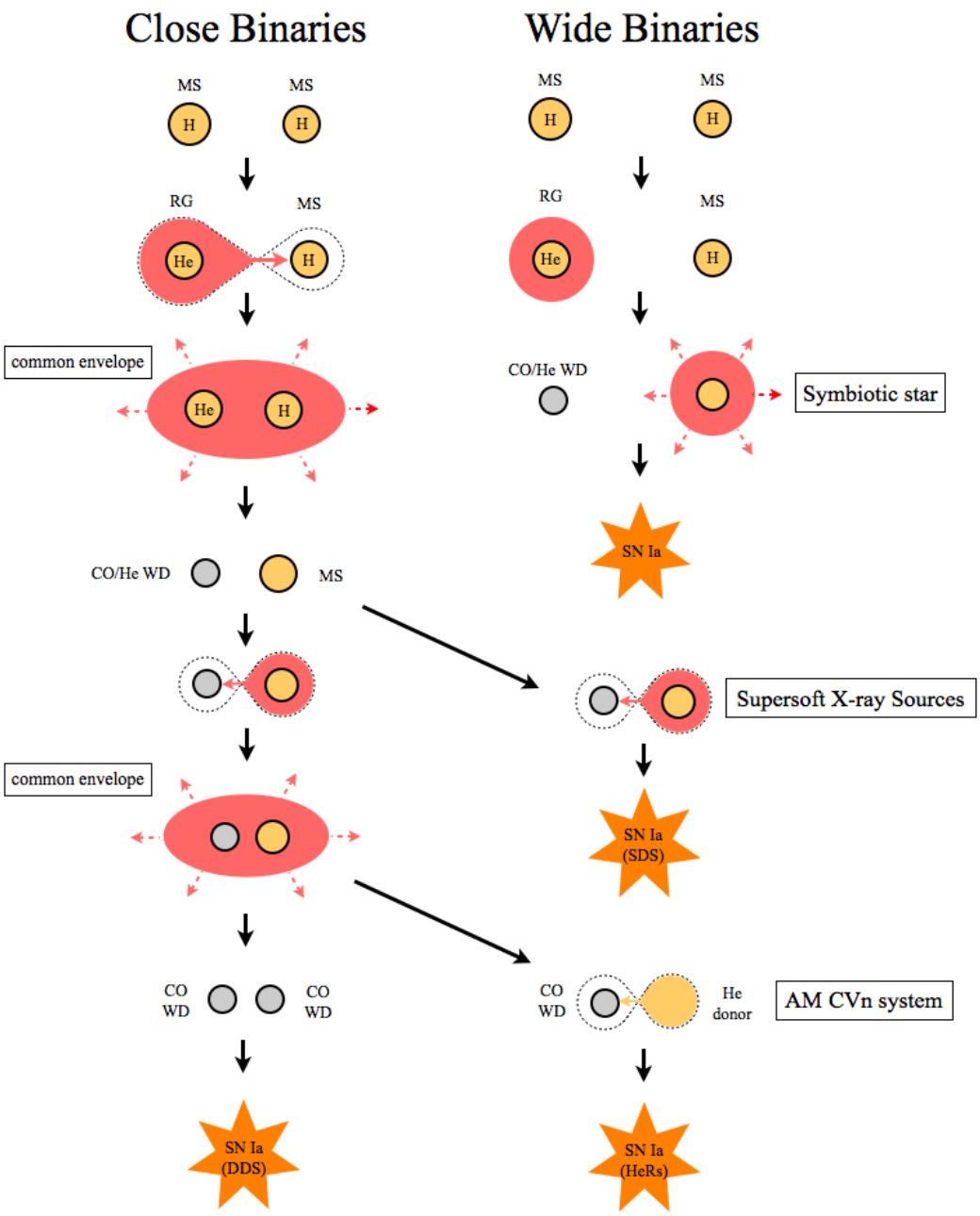

Figure 2.4: Evolutionary scenarios for typical progenitors of SN Ia.

the asymptonic giant branch (AGB) star, hydrogen-rich envelope expands, and transfer its mass to the secondary through the "Roche-lobe", a teardrop-shaped space defined by the region which material is bound to the secondary by gravity. Mass transfer from an evolved AGB star is dynamically unstable, and create a "common envelope", which finally disapear by recieving momentum from the orbiting star. As a result, the orbital separation shrink by tenth times, leaving a C+O WD (core of the primary) and non-degenerate secondary (likely still on the main sequence). Then the secondary starts to evolve with a delay. At some later stage, the secondary fills its Roche-lobe, and mass transfer to the primary should occur. This time, the mass transfer is stable and the primary WD can accumulate its mass to the Chandrasekhar limit. This track was first discussed by Whelan & Iben 1973, Nomoto 1982, Iben & Tutukov 1984, Paczynski 1985 (see Ruiter et al. 2009 and reference therein for recent models).

Whether these system lead to the thermonuclear explosion depends highly on the accretion rate from the secondary. Figure 2.5 illustrate this situation. In a lower accretion rate ($\dot{M} \leq 10^{-7}$), accreted hydrogen-rich material accumulate on the WD gradually. When the hydrogen-rich envelope on the WD reaches a critial mass, hydrogen ignites to trigger a *nova eruption*, or *hydrogen shell flash*. According to classical nova observations, nova ejecta contain white dwarf matter, i.e., carbon and oxygen for C+O WDs and oxygen, neon, and magnesium for O-Ne-Mg WDs (e.g. Prialnik 1986, Kovetz & Prialnik 1994). This lead to the consequence that classical novae cannot accumulate enough mass, but rather are eroded gradually after many cycles of nova outbursts.

Next, in a higher accretion rates, accreted material will be heated to the temperature enough to burn H and He stably, which converted materials (i.e., carbon and oxygen) are accumulated on the WD. Recurrent novae, whose eruption repeat in timescals of a decade to a century, are possible candidates of this track. Observationally, recurrent nova do not show heavy elements such as carbon, oxygen, and neon enriched in ejecta, and short recurrence periods are plausible to make massibe WDs close to the Chanrasekhar limit (Starrfield et al. 1985, Starrfield et al. 1988, Livio & Truran 1992, della Valle & Livio 1996).

Finally, in the case that the accreteion exceeds the consumption of hydrogen and helium,

$$\dot{M} > \dot{M}_{\rm cr} \sim 7.5 \times 10^{-7} \left(\frac{M_{\rm WD}}{M_\odot} - 0.4 \right) \quad M_\odot \ {\rm yr}^{-1} \tag{2.6}$$

unburned material ($\dot{M} - \dot{M}_{\rm cr}$) expands around WD and cause strong wind. Though consequences of this track is still unclear, a series of papers Hachisu et al. 1996, Hachisu et al. 1999b, Hachisu et al. 1999a discuss the effect that the wind stabilizes the mass transfer and limit the accretion rate suitable for mass accumulation to the WD.

Helium-burning donors: It is also possible that a WD accretes mass from helium-burning stars. Solheim & Yungelson 2005 showed that such systems like AM CVn may contribute to the SNe Ia population. The most characteristic feature for this group, since the secondary has rather larger ZAMS masses, is that the timescale to the explosion is faster than fiducial SD model (e.g. Ruiter et al. 2009, Iben et al. 1987, Wang et al. 2009a). Though these events are rare, it may be important sources to explain SN Ia with short evolutional timescales. These explosions are grouped as the acronym HeRS by some authors.

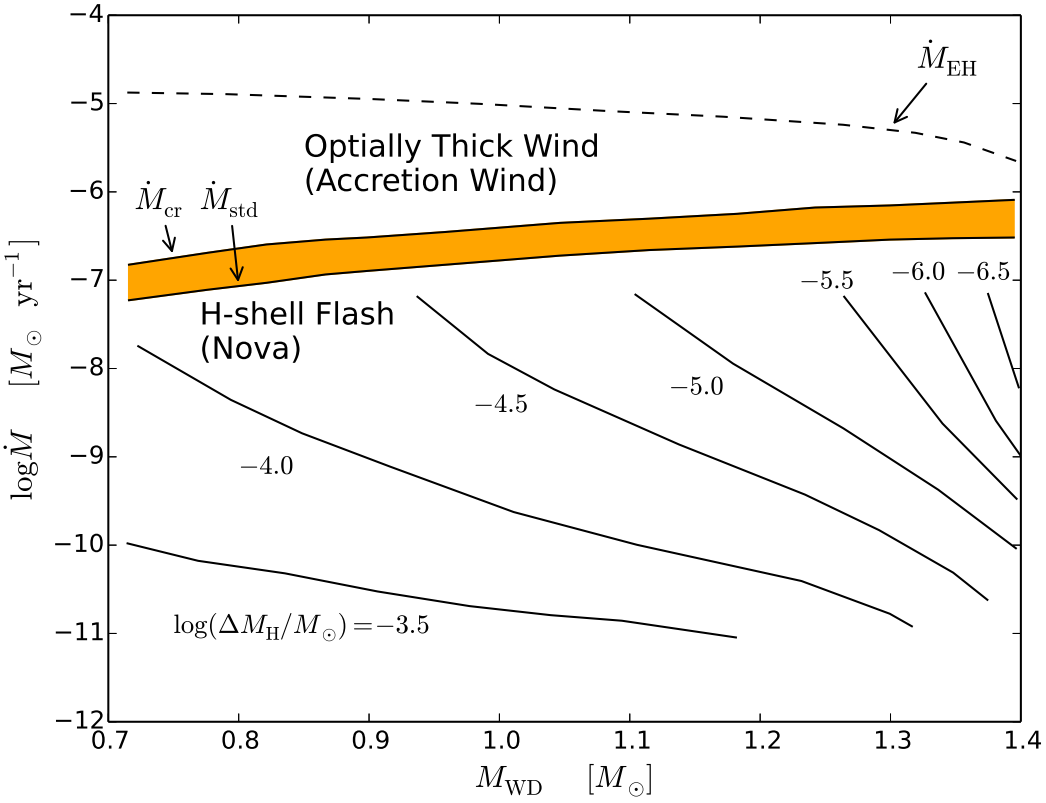

Figure 2.5: Response of white dwarfs to mass accretion is illustrated in the white dwarf mass and the mass accretion rate plane (reconstructed from Figure 9 of Nomoto 1982). $\dot{M}_{\rm EH}$ is the Eddington critical rate for hydrogen, $\dot{M}_{\rm std}$ is the accretion rate which is necessary for steady hydrogen burning, and $\dot{M}_{\rm cr}$ is the cretetical accretion rate that is comparable to the hydrogen consumption rate approximated as Equation 2.6. The value $\Delta M_{\rm H}$ is the mass of the accreted hydrogen-rich envelope at the ignition of hydrogen. In lower $\dot{M}$, WD experiences nova eruptions rather than accumulating mass, and orange hached region allow the stable hydrogen-burning, which lead WD to the Chandrasekhar limit. In higher $\dot{M}$, unburned material expands and cause strong wind. If we adopt the model of Hachisu & Kato 2001, accretion rate range allowed for SN Ia progenitor will expands to the higher end (thus $\dot{M}_{\rm EH}$ is plotted in dashed line).

2.2.3.2 Double Degenerate Model

Another promissing progenitor of SN Ia is double-degenerate model, proposed in classical studies of Iben & Tutukov 1984, Webbink 1984. If the mass transfer from the secondary through its Roche-lobe is unstable, the second common envelope takes place, leaving the primary C+O WD and the secondary C+O or He WD system (e.g. Ruiter et al. 2009). A detached WDs binary will eventually reach contact due to angular momentum loss from the emission of gravitational radiation. Then the less-massive WD finally accrete onto the primary WD, leading to a SN Ia explosion when the total mass exceed the Chandrasekhar mass (Tutukov & Yungelson 1979). According to the general relativity, the decline rate of the binary separation, a, can be expressed as below (in the case that the orbit is circular):

$$\frac{\dot{a}}{a} = 2\left(\frac{\dot{J}}{J}\right)_{\rm gw} = -\frac{64}{5}\frac{G^3}{c^5}\frac{M_1 M_2 (M_1+M_2)}{a^4} \propto a^{-4}, \tag{2.7}$$

where J is the angular momentum of the binary, and M_1 and M_2 are masses of the primary and the secondary, respectively.

Nevertheless this model explain the absence of hydrogen and the mass accumulation to the Chandrasekhar limit, it has been critisied by some aspects. First, according to the argument of Saio & Nomoto 1985, the accretion from the seconary WD whould not lead to central burning but rather burning in the outer layers of the primary WD, where the density is low. The outcome is that C+O WD transform into an O-Ne-Mg WD, but not a SN Ia explotion. This WD is thought to finally collapse to form a neutron star (accretion-induced collapse; AIC), since electron captures become impoartant at high central densities of the O-Ne-Mg WD (Miyaji et al. 1980). Mergers of massive WDs with a close mass ratio may avoid AIC ("violent merger"). Secondry, population synthesis calculations show that even if all C+O WDs with $M_{\rm tot} \leq M_{\rm Ch}$ become SN Ia, the estimated birthrates are facor of a few lower than observed SN Ia rates (e.g. van Kerkwijk et al. 2010, Badenes & Maoz 2012). Some event with $M_{\rm tot} < M_{\rm Ch}$ may contribute to SN Ia population (see section 1.3).

Recently, though there are still controvercial discussions, DD model is thought to be the major pathway to SN Ia population. Remarkable signatures are SN Ia rates, and absence of circum-stellar material and surviving secondary. All these observation constraints are introduced in section 2.3.

2.2.4 The explosion models

2.2.4.1 Ignition and explosion mechanism

Although the explosion physics is not clearly understood, theoretical stuedies are trying to provide reasonable models for SN Ia explosion (see Hillebrandt & Niemeyer 2000, Hillebrandt et al. 2013 for review). If the accreting WD reach to the Chandrasekhar limit, the energy budget near the core is governed by plasmon neutrino cooling and compressional heating. At later stage, higher temperature near the core cause convective carbon burning period (known as "simmering phase") for $\sim$ 1000 yrs. If the temperature become high

enough that the timescale for thermonuclear burning (τ_b) becomes much smaller than the timescale of convection (τ_c), the propagation of combustion waves starts. The reactive Euler equations allows two mode of combustion waves: one is called "deflagration", subsonic wave that burn carbon and oxgen to IMEs, and the other is called "detonation", supersonic wave which produce iron-peak elements. Combined with the observation signatures of typical SN Ia, the explosion cannot be explained by pure-detonation nor pure-deflagration model. Therefore, the consensus is that typical SN Ia starts to explode with subsonic deflagration, and then transisiton to the supersonic detonation occurs at some critical points (so-called "delayed-detonation model"). These waves propagate whole WD, and will explode as SN Ia. Some numerical simulations succeed in reproducding reasonable SN Ia spectrum (e.g. Röpke 2007, Woosley 2007, Woosley et al. 2009, Poludnenko et al. 2011), at the same time, some uncertainties (e.g. the way the deflagration ignites) makes it hard to realize SN Ia in simulations.

Alternative models are recently favored in the context of birthrates. One is called *sub-Chandrasekhar-mass double detonations*. According to this model, a C+O WD accretes mass from helium donor (either degenerated WD or non-degenerated star), creating thin He layer onto WD. After He layer grow enough massive to ignite He material, a detonation in the layer starts. This shock propagates into the C+O core, and finally the core experiences second detonation ("edge-lit detonation") even if WD does not reach M_{ch}. Recent studies (e.g. ref) indicate that this model can reproduce normal SN Ia, however, it produce significant amount of Ti in the outer layers, which is inconsistent with normal SN Ia. This model would explain the feature of subluminous 91bg-like SN Ia. As to double-degenerate merger scemario ("violent merger"), the entire treatment of merger and explosion was hard to archieve in the past computational resources. However, recent studies report that normal SN Ia is acctually produced in the merger simulations (e.g. 207).

All these models yet have ups and downs, and further investigation and observational constraints are expected in the future.

2.2.4.2 After the explosion

After the explosion provides kinetic energy and unbind WD, the photosphere of SN Ia expands. Gamma rays produced by radioactive decay of ^{56}Ni (see Equation 2.4) hold majority of optical lights. The optical spectra is well characterized by black-body radiation of photosphere and absorption lines of IMEs. As the SN expands, the light-emitting region (photosphere) recedes and finally reach to the phase that the energy deposition rate become comparable with radiation, that is, the peak of light curve. Then the light curve starts to decline, and as photosphere unveil inner part of SN, Fe starts to characterize the spectra. In infrared, light curves for normal SN Ia show the secondary maximum after about 40 days. This is due to the ionization evolution of the iron-peak elements in the ejecta (Kasen 2006). After hundreds of days, the decline of light curve is equivalent with the decay of ^{56}Co, and spectra are dominated by emission lines from iron-peak elements. Free expansion of the ejecta continues, sweeping out circumstellar and interstellar gas, and eventually, after tens to hundred years, a shell of shocked gas cause strong X-ray emission ("Sedov phase"). Those objects are called "Supernova remmant".

2.2.5 As a cosmological tool

After the discovery of the expantion of the universe, its expansion history is one of the key issue in current physics. SN Ia, as a good distance indicator, has been contributed to unveil the geometry of the universe (see Howell 2011 for a review).

In non-Euclidean space such as expanding universe, the distance defined by the luminosity of the object with redshift z, $D_L(z)$, depends on the cosmological parameters:

$$D_L(z) = (1+z)\int_0^z \frac{c\,dz'}{H_0\sqrt{(1-\Omega_{tot})(1+z')^2 + (1+z')^3\Omega_M + \Omega_{rad}(1+z')^4 + \Omega_\Lambda}}, \quad (2.8)$$

where Ω_M, Ω_{rad}, and Ω_Λ, are the energy densities of matter, radiation, and dark energy.

Considering the small fraction of radiation ($\Omega_{rad} \sim 10^{-4}$) and assuming the flat universe ($\Omega_{tot} = 1$), "distance modulus", the difference between the apparent magnitude and the absolute magnitude of the object, can be expressed as a function of Ω_M and Ω_Λ.

$$\begin{aligned} \mu(z) &= m - M = 5\log_{10}\left(\frac{D_L(z)}{\mathrm{Mpc}}\right) + 25 \\ &= 5\log_{10}\left\{\int_0^z \frac{c\,dz'}{H_0\sqrt{(1+z')^3\Omega_M + \Omega_\Lambda}}\right\} + 5\log_{10}(1+z) + 25 \end{aligned} \quad (2.9)$$

Since z and m can be obtained by observation, one is able to constrain cosmological parameters by estimating the absolute magnitude, M. This is the basic idea of *supernova cosmology*. Actually, M can be estimated using well-known light curve shape-versus-luminosity relation (Phillips relation, see section 2.2.2). Most common formalism is explessed with stretch factor (s) and color of SN Ia (c).

$$\mu(z) = m_B - M_B + \alpha(s-1) - \beta c, \quad (2.10)$$

where α and β are the slopes of the relations, and m_B and M_B is the apparent/absolute magnitudes. Recently, alternative measurement for standarizing SN Ia luminosity is proposed. Bailey et al. 2009 and Blondin et al. 2011 showed that some flux ratios (e.g. $\mathcal{R}_{642nm/443nm}$) can reduce the scatter in the luminosity calibration. Various techniques are used to determine the absolute magnitude, and many light curve fitter were developped so far (e.g. SALT2 by Guy et al. 2007; SNANA by Kessler et al. 2009b ; MLCS2k2 by Jha et al. 2007; SiFTO by Conley et al. 2008).

The expansion history of the universe is often characterised by the equation of state, w, which can be constrained by cosmologial parameters. If we take a arbitrary length scale in the universe, a, the universe evolves according to dominant components as

$$\rho \propto a^{-3(1+w)} = \begin{cases} a^{-3} & (w = 0; \text{normal matter}) \\ a^{-4} & (w = \frac{1}{3}; \text{relativistic component}) \\ 1 & (w = -1; \text{corresponding to Enstein's cosmological constant, } \Lambda) \end{cases} \quad (2.11)$$

In the late 1990s, two independent supernova observation teams: the Supernova Cosmology Project (SCP) (Perlmutter et al. 1999) and the High-Z SN Search Team (Riess et al. 1998)

found the strong evidence of nonzero Ω_Λ, which suggest the accelerating cosmic expansion. Since then, many large SN surveys have been carried out to measure the cosmological parameters (e.g., Knop et al. 2003, Tonry et al. 2003, Astier et al. 2006, Riess et al. 2007, Wood-Vasey et al. 2007, Kowalski et al. 2008, Hicken et al. 2009, Amanullah et al. 2010, Sullivan et al. 2011, and Suzuki et al. 2012). Now there is a general concensus that this universe is dominated by dark energy ($\Omega_\Lambda \sim 70\%$), which perfoms as a $w \sim -1$ component.

Although the first results by SCP and High-Z Team were using just tenth of SNe Ia, thanks to many strategic surveys, the number of cosmological SN Ia sample is dramatically increasing to hundreds. Now the statistical error is subdominant in the estimation of w, meaning that the reduction of the systematics is highly needed. Several dominant systematics can be summarized as below.

Calibration

The primary systematic uncertainties afecting SNe Ia depends on survey, but there is a general agreement that the largest component is calibration. This include the measurement of standard stars (flux reference), the measurement of zero points (e.g. Kessler et al. 2009a), K-correction (e.g. Hsiao et al. 2007), calibration to the historic Landolt phyotometric system used for nearby historical supernova. These factors will be reduced if precise meaurements of standard stars are carried out and low-redshift samples observed in Landolt system are replaced with well-calibrated ones.

Reddening

When estimating the absolute brightness, reddening effect should be corrected properly. As a general trend, redder SNe Ia are fainter. However, it is not clearly understand how much of the effect is due to the intrinsic color-luminosity relation, or to the dust extinction. It is also controversial that that the slope of color-luminosity relation, β ($= R_B = R_V - 1$), prefer small value compared to Milky Way dust ($R_B = 4.1$). In most cases, the values of β come within the range of $\beta \sim 2.5 - 3.5$ (e.g.Elias-Rosa et al. 2006, Krisciunas et al. 2006, Krisciunas et al. 2007, Elias-Rosa et al. 2008, Folatelli et al. 2010). Some studies show that the value of β differs when devided to separate groups. For example, smaller β is prefered by SNe Ia with lower ejecta velocity (Wang et al. 2009b), smaller collor excess $E(B-V)$ (Nobili & Goobar 2008, but contradicting with Folatelli et al. 2010), and those SNe Ia at low star-formation rate hosts (Sullivan et al. 2010). Whereas the conclusion cannot be made yet, one way to avoid this problem is infrared observation, which the effect of dust is minimized (e.g. Krisciunas et al. 2004, Wood-Vasey et al. 2008).

Restframe U-band

In optical bands, the light from SNe Ia at higher redshift correspond to shorter wavelength at rest-frame. The weakpoint of this shift in wavelength is that SN Ia has a great deal of scatter in rest-frame U-band (e.g. Ellis et al. 2008). The uncertainty might arise from intrinsic dispersion or pool calibration in U-band. However, this systematics can be reduced by constructing a well-calibrated sample in low-redshift.

Host biases

It is known that the luminosity and the color of SN Ia have correlation between the host properties such as star-formation rate, stellar mass, and metallicity (e.g. Hamuy et al. 1996, Howell 2001, Sullivan et al. 2006, Gallagher et al. 2008, Howell et al. 2009, Sullivan et al. 2010). The problem here is that the residual in cosmological fit, i.e., *Hubble residual*, still show some dependence on the host properties. This may suggest that we need another correction term in Equation 2.10. For example, theoretical studies indicate that SNe Ia at low-metal environment become fainter, because high matallicity WD yeld stable ^{58}Ni rather than radioactive ^{56}Ni (Timmes et al. 2003). If the metallicity effect explain the host dependence, host mass or host metallicity will be the third correction factor. However, it is yet not sure where these dependences come from. Alternative explanation is that the bias arised from progenitor age. This scenario may have a role because young progenitor comes from massive star, or the density structure of WD changes with time (ref).

To summarize, supernova cosmology is restricted by several uncertainties. The largest one is calibration, but the situation will be better in the future. Other systematics of concern are reddening, intrinsic dispersion in rest-frame U-band, host bias and progenitor. This thesis is related to the progenitor issue, which is still unclear and can be investigated by statistical studies. In the next section, the current constraints on progenitor are introduced.

2.3 Progenitors problems of Type Ia Supernova

In spite of its importance of SNe Ia, their progenitors are yet to be conclusively identified. Various approaches to constrain the progenitor systems have been examined so far (see Maoz et al. 2013 for a review). The observational results are not yet conclusive, but recent studies appears to show that DD models may explain most of, if not all, SNe Ia. Generally speaking, SD models are expected to leave evidences for the surviving companion and circumstellar materials around the system, which cannot be seen in most of observations. In the other hand, DD models will pass these constraints. SN 20011fe, the nearest normal SN Ia event in 25 years occured at M101 (6.4 Mpc), was one of the best case to test the progenitor because it was discovered very early and extremely well studied. Some other individual events are shedding lights on progenitor questions. Other approaches are based on statistical studies, i.e. the occurence rates of SN Ia. Among them, the distribution of the delayt time (DTD) is a promissing way to test the detailed progenitor components. In this section, some major discussions around progenitor problem are introduced, and the rate studies are separately described in section 1.3.

2.3.1 Surviving companion

In a SD scenario, the secondary star (donar) will survive the explosion of the primary WD, identifiable by its anomalous features such as velocity, rotation, and temperature (e.g. Marietta et al. 2000, Pan et al. 2013). Thus, if these survivor are detected, it will be a *smoking gun* of SD progenitors. Various remnants were investigated, however, no clear evidence of survivor is reported.

SN 1572 (or Tycho's SN) is one of the well studied remnants and several stars are de-

tected around the center of the remnant. Many studies tried to find any signature such as proper motion, rotation velocities, and chemical composition (e.g., Ruiz-Lapuente et al. 2004, Ihara et al. 2007, González Hernández et al. 2009, Kerzendorf et al. 2009) but they have not reached to a clear concensus. Recently, Kerzendorf et al. 2012 have concluded that no good candidates for the survivor is found in the Tycho's SN. Similar approach is also applied to SN 1006 and no apparent survivor with $L_V > 0.5L_{\odot,V}$ is detected, suggesting that most of SD channels except for normal MS donors are rejected (Kerzendorf et al. 2013b, González Hernández et al. 2012). The case of SNR 0509-67.5 in the Large Magellanic Cloud (LMC) is more clusial. Schaefer & Pagnotta 2012 reported that no stars with $L_V > 0.04L_{\odot,V}$ around the center of the remnant. Though late K-type MS stars with $M \sim 0.5M_{\odot}$ are still acceptable under this constraint, the fact rule out all traditional SD models. Edwards et al. 2012 conducted a HST observation of SNR 0519-69.0 in LMC, and found no evidence for giant or sub-giant donors. SN 1604 (or Kepler's SN), though the SN type is controversial, Kerzendorf et al. 2013a ruled out the existence of giant donors. Recently, an alternative interpretation to support SD model is proposed by several authours (e.g. Di Stefano et al. 2011, Hachisu & Kato 2012, Justham 2011). According to their model, the rotation of the primary WD may lead to the delay to the explosion, which enable donor to evolve to a undetectable WD. This pathway may challenge other observation features (see Maoz et al. 2013).

To summarize, no clear evidence for SD survivor is observed so far. Especially, the case of SNR 0509-67.5 is the strongest constraint that disagree with traditional SD models.

2.3.2 Hydrogen signature

In SD scenario, signature of hydrogen or helium from non-degenerate companion should be observed; the ejecta is thought to strip some material of $M \sim 0.1-0.2$ and they are expected to be observable as line emission in the later spectra, when the ejecta become optically thin. Mattila et al. 2005, Leonard 2007 and Lundqvist et al. 2013 studied several SNe Ia and derived upper limits to the strength of Hα. Their constraint ($M_{\rm H} < 0.01 - 0.03M_{\odot}$) appears to disfavor SD models. The most strong contraint is the case of SN 2011fe, which a limit of $0.001M_{\odot}$ is set by Shappee et al. 2013.

Nevertheless, there are some exceptions. SN 2002ic (Hamuy et al. 2003) and SN 2005gj (Aldering et al. 2006; Prieto et al. 2005) are well known for their presence of strong variable Hα. Alhough it sounds to contradict with the definition of SN Ia, their spectrum is acctually SN Ia like except for the presence of Hα. Now it is comprehended that Hα comes from the interaction of the ejecta and the existing dence CSM, as well as the picture of SN IIn (Han & Podsiadlowski 2006, Wood-Vasey & Sokoloski 2006; but see Chugai & Yungelson 2004, Benetti et al. 2006, Trundle et al. 2008 for alternative explanations). Recent found "CSM-interacting" SN Ia, PTF11kx (Dilday et al. 2012, Silverman et al. 2013), is another well-studied object. According to Dilday et al. 2012, PTF11kx can be explained by the configuration similar to the symbiotic reccurent nova RS Ophiuchi. Silverman et al. 2013 studied a compilation of 16 strongly CSM-interacting SNe Ia and estimated the fraction of these events to be 0.1-1% (or even higher) based on PTF and SDSS-II surveys. Though strong resemberance of CSM-interacting SNe Ia to SNe IIn suggest

that CSM may come from a massive star rather than a SD donor, these SNe still bear a possibility to be SD candidates.

2.3.3 Radio and X-ray emission from CSM interaction

In the same context above, in SD scenario, the existence of CSM from donor star is expected to raise shock with the SN ejecta. As a consequence, radio synchrotron emission from accelarated electrons and X-ray emission from inverse Compton scattering will be produced (see Chevalier 1982 and Chevalier 1998 for detailed physics). None of these emissions have been detected, despite radio/X-ray emissions from CC SNe are reported for some cases. Hughes et al. 2007 set upper limits on X-ray flux using four SNe Ia, including strongly CSM-interacting SN 2002ci and SN 2005gj, and Russell & Immler 2012 set upper limits on 53 SNe Ia. Combined with expected parameters of SD SNe Ia, these results indicate that SD models with evolved donor star are not the case. In the radio observations, Panagia et al. 2006 studied 27 nearby SNe Ia and no radio emission was found. Hancock et al. 2011 derived deeper limits by stacking analysis, constraining pre-explosion mass loss rate of the secondary to be $\dot{M} \lesssim 10^{-7} M_{\odot}\mathrm{yr}^{-1}$. Here again, the result obtained from the observation of SN 2011fe is tighter. Horesh et al. 2012 considered radio and X-ray limits and set a limit of $\dot{M} \lesssim 10^{-8} M_{\odot}\mathrm{yr}^{-1}$ assuming typical CSM parameters. Using additional X-ray observations, Margutti et al. 2012 refined the limit to $\dot{M} \lesssim 2 \times 10^{-9} M_{\odot}\mathrm{yr}^{-1}$. Taken together, no detection of radio and X-ray emission for good number of SNe Ia rules out giant SD donor, even including SNe Ia showing CSM-interacting features. In particular, the case of SN 2011fe defenetively favors clean environment.

2.3.4 blue-shifted Na I D absorption

Although the evidence of CSM from SD donor is not clearly seen in most of SNe Ia, some objects show blue-shifted absorption lines which are feasible feature for classical SD model. If a circumstellar wind from the secondary through accretion overflows or pre-explosion nova-like outburst exists, variable narrow blueshifted absorption should be observed in the spectra. Recent statistical studies indicate that some fraction ($\sim 20\%$) of SNe Ia shows these variable blueshifted Na I D lines (Sternberg et al. 2011, Foley et al. 2012, Maguire et al. 2013, and Phillips et al. 2013). This is preferable to SD models, however, Shen et al. 2013 showed that these CSM features can be seen also in some DD explosion. The approach to CSM still suffer from small numers and systematics to define samples, and may need further investigation.

2.3.5 Searching possible candidates

As noted in section 2.2.3.1, reccurent novae are promissing candidate for SD model. For example, U Sco and CI Aql are well known reccurent novae which hold high mass WD in their system: $1.55 \pm 0.24 M_{\odot}$ for U Sco (Thoroughgood et al. 2001) and $1.00 \pm 0.14 M_{\odot}$ for CI Aql (Sahman et al. 2013). However, whether these systems will evolve as SNe Ia is not clear. Some observations suggest that the mass of ejected material may exceed accreted mass (e.g. Schaefer 2013). Another type of reccurent nova system is symbiotic binary, which the separation is larger and the WD accrete mass from the strong wind from the com-

panion. RS Oph, the system containing a massive WD and a red giant, is one of these candidate (e.g. Kato & Hachisu 2012). Recently, V407 is also found to be a similar system (Hachisu & Kato 2012, Nelson et al. 2012).

Nevertheless there are possible SD candidates, their detected number challenges the SN Ia occurence rate in the Galaxy ($\sim 0.005\mathrm{yr}^{-1}$; estimated from Li et al. 2011a and McMillan 2011). If reccurent nova channel dominate SN Ia progenitors, the Galaxy should produce ~ 3000 systems, assuming typical accretion rate and accreted mass. However, according to Schaefer 2010 estimation, the Galactic reccurent novae only explain ~ 300 systems. Furthermore, observation of supersoft X-ray sources set tighter constraints on SD models. During the stable burning of accreted material from the secondary, a SD progenitor is observed as supersoft X-ray sources peaking at 30-100eV, with typical luminosities of $10^{38}\mathrm{erg\ s}^{-1}$ (e.g. Hachisu et al. 1999a). However, Di Stefano 2010 and Gilfanov & Bogdán 2010 pointed out that observed numbers of supersoft X-ray sources in nearby galaxies are an order of magnitude smaller than expected. This means that reccurent novae contribute only a few percent to the SN Ia rate.

As to DD system, the first systematical search for binary WDs are conducted by SPY (Geier et al. 2007, Napiwotzki et al. 2004, Nelemans et al. 2005). Among ~ 100 discovered WDs binaries, only a few systems will merge within a Hubble time and none of thier total masses exceeded M_{ch} (The only candidate whose mass is close to M_{ch} was WD 2020-425 with $M_{\mathrm{tot}} \sim 1.35$). Other surveys also failed to find any $M_{\mathrm{tot}} \geq M_{\mathrm{ch}}$ and Hubble-time-marging double WD binaries. However, as noted in section 2.2.3.2, the condition of total mass is not necessarily requiered. Recent study by Maoz et al. 2012a and Badenes & Maoz 2012, based on analysis of 4000 DA WDs in SDSS, revealed that the Galactic merger rates is consistent with theoretical binaly population synthesis calculations (a few $10^{-2}\mathrm{yr}^{-1}$; e.g. Nelemans et al. 2001, Toonen et al. 2012).

To summarize, various tests are conducted to find SD/DD features for good numbers of SN Ia and possible candidates. These reults generally rule out the dominance of SD systems in all SN Ia. Some CSM-interacting SN Ia may arise from SD channels, but the question about how many SD/DD systems contribute to SN Ia population still remains unclear. Thus, statistical studies such as occurence rates of SN Ia and their properties are highly needed to answer the question.

Now is no time to think of what you do not have. Think of what you can do with that there is.

Ernest Miller Hemingway (1899 - 1961)

3 Observations and Sample Selection

3.1 Subaru XMM-Newton Deep Survey

The Subaru/XMM-Newton Deep Survey (SXDS) is a multi-wavelength survey from X-ray to radio (Sekiguchi & SXDS Team 2004). The survey targets a 1.22 deg^2 field centered on ($02^{\rm h}18^{\rm m}00^{\rm s}$,$-05°00'00''$), hereafter referred to as the Subaru/XMM-Newton Deep Field (SXDF[4]; Figure 3.1).

3.2 Imaging observations

Optical:
The optical imaging component of the survey was carried out using Suprime-Cam (Miyazaki et al. 2002) on the 8.2–m Subaru telescope, starting in September 2002. With Suprime-Cam's very wide field of view ($34' \times 27'$), the field is covered in five pointings (SXDF-C, SXDF-N, SXDF-S, SXDF-E and SXDF-W; see Furusawa et al. 2008). In order to detect and follow the light curves of optically faint variable objects, the Suprime-Cam observations were split into exposures of 1800−7200 seconds separated by periods of days to weeks. Between September 2002 and December 2002, the fields were observed 5−7 times in the i'-band and 2−4 times in the R_c- and z'-bands. After the 2002 observations finished, we took reference images in the i'-band in 2003 and 2005, in the z'-band in 2005, and in the R_c-band in 2008. The observations are described in detail in Morokuma et al. 2008. Here, the number of the epochs of the observations, each exposure time, and each detection limit are summarized in Table 3.1. For our SN study we exclude regions around bright objects to ensure reliable detection of object variability. This reduces the total effective area to 0.918 deg^2.

Infrared:
As part of the SXDS, the field was observed by the Wide Field Camera (WF-

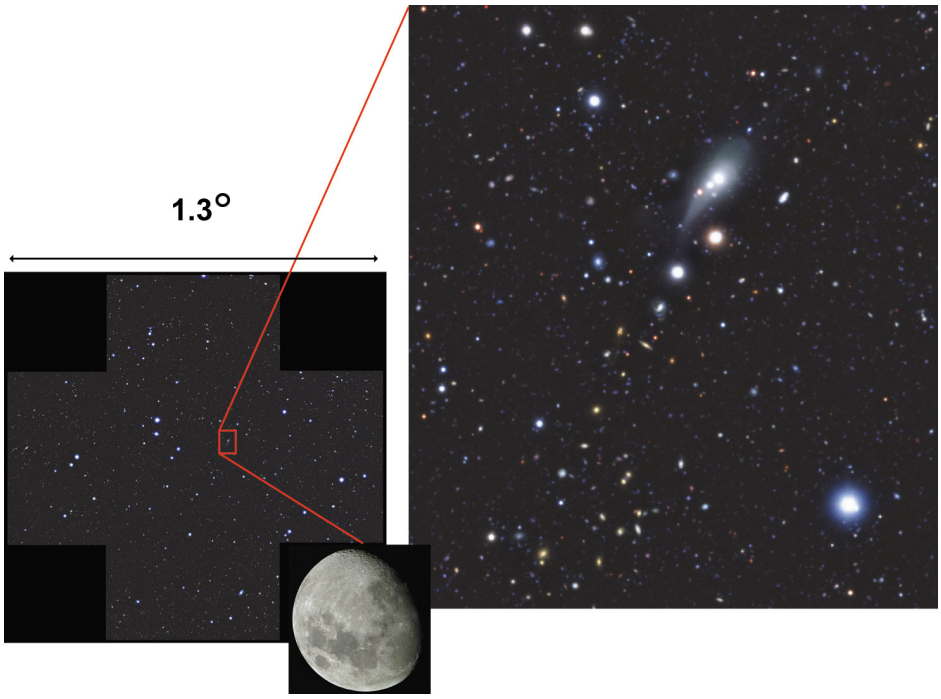

Figure 3.1: Field overview of Subaru/XMM-Newton Deep Survey (SXDS), synthetic images of the $B-$, $R-$, and $z'-$ bands (©NAOJ).

CAM) on the UKIDSS (United Kingdom Infrared Deep Sky Survey) Ultra Deep Survey (Warren et al. 2007) in the J, H, and K bands, with respective limiting magnitudes of 24.9, 24.2, 24.6 (5σ, 2 arcsecond diameter aperture). Additionally, the Spitzer Space Telescope (SST) as part of the SWIRE legacy program (Lonsdale et al. 2004) obtained data in 3.6 μm and 4.5 μm bands, with respective limiting magnitudes of 23.1 and 22.4 (3σ, 3.8 arcsecond diameter aperture).

X-ray:
X-ray imaging observations in the SXDF were carried out with the European Photon Imaging Camera (EPIC) on the XMM-Newton. The X-ray imaging covers most of the SXDF fields. The X-ray observation details are described in Ueda et al. 2008. The limiting fluxes are 1×10^{-15} erg^{-1} cm^{-2} s^{-1} in the soft band (0.5-2.0 keV) and 3×10^{-15} erg^{-1} cm^{-2} s^{-1} in the hard band (2.0-10.0 keV).

3.3 Spectroscopic observations

Follow-up spectroscopic observations to identify transients and obtain redshifts were taken during the survey in 2002. The follow-up was done with several ground-based 8-10m telescopes and the ACS grism on HST and is described in Lidman et al. 2005, Morokuma et al. 2010 and Suzuki et al. 2012. Given the large number of transients, priority was given to transients that were likely to be SNe Ia at z $>$ 1. A number of factors

went into computing the priority: the significance of the detection, the percentage increase in the brightness, the distance from the centre of the apparent host, the brightness of the candidate and the quality of the subtrac- tion (the follow-up procedure is summarized in Lidman et al. 2005). In total, 8 transients, half of which are beyond $z = 1$, were classified as SN Ia. In later years, additional spectroscopic observations were taken with FOCAS on Subaru to obtain redshifts of host galaxies after the transients had faded from view.

3.4 SN candidate selection

In order to obtain a sample of SNe Ia we have selected variable objects from our multi-epoch data and then applied a series of procedures to further purify the sample. The first such procedure consists of lightcurve fitting to reject objects whose lightcurves are inconsistent with an SN Ia. This procedures can be applied to all candidates. Additional procedures make use of color, spectroscopic and additional information available for subsamples of the full sample to further cull the sample. These procedures are now described in detail.

The details of the initial selection of variable objects in the SXDF are described in detail by Morokuma et al. 2008. In brief, we use an imaging subtraction method introduced by Alard & Lupton 1998 and developed by Alard 2000, which enables us to match one image against another image with a different PSF. We can then detect and measure variable objects in the subtracted images. This method is applied for all possible pairs of stacked images at different epochs. In the subtracted images, we select objects having a flux greater than $5\sigma_b$ in an aperture of 2 arcsecond in diameter, where σ_b is the background fluctuation within an aperture of this size. A total of 1040 variable objects were detected. The procedure to select SN candidates from 1040 variable objects is illustrated in Figure 3.2. We are selecting supernovae that occurred in 2002; since supernovae light curves last only a few months, there should be no variability detected in 2003 or 2005. Of 1040 variable objects, only 371 did not show variability (above $5\sigma_b$) in 2003 and 2005. These 371 objects are classified as transients. For computing light curves, we then assume that there is no flux from the transient in images taken from 2003 onwards. Finally, we require that objects show at least a $5\sigma_b$ increase in 2 or more epochs in the i'-band. If a variable object is only detected in one epoch, the object might be a false detection due to galaxy missubtraction, or another kind of transient phenomenon. Note that this requirement is accounted for in the rate calculation during the calculation of the control time (section 5.1).

We applied one further consideration at this stage; at redshift $z \sim 1.4$, the central wavelength of the Suprime-Cam i' band corresponds a rest-frame wavelength of ∼3250Å. The properties of supernovae, of all types, are not well characterized over this wavelength region, limiting the effectiveness of non-spectroscopic classification methods. For this reason we remove 5 objects whose spectroscopic redshift are $z > 1.4$. However, we also note that it is still possible to detect a SN Ia with $z > 1.4$ (see section 4.2 for a possible candidate). After this stage, 141 variable objects remain as SN candidates.

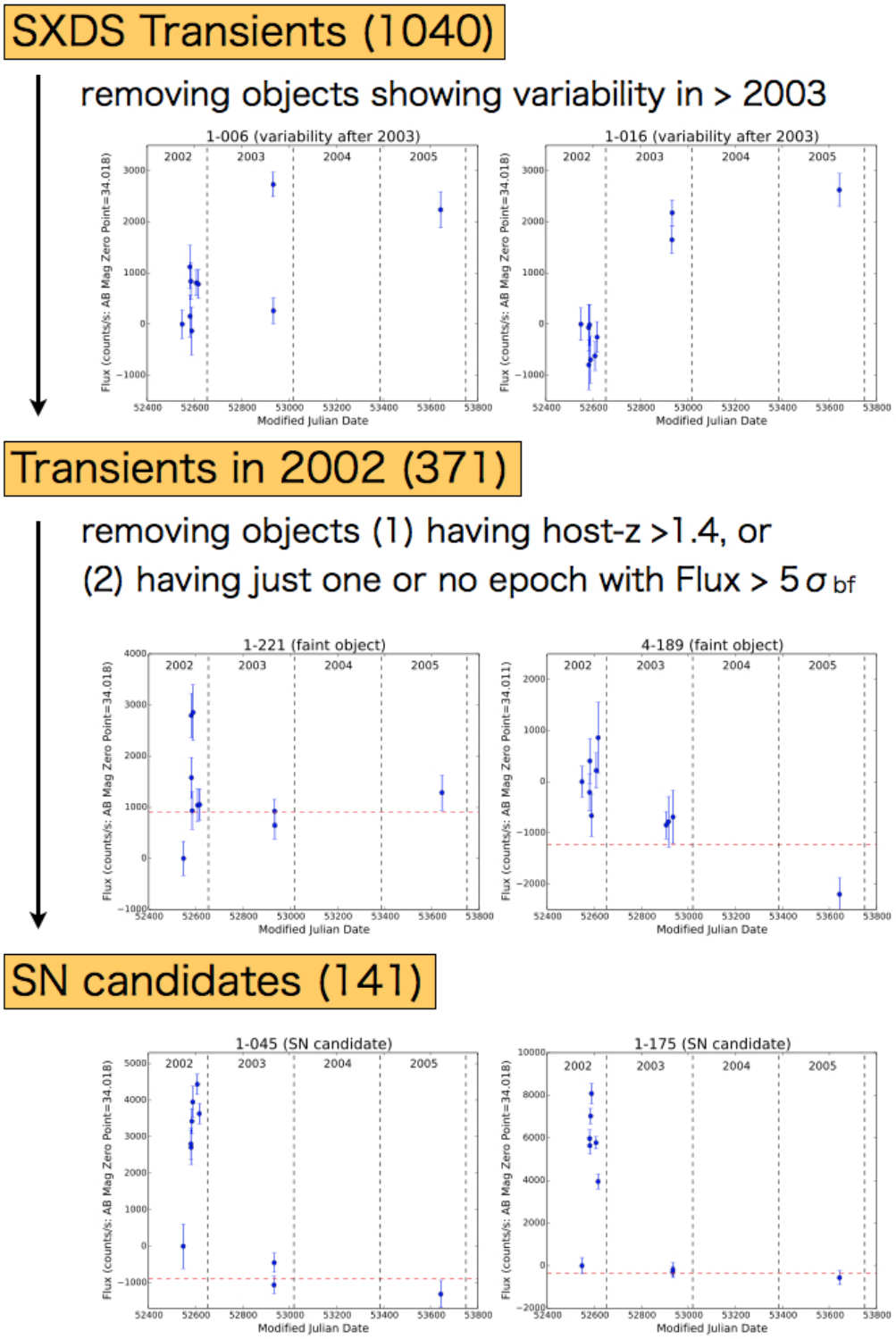

Figure 3.2: The flow chart of the SN candidate selection. Starting with 1040 SXDS transients, objects showing variability after 2003 are removed. Then high-z objects ($z_{ph} > 1.4$) and faint objects (having just one or no epoch with flux $> 5\sigma_b$). Finally, 141 SN candidates are selected. For each phase, two lightcurves are shown as examples. Horizontal red dashed line represents the zero flux measurement by taking the weighted mean of the data points later than 2003.

3.5 Host galaxy redshifts

Although we would need spectra of both host galaxies and supernovae in order to identify host galaxies with absolute certainty, here we simply identify the galaxy closest on the sky to each SN candidate as its host Morokuma et al. 2008. The stacked images of SXDF are much deeper than the individual images, which enables us to detect a reliable host galaxy for every SN candidate. Of the 141 host galaxies, only 22 have a spectroscopic redshift. Redshifts for the SN host galaxies without spectroscopic redshifts are derived from photometric redshifts of the host galaxies using the multi-color photometric dataset of SXDS. The stacked images from the Suprime-Cam observations have depths of $B = 28.4$, $V = 27.8$, $R_c = 27.7$, $i' = 27.7$, and $z' = 26.6$ (3σ, 2 arcsecond diameter aperture; Furusawa et al. 2008).

Photometric redshifts are calculated using this 10 band dataset. Photometric redshift calculations are performed using the publicly available code *LePhare* (Arnouts et al. 1999, Ilbert et al. 2006. We fit our B, V, R_c, i' z', J, H, K, $3.6\mu m$, $4.5\mu m$ host magnitudes with spectral energy distributions (SEDs) from PEGASE2 (Fioc & Rocca-Volmerange 1997, Fioc & Rocca-Volmerange 1999) stellar population synthesis models. We use the initial mass function of Scalo 1986 and 15 models for star formation (SF) history. These include a constant star formation rate (SFR) scenario, starburst scenario, and star formation history having an exponentially decaying SFR with exponential time scales of $\tau_{\rm SF} = 0.1$, 0.3, 0.5, 0.7, 1, 2, 3, 5, 7, 9, 10, 15, and 20 Gyrs.

To test the reliability of the photometric redshifts (z_{ph}), we use 786 SXDS galaxies that have both a photometric redshift and a spectroscopic one. The comparison is shown in Figure 3.3. The reliability depends on the redshift range and the undertainty of the host-galaxy photometry. Most galaxies ($\gtrsim 80\%$) are in the range $-0.1 < (z_{sp} - z_{ph})/z_{ph} < 0.2$. Since our work concentrates on the determination of SN Ia redshifts, we use the probability distribution function (PDF) of the host galaxy redshift when classifying its type and redshift.

It is possible that some host associations are erroneous, which could result in the rejection of a bona fide SN Ia due to an error in the lightcurve timescale. An erroneous association between objects with similar redshifts — such as those in the same group or cluster — is not of concern here. To check for possible host galaxy misidentification, for the objects which we later classify as SN Ia we show in Figure 4.6 the distribution of separations between the SN and the center of its designated host galaxy. According to Yasuda & Fukugita 2010, the radial distribution of SNe Ia is nearly consistent with the luminosity profiles of their host galaxies. In the case of our SXDS candidates, a Kolmogorov-Smirnov test finds the distribution of the SN Ia candidates to be consistent with the luminosity profiles of galaxies (Yasuda & Fukugita 2010). Therefore, we assume that erroneous host associations are unimportant for the present analysis.

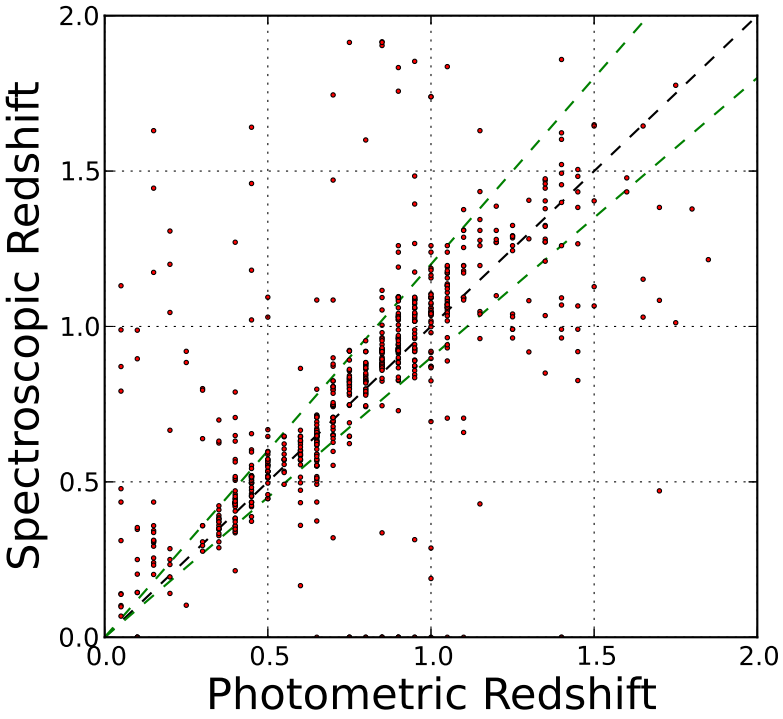

Figure 3.3: Spectroscopic redshifts (z_{sp}) versus photometric redshifts (z_{ph}) of SXDS galaxies. The green dashed lines indicate the region bounding $-0.1 < (z_{sp} - z_{ph})/z_{ph} < 0.2$.

Table 3.1: Summary of Suprime-Cam photometry

Field	Epoch	Date (UT)[a]	Δt[b]	t_{exp} [sec]	Seeing ["][c]	m_{lim}[d]
			i'-band			
SXDF-C	1	02/09/29,30	0.0	2700	0.54	26.19
SXDF-C	2	02/11/01	32.6	1860	0.92	25.76
SXDF-C	3	02/11/02	33.5	1800	0.68	25.85
SXDF-C	4	02/11/05	36.7	2400	0.70	26.11
SXDF-C	5	02/11/09	40.5	2460	0.60	25.77
SXDF-C	6	02/11/27,29	59.8	4200	0.72	26.38
SXDF-C	7	02/12/07	68.4	3000	0.78	26.32
SXDF-C	8	03/10/20	385.7	5760	1.14	26.53
SXDF-C	9	03/10/21	386.5	7500	0.58	26.71
SXDF-C	10	05/09/28	1094.6	3600	1.00	26.04
SXDF-N	1	02/09/29,30	0.0	3300	0.56	26.26
SXDF-N	2	02/11/01	32.4	2640	0.96	25.88
SXDF-N	3	02/11/02	33.3	1800	0.68	25.86
SXDF-N	4	02/11/09	40.3	2100	0.64	25.78
SXDF-N	5	02/11/29	60.3	3300	0.74	26.27
SXDF-N	6	03/09/22	357.5	4264	0.60	26.37
SXDF-N	7	03/10/02	367.6	1500	0.70	25.88
SXDF-N	8	03/10/21	386.5	3000	0.72	26.14
SXDF-S	1	02/09/29,30	0.0	3300	0.52	26.28
SXDF-S	2	02/11/01	32.5	3600	1.04	25.91
SXDF-S	3	02/11/02	33.4	1800	0.70	25.83
SXDF-S	4	02/11/09	40.4	2580	0.66	25.60
SXDF-S	5	02/11/29	60.6	1500	0.82	26.00
SXDF-S	6	03/09/22	357.6	4500	0.54	26.45
SXDF-S	7	03/10/02	367.7	2040	0.68	26.00
SXDF-S	8	05/09/28	1094.6	3900	0.96	26.04
SXDF-E	1	02/09/29,30	0.0	3300	0.60	26.25
SXDF-E	2	02/11/01	32.5	3000	1.04	25.97
SXDF-E	3	02/11/02	33.4	1800	0.70	25.83
SXDF-E	4	02/11/09	40.4	2820	0.66	26.78
SXDF-E	5	02/11/29	60.6	1800	0.80	26.03
SXDF-E	6	02/12/07	68.6	1209	1.54	25.19
SXDF-E	7	03/09/22	357.6	6000	0.62	26.58
SXDF-E	8	03/10/02	367.7	1271	0.68	25.71
SXDF-E	9	03/10/21	386.7	1400	0.88	25.51
SXDF-E	10	05/09/28	1094.6	3600	0.96	26.11

[a] Observed date in yy/mm/dd. When the images were stacked together, all dates for observations are included.

[b] Days from the first observation in each field.

[c] FWHM of PSF in stacked images.

[d] Limiting magnitude of 5σ in 2.0 arcsec aperture.

Table 3.1: Summary of Suprime-Cam photometry

Field	Epoch	Date (UT)[a]	Δt[b]	t_{exp} [sec]	Seeing ["][c]	m_{lim}[d]
SXDF-W	1	02/09/29,30	0.0	2400	0.54	26.14
SXDF-W	2	02/11/01	32.7	3000	0.96	25.96
SXDF-W	3	02/11/02	33.5	1800	0.66	25.84
SXDF-W	4	02/11/05	36.8	3060	0.76	25.98
SXDF-W	5	02/11/09	40.5	2100	0.64	25.97
SXDF-W	6	02/11/27,29	59.8	4200	0.74	26.39
SXDF-W	7	02/12/07	68.5	6483	1.04	26.34
SXDF-W	8	03/10/20,21	386.5	5460	0.66	26.46
			R_c-band			
SXDF-N	1	02/11/01	32.5	2400	0.85	26.37
SXDF-N	2	02/11/09	40.5	1920	0.81	26.02
SXDF-N	3	08/01/09	1927.3	2400	0.79	26.41
SXDF-S	1	02/11/01	32.6	2400	0.83	26.32
SXDF-S	2	02/11/09	40.6	1920	0.71	26.29
SXDF-S	3	08/01/09	1927.4	2400	0.69	26.52
SXDF-E	1	02/11/01	33.6	2400	0.89	26.26
SXDF-E	2	02/11/09	40.6	1920	0.87	26.12
SXDF-E	3	08/01/09	1927.4	2400	0.73	26.46
SXDF-W	1	02/11/01	33.7	3360	0.91	26.27
SXDF-W	2	02/11/09	40.7	1920	0.65	25.92
SXDF-W	3	08/01/09	1927.5	2400	0.81	26.33
			z'-band			
SXDF-N	1	02/11/04	35.3	2400	0.81	25.16
SXDF-N	2	02/11/05	36.2	600	0.79	24.22
SXDF-N	3	02/11/10	41.3	2340	1.03	24.93
SXDF-N	4	03/09/27	362.4	4860	0.71	25.99
SXDF-S	1	02/11/04	35.4	2400	0.77	25.11
SXDF-S	2	02/11/05	36.3	600	0.81	24.18
SXDF-S	3	02/11/10	41.4	2700	0.85	24.97
SXDF-S	4	03/09/22	357.7	4800	0.69	25.61
SXDF-E	1	02/11/04	35.4	2280	0.71	25.26
SXDF-E	2	02/11/05	36.3	1200	1.07	24.42
SXDF-E	3	02/11/10	41.4	4440	0.85	25.32
SXDF-E	4	03/09/26	361.5	4800	0.69	25.81
SXDF-W	1	02/11/04	35.6	2700	0.81	25.19
SXDF-W	2	02/11/05	36.4	750	0.75	24.37
SXDF-W	3	02/11/10	41.6	6210	1.05	25.41
SXDF-W	4	03/09/27	362.4	4800	0.69	25.92

[a] Observed date in yy/mm/dd. When the images were stacked together, all dates for observations are included.

[b] Days from the first observation in each field.

[c] FWHM of PSF in stacked images.

[d] Limiting magnitude of 5σ in 2.0 arcsec aperture.

If you don't know where you are going, any road will get you there.

Lewis Carroll (1832 - 1898)

4 Sample Refinement

4.1 Overview of the sample refinement

Among 1040 SXDS transients, 141 SN candidates are finally sampled in chapter 3. These objects, as noted in the previous chapter, have at least two epochs with flux greater than $5\sigma_b$ in i'-band. In this chapter, we introduces the method to construct SN Ia sample from 141 SN candidates. The refinements mainly consist of two parts. First, since light curves of SNe II differ from those of SNe Ia, SNe II are discriminated by single-band (i') lightcurve fitting (section 4.2). Though SNe II can be removed easily by single-band lightcurves, SNe Ibc are hard to discriminate due to the resemblance of light curves with SN Ia. Thus, we exploited subsample which other broad-band photometries (R_c, z') are available to safely estimate the number of possible SNe Ibc(section 4.4). Finally, 39 SN Ia candidates are sampled and their properties are tested in section 4.5. These refinement procedure is shown in Figure 4.1.

4.2 Discriminating Type II SNe

The lightcurves of SNe II are generally significantly broader than those of SNe Ia or SNe Ib/c. Therefore, as a first step we distinguishes between SNe I (including Ia, Ib and Ic) and SNe II using the lightcurve shape. To do this, we compare the lightcurve of each candidate to template lightcurves of the various SN subtypes. As we will see, the lightcurves of most candidates are adequately sampled to distinguish unambiguously between SNe I and SNe II. Where available, we use the spectroscopic redshift of the SN or host galaxy in the light-curve fitting. Where there is only a photometric redshift available, we use the PDF of the host galaxy calculated by *LePhare* as a redshift prior.

We construct SN Ia and SN II template lightcurves in the observed i'-band using K-corrections derived from the spectral time-series templates of Hsiao et al. 2007 and Nugent et al. 2002. The shape of various SN Ia lightcurves can be well-represented by a single

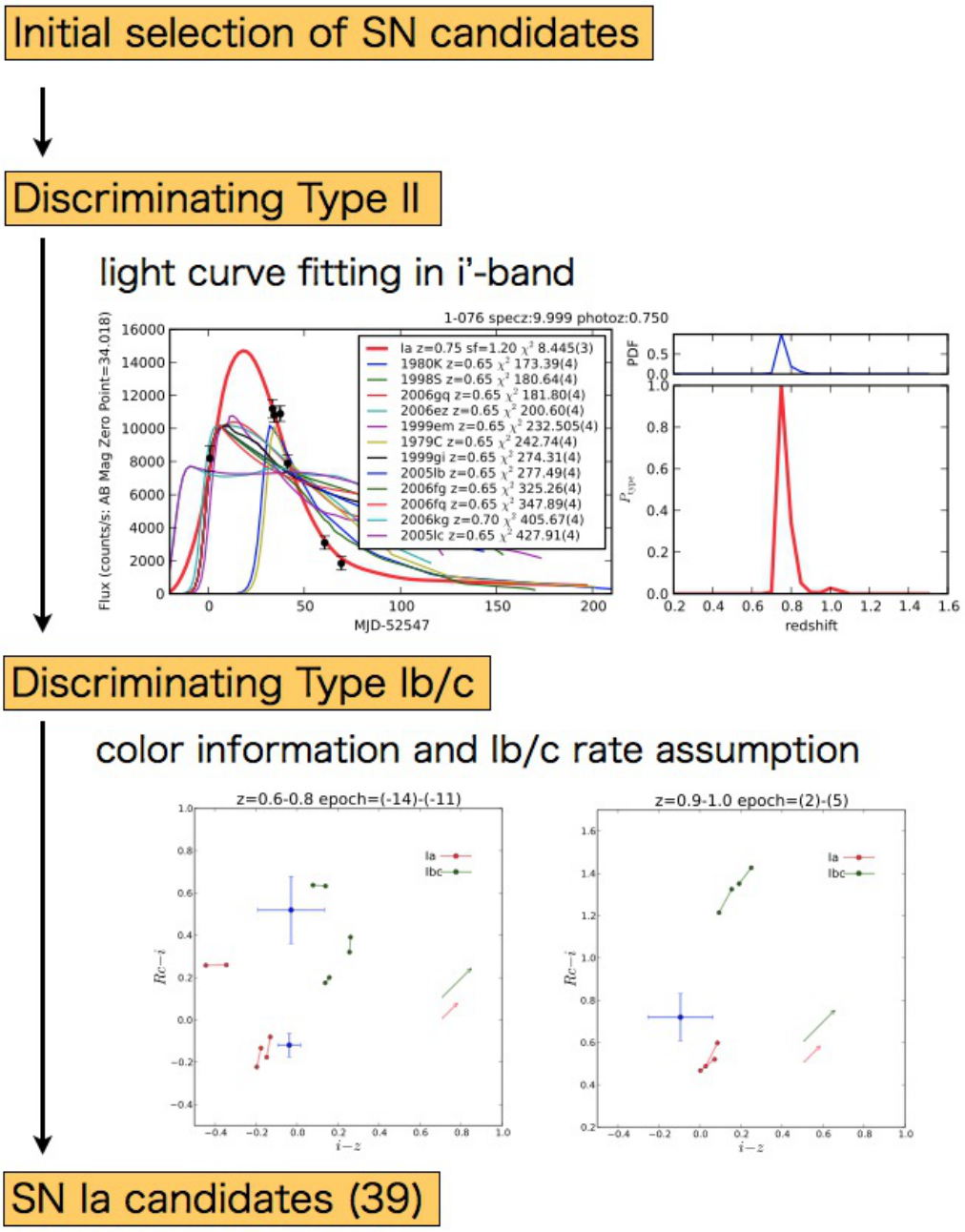

Figure 4.1: The flow chart of the sample refinements. Since the SN classification has a bias, we need to correct the number of SNe Ia identified by their light curves using artificial light curves made by the Monte Carlo simulations.

template and a stretch factor (Perlmutter et al. 1997). For the SN Ia lightcurves we perform K-corrections with the spectral template of Hsiao et al. 2007. This template accurately describes the UV features of SNe Ia, which is particularly important for high-redshift SNe Ia. SN Ia lightcurve shape diversity can be neglected as it has been shown to be small compared to the difference between SNe Ia and SNe II lightcurve shapes (Takanashi et al. 2008). The time series of spectral template are converted to magnitudes using following formula:

$$\begin{aligned} m_{\rm AB}(R) &= -2.5\log_{10}\frac{\int f_\nu \frac{R}{\nu}d\nu}{\int \frac{R}{\nu}d\nu} - 2.5\log_{10}(3631{\rm Jy}) + \mu(z) \\ &= -2.5\log_{10}\frac{\int \lambda f_\lambda R d\lambda}{\int \frac{R}{\lambda}d\lambda} - 2.408 + \mu(z), \end{aligned} \tag{4.1}$$

where R is the filterpass, $f_{\lambda,\nu}$ is the observed flux, and μ is distance modulus at redshift z.

In contrast to SNe Ia, it is impossible to describe SNe II with only one template. Type II SNe can be divided into several subtypes (e.g., IIP, IIL and IIn) each of which exhibits a broadly different light-curve shape. Even within subtypes there is significant light-curve shape diversity. Therefore, we use a set of 12 well-observed SN II light curves as templates. Our observed SNe II consist of 5 of the best-observed published SNe II and 7 SNe II from the SDSS-II SN survey (Sako et al. 2008). In total, the SDSS-II SN survey observed more than 50 SNe II over three years. The 7 used here are selected based on their discovery at an early phase and many repeat observations ($>$ 10) with long time coverage ($\sim$60 days) in the SDSS u'-, g'-, and r'-bands. Details for the 12 SNe II used as templates are listed in Table 4.1. For each candidate, an i'-band template light curve is made by K-correcting the observed multi-band photometry to the redshift of the candidate, using the templates of Nugent et al. 2002. Generally, the observed SN II light curves lack data points during their rising phase due to the rapid increase to maximum after explosion. Thus, we also use the Nugent et al. 2002 templates to interpolate the rising phase of the light curve. Example template light curves for Type Ia and II SNe are shown in Figure 4.2.

Using the observed i'-band light curve of each SXDS SN candidate, we perform the following fitting method to refine candidates.

First, we use the probability of being a certain type of SN as a function of redshift using the following formula:

$$P_{\rm type}(z) \propto PDF(z) \times \exp\left\{-\frac{\chi^2_{\rm LC}(z)}{2}\right\} \tag{4.2}$$

Here, $PDF(z)$ is the probability function derived by *LePhare*, and $\chi^2_{\rm LC}$ is the χ^2 calculated by light curve (LC) fitting.

$$\chi^2_{\rm LC}(z) = \sum_{k=1}^{n}\left\{\frac{f_{obs} - f_{temp}(z)}{\Delta f_{obs}}\right\}^2, \tag{4.3}$$

where f_{obs} is the observed i'-band flux, Δf_{obs} is the observational error, $f_{temp}(z)$ is the i'-band flux of the template light curve at redshift z, and n is the number of observing epochs during 2002: 7 in SXDF-C and SXDF-W, 6 in SXDF-E, and 5 in SXDF-N and SXDF-S. Note that $f_{temp}(z)$ represents a set of templates of SNe of different types. In the light-curve fit, the free parameters on the template light curve are the peak magnitude, the date at peak

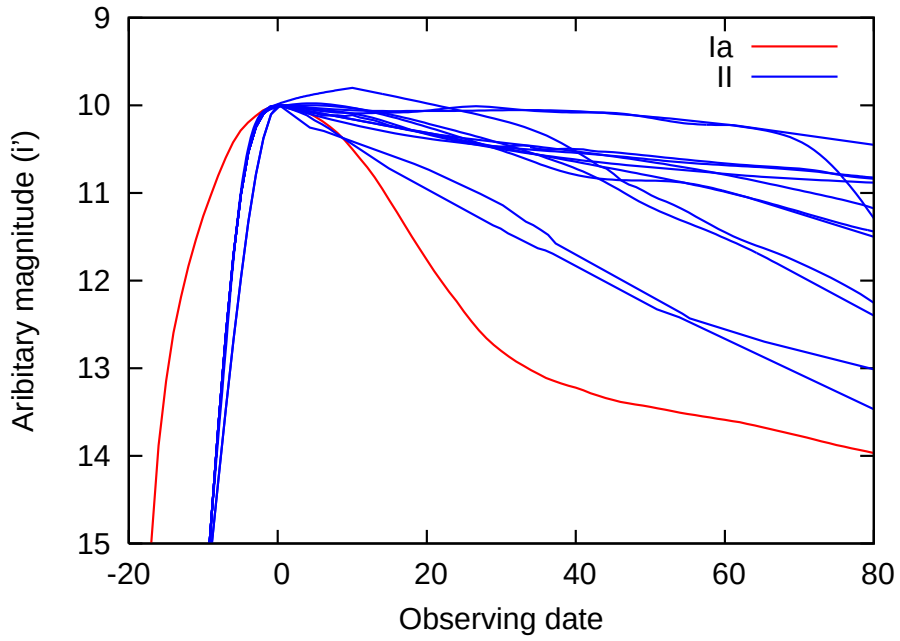

Figure 4.2: Examples of light curve templates in the observed i'-band: A single SN Ia template at $z = 0.9$ (*red line*) and 12 SN II templates at $z = 0.5$ (*blue lines*) are shown.

brightness, the stretch factor, and the redshift. Then we calculate the value of $\chi^2_{\rm LC}$ for each SN template. The date at peak brightness is allowed to vary between day -10 and 70 where day 0 corresponds to the beginning date of the SXDS variable object survey (September 30, 2002). The stretch factor is only used in fitting the Type Ia template. It is constrained to the range $0.75 - 1.2$ and moves independently of peak magnitude. For SNe Ia templates, the B-band absolute magnitude is allowed to vary in the range $-20.0 < M_B < -17.5$. This magnitude range is based on the range of the real SN Ia distribution observed in the SDSS-II SN survey (Dilday et al. 2008). For SNe II templates, the V-band absolute magnitude is allowed to vary in the range $-19.0 < M_V < -15.0$. As for SNe Ia, this range is based on the distribution of SNe II in the SDSS-II SN survey (see Figure 5.4). In all cases, the absolute magnitude is converted to an observed i'-band magnitude using the luminosity distance and a K-correction with the appropriate spectral template (Hsiao et al. 2007 and Nugent et al. 2002). For SNe having spectroscopic redshifts, the redshift is fixed, and f_{temp} is calculated by K-correcting the light-curve template to that redshift.

We determine the SN type by inspecting the value of $P_{\rm type}(z)$. If the $P_{\rm type}(z)$ obtained by fitting the SN Ia template is greater than that obtained by fitting any of the SN II templates, the candidate is classified as a SN I. In order to remove candidates that are neither SNe I nor II (i.e., AGN or other variable objects), we also require that the $\chi^2/d.o.f.$ for the SN I template be lower than 5. Based on the simulation of completeness (section 6), 98.4% of real SNe Ia will satisfy this requirement.

Using this method, we classify 44 of the 141 candidates as SNe I. Though our control time shows a sharp drop off by $z \sim 1.4$, one object (1-081) has been classified as SN Ia

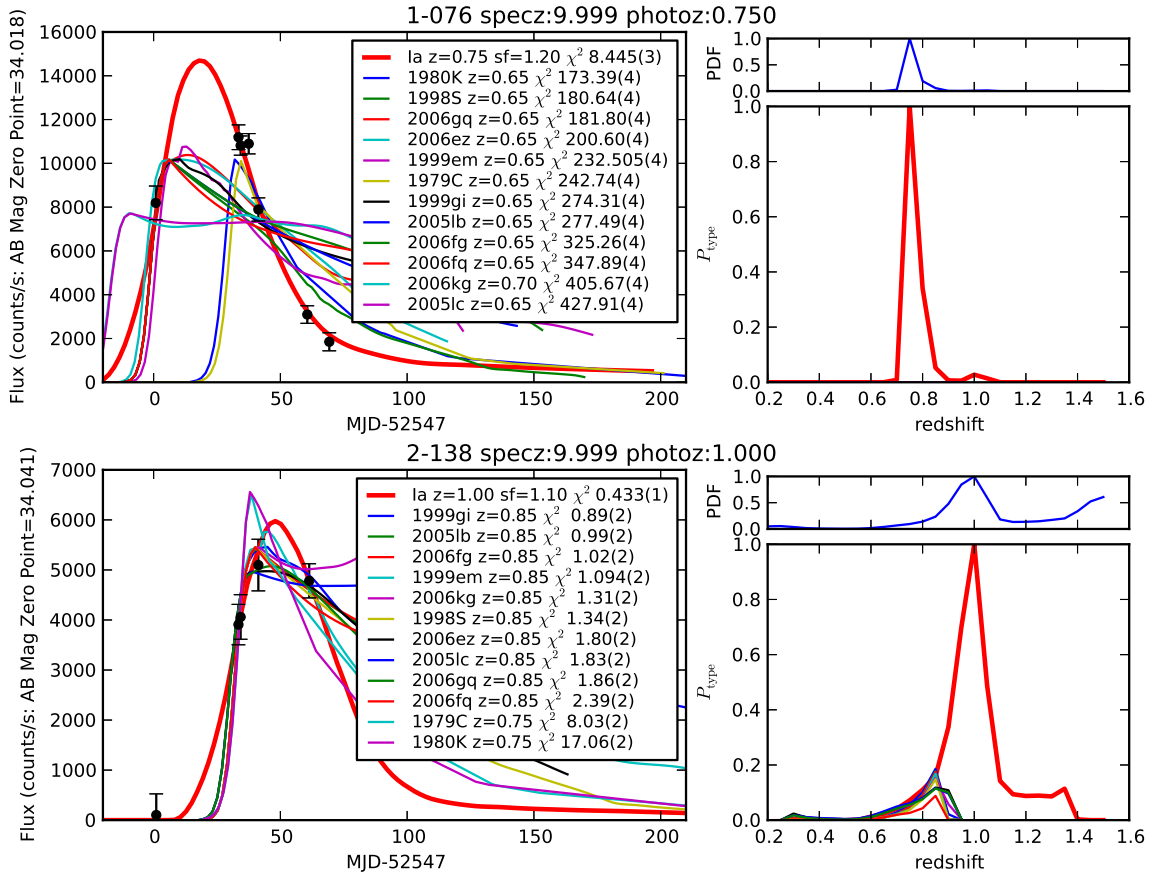

Figure 4.3: Two examples demonstrating the method we use to classify SNe (see appendix A for whole sample). On the left, we show the best fits using the templates used in this paper. The numbers in the parenthesis are reduced χ^2 values. The right-hand plots show the PDFs of the host galaxies and the normalized $P_{\rm type}$ as a function of redshift. The best fit for the object in the upper panels is a SN Ia at $z = 0.75$. This is a typical case. The object in the lower panels is an example of an object that has a type that is less clear. Though this object is best fit with a SN Ia template, the $P_{\rm type}$ distribution shows that SNe II are possible. However, the signature of SN Ia is still strong here and the object is classified as a SN Ia in our sample. The possible contamination of SN II from the fitting is taken into account (see section 5).

at $z = 1.45$ with $M_B = -19.53$. It is possible to detect a SN Ia with $z > 1.4$ if our observations cover at least two epochs around the maximum (see Figure 5.5). However, we do not include this object in the rate calculation and use only the 44 SNe Ia having $z < 1.4$. Examples of template light-curve fits are shown in Figure 4.3. Although we expect this method to distinguish between SNe I and II with good reliability (see following section), due to statistical fluctuations the classification will not be perfect. Therefore, we estimate and correct for completeness and SN II contamination in section 6.

4.3 Discriminating AGN

Another potential source of contamination are AGN that pass our variability cuts. X-ray detection is useful in confirming whether or not variable objects are AGN. Out of 43 SN Ia candidates, 42 objects were observed with XMM-Newton at some observation phase of SXDS, and only two object are detected in X-ray. This X-ray detection ratio is almost the same as the ratio of AGN to general galaxies (M08). Thus, the one object detected in X-ray might be supernova that occurred in a galaxy hosting an AGN.

We have a spectrum of one of the transients associated with an X-ray source, object 3-202 (SuF02-061). The spectrum exhibits an [Ne III] λ3869 emission line, suggesting the possibility of an AGN. [O II]$\lambda\lambda$3727 and Hδ are also detected. From these lines, we derive [Ne III]/H$\delta \sim 0.35$ and [O II]/H$\delta \sim 0.61$, which are consistent with either an AGN or starburst origin (Rola et al. 1997, Pérez-Montero et al. 2007).

Tests performed on the spectrum indicate that, had object 3-202 been a SN Ia, we would have detected the SN Ia features. Object 3-202 is also very close to the core of its host galaxy, as expected for an AGN. The offset is 0.19 pixels (0"04), which is larger than our expected measurement uncertainty. Thus, while we are unable to rule out the possibility of a SN Ib/c associated with a starburst, with this evidence we can conclusively reject the possibility that this object is a Type Ia SN.

We also reject object 1-143, due to the likelihood that it is an AGN. Unlike 3-202, we do not have a spectrum of object 1-143; however, it is detected in the X-rays and is closer to the core of its host galaxy than any other candidate.

X-ray observations are usually powerful tools to detect AGN, however not all AGN have X-ray detections and faint AGN populations are not traced by X-ray observations (M08). Since objects 3-202 and 1-143 passed the lightcurve test but are likely AGN, we may ask whether there are other such cases of AGN undetected by X-rays in our sample. Only one other object, 4-203, is as close to the core of its host as objects 3-202 and 1-143 are to theirs. If this was an AGN as well, our sample would have a deficit in the number of SNe Ia near core, so we deem it likely that this object is not an AGN.

4.4 Discriminating Type Ib/c SNe

At ths point we have 41 SN Ia candidates based on their light-curve shapes. It is impossible to further classify candidates into SNe Ia and Ib/c without additional data because the shapes

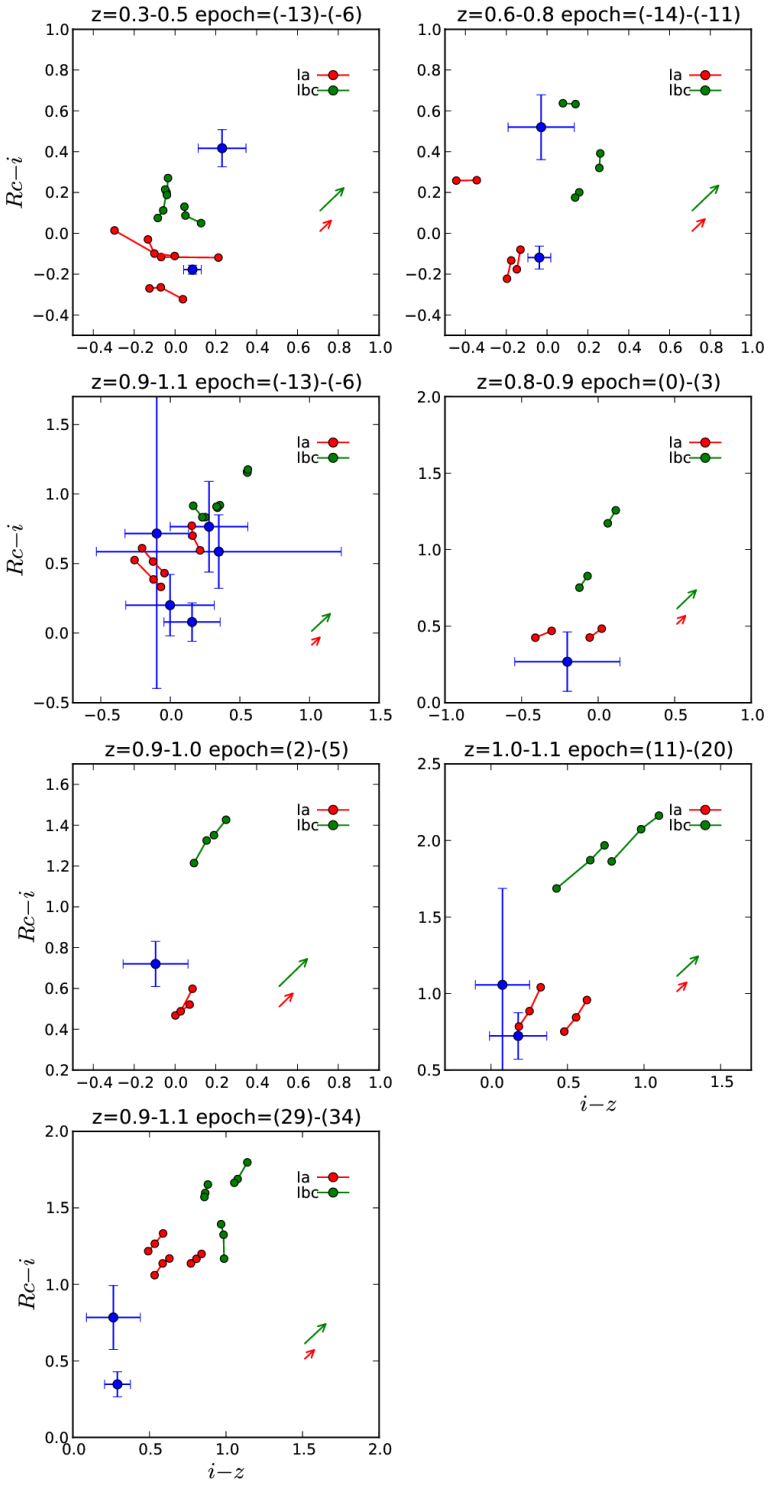

Figure 4.4: The color-color diagrams of SN I candidates in the observer frame. The *red lines* and *green lines* indicate the expected colors of unreddened SNe Ia and SNe Ib/c respectively at the given redshift. The points connected by the lines indicate the values at specific epochs in the epoch range given. Red and green arrows indicate average reddening of supernovae from their host galaxies: $A_B = 0.4$ for SNe Ia (Wang et al. 2006) and $A_B = 0.7$ for SNe Ib/c (Richardson et al. 2006). Blue circles show the colors of the SN I candidates in SXDS. Out of 15 candidates, two candidates have colors most similar to SNe Ib/c.

of SN Ia and Ib/c lightcurves are quite similar. Although SNe Ib/c are rarer events than SNe Ia, we expect that the classified SNe I will include a few SNe Ib/c.

In our observation, some transients were observed in R_c- and $z'-$bands. We make use of this photometry to discriminate SNe Ib/c from SNe Ia based on color information ($R_c - i'$ vs $i' - z'$); 14 of the remaining SNe I candidates have this color information. The AGN 3-202 also has a color measurement, as do 2 of the 8 spectroscopically-confirmed SNe Ia. We construct color-color diagrams of the candidates at each redshift and epoch where the colors are available (Figure 4.4). The color models of SNe Ia and Ib/c are obtained from the templates of Hsiao et al. 2007 and Nugent et al. 2002, respectively. We assume an average reddening from SN host galaxies and show the reddening as arrows on Figure 4.4. SN Ia candidates are grouped by similar redshift and epoch so that we can compare the expected SN Ia/Ibc colors and those of candidates.

Using Figure 4.4, we estimate that 2 out of the 14 remaining candidates have a color incompatible with SNe Ia. These objects, 2-038 and 4-100, are therefore rejected from the sample. Possible contamination of SN Ib/c on the rest of the sample is discussed in section 6.3 as a systematic uncertainties.

4.5 Properties of SN Ia candidates

We can use the small subset of the candidates that are spectroscopically confirmed SNe Ia as a basic consistency check. All 8 spectroscopically confirmed SNe Ia and probable SNe Ia (Ia*) found during the SXDS are classified as SNe I by the lightcurve fitting. All the fitting results are summarized in Table 4.2 and appendix A

Although the 39 SN Ia candidates will have some contamination from SNe II (estimated in section 6) and SNe Ib/c (section 6.3), we expect most of them to be SNe Ia. We can check that most of the 39 SN I candidates have properties broadly consistent with SNe Ia. The best fit lightcurve parameters for each of the 39 candidates are shown in Table 4.2. We note that the uncertainty in these parameters is often large, particularly for candidates lacking a spectroscopic redshift. This is not a problem however, as we are concerned with the broad light-curve characteristics of the sample as a whole rather than an precise determination of the light-curve parameters of any single SN. We discuss the distribution of absolute magnitude, lightcurve width, and host galaxy separation for the candidates.

Absolute magnitude. The distribution of the candidates' $B-$band absolute magnitudes (uncorrected for host galaxy extinction) is shown in Figure 4.5 (top). The distribution peaks around $M_B \sim -19.0$, the expected average magnitude of SNe Ia. The expected distribution of SN Ia magnitudes from this survey (based on the simulations described in section 5) is shown as a dotted line. There appears to be an overabundance of faint candidates, possibly due to contamination from SNe II. The lower panel of Figure 4.5 shows where the excess lies in redshift – the excess faint candidates are found mainly at lower redshift ($z < 0.8$). Note that the simulated expected distribution (green contours) takes into account the shift in the distribution of SNe toward higher luminosity and larger stretch with redshift (e.g., Howell et al. 2007). As a result, the top of the green contours slopes up with redshift.

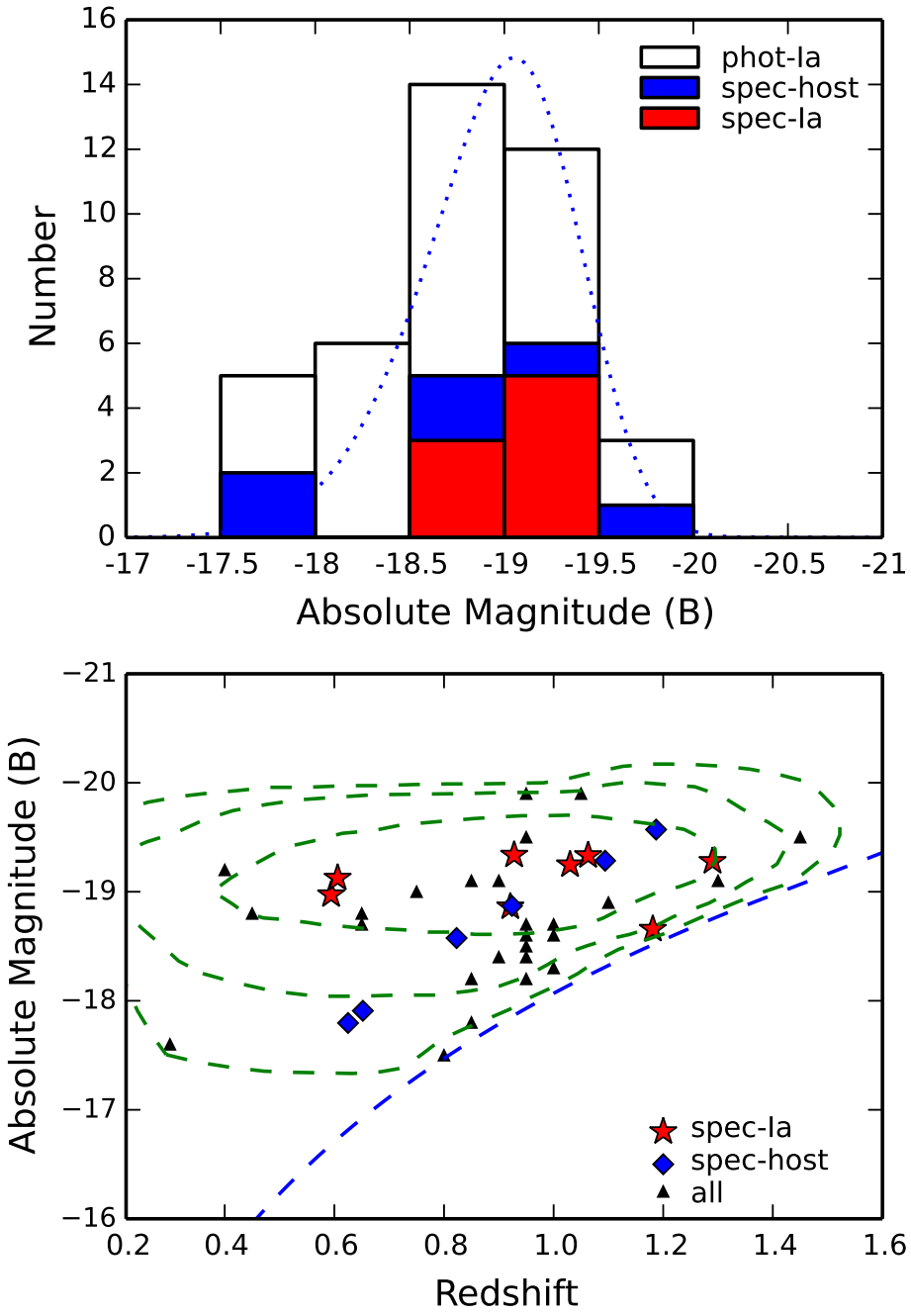

Figure 4.5: The observed peak magnitude distribution of SNe Ia candidates in our SXDF sample. The *top figure* shows the number distribution. Spectroscopically-confirmed SN Ia, not spectroscopically-confirmed SN Ia but objects with spectroscopic redshifts from host galaxies, and other SN Ia candidates are plotted as red, blue and open histograms, respectively The *bottom figure* shows the redshift distribution of the SN Ia candidates. In the bottom figure, the *red stars* describe the SNe Ia SNe confirmed by spectroscopic observations, the *blue diamonds* describe the candidates with spectroscopic redshifts from their host galaxies, and the *black triangles* describe the remaining SN Ia candidates. The *blue dotted line* describes the limiting magnitude of the SXDS observations. The *green contours* show the 1-, 2- and 3-σ confidence intervals for the distribution of a pure SN Ia sample calculated using the methods and SN rates from section 5.

Light curve width. Since our lightcurve fitting is based on at most seven epochs, constraining the light curve width (stretch parameter) is challenging compared to other parameters, e.g., M_B, and the day of maximum. Their errors are very large ($\Delta s \sim 0.1 - 0.2$). Furthermore, our stretch factors in Table 4.2 are not B-band stretch factors but observed $i'-$band stretch factors, which correspond to other rest-frame bands depending on redshift. This is not a problem here, however, since we are employing light curve fitting only to determine type and redshift. The observer-frame i'-band stretch distribution contains a broad peak around $s \sim 1$, which is the consistent with observations of nearby SNe Ia. At the same time, we found that some faint objects have large stretches ($s \sim 1.2$), though we expect large stretches for luminous objects. Some of these objects might be misclassified SNe II. We estimate the rate of misclassified SNe II in section 6.3.

Host galaxy separation. To check for possible host galaxy misidentification, we show the distribution of the distance from each candidate to the center of its designed host galaxy (Figure 4.6). According to Yasuda & Fukugita 2010, the radial distribution of SNe Ia is nearly consistent with the luminosity profiles of their host galaxies. In the case of our SXDS candidates, a Kolmogorov-Smirnov test finds the distribution of the SN I candidates to be consistent with the luminosity profiles of galaxies.

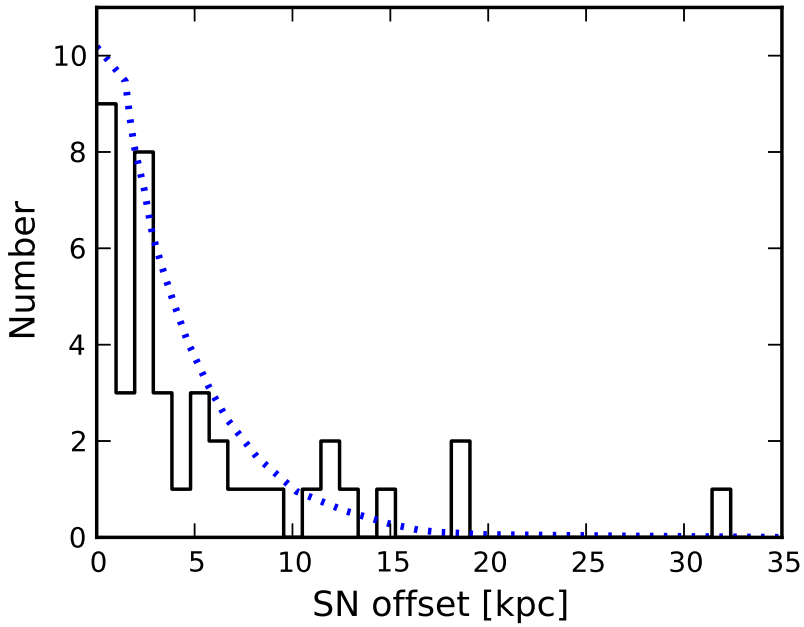

Figure 4.6: The distribution of distance between candidate and host galaxy center for the SN I candidates. The *black solid line* indicates the distribution of SN I candidates and the *blue dotted line* indicates the luminosity profiles of galaxies (Yasuda & Fukugita 2010).

4.6 The estimated number of observed SN Ia

To count the estimated number of observed SNe Ia (N_{est}), the easiest way might be to use the best-fit redshift derived from the fitting. However, some SN Ia candidates have large host photo-z uncertainties (see bottom right panel of Figure 4.3 for an example). Instead, we allocate the number of SN Ia according to their P_{type} distributions. For example, in the case of 2-138 illustrated in Figure 4.3, we allocate a fractional contribution of 0.55 to the $0.6 < z < 1.0$ bin and 0.45 to the $1.0 < z < 1.4$ bin. These allocations are summarized in Table 4.2, where it can be seen that the probability is concentrated in a single bin for each SN.

Table 4.1: Type II supernova templates

Name	Reference	Type	Lightcurve points
SN1979C	de Vaucouleurs et al. 1981[a]	II-L	23 (U), 32 (B), 31(V)
SN1980K	Buta 1982[b]	II-L	20 (U), 25 (B), 25 (V)
SN1998S	Fassia et al. 2000[c]	II-n	25 (B), 26 (V), 28 (R), 21 (I)
SN1999em	Leonard et al. 2002[d]	II-P	29 (U), 40 (B), 41 (V), 46 (R), 44 (I)
SN1999gi	Leonard et al. 2002[e]	II-P	29 (B), 30 (V), 30 (R), 30 (I)
SN2005lb	Sako et al. in prep.[f]	II	1 (u'), 15 (g'), 14 (r'), 12 (i'), 13 (z')
SN2005lc	Sako et al. in prep.[f]	II	20 (u'), 24 (g'), 24 (r'), 23 (i'), 25 (z')
SN2006ez	Sako et al. in prep.[f]	II	21 (u'), 21 (g'), 22 (r'), 20 (i'), 22 (z')
SN2006fg	D'Andrea et al. 2010[f]	II	13 (u'), 17 (g'), 16 (r'), 17 (i'), 19 (z')
SN2006fq	D'Andrea et al. 2010[f]	II	12 (u'), 22 (g'), 22 (r'), 21 (i'), 22 (z')
SN2006gq	D'Andrea et al. 2010[f]	II	0 (u'), 18 (g'), 16 (r'), 16 (i'), 13 (z')
SN2006kg	Sako et al. in prep.[f]	II	20 (u'), 20 (g'), 20 (r'), 20 (i'), 19 (z')

[a] 76-,91-,205-cm telescopes of the McDonald Observatory

[b] 76-,91-cm telescopes of McDonald Observatory and 1.55-m telescope of the U.S. Naval Observatory

[c] The 82-cm Instituto de AstrofoAsica de Canarias telescope (IAC80) on Tenerife, the 1.0-m Jacobus Kapteyn Telescope (JKT) on La Palma and the 3.5-m Wisconsin-Indiana-Yale-NOAO telescope (WIYN) at Kitt Peak

[d] 76-,91-,205-cm telescopes of the McDonald Observatory

[e] The Katzman Automatic Imaging Telescope (KAIT) and the 1.2-m telescope at the Fred Lawrence Whipple Observatory (FLWO)

[f] The SDSS's 2.5-meter telescope at Apache Point Observatory

Table 4.2: SN Ia candidates

Field-ID	SuF02-ID[a]	Offset[b]	RA	Dec	Host ID	z_{phot}	z_{spec}	z_{SN}[c]	The allocation of SN Ia to each bin [d]				M_B[e]	$m_{i'}$	s[f]	Day[g]
									0.2−0.6	0.6−1.0	1.0−1.4	1.4−				
1-018	SuF02-007	11.944	02:18:52.178	-05:01:13.17	iC-083788	0.85	-	0.950	0.028	0.650	0.313	0.009	-18.5	24.7	1.15	32
1-020	SuF02-012[h]2, 3	0.205	02:18:51.576	-04:47:25.97	iC-176827	1.15	1.290	1.290	-	-	1.000	-	-19.3	25.1	1.15	34
1-038	SuF02-J02	2.490	02:18:42.854	-05:04:12.50	iC-063533	0.70	0.652	0.652	-	1.000	-	-	-17.9	24.5	1.10	36
1-045	SuF02-082	4.756	02:18:40.690	-05:03:43.73	iC-065953	0.65	0.625	0.625	-	1.000	-	-	-17.8	24.5	1.20	52
1-076		7.785	02:18:31.195	-05:01:23.60	iC-081825	0.75	-	0.750	-	0.985	0.015	-	-19.0	23.6	1.20	18
1-090		3.360	02:18:22.051	-04:57:18.78	iC-107586	0.85	-	0.850	-	1.000	-	-	-18.2	24.7	1.20	14
1-120	SuF02-004	0.378	02:18:09.026	-04:54:18.71	iC-126749	1.00	1.187	1.187	-	-	1.000	-	-19.6	24.6	1.20	30
1-157		2.550	02:17:50.203	-05:03:45.62	iC-066598	0.45	-	0.450	0.993	0.007	-	-	-18.8	22.8	0.75	70
1-175	SuF02-000[h]3	2.953	02:17:42.590	-05:06:33.76	iC-049015	0.75	0.921	0.921	-	1.000	-	-	-18.9	24.2	1.15	44
1-192	SuF02-065[h]1	1.800	02:17:34.589	-05:00:16.78	iC-088216	0.58	1.181	1.181	-	-	1.000	-	-18.7	25.5	1.20	38
1-193	SuF02-060[h]1	1.044	02:17:34.565	-04:53:47.36	iC-129501	1.05	1.063	1.063	-	-	1.000	-	-19.3	24.2	1.00	44
1-202		1.496	02:17:32.114	-04:53:30.42	iC-131867	1.05	-	1.100	-	0.094	0.906	-	-18.9	24.9	0.75	52
1-203		5.611	02:17:32.160	-05:11:15.69	iC-017504	0.90	-	0.900	-	0.998	0.002	-	-19.1	24.0	1.10	0
1-242	SuF02-002	2.535	02:17:12.264	-04:55:08.82	iC-121417	0.75	0.823	0.823	-	1.000	-	-	-18.6	24.2	1.00	36
1-252		1.502	02:17:10.188	-04:50:43.91	iC-148634	0.95	-	0.950	-	0.945	0.054	-	-18.4	24.8	1.20	60
1-254		0.608	02:17:09.758	-04:57:47.89	iC-105194	0.95	-	0.950	-	0.906	0.094	-	-19.5	23.7	0.95	8
1-258	SuF02-071[h]3	8.003	02:17:08.772	-05:02:06.24	iC-076434	0.90	0.928	0.928	-	1.000	-	-	-19.3	23.8	0.95	36
1-280	SuF02-027[h]3	2.005	02:17:00.074	-04:58:20.14	iC-100962	0.60	0.594	0.594	1.000	-	-	-	-19.0	23.2	1.00	38
2-019	SuF02-026	1.720	02:18:51.905	-04:46:57.29	iN-013001	0.35	-	0.800	0.013	0.969	0.015	0.003	-17.5	25.2	0.75	24
2-033[f]		17.026	02:18:42.509	-04:34:17.99	iN-090581	0.35	-	0.400	1.000	-	-	-	-19.2	22.1	0.90	54
2-042		4.048	02:18:31.850	-04:25:13.52	iN-149479	0.65	-	0.650	0.416	0.584	-	-	-18.7	23.7	1.15	-4
2-138[j]		0.752	02:17:46.010	-04:36:46.59	iN-077467	1.00	-	1.000	0.002	0.532	0.464	-	-18.7	24.7	1.20	48
2-146[j]	SuF02-037	1.444	02:17:43.363	-04:30:57.22	iN-113117	0.85	0.924	0.924	-	1.000	-	-	-18.9	24.3	1.10	38
2-167[j]	SuF02-05	8.014	02:17:27.401	-04:40:45.42	iN-052480	0.85	-	0.850	-	0.970	0.021	0.009	-17.8	25.1	0.90	38
2-175		0.250	02:17:18.859	-04:30:26.53	iN-116245	1.00	-	1.000	-	0.243	0.757	-	-18.3	25.1	1.15	14
3-008[j]		0.294	02:19:04.080	-05:14:50.16	iS-162495	0.90	-	0.900	-	0.995	0.005	-	-18.4	24.7	1.20	56
3-156		4.336	02:17:48.098	-05:27:44.54	iS-074610	0.65	-	0.650	0.004	0.996	-	-	-18.8	23.6	1.15	66
4-083		11.480	02:20:13.834	-05:07:34.27	iE-135660	1.30	-	1.300	-	0.000	0.996	0.004	-19.1	25.3	1.05	38
4-105[j]		3.613	02:20:05.904	-05:05:31.83	iE-123124	0.95	-	0.950	-	0.608	0.281	0.111	-18.2	25.0	0.90	52
4-106[j]		4.766	02:19:26.021	-05:05:06.94	iE-059305	1.00	-	0.950	-	0.747	0.253	-	-18.7	24.5	0.75	54
4-117[j]		1.345	02:20:16.889	-05:03:50.67	iE-141288	0.95	-	0.950	-	0.999	0.001	-	-19.9	23.1	1.20	8
4-150		13.697	02:19:35.458	-04:57:42.26	iE-076200	3.00	-	0.300	1.000	-	-	-	-17.6	23.1	0.75	-6
4-174[j]		0.538	02:19:10.296	-04:54:19.19	iE-036303	1.10	-	1.050	-	0.006	0.994	-	-19.9	23.6	0.95	12
4-203		0.024	02:20:32.179	-04:49:58.86	iE-157248	0.95	-	0.950	-	0.666	0.334	-	-18.6	24.6	1.10	64
4-233		0.415	02:19:49.937	-04:45:53.30	iE-097735	0.80	-	0.850	-	1.000	-	-	-19.1	23.7	0.75	70
5-029[j]	SuF02-025[h]1	0.722	02:16:23.947	-04:49:29.51	iW-069337	0.55	0.606	0.606	-	1.000	-	-	-19.1	23.1	1.05	54
5-035		1.244	02:16:46.918	-04:51:21.98	iW-036122	1.00	-	1.000	-	0.579	0.421	-	-18.6	24.8	0.85	62
5-049[j]		5.846	02:16:50.143	-04:54:33.53	iW-032007	1.00	1.094	1.094	-	-	1.000	-	-19.3	24.5	0.80	54
5-149[j]	SuF02-017[h]1	20.365	02:16:45.530	-05:09:48.28	iW-038187	0.50	1.030	1.030	-	-	1.000	-	-18.9	24.5	1.00	30

Table 4.2: (Continued.)

Field-ID	SuF02-ID[a]	Offset[b]	RA	Dec	Host ID	z_{phot}	z_{spec}	z_{SN}[c]	M_B[e]	$m_{i'}$	s[f]	Day[g]
Candidates rejected as AGN or SN Ib/c, and one possible SN Ia at $z > 1.4$												
1-081[l]		1.134	02:18:29.273	-05:01:05.60	iC-083570	1.450	-	1.450	-19.5	25.3	0.95	62
1-143[i]	SuF02-058	0.047	02:17:59.674	-04:52:26.77	iC-138418	2.600	-	0.50	-17.7	24.1	1.20	56
2-038[k]	SuF02-077	2.736	02:18:35.210	-04:26:39.90	iN-140425	0.450	-	0.450	-17.6	24.0	0.90	48
3-202[i,j]	SuF02-061	0.192	02:17:22.769	-05:16:56.58	iS-148873	0.700	1.085	1.100	-19.7	24.0	0.85	22
4-100[k]		0.347	02:19:56.690	-05:05:55.86	iE-108255	0.750	-	0.750	-18.2	24.3	1.10	54

[a] The IDs correspond to the spectroscopic candidates in the other papers (see Lidman et al. 2005, Morokuma et al. 2010, and Suzuki et al. 2012).

[b] The offset means distance (pixel) from objects to the center of the host galaxy.

[c] The redshifts are estimated by the light curve fitting with photometric redshifts of host galaxies. When available, the spectroscopic redshifts are used.

[d] The allocation of SN Ia to $0.2 < z < 0.6$, $0.6 < z < 1.0$, $1.0 < z < 1.4$, and 1.4 bins according to $PDF(z)$ (see section 4.5)

[e] The absolute magnitudes are not corrected for extinction from SN host galaxies.

[f] The stretch factors are not B-band stretch but just observed i'-band stretch used in the light curve fitting.

[g] The days means the dates from the peak magnitude.

[h] Spectroscopically confirmed SNe Ia (including probable Ia). The numbers represents the reference: 1 is published in Lidman et al. 2005, 2 is published in Morokuma et al. 2010, and 3 is going to be included in Rubin et al. (in prep.)

[i] Detected in X-rays with XMM-Newton.

[j] Candidates with color information (detected in R_c, i' and z')

[k] Failed color cut.

[l] This object at $z = 1.45$ is not included in the rate calculation.

Theory is not the endpoint of work; it is work along the way to the work. To read it actively is just a process that will hopefully bring us to a less shadowed place.

Félix González-Torres (1957 - 1996)

5 Rate Calculation

Given the supernova rate per unit comoving volume $r_V(z)$, the average number of SNe we expect to observe in the redshift bin $[z_1, z_2]$ is given by

$$N_{exp}(z_1 < z < z_2) = \int_{z_1}^{z_2} r_V(z) \frac{CT(z)}{1+z} \frac{\Theta}{4\pi} V(z) dz, \tag{5.1}$$

where $V(z)dz$ is the comoving volume in a redshift slice of width dz, Θ is the solid angle observed in the survey (in units of steradians), and $CT(z)$ is the observer frame "control time". The control time can be thought of as an "effective visibility time"; it is the total time (in the observer frame) for which the survey is sensitive to a SN Ia at redshift z. In any survey of finite length, the observed number of SNe in any given bin will differ from the average expected number N_{exp} due to Poisson statistics. Given a functional form of the rate $r_V(z)$, we can estimate its parameters by comparing the observed number of SNe to N_{exp} in each redshift bin. Alternatively, we can make the approximation that the rate is constant within each bin. Under this approximation, $r_V(z)$ can be moved outside the integral in Equation 5.1. Using N_{Ia} as an unbiased estimator of N_{exp}, we get an estimate of the rate in the bin $z_1 < z < z_2$,

$$\widehat{r}_v(z_1 < z < z_2) = \frac{N_{Ia}(z_1 < z < z_2)}{\int_{z_1}^{z_2} \frac{CT(z)}{1+z} \frac{\Theta}{4\pi} V(z) dz}. \tag{5.2}$$

Since CT(z) differs by changing position (field) and survey epochs, CT(z) is calculated for all fields and corresponding survey parameters, then normalized for the rate calculations. In this paper, we use two methods. Assuming the rate follows a simple power law, $r_V(z) = r_0(1+z)^\alpha$ (Pain et al. 2002), we estimate its parameters using Equation 5.1. We also use Equation 5.2 to estimate the rate in three broad bins, $0.2 < z < 0.6$, $0.6 < z < 1.0$, $1.0 < z < 1.4$.

Because we have a spectroscopic classification for only a small minority of our SN candidates, we use a photometric typing method as our primary means of classifying into SNe I and II, thereby arriving at an estimated number of SNe Ia observed, N_{est}. This method can give a biased estimate of the true number of SNe Ia, N_{Ia}, due to the limited number and precision of observations. Specifically, some Type II SNe may be misclassified as SNe Ia, while some Type Ia SNe may be misclassified as SNe II. The estimated number of SNe Ia, N_{est}, can be expressed as follows:

$$N_{est}(z) = N_{Ia}(z)P_{Ia}(z) + N_{II}(z)F_{II}(z) + \widetilde{N}_{Ib/c} + \widetilde{N}_{AGN}, \tag{5.3}$$

where P_{Ia} is the probability of correctly classifying a SN Ia (completeness) and F_{II} is the probability of classifying a SN II as a SN Ia (contamination). Note that these two factors address only misclassification in the lightcurve fitting, not uncertainties in the SN Ia or II lightcurve templates. Those uncertainties are addressed in our estimate of the systematic error (section 6.4). $\widetilde{N}_{Ib/c}$ and $\widetilde{N}_{AGN}$ are possible residual contamination from SN Ib/c and AGN, as described in section 4.3 and section 4.4. The method we use to derive the rates is illustrated in Figure 5.1. In section 5.1 we calculate $CT(z)$ using simulated SN Ia light curves. In section 6 we calculate $P_{Ia}(z)$ and $F_{II}(z)$ using simulated SN Ia and II light curves. The number of SNe II, $N_{II}(z)$, is calculated assuming the nearby SN II rate and cosmic star formation history.

5.1 Control time

The control time is the time interval during which we can detect the SN explosion. Here we define the time in the observer-frame. We compute the control time as a function of redshift.

5.1.1 Simulated light curves of Ia

In order to calculate the control time, we carry out a Monte Carlo simulation to generate artificial "observed" SN Ia and SN II lightcurves based on the observation dates and depths of our SXDS variable object survey. To produce a distribution of artificial SNe Ia modeled on the true SN Ia distribution, we use a magnitude distribution based on SNe Ia from the SDSS-II SN survey (Frieman et al. 2008). As the SDSS-II sample is essentially complete at $z \leq 0.12$ (Dilday et al. 2008), we adopt the exact absolute magnitudes and stretch factors of 56 $z \leq 0.12$ SDSS-II SNe for our artificial SNe Ia. The 56 SNe include all spectroscopically-confirmed $z \leq 0.12$ SNe Ia obtained in the first two years (2005 and 2006) of the survey. The B-band absolute magnitude distribution (uncorrected for dust extinction) and B-band stretch factor distribution of these SNe Ia is shown in Figure 5.3. The stretch distribution of SNe Ia at high-redshift might be different from the local distribution; according to Howell et al. 2007 the average light curve width and average intrinsic luminosity of SNe Ia increase toward high-redshift for non-subluminous SNe Ia. Therefore we include the effect of the stretch evolution toward high-redshift in our simulation. At each redshift, we make an artificial light curve in the observed i'-band based on each of the 56 SNe. To do this, we use the absolute

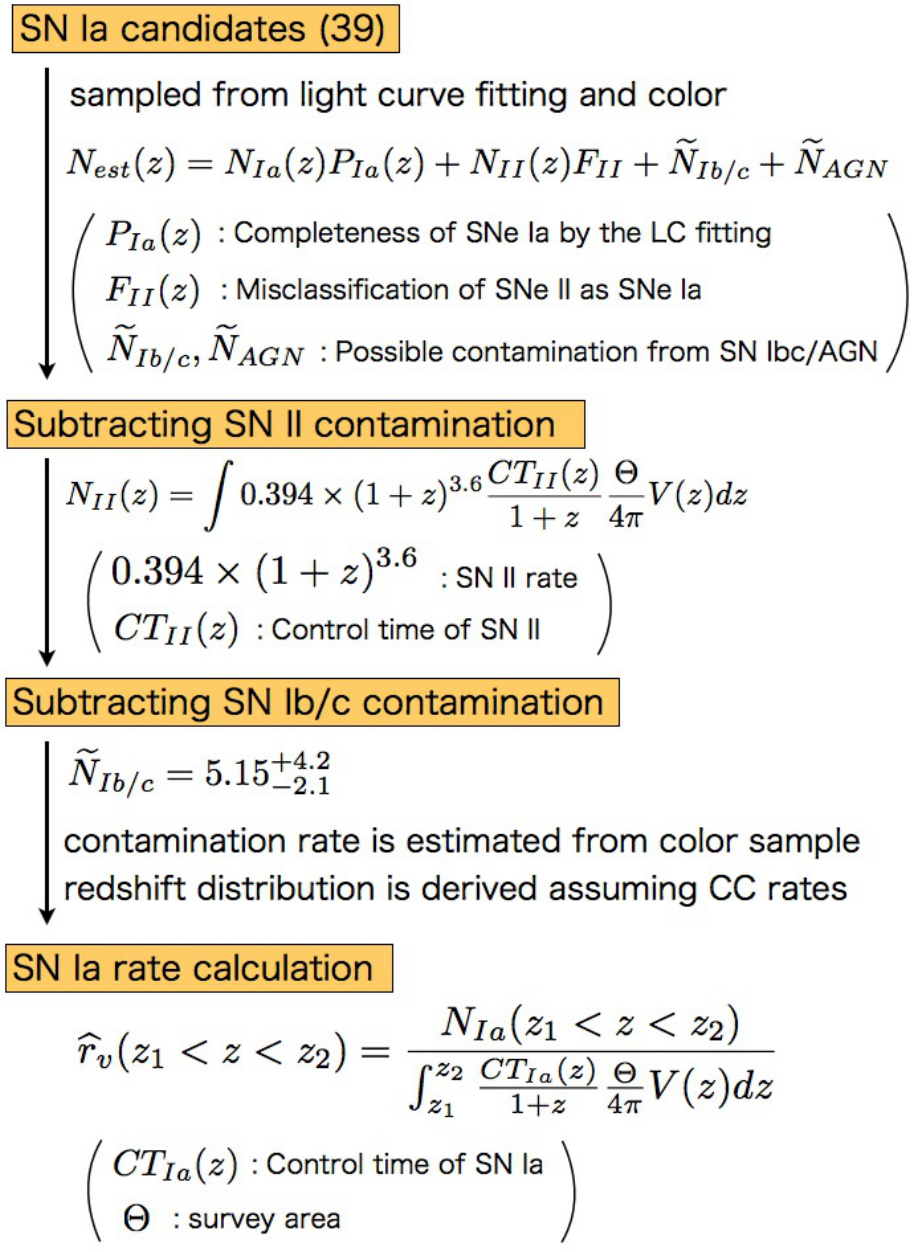

Figure 5.1: The flow chart of the rate calculation. From 39 SN Ia candidates, possible SN II and SN Ib/c contaminations are subtracted. The rate of possible AGN contamination is considered as a systematic uncertainty in section 6.4.

magnitude of the SN and a K-correction based on the $u'g'r'i'$ SDSS-II light curve and the Hsiao et al. 2007 template.

5.1.2 Dust modeling

Though we use real SNe Ia, including whatever dust extinction they suffer, for our control time simulation in order to represent the actual $M_B - s$ distribution, an alternative approach is to employ a simple parameterized family of lightcurves, e.g., using stretch and color, c. B12 simulated the magnitude distribution of SNe Ia using the model:

$$M_B = -19.31 - \alpha(s-1) + \beta c + I \tag{5.4}$$

where -19.31 is the fiducial magnitude, $\alpha = 1.24$, $\beta = 2.28$ (Kowalski et al. 2008), and I is an additional "intrinsic dispersion" characterized with $\mu = 0.0$ mag and $\sigma = 0.15$ gaussian distribution. To account for the dust effect, various dust models are usually included in the color distribution. Some conventional models are sammarized below.

Kessler et al. 2009 (K09; closest model to our sample)
This model is a good representative of host-galaxy SN extinction in the SDSS-II SN Survey (Kessler et al. 2009a).

$$P(A_V) = \frac{e^{-A_V/0.33}}{0.33} \tag{5.5}$$

Hatano et al. 1998 (Ha98; most dust-affected model)
Hatano et al. 1998 used a Monte Carlo technique to estimate the effect of dust in disk galaxy, assuming distribution of dust and supernova progenitors in a simple model. They derived an extinction distribution $P(A_V)$ showing long tail extending to high-A_V.

$$P(A_V) = 0.61\frac{e^{-A_V/2}}{2} + 0.39\frac{e^{-A_V/0.07}}{0.07} \tag{5.6}$$

Riello & Patat 2005
The model of Riello & Patat 2005 was aimed at generalizing the Hatano et al. 1998 models to a variety of dust properties and galaxy physics.

$$P(A_V) = 0.35\delta(A_V) + 0.40\frac{2}{0.6\sqrt{2\pi}}e^{-A_V^2/(2\times 0.6^2)} + 0.25e^{-A_V} \tag{5.7}$$

Neill et al. 2006
This model is used in the analysis of Neill et al. 2006, who estimated the SN Ia rate from SNLS sample.

$$P(A_V) = \frac{2}{0.62\sqrt{2\pi}}e^{-A_V^2/(2\times 0.62^2)} \tag{5.8}$$

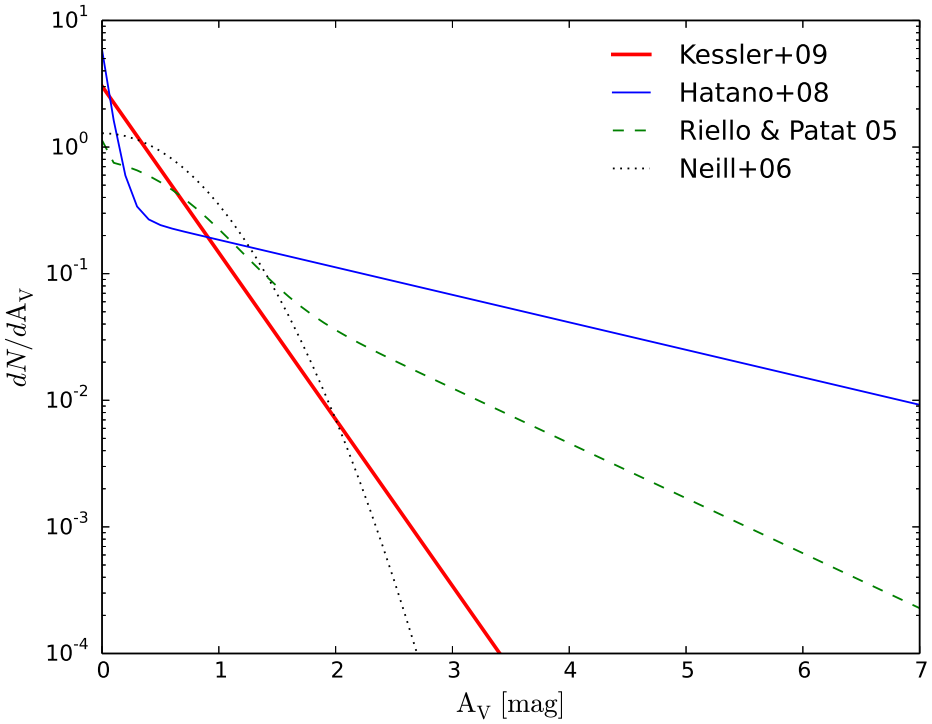

Figure 5.2: Comparison of various dust models.

Following the procedure of Barbary et al. 2012, these A_V distributions are converted to color distributions, $P_{host}(c)$, using the relation $A_V = R_V \times E(B-V) \approx (\beta - 1) \times c$. The final color distribution, $P(c)$, is a convolution of $P_{host}(c)$ and the intrinsic color distribution (assumed to be Gaussian). For example, in the Kessler et al. 2009a model, $P_{host}(c) \propto e^{-(\beta-1)c/0.33}$ is obtained and the final $P(c)$ is calculated as

$$P(c) = \frac{\lambda}{2} e^{\frac{\lambda^2\sigma^2}{2} - \lambda c} \,\mathrm{Erfc}\left(\frac{\lambda\sigma^2 - c}{\sqrt{2}\sigma}\right), \tag{5.9}$$

where λ represents $(\beta-1)/0.33$, Erfc is a complementary error function, and σ is the intrinsic color dispersion ($\sigma \sim 0.12$).

Figure 5.3 shows the magnitude distributions calculated for three dust models used in this thesis. Since our control time sample is based on SDSS-II SNe, the sample is well represented by the distribution with the Kessler et al. 2009a model (hereafter K09 dust model). Note that these three models are only used to estimate the dust effect and the base control time is calculated using observed distribution of SDSS-II SNe Ia. The uncertainty caused by the choice of extinction models is discussed in section 6.4.

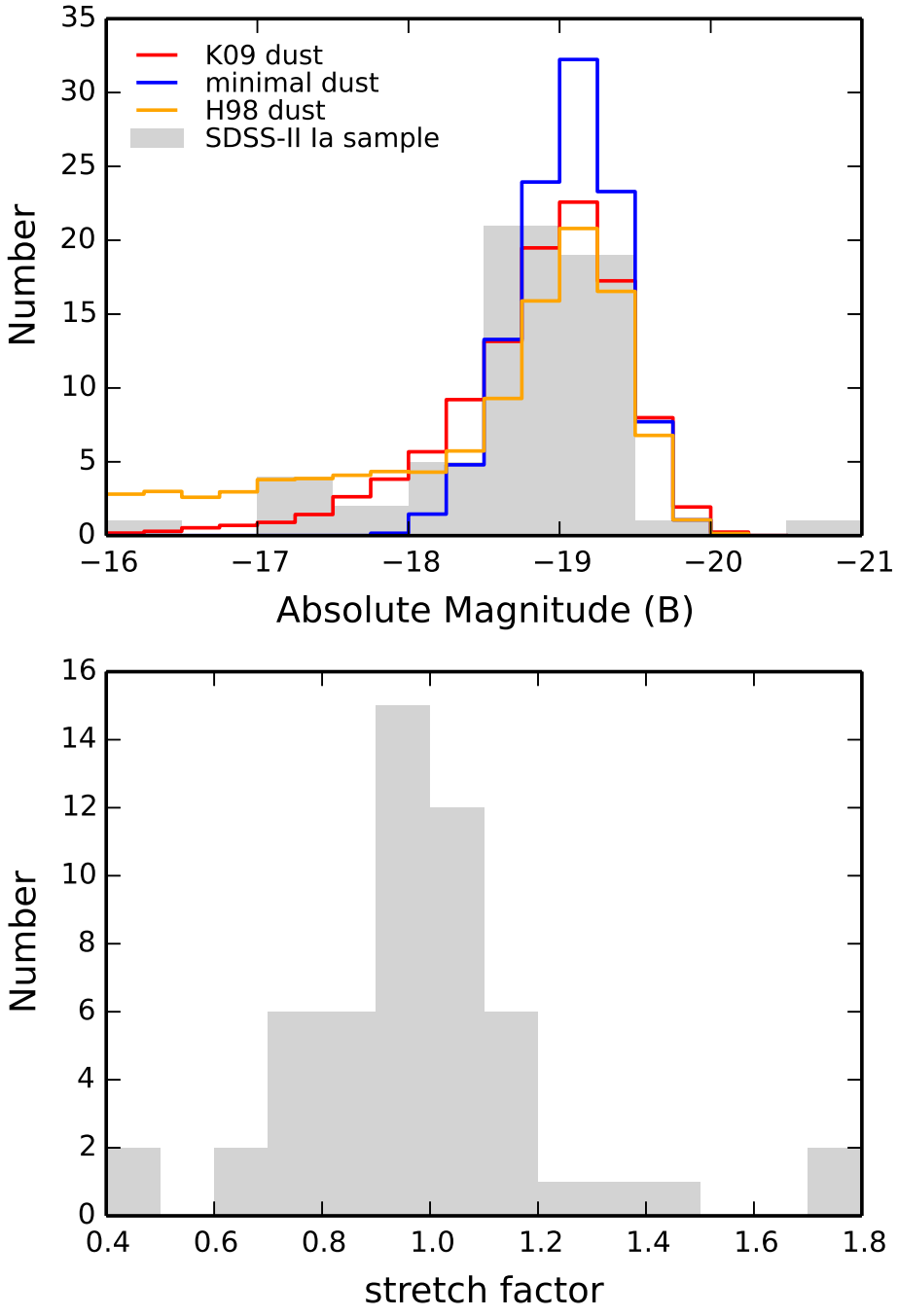

Figure 5.3: The absolute magnitude (*top*) and stretch (*bottom*) distributions of the 56 $z < 0.12$ SDSS-II SNe Ia. We make artificial lightcurves from a SN Ia template using these distributions. Solid lines plotted in the top panel represent the simulated SN Ia distribution using assumptions in Barbary et al. 2012. The red line indicates the distribution using the K09 dust model, and the blue line indicates the minimal dust model.

5.1.3 Simulated light curves of II

Next, we make artificial SN II lightcurves from the Type II templates of section 4.2. As for SNe Ia, the absolute magnitude distribution for these lightcurves is based on real SDSS-II SNe. However, it is more difficult to achieve a complete sample for SNe II because they are intrinsically fainter than SNe Ia on average. If we use the same redshift cut off as for SNe Ia ($z = 0.12$), the number of faint SNe II will be underestimated (see Figure 5.4). To resolve this problem, we have constructed a new luminosity function that accounts for incompleteness using the formula below:

$$N_{eff}(L)dL = N_{sdss}(L)dL \times \frac{V_{z<0.17}}{V_{z_{max}|L}} \tag{5.10}$$

where $N_{SDSS}(L)dL$ is the number of SDSS SNe II with luminosity $L - \frac{dL}{2} < L < L + \frac{dL}{2}$ and $V_{z_{max}|L}$ is the volume to which a SN II can be seen above the SDSS flux limit given the luminosity, L. Thus, we can simulate lightcurves using essentially all of the real SNe II from SDSS-II. We will estimate the systematic error due to the correction factors in section 6.4 by varying the SDSS flux limit. In addition to a distribution in absolute magnitude, we use two different subtypes (Type IIP and IIL) in our generated artificial SN II light curves. We use a ratio of Type II-P to Type II-L of 2:1 (Richardson et al. 2002). Also as part of our systematic error estimate in section 6.4, we vary this ratio. We generate a total of about 100,000 SN Ia and SN II lightcurves. We note that statistical error and systematic error of 2% in the flux is included in the lightcurve simulation.

5.2 Control time calculation

We calculate how many days the artificial SNe Ia can be observed. We add observation errors to the artificial SN Ia light curves. The observing errors are calculated from the limiting magnitudes of the SXDS observations, which includes the effect of decreasing signal-to-noise ratio due to the subtraction of two images.

We also include the detection efficiency in the control time calculation. The detection efficiency of the SXDS variable object survey was obtained by Morokuma et al. 2008. They estimated the detection efficiency as a function of magnitude in each subtraction image. They added artificial stars to images and detected them in the same manner as for the real images. The results are shown in Figure 8 of Morokuma et al. 2008.

The observable time duration (control time) of artificial SNe Ia is calculated for each redshift bin of width $\Delta z = 0.05$. The control time of SNe II is calculated in the same way as the SN Ia control time, but is only used for the estimation of contamination. Since the observations consist of 5 fields of Suprime-Cam with different survey parameters, we calculate the control times for each field, and then weight them according to field areas (see Equation 3 of Barbary et al. 2012). In addition, we use the data from the center field when it overlaps with other fields. The result of the weighted control time is shown in Figure 5.5.

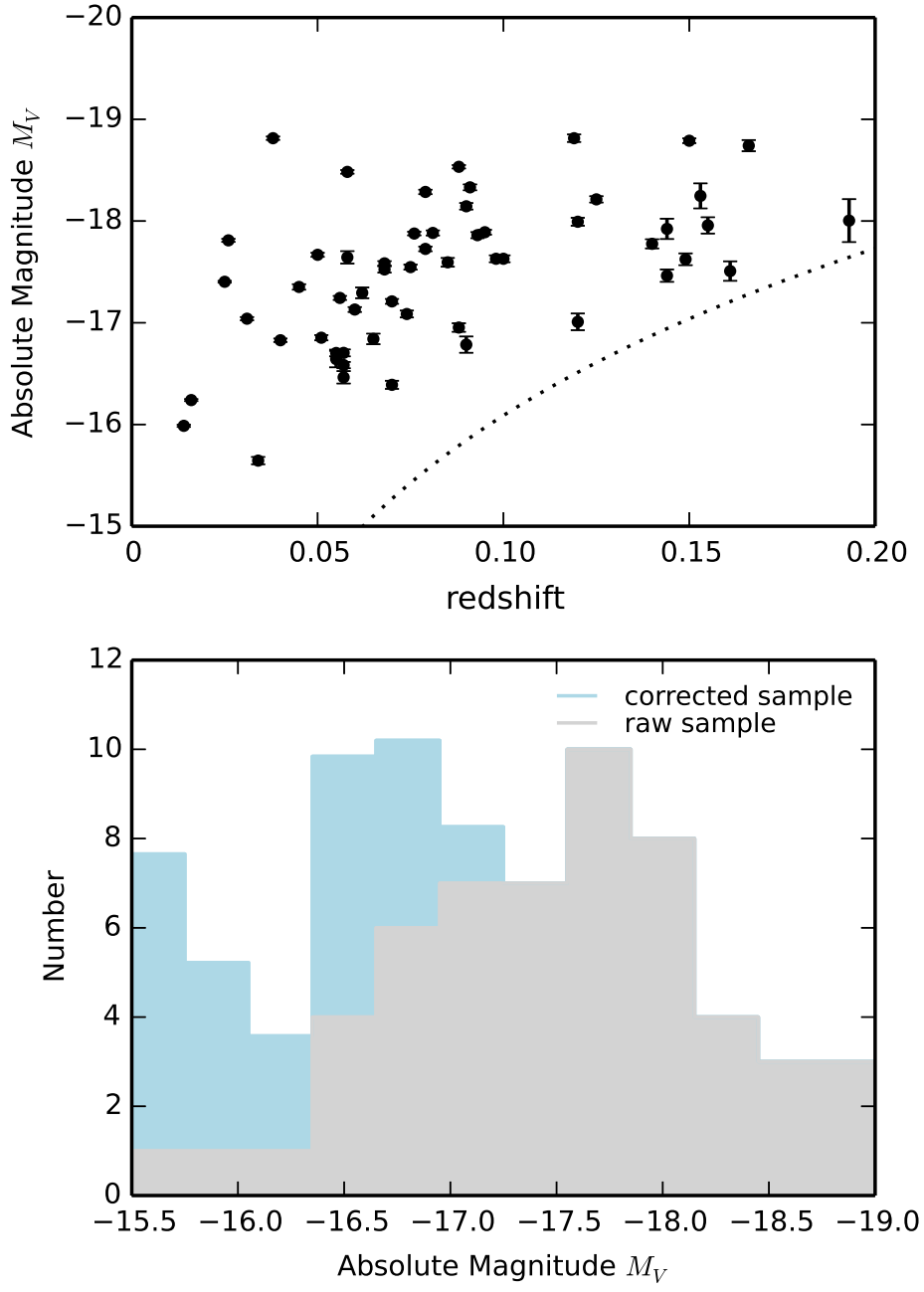

Figure 5.4: The absolute magnitude and redshifts of Type II supernovae found by SDSS-II SN survey at $z < 0.17$ (*top*). The dashed line shows the 5σ detection limit of SDSS-II SN survey. At higher redshifts fainter SNe are lost, therefore we construct a luminosity function that accounts or incompleteness (*bottom*; see Equation 5.10). We vary the magnitude limit curve 0.2 mag brighter/fainter to estimate systematics.

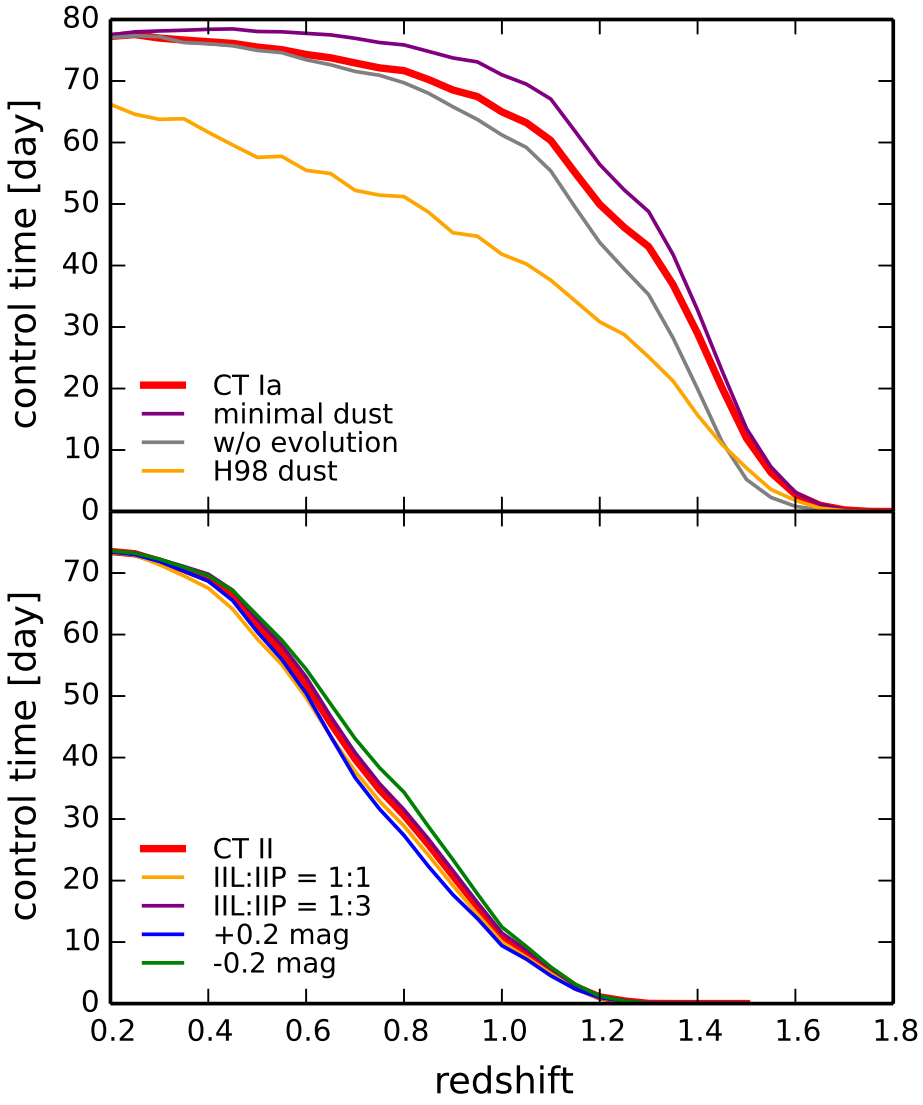

Figure 5.5: *top*: The observer-frame control time for SNe Ia (red line). The models for minimal dust (purple), without evolution effects in Howell et al. 2007 (gray), and the model based on Hatano et al. 1998 are plotted as well. *bottom*: The observer-frame control time for SNe II (red line). The models for different SN IIL and SN IIP ratio (1:1 in yellow, 1:3 in purple) are plotted. In addition, the choice of magnitude limit curve in Figure 5.4 affects the luminosity function of SN II (see the discussion in section 5.1.1). We therefore show the control time for the case of 0.2 mag brighter limit (blue) and 0.2 mag fainter limit (green).

To truly laugh, you must be able to take your pain, and play with it!

Charlie Chaplin (1889 - 1977)

6 Typing Completeness and Contamination

6.1 Estimating typing completeness

In order to determine the completeness of our light curve classification technique, we fit lightcurve templates to our sample of artificial SNe Ia. Because the total number of observing epochs is different for the different fields of the SXDF, we calculate the completeness separately for each field. The completeness for each field (represented as 7 epoch, 6 epoch, and 5 epoch mode) is shown in the different panels of Figure 6.1.

As a general trend, the completeness improves as more epochs are observed (the second column of Table 3.1) because the maximum is easily detectable. The result also shows that SNe Ia are safely classified with high completeness ($\sim$ 80% in average). Though this fraction is higher than the most efficient classification method in Kessler et al. 2010 ($\sim$ 75% of Sako et al. 2011, our fitting code is only used for eliminating SNe IIL and SNe IIP from SNe Ia, whereas Kessler et al. 2010 attempted to eliminate SNe Ib/c in this way. As mentioned in section 4.2, SNe II are more easily distinguished from SNe Ia based on light curves. Also our calculations do not include the rare luminous SNe Ib/c such as SN2005ap (Quimby et al. 2007); these will be handled as a systematic uncertainty in section 6.4. Figure 6.1 also shows that when there are fewer epochs the classification becomes less secure because the epoch of maximum brightness may be missed.

6.2 Estimating the misclassification ratio

We also estimate how often SNe II are misclassified as SNe Ia (the contamination F_{II}). Using the same method as for SNe Ia, we made artificial SNe II and fit those SNe with light curve templates to estimate the misclassification ratio (the ratio of SN II classified SN Ia). The results are shown in Figure 6.2. The misclassification becomes large toward high redshift,

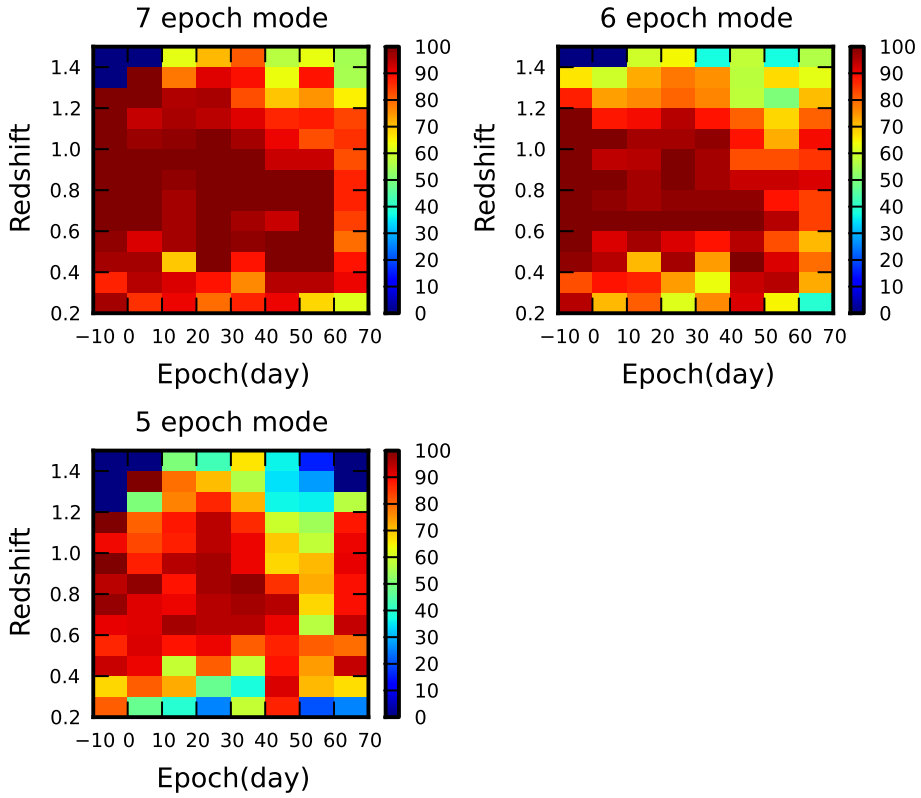

Figure 6.1: The completeness of the lightcurve fitting classification. These figures describe how many artificial SNe Ia are identified as Type Ia. The reliability depends on the number of observing epochs. The left top figure is for the 7 epoch observing mode (SXDF-C and SXDF-W). The right top figure is for the 6 epoch observing mode (SXDF-E). The left bottom figure is for the 5 epoch observing mode (SXDF-N and SXDF-S). The horizontal axis represents the observer-frame date of teh first epoch relative to maximum light. The figures show that we can classify SNe Ia with high completeness.

but it is not a serious problem because the detection efficiency of SNe II is much less than that of SNe Ia at high redshift (see Figure 5.5).

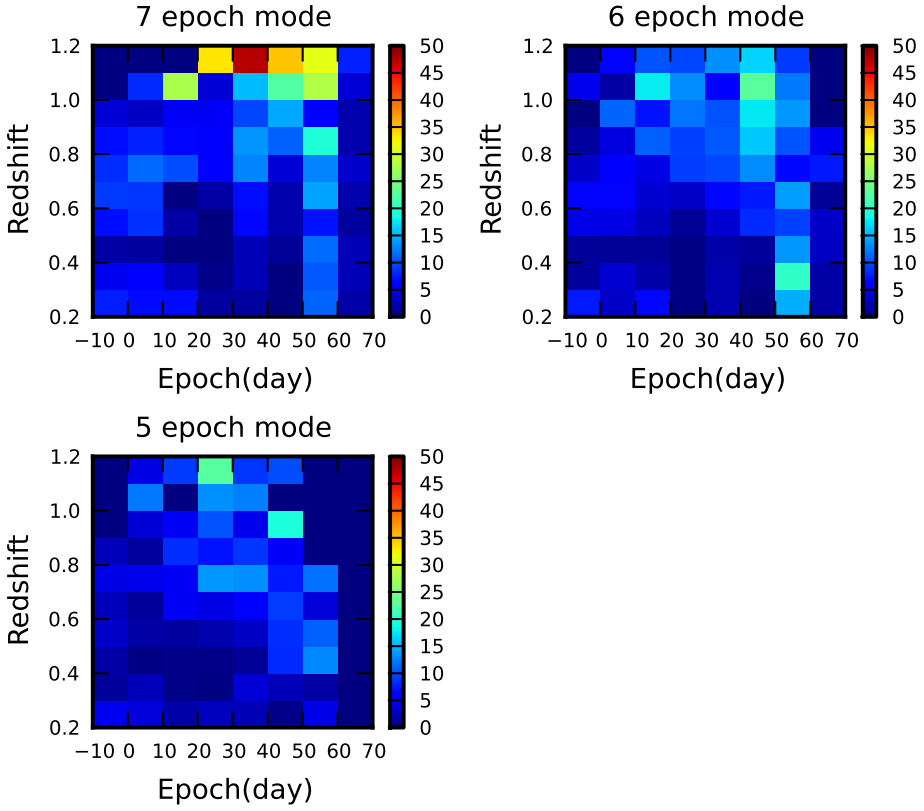

Figure 6.2: The fraction, F_{II}, of instances where artificial SNe II are misclassified as SNe Ia. Three panels represent the 7 epoch, 6 epoch, and 5 epoch mode as Figure 6.1. The misclassification increases toward high redshift. In contrast, the detection efficiency of SNe II decreases toward high redshift. As a result, the contamination is also small at high redshift.

Now, in order to find the true number (N_{Ia} in Equation 5.3) of SNe Ia and II at each redshift, we need to estimate the contamination of our SNe Ia sample by SNe II. There are many studies to derive core collapse supernova rates, and these results are consistent each other (Dahlen et al. 2012, Melinder et al. 2012, Graur et al. 2011, Bazin et al. 2009, Botticella et al. 2008, Mattila et al. 2012, Li et al. 2011a, Smartt et al. 2009, Cappellaro et al. 1999, Horiuchi et al. 2011, Magnelli et al. 2009). These reults are summarized in Figure 6.3 and Table 6.1. Since higher redshift SN II rates have larger uncertainty, we use the measured nearby SN II rate and assume that the SN II rate is increasing in proportion to the cosmic star formation rate. The progenitors of SNe II are massive stars and have a very short delay time between star formation and explosion, which justifies this assumption. We use a nearby SN II rate of 0.394×10^{-4} yr^{-1} Mpc^{-3} at $z \sim 0$ (Li et al. 2011a), and a star formation rate $\propto (1+z)^{3.6}$ (Hopkins & Beacom 2006). The SN II rate is then $0.394 \times (1+z)^{3.6}$. Using this assumption, the number of SNe II

available that potentially could be misclassified as SNe Ia, $N_{II}(z)$, can be calculated using the equation below.

$$N_{II}(z) = \int 0.394 \times (1+z)^{3.6} \frac{CT_{II}(z)}{1+z} \frac{\Theta}{4\pi} V(z) dz, \tag{6.1}$$

where $CT_{II}(z)$ represents the control times of SNe II. We note in particular that this model for the SN II rates is in agreement with the $z \sim 1$ SN II rate from Dahlen et al. 2012.

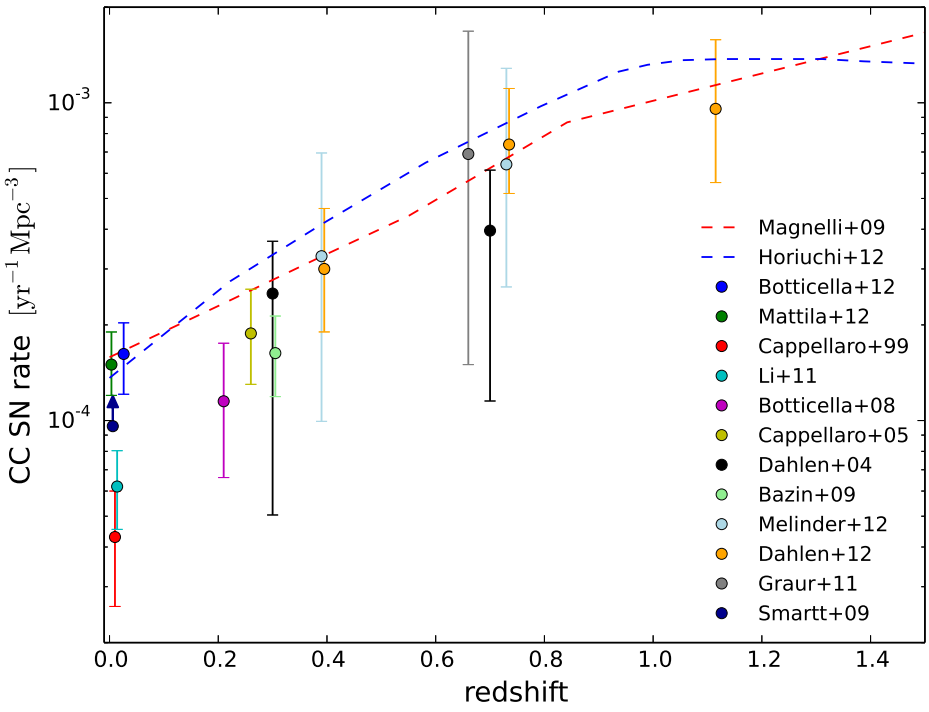

Figure 6.3: The CC SN rate measurements from various survey listed in Table 6.1. Since CC SNe observation is easily affected by the dust extinction, measured rates vary with different dust modeling. The *dot-dashed lines* are the result from Magnelli et al. 2009 and Horiuchi et al. 2011, witch assumed SFH and a relation between star formation and CC SN rate.

Table 6.1: The published CC SN rate measurements

Redshift	N_{Ia}	Rate [10^{-4} yr^{-1} Mpc^{-3}]	Refference
< 0.0026	14^a	$1.62^{+0.41}_{-0.41}$	Botticella et al. 2012
< 0.0035	36^b	$1.5^{+0.4}_{-0.3}$	Mattila et al. 2012
< 0.0066	92^c	> 0.96	Smartt et al. 2009
0.01	67^d	$0.43^{+0.17}_{-0.17}$	Cappellaro et al. 1999
< 0.014	440^e	$0.62^{+0.07+0.17}_{-0.07-0.15}$	Li et al. 2011a
0.21	44.95^f	$1.15^{+0.43+0.42}_{-0.33-0.36}$	Botticella et al. 2008
0.26	31.2^g	$1.88^{+0.71}_{-0.58}$	Cappellaro et al. 2005
0.3	17^h	$2.51^{+0.88+0.75}_{-0.75-1.86}$	Dahlen et al. 2004
0.3	117^i	$1.63^{+0.34+0.37}_{-0.34-0.28}$	Bazin et al. 2009
0.39	$3.28(3)^j$	$3.29^{+3.08+1.98}_{-1.78-1.45}$	Melinder et al. 2012
0.39	$9.99(9)^k$	$3.00^{+1.28+1.04}_{-0.94-0.57}$	Dahlen et al. 2012
0.66	8.7^l	$6.9^{+9.9}_{-5.4}$	Graur et al. 2011
0.7	17^h	$3.96^{+1.03+1.92}_{-1.06-2.60}$	Dahlen et al. 2004
0.73	$3.27(5)^j$	$6.40^{+5.30+3.65}_{-3.12-2.11}$	Melinder et al. 2012
0.73	$23.56(25)^k$	$7.39^{+1.86+3.20}_{-1.52-1.60}$	Dahlen et al. 2012
1.11	$11.44(11)^k$	$9.57^{+3.76+4.96}_{-2.80-2.80}$	Dahlen et al. 2012

[a] compilation of published CC SNe within 11Mpc

[b] compilation of published CC SNe in 6-15Mpc

[c] compilation of published CC SNe within 28Mpc

[d] SNe sample from Asiago, Crimea, OCA, Calan/Tololo, and Evans ' SN searches

[e] SNe sample within 60Mpc from Lick Observatory Supernova Search (LOSS)

[f] SNe sample from the Southern inTermediate Redshift ESO Supernova Search (STRESS)

[g] SN search program with ESO/MPI 2.2 m telescope at ESO, La Silla

[h] HST observation as a part of the Great Observatories Origins Deep Survey (GOODS)

[i] SNe from the Supernova Legacy Survey (SNLS)

[j] SNe from the Stockholm VIMOS Supernova Survey (SVISS). The numbers in parencesis represents the raw detected number. In the rate calculation, the real numbers which takes the redshift uncertainty into account are used.

[k] updated sample from Dahlen et al. 2004

[l] SN servey program in the Subaru Deep Field (SDF)

6.3 SN Ib/c contamination

In this subsection, we estimate the number of SNe Ib/c in our sample of 39 SNe Ia. In addition to the 2 SNe Ib/c that are found from their colors, we estimate that there are another $3.15^{+4.20}_{-2.10}$ SNe Ib/c are in the sample. We compare this number with the number that one would infer from evolving local SNe Ib/c rates to higher redshift and we estimate the redshift distribution of the SNe Ib/c in our SN Ia sample.

As described in section 4.4, the candidate refinement indicates that approximately 2 out of the 14 SNe I with color information are SNe Ib/c. This yields an estimated observed SN Ib/c contamination percentage of $14.3^{+18.8}_{-9.2}$ based on the combined application of lightcurve shape and color-color selection.

Of the 39 lightcurve-selected SN Ia candidates 8 have spectroscopic confirmation and an additional 10 possess colors expected for SNe Ia, leaving a pool of 21 lightcurve-selected candidates that could still harbour SNe Ib/c. While it is encouraging that color classification has revealed only minor contamination from SNe Ib/c, the implication is that roughly 3 additional SNe Ib/c remain in this unconfirmed pool. For these a statistical correction can be applied if their number and redshift distribution can be estimated.

Since spectroscopically-confirmed SNe Ia are not present in the unconfirmed pool, it could be argued that such objects should also be removed from the color-color classified subsample. The rationale here is that since spectroscopic observations may suffer greater selection biases than color observations, the set of spectroscopically-confirmed objects may be less representative of the unconfirmed pool than is the set of objects with colors. Kolmogorov-Smirnov tests of either the redshift distributions or the peak magnitudes indicate that the spectroscopically-confirmed and color-color subsamples are consistent with the unconfirmed pool with $P = 0.74$. While there is no direct evidence of differential bias, this approach may be considered more conservative. In this case the removal of 2 spectroscopically-typed SNe from the sample of 14 objects with color-color information would raise the observed contamination rate to 2 out of 12 objects, or $16.7^{+21.9}_{-10.8}\%$.

While correlated, these various estimates are consistent with a SN Ib/c contamination rate of $15^{+20}_{-10}\%$. Though the uncertainty is large due to the small number of color samples, we adopt this rate for the unconfirmed subsample. This would imply an additional $3.15^{+4.20}_{-2.10}$ undetected SNe Ib/c in the unconfirmed pool. Combined with the 2 SNe Ib/c detected via color selection this leads to a estimated total of $5.15^{+4.20}_{-2.10}$ SNe Ib/c in the lightcurve-shape selected sample. This residual SN Ib/c contamination is treated as a systematic uncertainty.

The second component of the statistical correction of the unconfirmed pool is to determine the expected redshift distribution. The core-collapse SN rate, the SN Ib/c luminosity function and the survey control time must then be included to predict the final redshift distribution. Figure 6.4 shows the result of such a calculation using the luminotisy function of SN Ib/c from nearby complete survey (Li et al. 2011a) to calculate the control time, and assuming the observed fraction of SN Ib/c to SN Ia (Li et al. 2011a) and core-collapse SN rate evolution (Dahlen et al. 2012). The expected number of contaminating SNe Ib/c is $8.34^{+3.34}_{-3.34}$. This number is consistent with the number estimated directly from the observation, $5.15^{+4.20}_{-2.10}$. The two objects, 2-038 and 4-100, classified as a SN Ib/c via their color are at $z \sim 0.45$ and $z \sim 0.75$, respectively — right near the peak of the calculated distribution in Figure 6.4.

In summary, we estimate that a total of $5.15^{+4.20}_{-2.10}$ SNe Ib/c contaminate the lightcurve-selected SN I sample. We use color information to directly remove objects 2-038 and 4-100. The remaining $3.15^{+4.20}_{-2.10}$ SNe are subtracted using the redshift distribution of Figure 6.4 using the appropriate scaling. Since we have only a limited color sample to estimate SN Ib/c contamination, the impact of the uncertainty is large in the lowest bin ($0.2 < z < 0.6$), and is comparable to the Poisson uncertainties associated with the detected SN Ia sample (Table 6.2). However, this effect becomes much smaller beyond $z = 0.6$, where we want to constrain the rate. We note that reasonable changes to the color selection procedure, or to the shape of the SN Ib/c redshift distribution, have negligible effect relative to the Poisson errors.

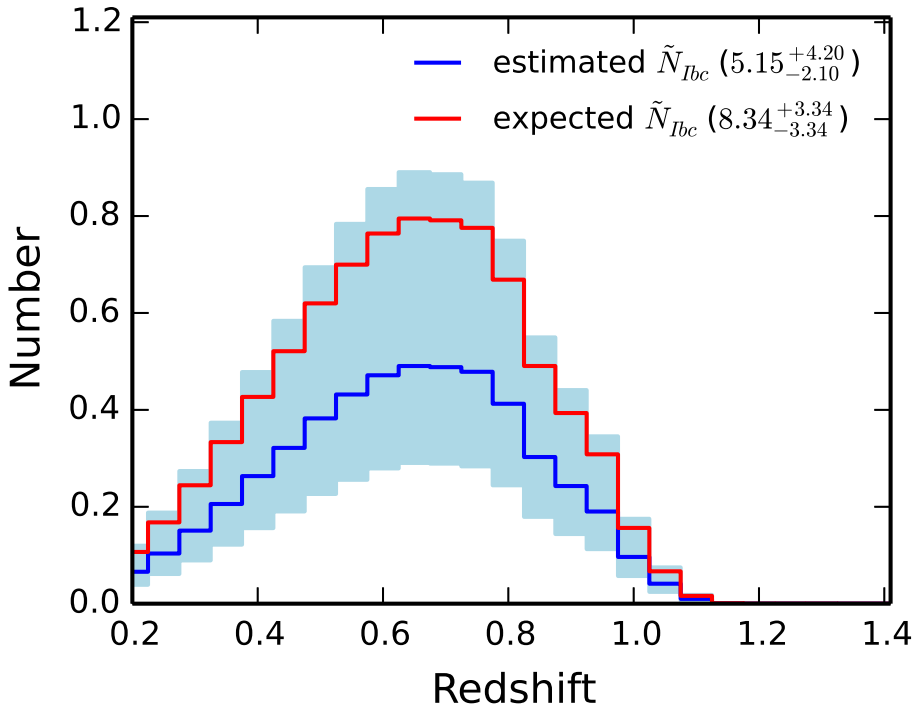

Figure 6.4: The estimated number of possible SNe Ib/c contamination ($\widetilde{N}_{Ib/c}$ in Equation 5.3) in the lightcurve-selected SN I sample. The *red solid line* indicates the expected number simulated assuming nearby SN Ib/c rate and its evolution (Li et al. 2011b, Dahlen et al. 2012). The *blue solid line* and *light blue region* represents the number estimated from color-color selection and corresponding error region.

6.4 Results and systematic error estimation

The SN Ia rate is obtained from Equations 5.1–5.3. The observed number (N_{Ia}) of SNe Ia in each redshift bin is obtained from Equation 5.3, and is shown in Figure 6.5. We show

the SN Ia rate in each redshift bin of $\Delta z = 0.4$ in Table 6.3. The results include systematic and statistical errors. These redshift bins are the same as those of Dahlen et al. 2008. The effective redshift $\bar{z}$ of each bin is the average redshift in the bin, weighted by the control time and volume, and is given by

$$\bar{z} = \frac{\int_{z_1}^{z_2} z \frac{CT_{Ia}(z)}{1+z} V(z) dz}{\int_{z_1}^{z_2} \frac{CT_{Ia}(z)}{1+z} V(z) dz}. \tag{6.2}$$

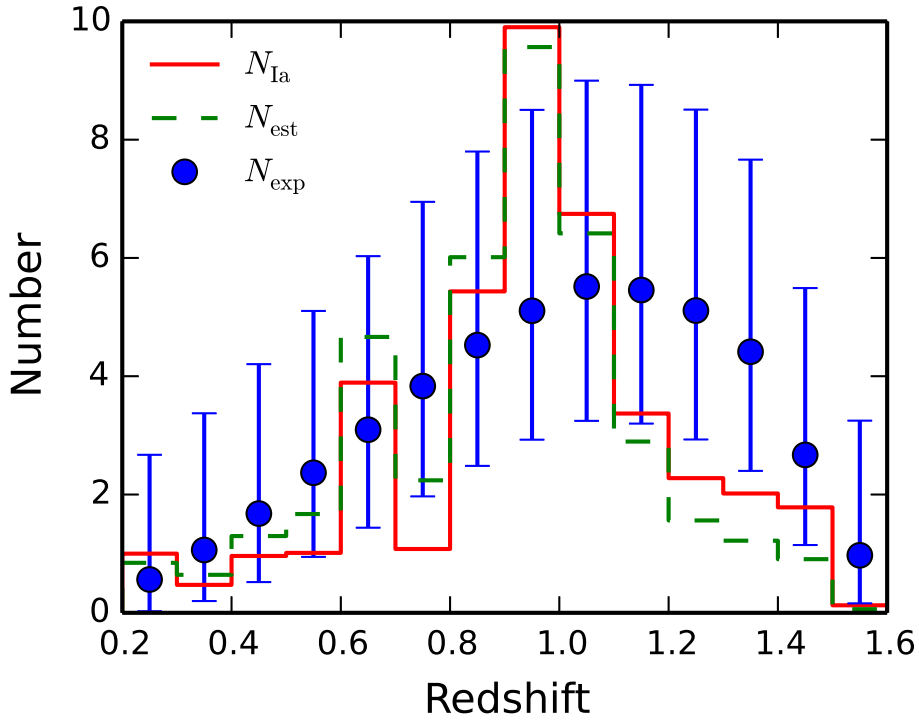

Figure 6.5: The number of SNe Ia from SXDS observations. The *green dashed histogram* indicates the estimated number (N_{est}) of SN Ia candidates obtained by the light-curve fitting. The *red solid histogram* indicates the observed number (N_{Ia}) of SNe Ia, after correction for completeness and contamination. The *blue points* with statistical error bars indicate the expected number (N_{exp}) obtained by the model-dependent rate calculation of Equation 5.1. In this figure, one SN Ia, 1-081, at $z = 1.45$ is included in the histogram.

We now itemize the causes of systematic uncertainties and the methods used to estimate their sizes, and then summarize the results in Table 6.2.

(1) In generating artificial SNe II, we adopted a ratio of Type II-P to Type II-L of 2:1 (Richardson et al. 2002). However the real distribution of Type II subtypes is not well-known. Using a different ratio will change the fraction of misclassifications of SN II as SN Ia, F_{II}. We adopt different ratios of 1:1 and 3:1 and recalculate the SN Ia rates in each case. As plotted in Figure 5.5, the effect of changing the ratio is minor (up to $\sim 2\%$). The impact on

the final SN Ia rate depends on the redshift range (shown in Table 6.2).

(2) Artificial SNe II were generated using the peak magnitude distribution of low-redshift SNe II found by the SDSS-II SN survey. Since the observed luminosity distribution is not complete for fainter SNe II, we carefully corrected the magnitude distribution using the magnitude limit curve (see the discussion in section 5.1.1). We checked how the correction factor changes if the magnitude limit is moved 0.2 mag brighter/fainter. As in Figure 5.5, the effect of changing this threshold is minor; resulting in $\sim 2\%$ changes in the rate. We take the half of this difference as a systematic.

(3) In our baseline calculation we accounted for contamination from SNe Ib/c by color-color selection discussed in section 6.3. This makes $3.15^{+4.20}_{-2.10}$ additional SN Ib/c contaminating the SN Ia sample after removing two objects classified as SN Ib/c (2-038 and 4-100). The effect of changing the number of SN Ib/c is greatest in the lowest-bin. In a bin with small number of SN Ia, the contamination from SN Ib/c can be the biggest uncertainty. This means that more color information would have helped to better constrain the rate at $z < 0.6$, and such color information will be important in future surveys.

(4) In section 4.3, we removed two likely AGN. There remained one source near core without X-ray detections or spectroscopic or color constraints. If that source were an AGN, or if one of the rejected X-ray detections were a SN Ia, the resulting error would be 2.6%. We take this as the systematic error due to AGN (i.e., $\widetilde{N}_{AGN} = 1$ in Equation 5.3).

(5) We separately consider the contamination from the core collapse SNe in the high-redshift bin ($1.0 \leq z < 1.4$). As noted in section 5.2, the control time for Type II SNe is very small at $z \geq 1.0$, but there might exist very bright core collapse SNe. Boissier & Prantzos 2009 show the magnitude distribution of SNe Ib/c and II from a large but heterogenous sample. Most of these SNe are fainter than ~ -18.0 mag and there are very few bright SNe of ~ -19.0 mag. However the magnitudes are discovery magnitudes, and serve only as lower limits on the peak magnitudes. The Ib/c sample of Richardson et al. 2006 contains three very bright SNe Ic that would be detectable and possibly mistaken for SNe Ia at high-redshift ($z > 1.0$). We estimate the contamination ratio of bright SNe using the magnitude distribution of Figure 6 of Bazin et al. 2009. There are four core collapse SNe (one object is a SN Ib/c and three objects are SNe II) that have peak absolute magnitudes that are around -19. In this figure, there are approximately 50 SNe Ia with a similar magnitude. Therefore the contamination from core collapse SNe in the high-redshift bin is estimated to be $\sim 8\%$.

(6) In the control time calculation we assumed that the average stretch changes with redshift in the manner prescribed by to Howell et al. 2007. If instead we recalculate the control time using the local stretch distribution in every redshift bin we find a somewhat lower control time in the highest redshift bin, leading to a $\sim 15\%$ increase in the estimated SN Ia rate for $1.0 \leq z < 1.4$. This is the dominant source of systematic uncertainty in this bin.

(7) The effect from the dust extinction of host galaxy is the most uncertain factor in the rate calculation. Recall that the sample used for the control calculation was based on SNe Ia uncorrected for dust extinction. This sample has a tail extending fainter than the $M_B \sim -18.0$ limit given by the minimal dust model. Thus, if the minimal dust model is taken as a reference, our rates decrease by 2.9%, 6.5%, and 11.9%, respectively, in each redshift bin. If instead extinction is much stronger than in our observed reference sample, our rates will be underestimated. Barbary et al. 2012 examined various dust models to investigate the extinction effects. According to their estimate, the most extreme dust model based on Hatano et al. 1998 ("dust model A" in their paper) resulted in up to ~ 50 changes in rates. Though our approach is different from Barbary et al. 2012 (i.e., they constructed SN Ia luminosity function from two parameter families), we examined how large the effect of this extreme dust model is. We simulated the control time in the same manner as Barbary et al. 2012 (see Figure 5.5), and estimated the differences to be +28.2%, +43.0%, and +47.8%, respectively, in each redshift bin. This result is consistent with the estimate of Barbary et al. 2012. We wish to include this as a systematic uncertainty, but we will report it separately in the systematics in Table 6.2 because, unlike our other systematics, the size of this systematic is highly speculative.

Several studies have indicated that the mean extinction increases with redshift (Mannucci et al. 2007, Holwerda 2008), so this issue may be most important in our highest redshift bin. Barbary et al. 2012 took a systematic uncertainty of 50% due to possible unaccounted for dust extinction. As examples, Figure 7.1 we show uncertainties of 50%, and that of the minimal dust model. We note that even though the extinction-corrected rate is uncertain, our measurement is a good representation of the rate to be used for predicting future SN searches at high redshift.

Table 6.2: Summary of systematic uncertainties in percent

Source items		$0.2 \leq z < 0.6$	$0.6 \leq z < 1.0$	$1.0 \leq z < 1.4$
(1) Ratio of IIP and IIL	num.	$^{+0.6}_{-0.3}$	$^{+0.8}_{-0.4}$	$^{+0.8}_{-0.4}$
(2) Luminosity function of SN II	num.	$^{+0.3}_{-0.6}$	$^{+1.4}_{-1.4}$	$^{+1.1}_{-0.9}$
(3) Discrimination of Type Ib/c	num.	$^{+22.6}_{-45.5}$	$^{+6.2}_{-12.4}$	$^{+0.4}_{-0.8}$
(4) AGN contamination	num.	$^{+0.0}_{-2.6}$	$^{+0.0}_{-2.6}$	$^{+0.0}_{-2.6}$
(5) CC SN contamination at high-z	num.	-	-	$^{+0.0}_{-8.0}$
(6) Evolution effect of SNe Ia	denom.	$^{+0.5}_{-0.0}$	$^{+3.2}_{-0.0}$	$^{+14.5}_{-0.0}$
(7) Extinction (known)	denom.	$^{+0.0}_{-2.9}$	$^{+0.0}_{-6.5}$	$^{+0.0}_{-11.9}$
Total known systematics		$^{+22.6}_{-45.7}$	$^{+7.1}_{-14.3}$	$^{+14.5}_{-14.7}$
(7)' Extinction (unknown)	denom.	$^{+50.0}_{-0.0}$	$^{+50.0}_{-0.0}$	$^{+50.0}_{-0.0}$
Total known and unknown dust systematics		$^{+54.9}_{-45.7}$	$^{+50.5}_{-14.3}$	$^{+52.1}_{-14.7}$

Note: "num." and "denom." refer to "numerator" and "denominator" of Equation 5.2.

Table 6.3: The SN Ia rates in SXDF

Redshift bin	z_{eff}[a]	SNR[b]	error(stat)	error(sys)[c]	Denom.[d]	N_{est}[e]	N_{II}[f]	$N_{Ib/c}$[g]	N_{comp}[h]	N_{Ia}[i]
$0.2 \leq z < 0.6$	0.44	0.262	$^{+0.229}_{-0.133}$	$^{+0.059+0.131}_{-0.120}$	13.179	4.46	0.61	1.18	0.78	$3.45^{+3.02}_{-1.76}$
$0.6 \leq z < 1.0$	0.80	0.839	$^{+0.230}_{-0.185}$	$^{+0.060+0.419}_{-0.120}$	24.199	22.48	2.52	1.88	2.23	$20.31^{+5.58}_{-4.47}$
$1.0 \leq z < 1.4$	1.14	0.705	$^{+0.239}_{-0.183}$	$^{+0.102+0.352}_{-0.103}$	20.442	12.09	0.91	0.09	3.32	$14.41^{+4.88}_{-3.75}$

[a] Effective redshift.

[b] Supernova rates are given in units $10^{-4}h_{70}^{3}yr^{-1}Mpc^{-3}$.

[c] Know systematic, followed by *ad hoc* due to dust.

[d] Denominator of Equation 5.2 uncertainty in units $10^{4}h_{70}^{-3}yrMpc^{3}$.

[e] Estimated numbers of observed SNe Ia (see section 5).

[f] Estimated number of contaminating Type II SNe.

[g] Estimated number of contaminating Type Ib/c SNe after removing two objects classified as SN Ib/c, i.e., 2-038 and 4-100

[h] Estimated number due to SN typing incompleteness.

[i] The number of SN Ia used in the rate calculation. The errors show statistical uncertainty.

Learn from yesterday, live for today, hope for tomorrow.
The important thing is not to stop questioning.

Albert Einstein (1879 - 1955)

7

Discussion and Application to the Future Survey

7.1 Discussion

7.1.1 SN Ia rate function

We fit the SN Ia rates with a power law (e.g.,Pain et al. 2002),

$$r_V(z) = r_0(1+z)^{\alpha}. \tag{7.1}$$

In this fit, we use the SN Ia rate obtained in redshift bins of $\Delta z = 0.1$. The best fit values of r_0 and α are

$$r_0 = 0.20^{+0.52}_{-0.16}(\text{stat.})^{+0.26}_{-0.07}(\text{syst.}) \times 10^{-4}\text{yr}^{-1}\text{Mpc}^{-3} \tag{7.2}$$

$$\alpha = 2.04^{+1.84}_{-1.96}(\text{stat.})^{+2.11}_{-0.86}(\text{syst.}) \tag{7.3}$$

We show the fit in Figure 7.1, and the expected number (N_{exp}) obtained by this fit in Figure 6.5.

7.1.2 Comparison with previous SN rate studies

Here, we check the consistency of our results with previous works (Figure 7.2). First, we compare nearby and mid-redshift SN Ia rates with our results. Li et al. 2011a derived a nearby SN Ia rate from 274 SNe Ia from the Lick Observatory Supernova Search (LOSS). Dilday et al. 2008 measured the nearby SN Ia rate at $z = 0.12$ using SNe Ia obtained by the SDSS-II SN survey. Recently, Perrett et al. 2012 determined the SN Ia rate in $0.1 \leq z \leq 1.1$ range with a very small uncertainty using the dataset of SNLS. These results are quite consistent with our fitted power-law curve. We also compare our measurements to those at similar or slightly higher redshifts. Graur et al. 2011 obtained high-redshift SN Ia rates in the Subaru Deep Field (SDF) using the multi-color SED fitting classification method

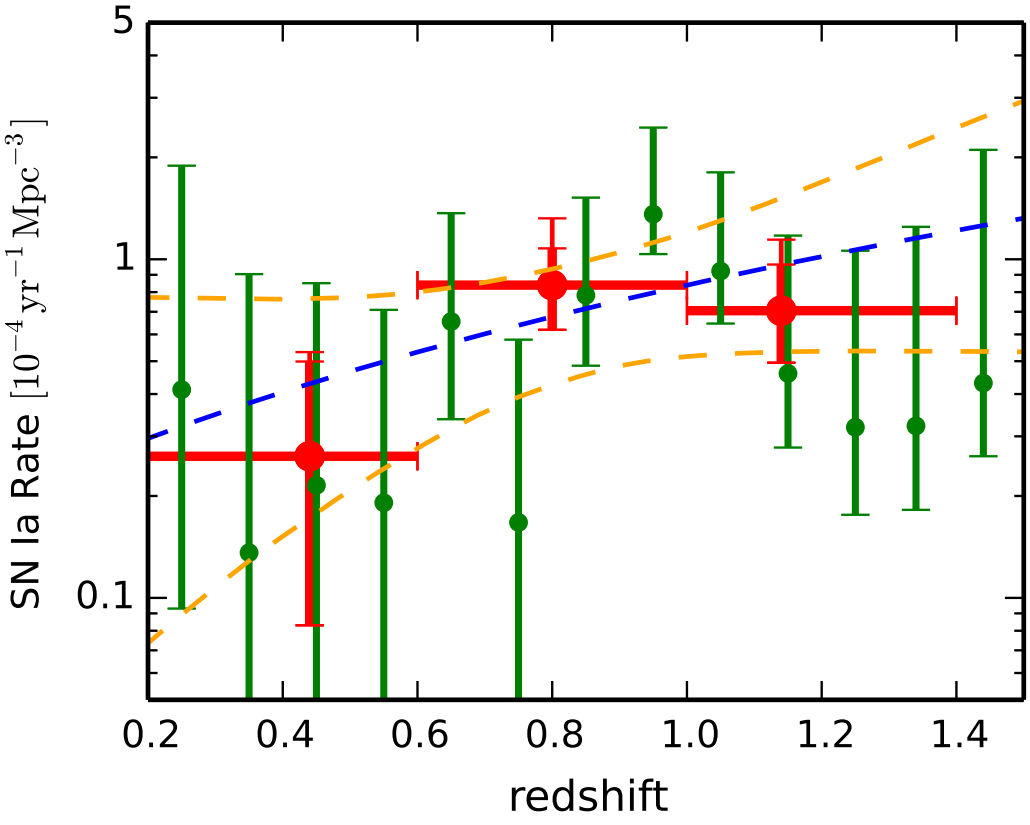

Figure 7.1: SN Ia rates in SXDF. *Red circles* show the rate in redshift bins of width $\Delta z = 0.4$, the same bin width used by Dahlen et al. 2008, calculated using Equation 5.2. *Green crosses* show the rate in redshift bins of width $\Delta z = 0.1$. For the upper error bar in $\Delta z = 0.4$ rates, the 2nd bar represents the observed + known systematics and the top bar represents the case of adding 50% *ad hoc* errors for the dust extinction. The *blue dashed line* shows $r_V(z) = r_0(1+z)^\alpha$, where $r_0 = 0.20^{+0.52}_{-0.16}(\mathrm{stat.})^{+0.26}_{-0.07}(\mathrm{syst.})\times10^{-4}\mathrm{yr}^{-1}\mathrm{Mpc}^{-3}$, and $\alpha = 2.04^{+1.84}_{-1.96}(\mathrm{stat.})^{+2.11}_{-0.86}(\mathrm{syst.})$. The orange dashed lines correspond to the $\pm1\sigma$ error region.

(Poznanski et al. 2007a). Graur et al. 2011 carried out very deep photometric observations and detected very high-redshift SNe Ia up to $z \sim 2.0$. They used one epoch with a reference epoch, and thus could not employ our light curve fitting method.

On the other hand, Dahlen et al. 2008 identified SNe with spectroscopic observations of GOODS SN survey, and measured SN Ia rates up to $z \sim 1.6$. Barbary et al. 2012 also derived SN Ia in this same redshift range from *Hubble Space Telescope* Cluster Supernova Survey. Even though these studies used different samples and techniques, our result and the results from these studies are consistent within the uncertainties.

In the highest redshift regime ($z \gtrsim 1.4$), the SN Ia rate is still uncertain. Graur et al. 2011 show that the SN Ia rate remains high beyond this redshift, while the SN Ia rates of Dahlen et al. 2008 are flat from $z \sim 0.8$ to $z \sim 1.2$, and then show a sharp decline at $z \sim 1.6$. As noted in section 6.4, Barbary et al. 2012 also found that different assumptions about host-galaxy dust extinction can induce systematic differences between measurements. It is therefore not yet clear if we have observed the peak in the volumetric SN Ia rate. According to galaxy studies (e.g., Hopkins & Beacom 2006), the peak of the cosmic star formation rate is at $z \sim 2$–3. Based on the peak in the cosmic star formation rate, we estimate that the delay time of SNe Ia at high redshifts is $\lesssim$ 2-3 Gyr. In order to determine whether SNe Ia with the shortest delay times are dominant or not, it is necessary to observe more samples at $z \geq 1.4$. This will be a key issue for future SN Ia surveys. One of these is the HSC transient survey, which will use *Hyper Suprime-Cam* on the Subaru Telescope. In this survey, ~ 100 SNe Ia will be detected with $z \gtrsim 1.0$, and thus provide useful information about the high-redshift SN Ia rates. At the same time, at low redshift it will construct a complete sample of SNe of all types, to faint luminosities and/or high values of dust extinction. Both the luminosity and extinction distributions will help in refining future rates calculations at high redshift.

We also check for consistency with Totani et al. 2008. They measured the delay time distribution of SNe Ia using the same variable object catalog of M08, but used a different method to select SNe Ia. They selected 65 SN Ia candidates showing significant spatial offset from the center of host galaxies with an old stellar population. However, not all of their candidates are SNe Ia due to the uncertainty in the selection method. They estimated that 82% of the 65 candidates were actually SNe Ia. We check their candidates by our light-curve fitting method. Out of the 65 candidates in Totani et al. 2008, 19 candidates have light curves with a sufficient number of epochs and sufficient signal-to-noise to perform our light-curve fitting. Fifteen candidates (79% of the 19 candidates) are identified as SNe Ia. This result indicates that our selection of SNe Ia is consistent with the selection of Totani et al. 2008.

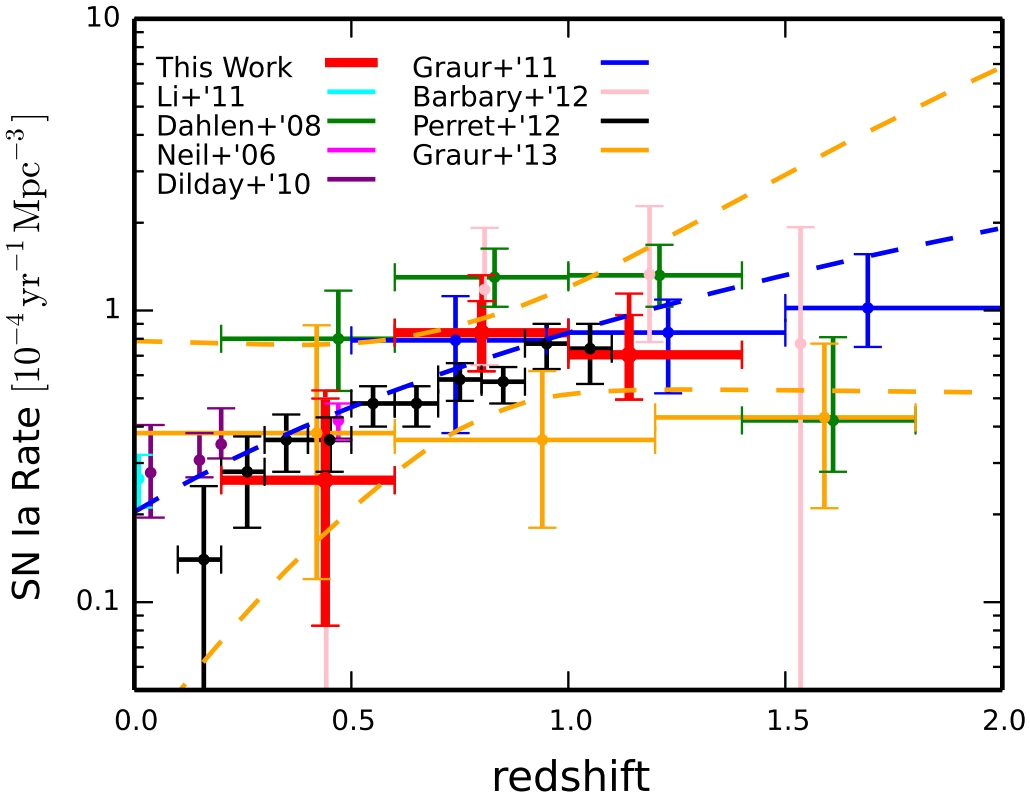

Figure 7.2: Comparison of various previous works with our results. The *red data* show our results. As in Figure 7.1, the systematic uncertainty is divided into observed + known systematics (2nd error bar), and the case of adding 50% *ad hoc* errors for the dust extinction (top error bar). The *cyan data* are the results by Li et al. 2011a. The *green data* are the results by Dahlen et al. 2008. The *pink data* is the result at $z = 0.47$ by Neill et al. 2006. The *purple data* is the result at $z = 0.12$ by Dilday et al. 2008. The *blue data* are the result of Graur et al. 2011. The *pink data* are the result of Barbary et al. 2012. The *black open triangles* are the result of Perrett et al. 2012.

Table 7.1: The published SN Ia rate measurements

Redshift	N_{Ia}	Rate [10^{-4} yr^{-1} Mpc^{-3}]	Refference
0.01	70^{a}	$0.183^{+0.046}_{-0.046}$	Cappellaro et al. 1999
< 0.019	274^{b}	$0.265^{+0.034+0.043}_{-0.033-0.043}$	Li et al. 2011a
0.0375	516^{c}	$0.278^{+0.112+0.015}_{-0.083-0.000}$	Dilday et al. 2010
0.1	516^{c}	$0.259^{+0.052+0.018}_{-0.044-0.001}$	Dilday et al. 2010
0.11	90^{d}	$0.247^{+0.029+0.016}_{-0.026-0.031}$	Graur & Maoz 2013
0.15	516^{c}	$0.307^{+0.038+0.035}_{-0.034-0.005}$	Dilday et al. 2010
0.15	1.95^{e}	$0.32^{+0.23+0.07}_{-0.23-0.06}$	Rodney & Tonry 2010
0.16	4^{f}	$0.16^{+0.10+0.07}_{-0.10-0.14}$ ^{g}	Perrett et al. 2012
0.2	17^{h}	$0.189^{+0.042+0.046}_{-0.034-0.045}$	Horesh et al. 2008
0.2	516^{c}	$0.348^{+0.032+0.082}_{-0.030-0.007}$	Dilday et al. 2010
0.25	516^{c}	$0.365^{+0.031+0.182}_{-0.028-0.012}$	Dilday et al. 2010
0.26	16^{e}	$0.32^{+0.08+0.07}_{-0.08-0.08}$ ^{g}	Perrett et al. 2012
0.3	31.05^{i}	$0.34^{0.16+0.21}_{-0.15-0.22}$	Botticella et al. 2008
0.3	516^{c}	$0.434^{+0.037+0.396}_{-0.034-0.016}$	Dilday et al. 2010
0.35	4.01^{e}	$0.34^{+0.19+0.07}_{0.19-0.03}$	Rodney & Tonry 2010
0.35	31^{f}	$0.41^{+0.07+0.06}_{-0.07-0.07}$ ^{g}	Perrett et al. 2012
0.42	2.0^{j}	$0.38^{+0.51+0.06}_{-0.25-0.06}$	Graur et al. 2013
0.44	**3.45**	$0.262^{+0.229+0.144}_{-0.133-0.120}$	**This Work**
0.442	0^{k}	$0.00^{+0.50+0.00}_{-0.00-0.00}$	Barbary et al. 2012
0.45	5.11^{e}	$0.31^{+0.15+0.12}_{-0.15-0.04}$	Rodney & Tonry 2010
0.45	42^{f}	$0.41^{+0.07+0.05}_{-0.07-0.06}$ ^{g}	Perrett et al. 2012

[a] SNe sample from Asiago, Crimea, OCA, Calan/Tololo, and Evans ' SN searches

[b] SNe sample within 60Mpc from Lick Observatory Supernova Search (LOSS)

[c] 516 SNe Ia at $z < 0.5$ from SDSS-II Supernova Survey sample. This is the extended result of Dilday et al. 2008, which measured SN Ia rate at $z = 0.09$ with 17 SNe Ia.

[d] SNe Ia recovered from $\sim$ 700000 galaxy spectra in SDSS

[e] $\sim$ 130 SN Ia candidtates in $0.1 < z < 1$ from the IfA Deep Survey

[f] SNe from the Supernova Legacy Survey (SNLS). About $\sim$ 40% of sample have spectroscopic confirmation.

[g] The rates are scaled +15% assuming 91bg-like fraction in LOSS (see section 6 of Perrett et al. 2012)

[h] SNe sample from SDSS-I

[i] SNe sample from the Southern inTermediate Redshift ESO Supernova Search (STRESS)

[j] SNe sample from the Cluster Lensing And Supernova survey with Hubble (CLASH)

[k] SNe from HST Cluster Supernova Survey

Table 7.1: The published SN Ia rate measurements (Contd.)

Redshift	N_{Ia}	Rate [10^{-4} yr^{-1} Mpc^{-3}]	Refference
0.55	6.49^{e}	$0.32^{+0.14+0.07}_{-0.14-0.07}$	Rodney & Tonry 2010
0.55	72^{f}	$0.55^{+0.07+0.05}_{-0.07-0.06}$ ^{g}	Perrett et al. 2012
0.62	7^{n}	$1.29^{+0.88+0.27}_{-0.57-0.28}$	Melinder et al. 2012
0.65	10.09^{e}	$0.49^{+0.17+0.14}_{-0.17-0.08}$	Rodney & Tonry 2010
0.65	91^{f}	$0.55^{+0.06+0.05}_{-0.06-0.07}$ ^{g}	Perrett et al. 2012
0.74	20.3^{o}	$0.79^{+0.33}_{-0.41}$	Graur et al. 2011
0.75	14.29^{e}	$0.68^{+0.21+0.23}_{-0.21-0.14}$	Rodney & Tonry 2010
0.75	110^{f}	$0.67^{+0.07+0.06}_{-0.07-0.08}$ ^{g}	Perrett et al. 2012
0.80	**20.31**	$0.839^{+0.230+0.423}_{-0.185-0.120}$	**This Work**
0.807	5.25^{k}	$1.18^{+0.60+0.44}_{-0.45-0.28}$	Barbary et al. 2012
0.83	25^{m}	$1.30^{+0.33+0.73}_{-0.27-0.51}$	Dahlen et al. 2008
0.85	128^{f}	$0.66^{+0.06+0.07}_{-0.06-0.08}$ ^{g}	Perrett et al. 2012
0.94	5.1^{j}	$0.36^{+0.24+0.10}_{-0.15-0.10}$	Graur et al. 2013
0.95	141^{f}	$0.89^{+0.09+0.12}_{-0.09-0.14}$ ^{g}	Perrett et al. 2012
1.05	50^{f}	$0.85^{+0.14+0.12}_{-0.14-0.15}$ ^{g}	Perrett et al. 2012
1.14	**14.41**	$0.705^{+0.239+0.366}_{-0.183-0.103}$	**This Work**
1.187	5.63^{k}	$1.33^{+0.65+0.69}_{-0.49-0.26}$	Barbary et al. 2012
1.21	20^{m}	$1.32^{+0.36+0.38}_{-0.29-0.32}$	Dahlen et al. 2008
1.23	27.0^{o}	$0.84^{+0.25}_{-0.28}$	Graur et al. 2011
1.535	1.12^{k}	$0.77^{+1.07+0.44}_{-0.54-0.77}$	Barbary et al. 2012
1.59	3.9^{j}	$0.43^{+0.34+0.04}_{-0.21-0.08}$	Graur et al. 2013
1.61	3^{m}	$0.42^{+0.39+0.19}_{-0.23-0.14}$	Dahlen et al. 2008
1.69	10.0^{o}	$1.02^{+0.54}_{-0.37}$	Graur et al. 2011
2.1	0^{j}	< 1.7	Graur et al. 2013

^{l} SNe derived from the first two yrs of SNLS

^{m} SNe from HST ACS imaging of the two GOODS fields

^{n} SNe from the Stockholm VIMOS Supernova Survey (SVISS)

^{o} SN servey program in the Subaru Deep Field (SDF). This is the updated version of Poznanski et al. 2007b

7.2 Application to the Future Survey

As noted in section 1.4, several large systematic surveys have been conducted. In the near future, deeper and wider surveys are going to be carried out. Here we briefly summarize prospect to the future surveys, especially in the context of SN Ia rate and application of the method used in this thesis.

7.2.1 Hyper Suprime-Cam Transient Survey

This thesis is based on the analysis of Suprime-Cam (SC) imaging observation. From 2013, the updated CCD camera, the Hyper Suprime-Cam (HSC), is available. HSC has a wide Field of View of 1.77 deg^2 ($\sim$ 7 times larger than SC) and, coupled with the 8.2m Subaru Telescope, is the most powerful survey imaging camera in the world. Using this instrument, the deep imaging survey (HSC survey [6]) is scheduled to start from early 2014. The survey include repeat imaging observation to detect transient objects such as SNe, AGNs, and variable stars. The survey field is wide and deep (Deep field: 27 deg^2, $r \simeq 27$; Ultradeep field: 3.5 deg^2, $r \simeq 28$) enough to detect many SNe Ia at $z > 1$. Furthermore, HSC survey is carried out multi-band ($grizy$) imaging (see Figure 7.4 for the comparison with SXDS photometries). Recall that SN Ia rate from SXDS has a constraint that most of transients were observed only in i'-band, whereas, in HSC, SN candidates are much safely classified using their photometries. The SNe sample constructed from HSC survey with good quality and enough color information will provide us a good opportunity to investigate statistical nature of SNe at high-redshift. Figure 7.3 (top panel) shows the expected number of SNe Ia with $S/N > 5.0$. The comparison with the SXDS is obvious.

7.2.2 SN Ia rate studies in HSC

Figure 7.5 is the simulated SN Ia rate estimate in HSC survey (only statistical error are considered). Note that all these data have at least three-band observation, and thus, the systematic errors caused by CC SNe contamination will be much reduced at $z < 1$. Even more, the deep imaging will enable us to study SN Ia rates above $z \sim 1.4$, in which we could not reach in this work.

Besides HSC transient survey, one may expect to detect very high redshift SNe Ia ($z > 1.8$) using this instrument. Figure 7.3 (bottom panel) shows the expected number of SNe Ia under the assumption of 6-hr ultradeep z-band imaging and two-week cadence. In this survey parameter, though only single z-band imaging is assumed, about 10 SNe Ia are detectable (also the possibility of detecting SN Ia at $z > 2.0$ is not small).

7.2.3 Other plannes transient surveys

Considering these results, the rate estimates will be improved in HSC era. Possible competitor will be the Dark Energy Survey[7]. This survey uses the prime focus Dark Energy Camera (DECam) on the Blanco 4-m telescope at Cerro Tololo Inter-American Observatory (CTIO). The DECam has a 3 deg^2 field of view, and the survey began in August 2013. The

[6] http://www.naoj.org/Projects/HSC/index.html

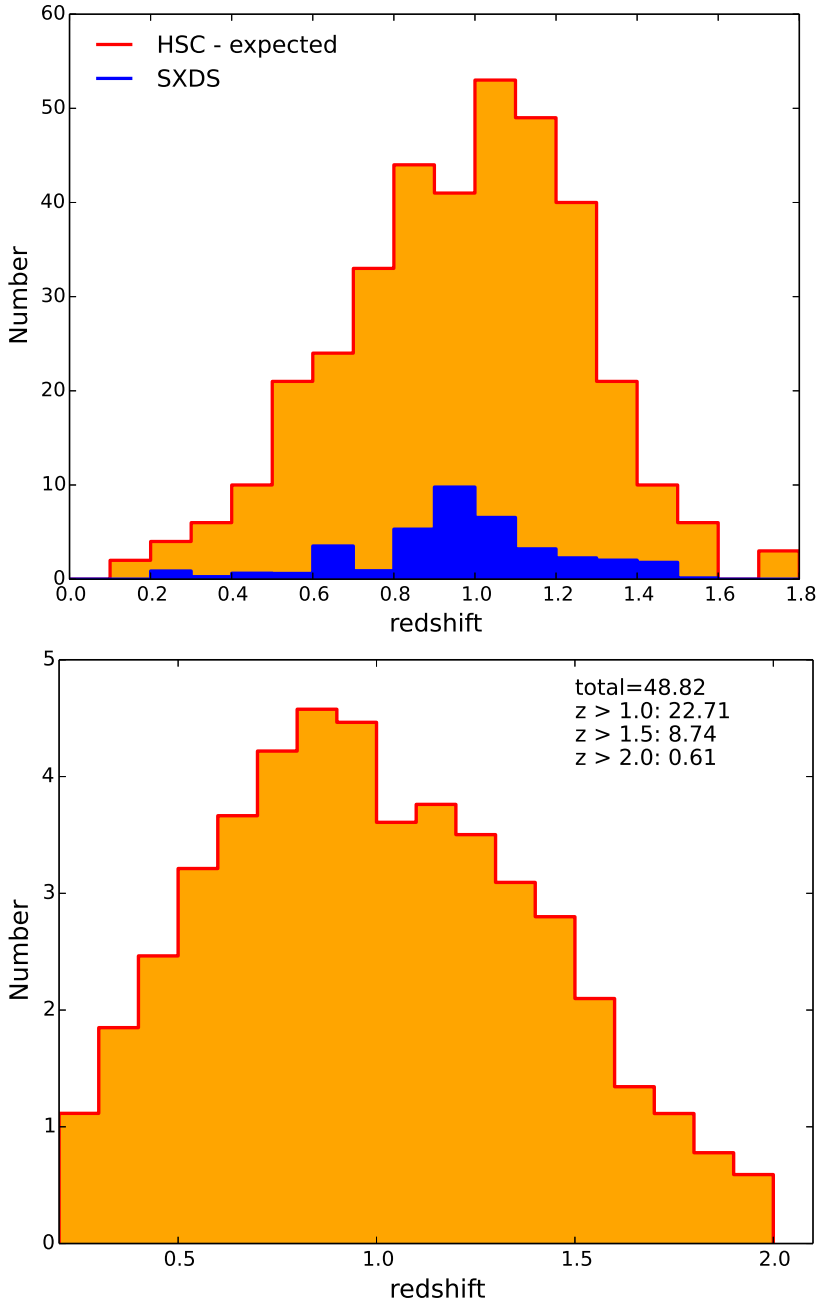

Figure 7.3: *Top*: The expected redshift distribution of SNe Ia observable in HSC transient survey. About 100 SNe Ia above $z = 1.0$ are available with good photometric quality ($S/N >$ 5.0 in at least three optical broad bands). In total, $\sim$ 300 SNe Ia will be detected in $0.2 < z < 1.8$. *Bottom*: The expected redshift distribution of SNe Ia assuming 6-hr z'-band imaging in two-week cadence. HSC have an enough power to detect SNe Ia at $z > 1.8$.

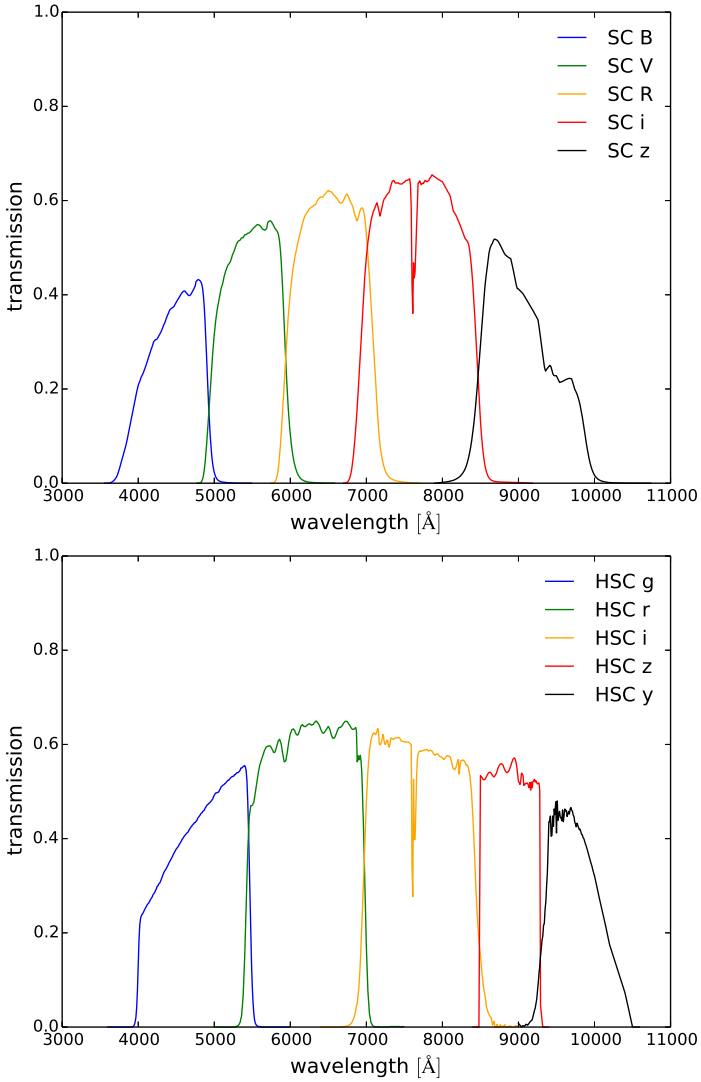

Figure 7.4: The comparison of filter passbands between Suprime-Cam and Hyper Suprime-Cam. The filter of HSC survey have much sensitivity to redder side, meaning that high-redshift objects are more detectable.

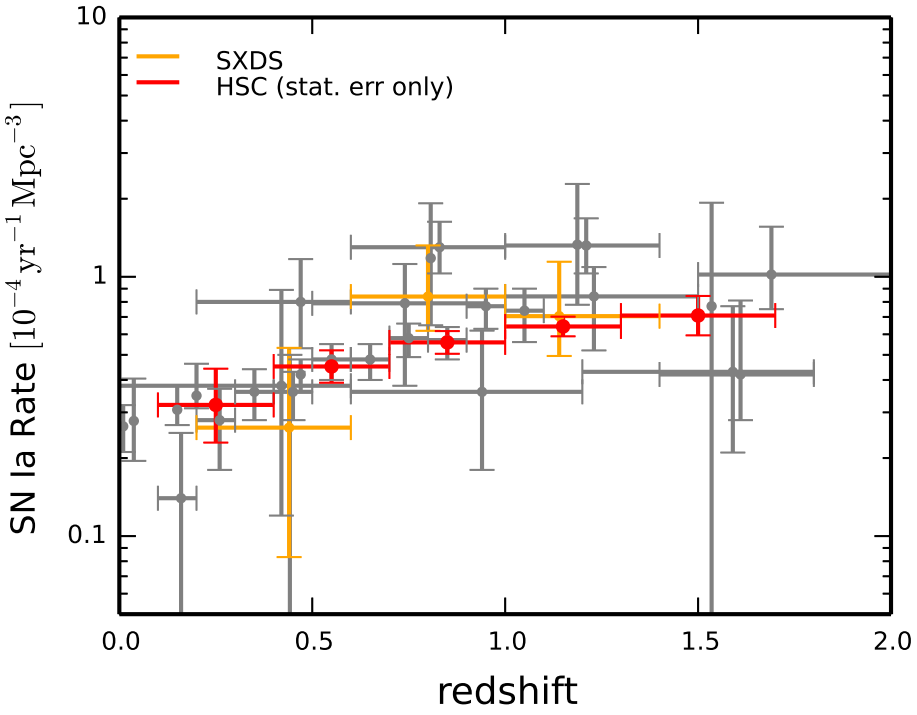

Figure 7.5: The expected SN Ia rates constraint in HSC transient survey (*the red points*; only statistical errors are plotted). The result of this thesis is shown in *the orange points*, and *the gray points* represent published SN Ia rate measurements summarized in Table 7.1.

DES supernova search will cover 30 deg^2 in *griz* with 5-day cadence throughout each DES observation season. They will discover 4000 SNe Ia over the redshift range $0.5 < z < 1.2$ (also about 20% of DES SNe Ia will be followed up with real-time spectroscopy from other telescopes). Hence, in the near future, DES and other transient surveys (e.g., Pan-STARRS, iPTF) will investigate $z < 1.2$ SNe with very rich sample, and HSC and HST will target the $z > 1.4$ universe. After that, the Large Synoptic Survey Telescope (LSST[8]) and the Wide Field Infrared Survey Telescope (WFIRST[9]) will lead the transient science. LSST is a wide-field, ground-based telescope, designed to image a substantial fraction of the sky in six optical bands every few nights. According to their plan, at least 500 SNe Ia per season are discovered, and LSST will give tens of thousands of well-measured SNe Ia light curves up to $z \sim 1$ over the full ten-year survey. WFIRST is the space telescope which IR camera with a 0.281 deg^2 field of view is installed. This survey will confirm 2700 SNe Ia over the redshift range $z = 0.1 - 1.7$.

[7] http://www.darkenergysurvey.org/reports/proposal-standalone.pdf
[8] http://www.lsst.org/lsst/
[9] http://wfirst.gsfc.nasa.gov/

He is the happiest man who can set the end of his life in connection with the beginning.

Johann Wolfgang von Goethe (1749 - 1832)

8 Summary

In this thesis, a new measurements of the high-redshift SN Ia rate has been presented, using objects selected from the SXDS variable object survey. Each variable object was observed in the i'-band at 5-7 epochs for about two months, which is sufficient to build lightcurves. The variable objects are classified by comparing their lightcurves with template light curves. Out of 1040 variable objects, 44 SN I candidates are selected. After excluding SNe Ia beyond $z = 1.4$, and using ancillary data to exclude two likely AGNs and two likely SNe Ib/c, we construct a sample of 39 SNe Ia that are then used to derive the rates. Using simulated lightcurves, we correct the number of SN Ia candidates for incompleteness due to misclassification. The control time is also calculated with artificial SN light curves. Finally, we derive the SN Ia rate in several redshift bins between $0.2 < z < 1.4$. Our rate measurements are the most distant yet obtained using lightcurves from ground-based telescopes. A number of systematic factors affecting the rates are also examined carefully. In the low redshift bin, chief among these is the contamination from core-collapse SN because for most of object we lack color information. In the higher redshift bin, the correction for extinction is the dominant systematics. However, even using conservative estimates of the systematic error, the statistical errors are comparable in size. Improved systematics control will be much more important for future rates measurements based on much larger samples.

Our SNe Ia rates are consistent with the rates that have been derived in earlier studies. Up to $z \sim 0.8$, the rate increase and may then flatten at higher redshift. The SDXS survey was relatively inefficient at finding SNe Ia beyond $z \sim 1.4$, so we are unable to either confirm or refute the downturn that has been seen in searches done with HST beyond this redshift. The upcoming HSC transient survey is considerably more efficient in finding SNe beyond $z \sim 1.4$ than the SXDS survey, thus offering us the possibility of measuring the rates of SNe Ia in this important redshift range with unprecedented precision.

A

The results of light curvefitting

Here we summarize all the lightcurve fitting results for 39 SN Ia candidates in SXDS. In each object, left panel show the fitting light curves (solid lines) with observed light curve (black points). In the middle panel, the probability distribution of beeing certain SN types, i.e. $P_{\rm type}(z)$, is plotted as a function of redshift. The inserted four numbers are the allocation to the each redshift bins (see the discussion in section 4.6). In the right panel, the best fit parameters (redshift, stretch factor, absolute magnitude at the peak, and chi-square of the fitting) are reported.

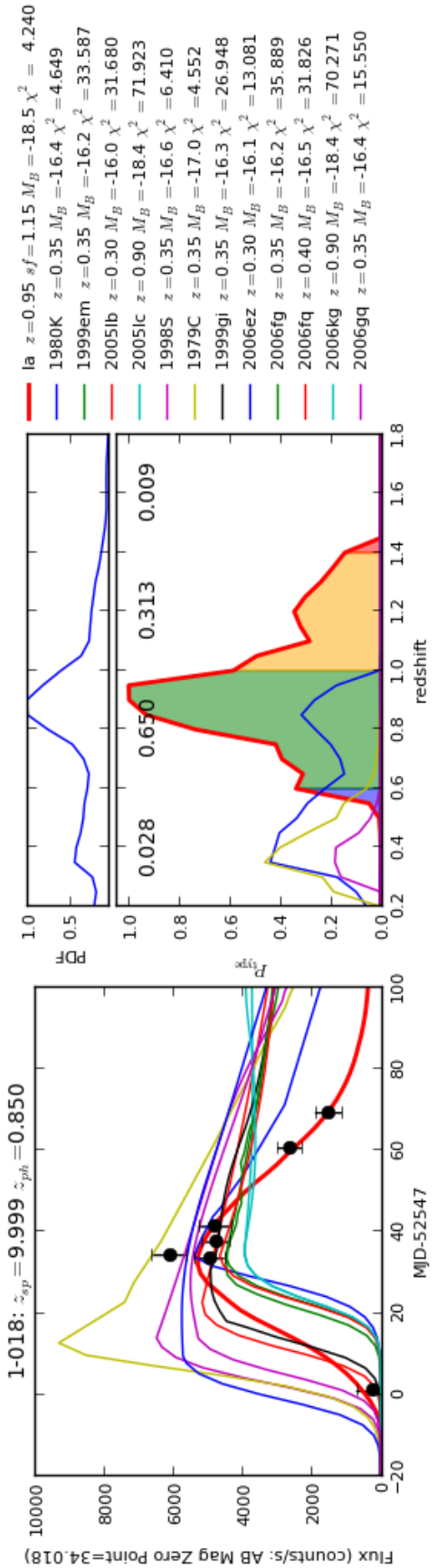
Ia z=0.95 sf=1.15 M_B=-18.5 χ^2 = 4.240
1980K z=0.35 M_B=-16.4 χ^2 =4.649
1999em z=0.35 M_B=-16.2 χ^2 =33.587
2005lb z=0.30 M_B=-16.0 χ^2 =31.680
2005lc z=0.90 M_B=-18.4 χ^2 =71.923
1998S z=0.35 M_B=-16.6 χ^2 =6.410
1979C z=0.35 M_B=-17.0 χ^2 =4.552
1999gi z=0.35 M_B=-16.3 χ^2 =26.948
2006ez z=0.30 M_B=-16.1 χ^2 =13.081
2006fg z=0.35 M_B=-16.2 χ^2 =35.889
2006fq z=0.40 M_B=-16.5 χ^2 =31.826
2006kg z=0.90 M_B=-18.4 χ^2 =70.271
2006gq z=0.35 M_B=-16.4 χ^2 =15.550
0.028
0.650
0.313
0.009
PDF
P_{type}
redshift
1-018: z_{sp}=9.999 z_{ph}=0.850
MJD-52547
Flux (counts/s: AB Mag Zero Point=34.018)

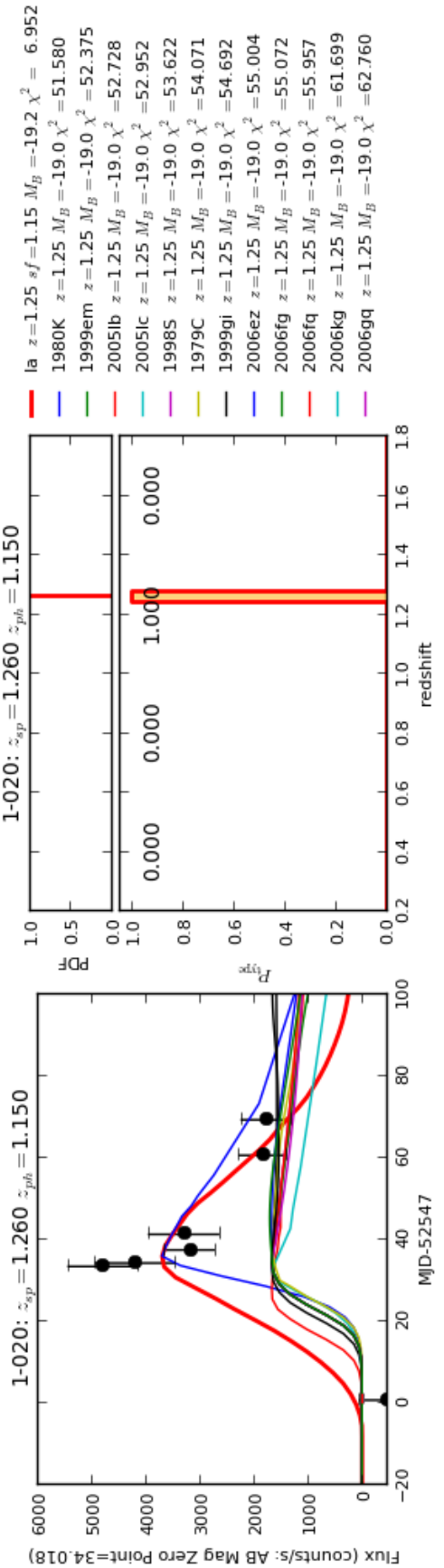
Ia z=1.25 sf=1.15 M_B=-19.2 χ^2 = 6.952
1980K z=1.25 M_B=-19.0 χ^2 =51.580
1999em z=1.25 M_B=-19.0 χ^2 =52.375
2005lb z=1.25 M_B=-19.0 χ^2 =52.728
2005lc z=1.25 M_B=-19.0 χ^2 =52.952
1998S z=1.25 M_B=-19.0 χ^2 =53.622
1979C z=1.25 M_B=-19.0 χ^2 =54.071
1999gi z=1.25 M_B=-19.0 χ^2 =54.692
2006ez z=1.25 M_B=-19.0 χ^2 =55.004
2006fg z=1.25 M_B=-19.0 χ^2 =55.072
2006fq z=1.25 M_B=-19.0 χ^2 =55.957
2006kg z=1.25 M_B=-19.0 χ^2 =61.699
2006gq z=1.25 M_B=-19.0 χ^2 =62.760
0.000
1.000
0.000
0.000
PDF
P_{type}
redshift
1-020: z_{sp}=1.260 z_{ph}=1.150
MJD-52547
Flux (counts/s: AB Mag Zero Point=34.018)

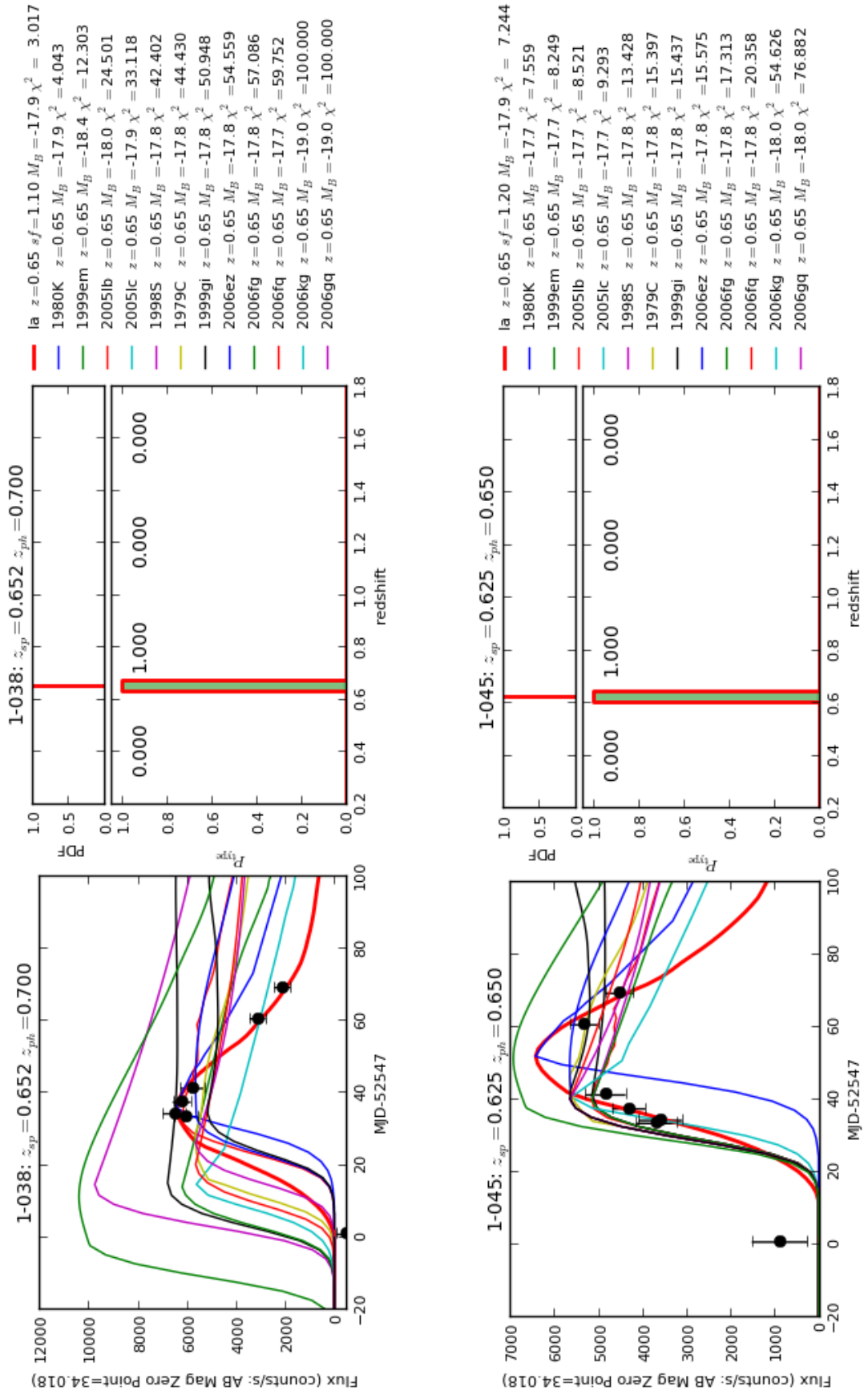
Ia z=0.65 sf=1.10 M_B=-17.9 χ^2= 3.017
1980K z=0.65 M_B=-17.9 χ^2=4.043
1999em z=0.65 M_B=-18.4 χ^2=12.303
2005lb z=0.65 M_B=-18.0 χ^2=24.501
2005lc z=0.65 M_B=-17.9 χ^2=33.118
1998S z=0.65 M_B=-17.8 χ^2=42.402
1979C z=0.65 M_B=-17.8 χ^2=44.430
1999gi z=0.65 M_B=-17.8 χ^2=50.948
2006ez z=0.65 M_B=-17.8 χ^2=54.559
2006fg z=0.65 M_B=-17.8 χ^2=57.086
2006fq z=0.65 M_B=-17.7 χ^2=59.752
2006kg z=0.65 M_B=-19.0 χ^2=100.000
2006gq z=0.65 M_B=-19.0 χ^2=100.000
1-038: z_{sp}=0.652 z_{ph}=0.700
PDF
P_{type}
redshift
0.000
1.000
0.000
0.000
1-038: z_{sp}=0.652 z_{ph}=0.700
MJD-52547
Flux (counts/s: AB Mag Zero Point=34.018)
Ia z=0.65 sf=1.20 M_B=-17.9 χ^2= 7.244
1980K z=0.65 M_B=-17.7 χ^2=7.559
1999em z=0.65 M_B=-17.7 χ^2=8.249
2005lb z=0.65 M_B=-17.7 χ^2=8.521
2005lc z=0.65 M_B=-17.7 χ^2=9.293
1998S z=0.65 M_B=-17.8 χ^2=13.428
1979C z=0.65 M_B=-17.8 χ^2=15.397
1999gi z=0.65 M_B=-17.8 χ^2=15.437
2006ez z=0.65 M_B=-17.8 χ^2=15.575
2006fg z=0.65 M_B=-17.8 χ^2=17.313
2006fq z=0.65 M_B=-17.8 χ^2=20.358
2006kg z=0.65 M_B=-18.0 χ^2=54.626
2006gq z=0.65 M_B=-18.0 χ^2=76.882
1-045: z_{sp}=0.625 z_{ph}=0.650
PDF
P_{type}
redshift
0.000
1.000
0.000
0.000
1-045: z_{sp}=0.625 z_{ph}=0.650
MJD-52547
Flux (counts/s: AB Mag Zero Point=34.018)

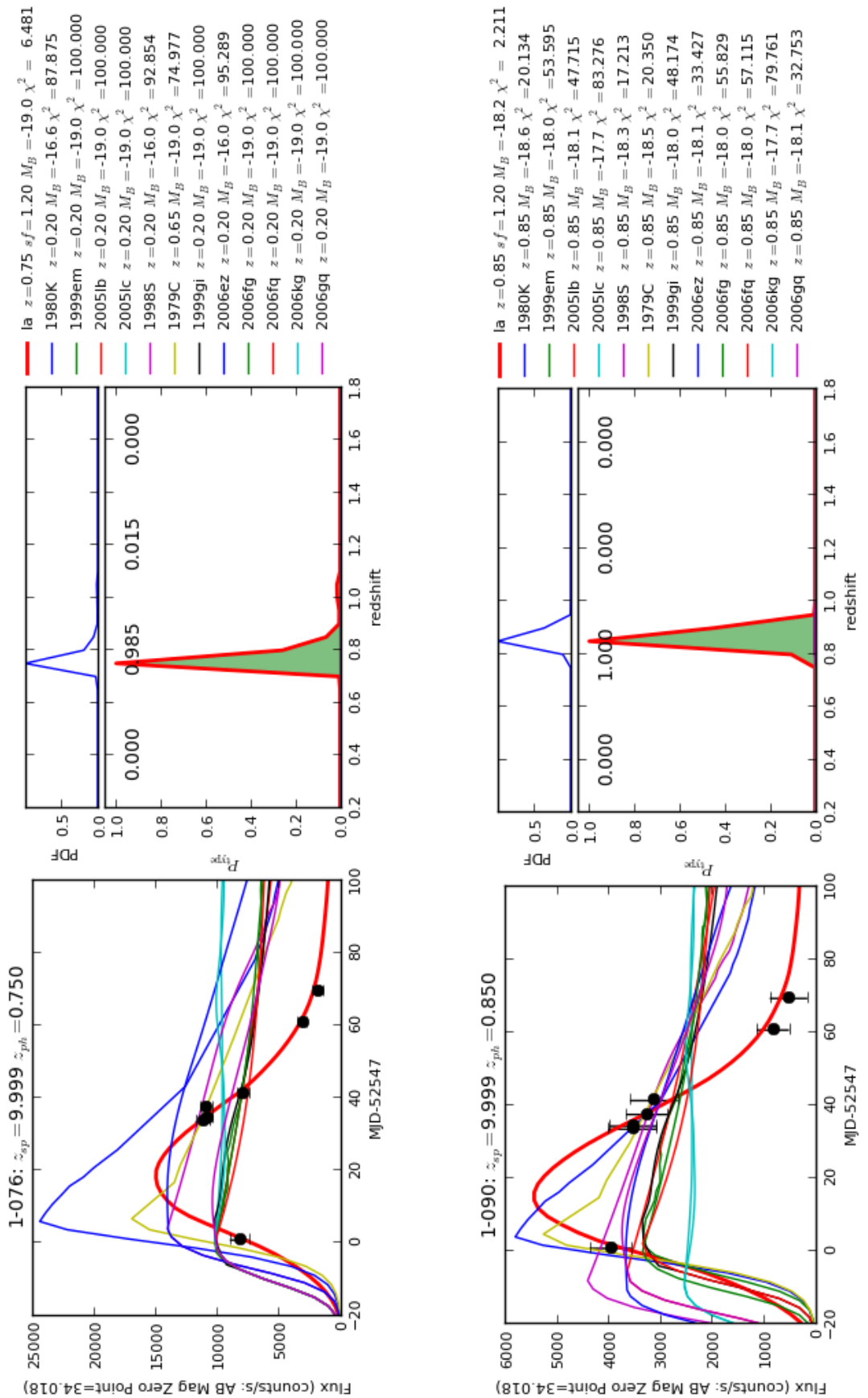
1-076: z_{sp}=9.999 z_{ph}=0.750
1-090: z_{sp}=9.999 z_{ph}=0.850
Flux (counts/s: AB Mag Zero Point=34.018)
MJD-52547
P_{type}
PDF
redshift
Ia z=0.75 sf=1.20 M_B=-19.0 χ^2= 6.481
1980K z=0.20 M_B=-16.6 χ^2=87.875
1999em z=0.20 M_B=-19.0 χ^2=100.000
2005lb z=0.20 M_B=-19.0 χ^2=100.000
2005lc z=0.20 M_B=-19.0 χ^2=100.000
1998S z=0.20 M_B=-16.0 χ^2=92.854
1979C z=0.65 M_B=-19.0 χ^2=74.977
1999gi z=0.20 M_B=-19.0 χ^2=100.000
2006ez z=0.20 M_B=-16.0 χ^2=95.289
2006fq z=0.20 M_B=-19.0 χ^2=100.000
2006fq z=0.20 M_B=-19.0 χ^2=100.000
2006kg z=0.20 M_B=-19.0 χ^2=100.000
2006gq z=0.20 M_B=-19.0 χ^2=100.000
Ia z=0.85 sf=1.20 M_B=-18.2 χ^2= 2.211
1980K z=0.85 M_B=-18.6 χ^2=20.134
1999em z=0.85 M_B=-18.0 χ^2=53.595
2005lb z=0.85 M_B=-18.1 χ^2=47.715
2005lc z=0.85 M_B=-17.7 χ^2=83.276
1998S z=0.85 M_B=-18.3 χ^2=17.213
1979C z=0.85 M_B=-18.5 χ^2=20.350
1999gi z=0.85 M_B=-18.0 χ^2=48.174
2006ez z=0.85 M_B=-18.1 χ^2=33.427
2006fq z=0.85 M_B=-18.0 χ^2=55.829
2006fq z=0.85 M_B=-18.0 χ^2=57.115
2006kg z=0.85 M_B=-17.7 χ^2=79.761
2006gq z=0.85 M_B=-18.1 χ^2=32.753

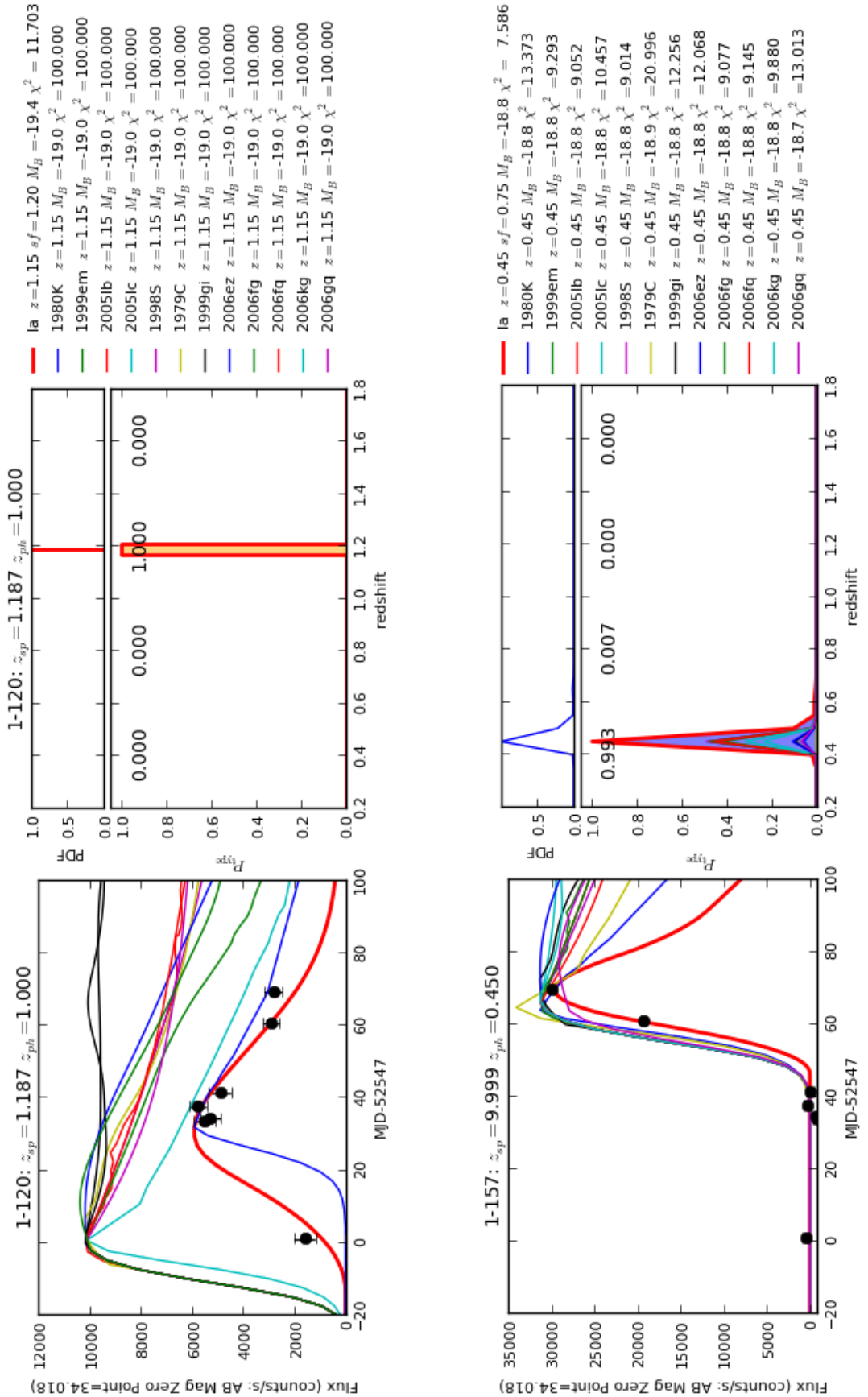
Ia z=1.15 sf=1.20 M_B=-19.4 χ^2 = 11.703
1980K z=1.15 M_B=-19.0 χ^2 =100.000
1999em z=1.15 M_B=-19.0 χ^2 =100.000
2005lb z=1.15 M_B=-19.0 χ^2 =100.000
2005lc z=1.15 M_B=-19.0 χ^2 =100.000
1998S z=1.15 M_B=-19.0 χ^2 =100.000
1979C z=1.15 M_B=-19.0 χ^2 =100.000
1999gi z=1.15 M_B=-19.0 χ^2 =100.000
2006ez z=1.15 M_B=-19.0 χ^2 =100.000
2006fg z=1.15 M_B=-19.0 χ^2 =100.000
2006fq z=1.15 M_B=-19.0 χ^2 =100.000
2006kg z=1.15 M_B=-19.0 χ^2 =100.000
2006gq z=1.15 M_B=-19.0 χ^2 =100.000
1-120: z_{sp}=1.187 z_{ph}=1.000
PDF
P_{type}
redshift
MJD-52547
Flux (counts/s: AB Mag Zero Point=34.018)
Ia z=0.45 sf=0.75 M_B=-18.8 χ^2 = 7.586
1980K z=0.45 M_B=-18.8 χ^2 =13.373
1999em z=0.45 M_B=-18.8 χ^2 =9.293
2005lb z=0.45 M_B=-18.8 χ^2 =9.052
2005lc z=0.45 M_B=-18.8 χ^2 =10.457
1998S z=0.45 M_B=-18.8 χ^2 =9.014
1979C z=0.45 M_B=-18.9 χ^2 =20.996
1999gi z=0.45 M_B=-18.8 χ^2 =12.256
2006ez z=0.45 M_B=-18.8 χ^2 =12.068
2006fg z=0.45 M_B=-18.8 χ^2 =9.077
2006fq z=0.45 M_B=-18.8 χ^2 =9.145
2006kg z=0.45 M_B=-18.8 χ^2 =9.880
2006gq z=0.45 M_B=-18.7 χ^2 =13.013
1-157: z_{sp}=9.999 z_{ph}=0.450
PDF
P_{type}
redshift
MJD-52547
Flux (counts/s: AB Mag Zero Point=34.018)

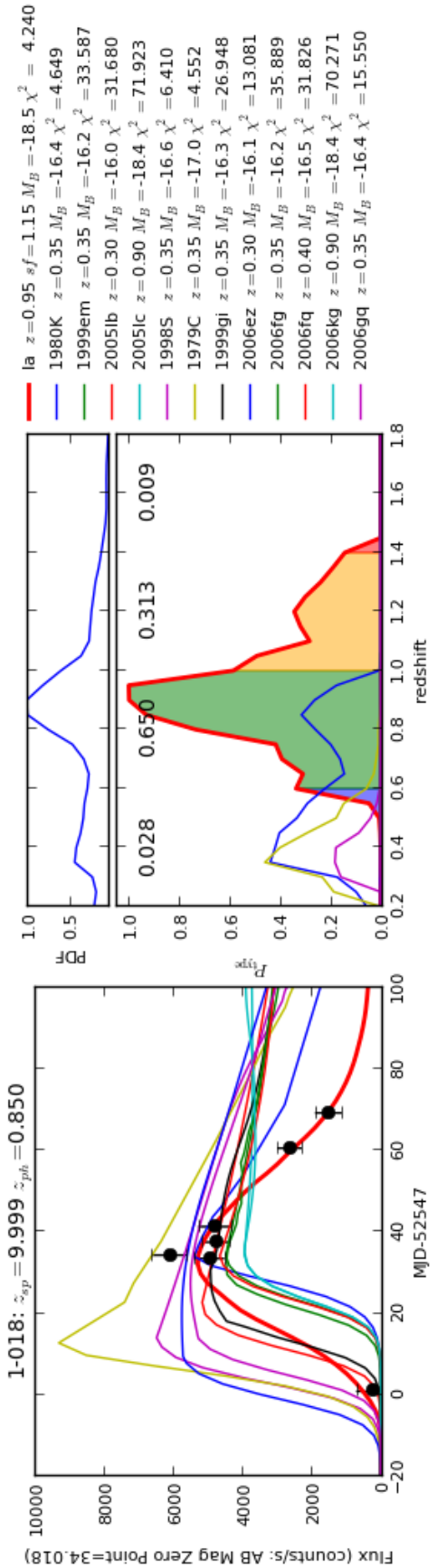
Ia z=0.95 sf=1.15 M_B=-18.5 χ^2 = 4.240
1980K z=0.35 M_B=-16.4 χ^2 =4.649
1999em z=0.35 M_B=-16.2 χ^2 =33.587
2005lb z=0.30 M_B=-16.0 χ^2 =31.680
2005lc z=0.90 M_B=-18.4 χ^2 =71.923
1998S z=0.35 M_B=-16.6 χ^2 =6.410
1979C z=0.35 M_B=-17.0 χ^2 =4.552
1999gi z=0.35 M_B=-16.3 χ^2 =26.948
2006ez z=0.30 M_B=-16.1 χ^2 =13.081
2006fg z=0.35 M_B=-16.2 χ^2 =35.889
2006fq z=0.40 M_B=-16.5 χ^2 =31.826
2006kg z=0.90 M_B=-18.4 χ^2 =70.271
2006gq z=0.35 M_B=-16.4 χ^2 =15.550
PDF
P_{type}
0.028
0.650
0.313
0.009
redshift
1-018: z_{sp}=9.999 z_{ph}=0.850
MJD-52547
Flux (counts/s: AB Mag Zero Point=34.018)

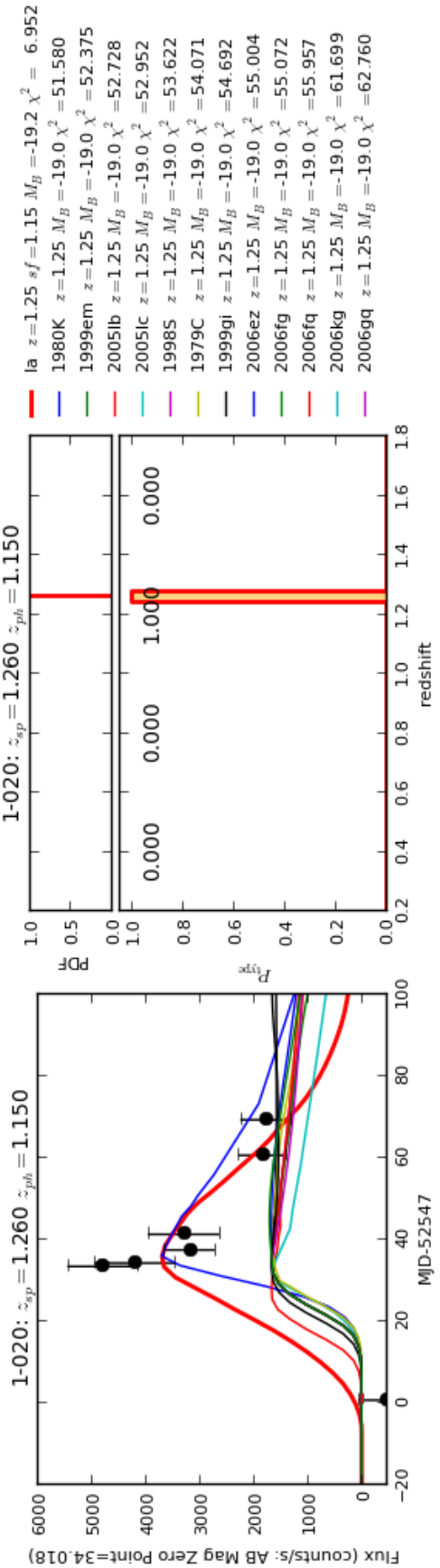
Ia z=1.25 sf=1.15 M_B=-19.2 χ^2 = 6.952
1980K z=1.25 M_B=-19.0 χ^2 =51.580
1999em z=1.25 M_B=-19.0 χ^2 =52.375
2005lb z=1.25 M_B=-19.0 χ^2 =52.728
2005lc z=1.25 M_B=-19.0 χ^2 =52.952
1998S z=1.25 M_B=-19.0 χ^2 =53.622
1979C z=1.25 M_B=-19.0 χ^2 =54.071
1999gi z=1.25 M_B=-19.0 χ^2 =54.692
2006ez z=1.25 M_B=-19.0 χ^2 =55.004
2006fg z=1.25 M_B=-19.0 χ^2 =55.072
2006fq z=1.25 M_B=-19.0 χ^2 =55.957
2006kg z=1.25 M_B=-19.0 χ^2 =61.699
2006gq z=1.25 M_B=-19.0 χ^2 =62.760
PDF
P_{type}
0.000
1.000
redshift
1-020: z_{sp}=1.260 z_{ph}=1.150
MJD-52547
Flux (counts/s: AB Mag Zero Point=34.018)

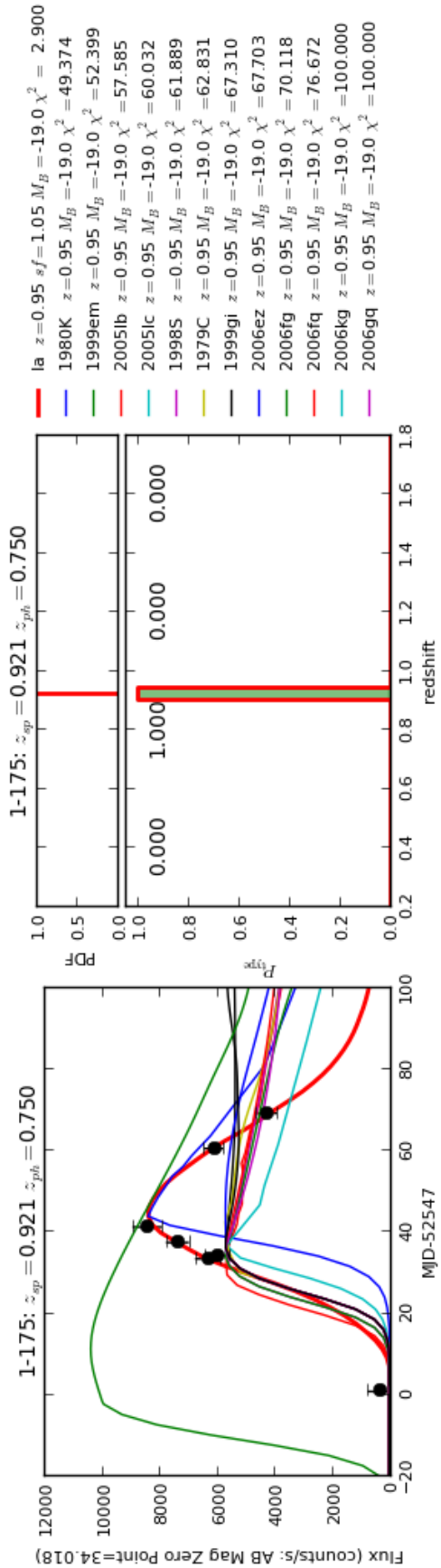
Ia z=0.95 sf=1.05 M_B=-19.0 χ^2= 2.900
1980K z=0.95 M_B=-19.0 χ^2=49.374
1999em z=0.95 M_B=-19.0 χ^2=52.399
2005lb z=0.95 M_B=-19.0 χ^2=57.585
2005lc z=0.95 M_B=-19.0 χ^2=60.032
1998S z=0.95 M_B=-19.0 χ^2=61.889
1979C z=0.95 M_B=-19.0 χ^2=62.831
1999gi z=0.95 M_B=-19.0 χ^2=67.310
2006ez z=0.95 M_B=-19.0 χ^2=67.703
2006fg z=0.95 M_B=-19.0 χ^2=70.118
2006fq z=0.95 M_B=-19.0 χ^2=76.672
2006kg z=0.95 M_B=-19.0 χ^2=100.000
2006gq z=0.95 M_B=-19.0 χ^2=100.000
1-175: z_{sp}=0.921 z_{ph}=0.750
PDF
P_{type}
redshift
0.000
1.000
0.000
0.000
1-175: z_{sp}=0.921 z_{ph}=0.750
MJD-52547
Flux (counts/s: AB Mag Zero Point=34.018)

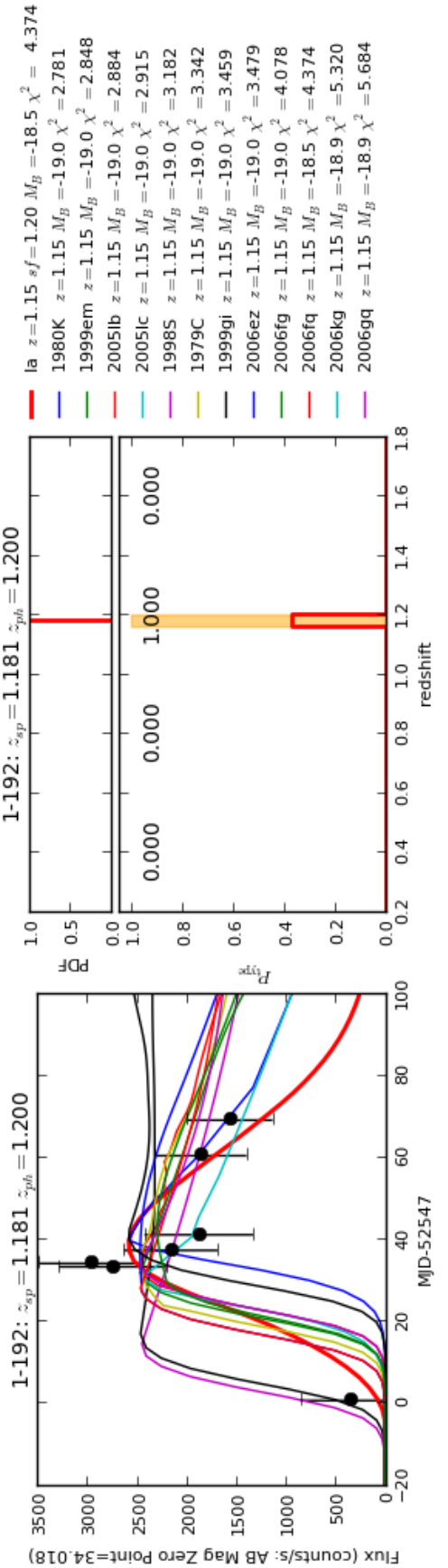
Ia z=1.15 sf=1.20 M_B=-18.5 χ^2= 4.374
1980K z=1.15 M_B=-19.0 χ^2=2.781
1999em z=1.15 M_B=-19.0 χ^2=2.848
2005lb z=1.15 M_B=-19.0 χ^2=2.884
2005lc z=1.15 M_B=-19.0 χ^2=2.915
1998S z=1.15 M_B=-19.0 χ^2=3.182
1979C z=1.15 M_B=-19.0 χ^2=3.342
1999gi z=1.15 M_B=-19.0 χ^2=3.459
2006ez z=1.15 M_B=-19.0 χ^2=3.479
2006fg z=1.15 M_B=-19.0 χ^2=4.078
2006fq z=1.15 M_B=-18.5 χ^2=4.374
2006kg z=1.15 M_B=-18.9 χ^2=5.320
2006gq z=1.15 M_B=-18.9 χ^2=5.684
1-192: z_{sp}=1.181 z_{ph}=1.200
PDF
P_{type}
redshift
0.000
0.000
1.000
0.000
1-192: z_{sp}=1.181 z_{ph}=1.200
MJD-52547
Flux (counts/s: AB Mag Zero Point=34.018)

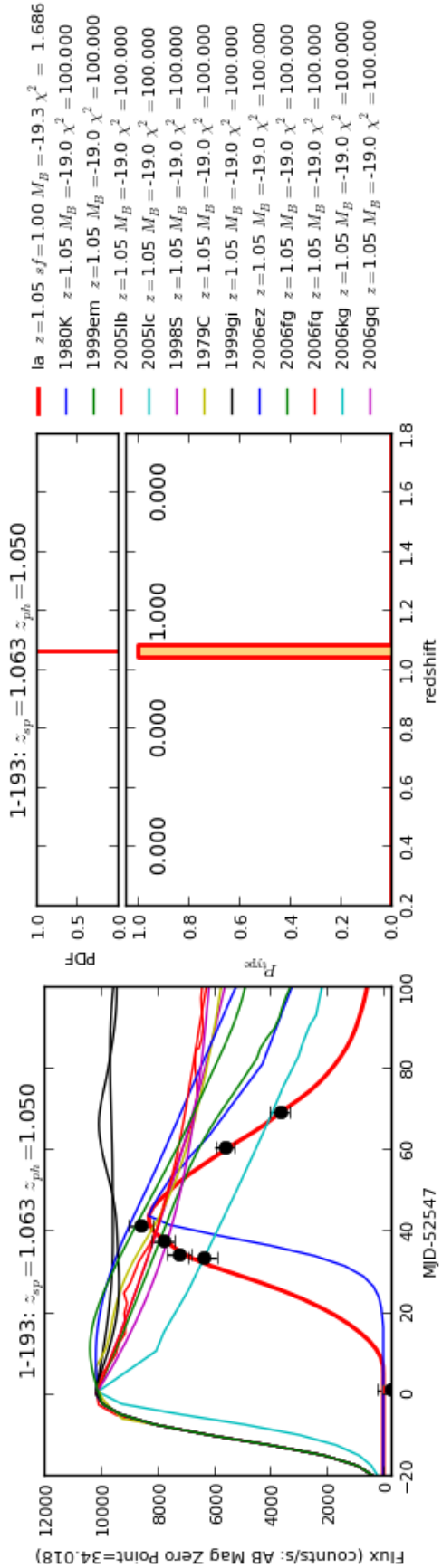
Ia z=1.05 sf=1.00 M_B=-19.3 χ^2 = 1.686
1980K z=1.05 M_B=-19.0 χ^2=100.000
1999em z=1.05 M_B=-19.0 χ^2=100.000
2005lb z=1.05 M_B=-19.0 χ^2=100.000
2005lc z=1.05 M_B=-19.0 χ^2=100.000
1998S z=1.05 M_B=-19.0 χ^2=100.000
1979C z=1.05 M_B=-19.0 χ^2=100.000
1999gi z=1.05 M_B=-19.0 χ^2=100.000
2006ez z=1.05 M_B=-19.0 χ^2=100.000
2006fg z=1.05 M_B=-19.0 χ^2=100.000
2006fq z=1.05 M_B=-19.0 χ^2=100.000
2006kg z=1.05 M_B=-19.0 χ^2=100.000
2006gq z=1.05 M_B=-19.0 χ^2=100.000
1-193: z_{sp}=1.063 z_{ph}=1.050
PDF
P_{type}
redshift
0.000
0.000
1.000
0.000
1-193: z_{sp}=1.063 z_{ph}=1.050
MJD-52547
Flux (counts/s: AB Mag Zero Point=34.018)

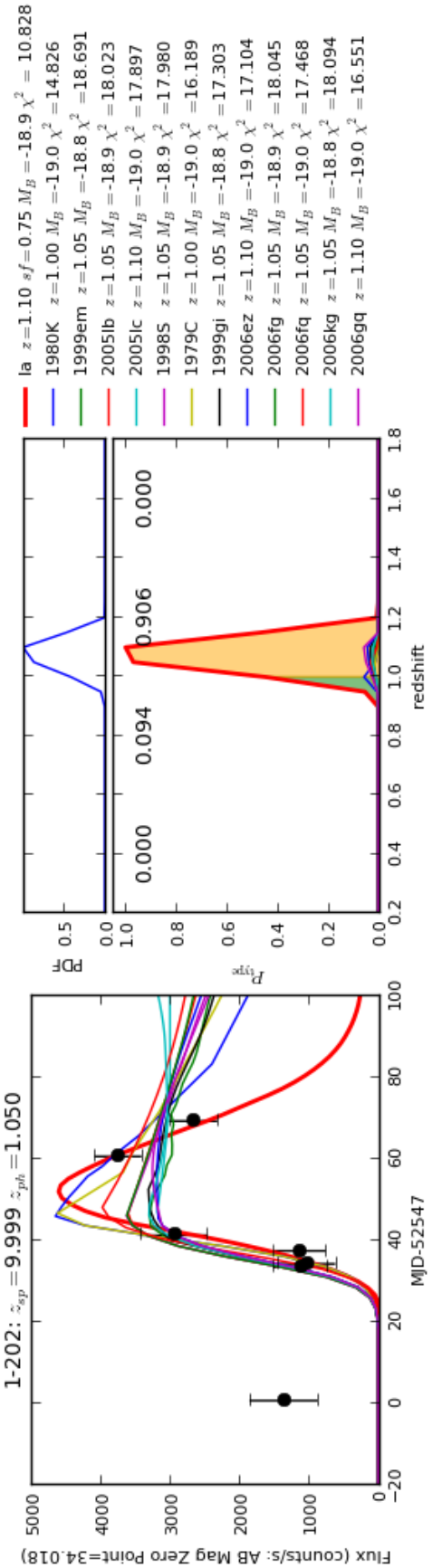
Ia z=1.10 sf=0.75 M_B=-18.9 χ^2 = 10.828
1980K z=1.00 M_B=-19.0 χ^2=14.826
1999em z=1.05 M_B=-18.8 χ^2=18.691
2005lb z=1.05 M_B=-18.9 χ^2=18.023
2005lc z=1.10 M_B=-19.0 χ^2=17.897
1998S z=1.05 M_B=-18.9 χ^2=17.980
1979C z=1.00 M_B=-19.0 χ^2=16.189
1999gi z=1.05 M_B=-18.8 χ^2=17.303
2006ez z=1.10 M_B=-19.0 χ^2=17.104
2006fg z=1.05 M_B=-18.9 χ^2=18.045
2006fq z=1.05 M_B=-19.0 χ^2=17.468
2006kg z=1.05 M_B=-18.8 χ^2=18.094
2006gq z=1.10 M_B=-19.0 χ^2=16.551
PDF
P_{type}
redshift
0.000
0.094
0.906
0.000
1-202: z_{sp}=9.999 z_{ph}=1.050
MJD-52547
Flux (counts/s: AB Mag Zero Point=34.018)

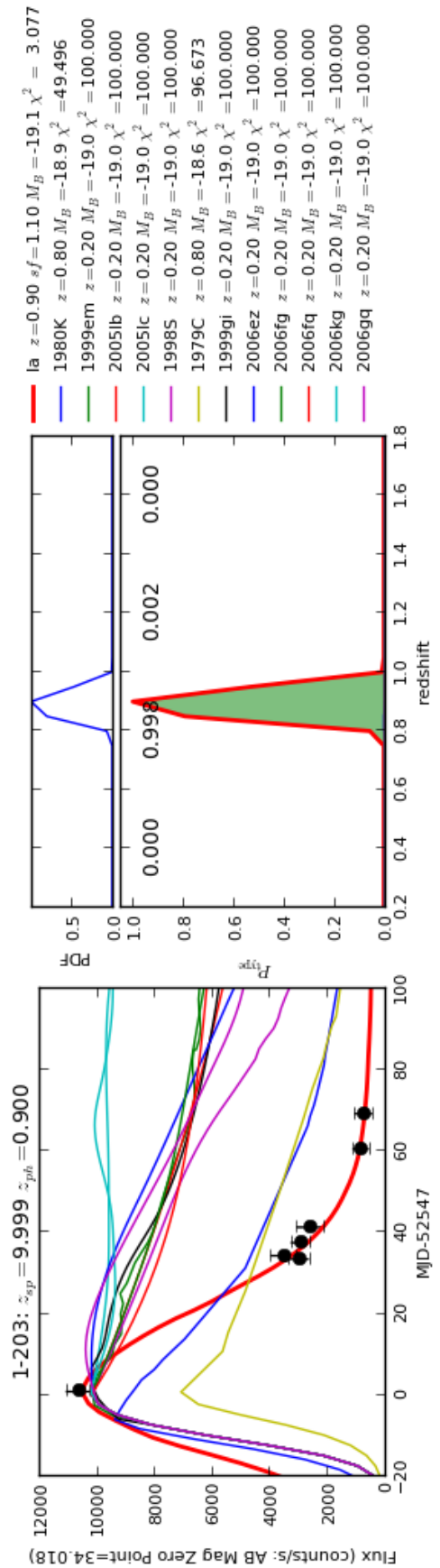
1-203: z_{sp}=9.999 z_{ph}=0.900
Flux (counts/s: AB Mag Zero Point=34.018)
MJD-52547
P_{type}
PDF
redshift
Ia z=0.90 sf=1.10 M_B=-19.1 χ^2= 3.077
1980K z=0.80 M_B=-18.9 χ^2=49.496
1999em z=0.20 M_B=-19.0 χ^2=100.000
2005lb z=0.20 M_B=-19.0 χ^2=100.000
2005lc z=0.20 M_B=-19.0 χ^2=100.000
1998S z=0.20 M_B=-19.0 χ^2=100.000
1979C z=0.80 M_B=-18.6 χ^2=96.673
1999gi z=0.20 M_B=-19.0 χ^2=100.000
2006ez z=0.20 M_B=-19.0 χ^2=100.000
2006fg z=0.20 M_B=-19.0 χ^2=100.000
2006fq z=0.20 M_B=-19.0 χ^2=100.000
2006kg z=0.20 M_B=-19.0 χ^2=100.000
2006gq z=0.20 M_B=-19.0 χ^2=100.000
0.998
0.002
0.000

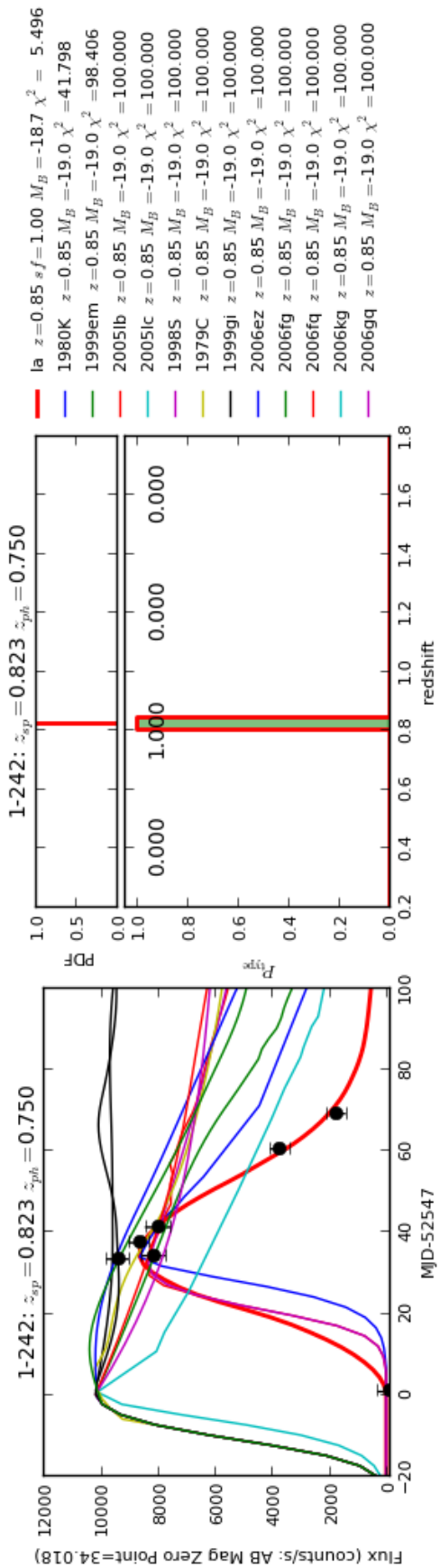
1-242: z_{sp}=0.823 z_{ph}=0.750
Flux (counts/s: AB Mag Zero Point=34.018)
MJD-52547
P_{type}
PDF
redshift
Ia z=0.85 sf=1.00 M_B=-18.7 χ^2= 5.496
1980K z=0.85 M_B=-19.0 χ^2=41.798
1999em z=0.85 M_B=-19.0 χ^2=98.406
2005lb z=0.85 M_B=-19.0 χ^2=100.000
2005lc z=0.85 M_B=-19.0 χ^2=100.000
1998S z=0.85 M_B=-19.0 χ^2=100.000
1979C z=0.85 M_B=-19.0 χ^2=100.000
1999gi z=0.85 M_B=-19.0 χ^2=100.000
2006ez z=0.85 M_B=-19.0 χ^2=100.000
2006fg z=0.85 M_B=-19.0 χ^2=100.000
2006fq z=0.85 M_B=-19.0 χ^2=100.000
2006kg z=0.85 M_B=-19.0 χ^2=100.000
2006gq z=0.85 M_B=-19.0 χ^2=100.000
1.000
0.000

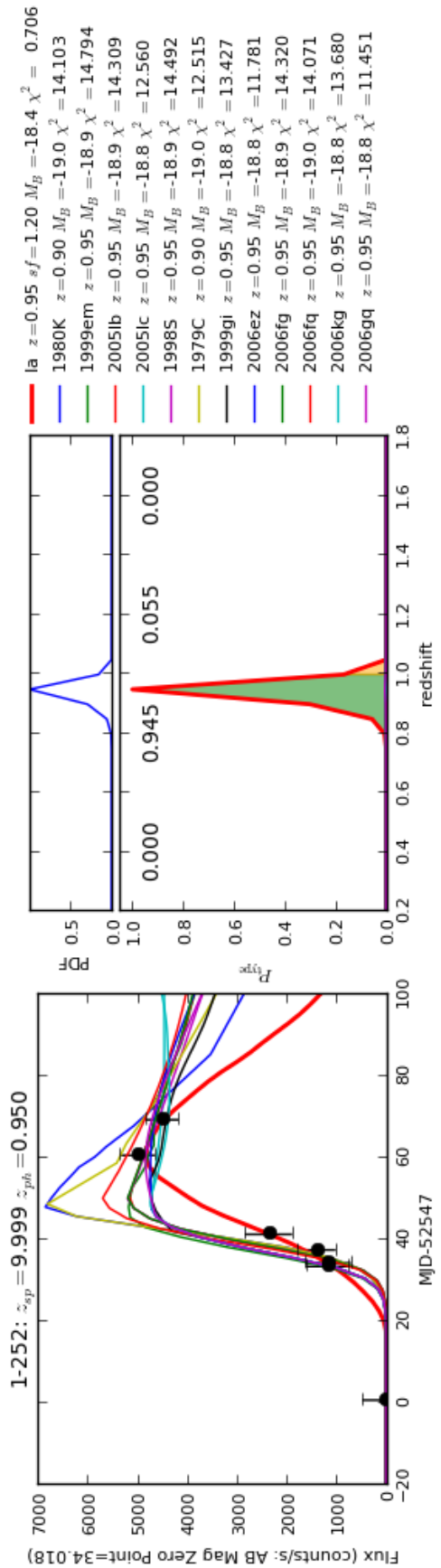
Ia z=0.95 sf=1.20 M_B=-18.4 χ^2= 0.706
1980K z=0.90 M_B=-19.0 χ^2=14.103
1999em z=0.95 M_B=-18.9 χ^2=14.794
2005lb z=0.95 M_B=-18.9 χ^2=14.309
2005lc z=0.95 M_B=-18.8 χ^2=12.560
1998S z=0.95 M_B=-18.9 χ^2=14.492
1979C z=0.90 M_B=-19.0 χ^2=12.515
1999gi z=0.95 M_B=-18.8 χ^2=13.427
2006ez z=0.95 M_B=-18.8 χ^2=11.781
2006fg z=0.95 M_B=-18.9 χ^2=14.320
2006fq z=0.95 M_B=-19.0 χ^2=14.071
2006kg z=0.95 M_B=-18.8 χ^2=13.680
2006gq z=0.95 M_B=-18.8 χ^2=11.451
1-252: z_{sp}=9.999 z_{ph}=0.950
0.000
0.945
0.055
0.000
redshift
PDF
P_{type}
MJD-52547
Flux (counts/s: AB Mag Zero Point=34.018)

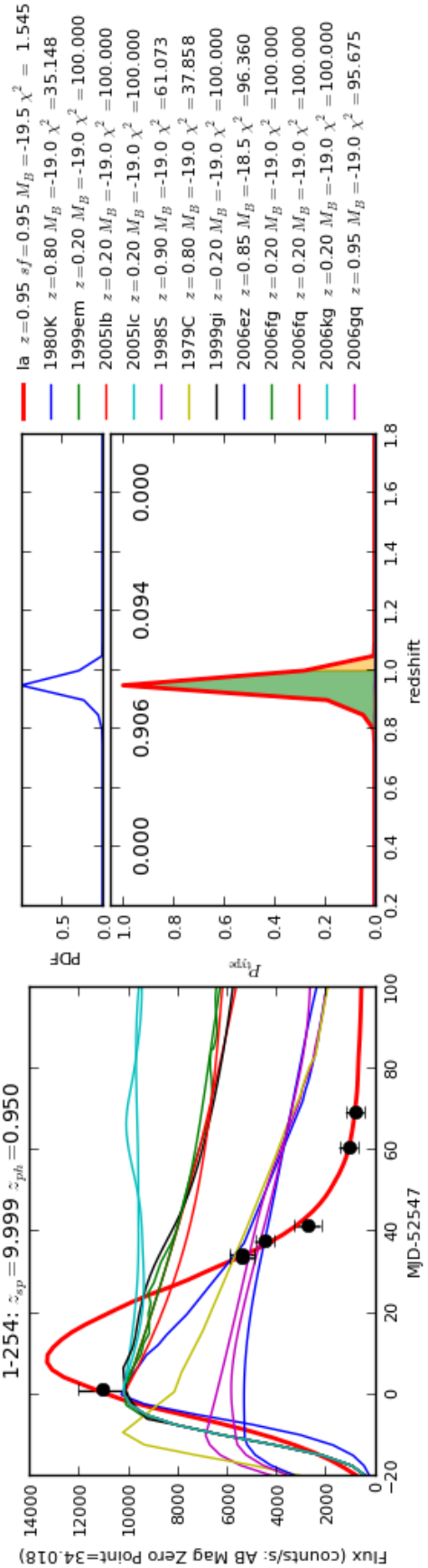
Ia z=0.95 sf=0.95 M_B=-19.5 χ^2= 1.545
1980K z=0.80 M_B=-19.0 χ^2=35.148
1999em z=0.20 M_B=-19.0 χ^2=100.000
2005lb z=0.20 M_B=-19.0 χ^2=100.000
2005lc z=0.20 M_B=-19.0 χ^2=100.000
1998S z=0.90 M_B=-19.0 χ^2=61.073
1979C z=0.80 M_B=-19.0 χ^2=37.858
1999gi z=0.20 M_B=-19.0 χ^2=100.000
2006ez z=0.85 M_B=-18.5 χ^2=96.360
2006fg z=0.20 M_B=-19.0 χ^2=100.000
2006fq z=0.20 M_B=-19.0 χ^2=100.000
2006kg z=0.20 M_B=-19.0 χ^2=100.000
2006gq z=0.95 M_B=-19.0 χ^2=95.675
1-254: z_{sp}=9.999 z_{ph}=0.950
0.000
0.906
0.094
0.000
redshift
PDF
P_{type}
MJD-52547
Flux (counts/s: AB Mag Zero Point=34.018)

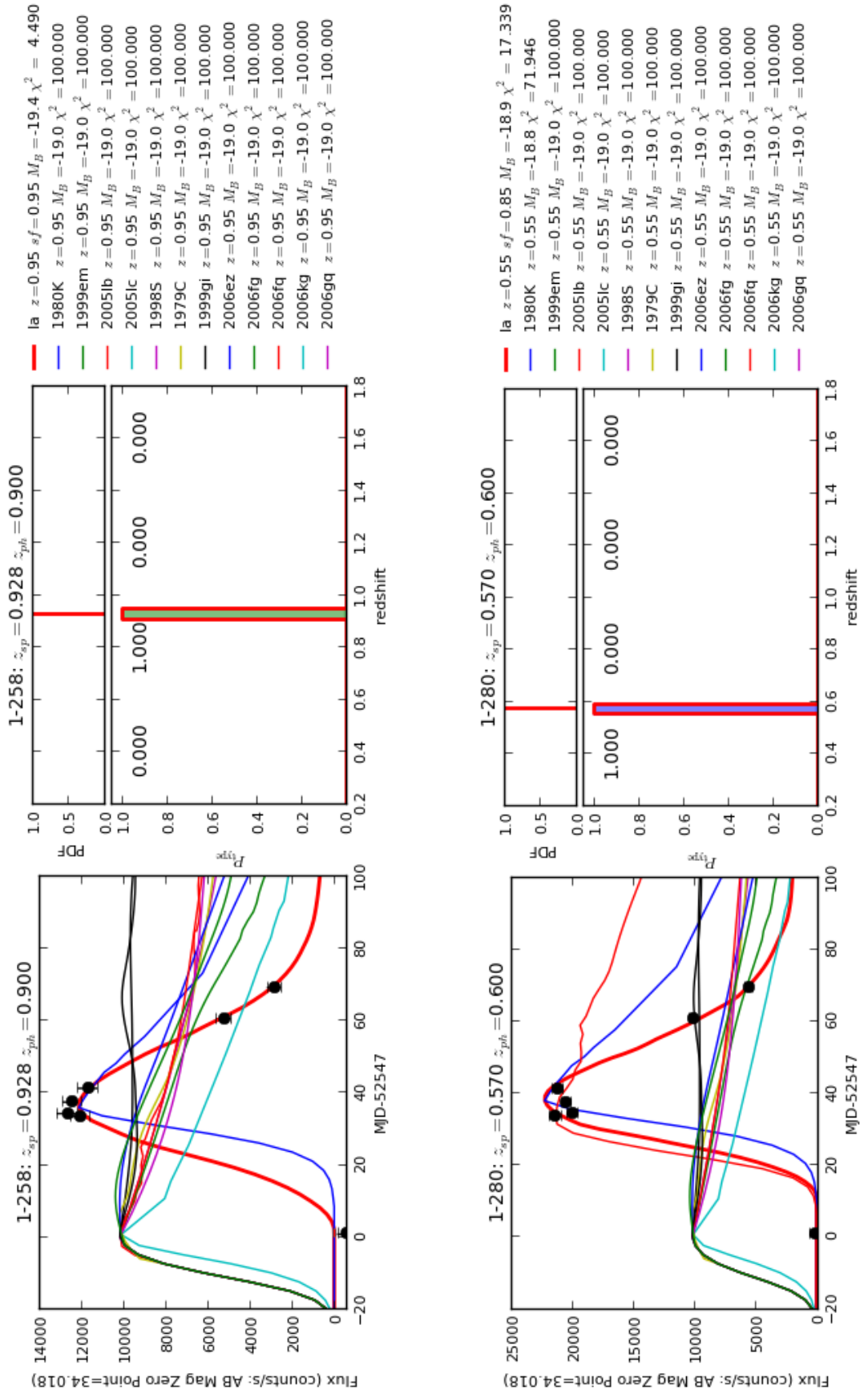
Ia z=0.95 sf=0.95 M_B=-19.4 χ^2 = 4.490
1980K z=0.95 M_B=-19.0 χ^2=100.000
1999em z=0.95 M_B=-19.0 χ^2=100.000
2005lb z=0.95 M_B=-19.0 χ^2=100.000
2005lc z=0.95 M_B=-19.0 χ^2=100.000
1998S z=0.95 M_B=-19.0 χ^2=100.000
1979C z=0.95 M_B=-19.0 χ^2=100.000
1999gi z=0.95 M_B=-19.0 χ^2=100.000
2006ez z=0.95 M_B=-19.0 χ^2=100.000
2006fg z=0.95 M_B=-19.0 χ^2=100.000
2006fq z=0.95 M_B=-19.0 χ^2=100.000
2006kg z=0.95 M_B=-19.0 χ^2=100.000
2006gq z=0.95 M_B=-19.0 χ^2=100.000
1-258: z_{sp}=0.928 z_{ph}=0.900
PDF
redshift
P_{type}
MJD-52547
Flux (counts/s: AB Mag Zero Point=34.018)
Ia z=0.55 sf=0.85 M_B=-18.9 χ^2 = 17.339
1980K z=0.55 M_B=-18.8 χ^2=71.946
1999em z=0.55 M_B=-19.0 χ^2=100.000
2005lb z=0.55 M_B=-19.0 χ^2=100.000
2005lc z=0.55 M_B=-19.0 χ^2=100.000
1998S z=0.55 M_B=-19.0 χ^2=100.000
1979C z=0.55 M_B=-19.0 χ^2=100.000
1999gi z=0.55 M_B=-19.0 χ^2=100.000
2006ez z=0.55 M_B=-19.0 χ^2=100.000
2006fg z=0.55 M_B=-19.0 χ^2=100.000
2006fq z=0.55 M_B=-19.0 χ^2=100.000
2006kg z=0.55 M_B=-19.0 χ^2=100.000
2006gq z=0.55 M_B=-19.0 χ^2=100.000
1-280: z_{sp}=0.570 z_{ph}=0.600
PDF
redshift
P_{type}
MJD-52547
Flux (counts/s: AB Mag Zero Point=34.018)

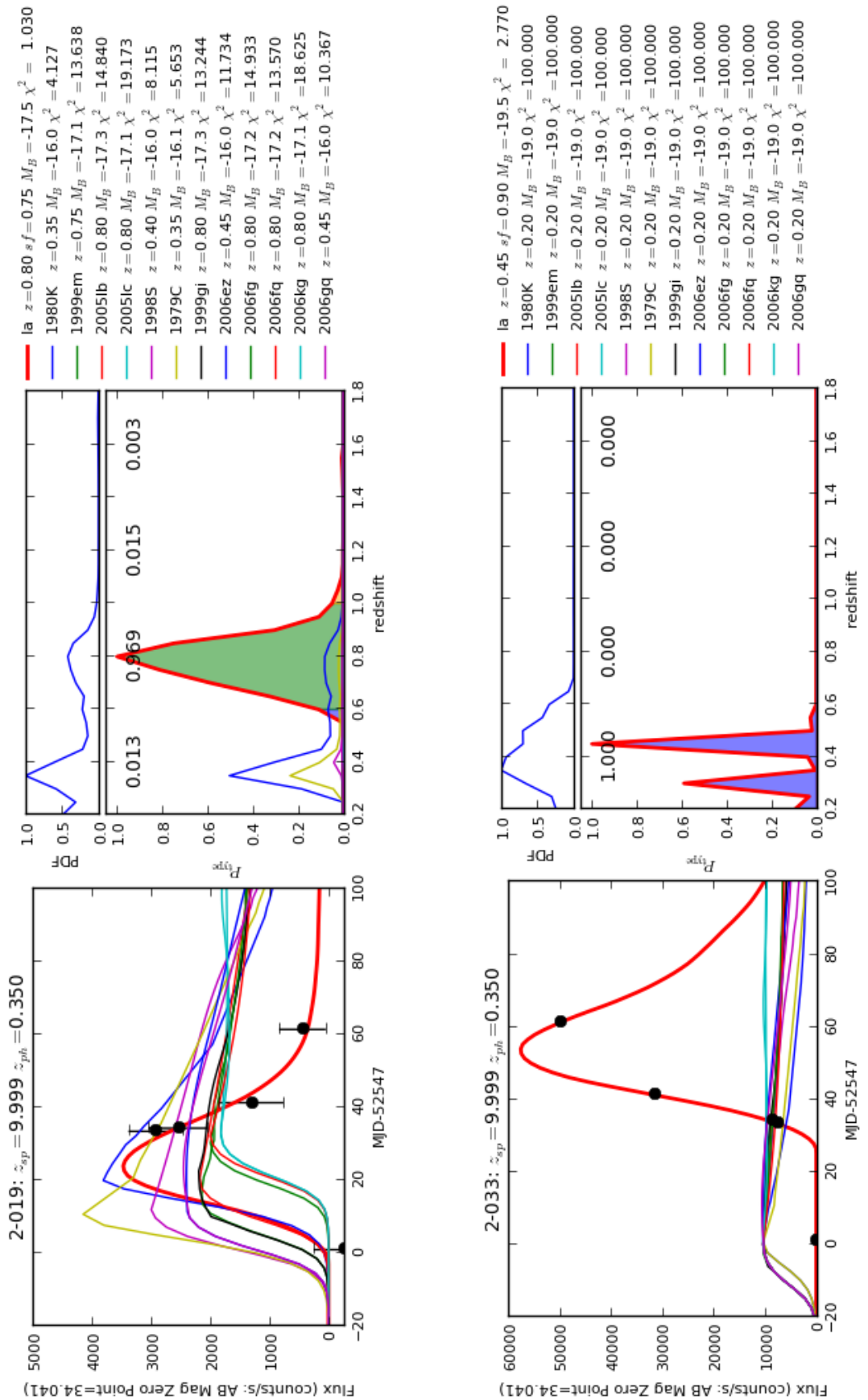
Ia z=0.80 sf=0.75 M_B=-17.5 χ^2= 1.030
1980K z=0.35 M_B=-16.0 χ^2=4.127
1999em z=0.75 M_B=-17.1 χ^2=13.638
2005lb z=0.80 M_B=-17.3 χ^2=14.840
2005lc z=0.80 M_B=-17.1 χ^2=19.173
1998S z=0.40 M_B=-16.0 χ^2=8.115
1979C z=0.35 M_B=-16.1 χ^2=5.653
1999gi z=0.80 M_B=-17.3 χ^2=13.244
2006ez z=0.45 M_B=-16.0 χ^2=11.734
2006fg z=0.80 M_B=-17.2 χ^2=14.933
2006fq z=0.80 M_B=-17.2 χ^2=13.570
2006kg z=0.80 M_B=-17.1 χ^2=18.625
2006gq z=0.45 M_B=-16.0 χ^2=10.367
PDF
P_{type}
0.013
0.969
0.015
0.003
redshift
2-019: z_{sp}=9.999 z_{ph}=0.350
Flux (counts/s: AB Mag Zero Point=34.041)
MJD-52547
Ia z=0.45 sf=0.90 M_B=-19.5 χ^2= 2.770
1980K z=0.20 M_B=-19.0 χ^2=100.000
1999em z=0.20 M_B=-19.0 χ^2=100.000
2005lb z=0.20 M_B=-19.0 χ^2=100.000
2005lc z=0.20 M_B=-19.0 χ^2=100.000
1998S z=0.20 M_B=-19.0 χ^2=100.000
1979C z=0.20 M_B=-19.0 χ^2=100.000
1999gi z=0.20 M_B=-19.0 χ^2=100.000
2006ez z=0.20 M_B=-19.0 χ^2=100.000
2006fg z=0.20 M_B=-19.0 χ^2=100.000
2006fq z=0.20 M_B=-19.0 χ^2=100.000
2006kg z=0.20 M_B=-19.0 χ^2=100.000
2006gq z=0.20 M_B=-19.0 χ^2=100.000
PDF
P_{type}
1.000
0.000
0.000
0.000
redshift
2-033: z_{sp}=9.999 z_{ph}=0.350
Flux (counts/s: AB Mag Zero Point=34.041)
MJD-52547

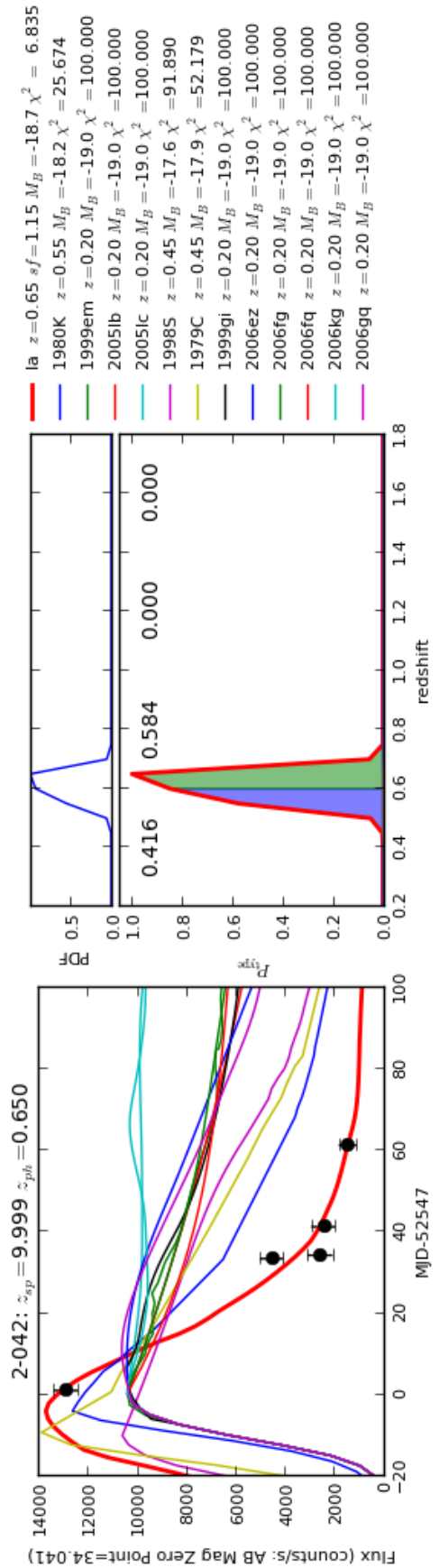
Ia z=0.65 sf=1.15 M_B=-18.7 χ^2= 6.835
1980K z=0.55 M_B=-18.2 χ^2=25.674
1999em z=0.20 M_B=-19.0 χ^2=100.000
2005lb z=0.20 M_B=-19.0 χ^2=100.000
2005lc z=0.20 M_B=-19.0 χ^2=100.000
1998S z=0.45 M_B=-17.6 χ^2=91.890
1979C z=0.45 M_B=-17.9 χ^2=52.179
1999gi z=0.20 M_B=-19.0 χ^2=100.000
2006ez z=0.20 M_B=-19.0 χ^2=100.000
2006fg z=0.20 M_B=-19.0 χ^2=100.000
2006fq z=0.20 M_B=-19.0 χ^2=100.000
2006kg z=0.20 M_B=-19.0 χ^2=100.000
2006gq z=0.20 M_B=-19.0 χ^2=100.000
0.416
0.584
0.000
0.000
0.000
PDF
P_{type}
redshift
2-042: z_{sp}=9.999 z_{ph}=0.650
MJD-52547
Flux (counts/s: AB Mag Zero Point=34.041)

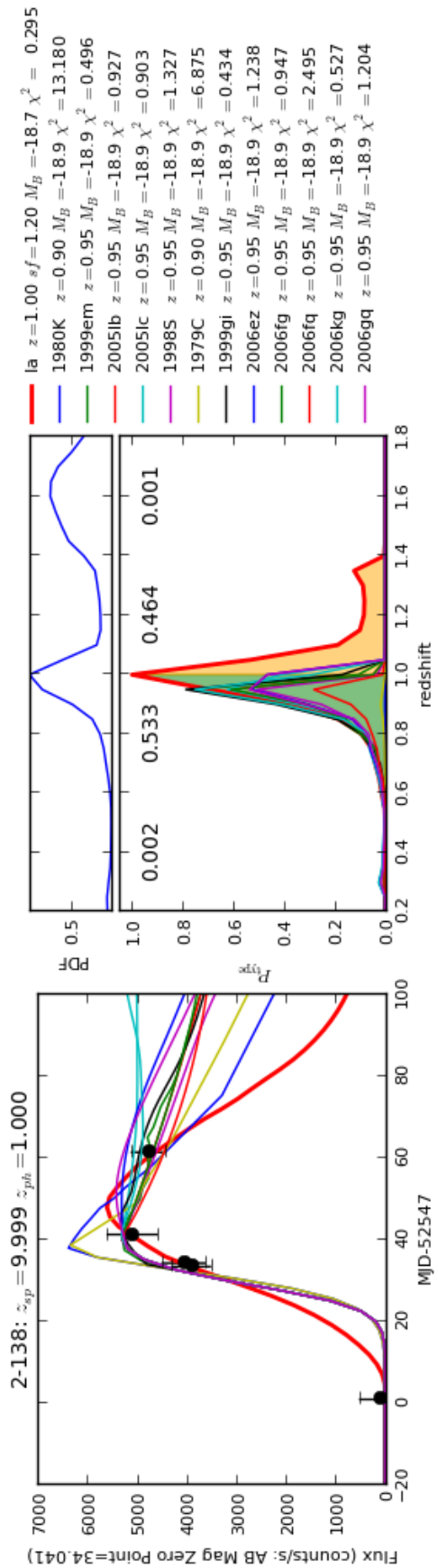
Ia z=1.00 sf=1.20 M_B=-18.7 χ^2= 0.295
1980K z=0.90 M_B=-18.9 χ^2=13.180
1999em z=0.95 M_B=-18.9 χ^2=0.496
2005lb z=0.95 M_B=-18.9 χ^2=0.927
2005lc z=0.95 M_B=-18.9 χ^2=0.903
1998S z=0.95 M_B=-18.9 χ^2=1.327
1979C z=0.90 M_B=-18.9 χ^2=6.875
1999gi z=0.95 M_B=-18.9 χ^2=0.434
2006ez z=0.95 M_B=-18.9 χ^2=1.238
2006fg z=0.95 M_B=-18.9 χ^2=0.947
2006fq z=0.95 M_B=-18.9 χ^2=2.495
2006kg z=0.95 M_B=-18.9 χ^2=0.527
2006gq z=0.95 M_B=-18.9 χ^2=1.204
0.002
0.533
0.464
0.001
PDF
P_{type}
redshift
2-138: z_{sp}=9.999 z_{ph}=1.000
MJD-52547
Flux (counts/s: AB Mag Zero Point=34.041)

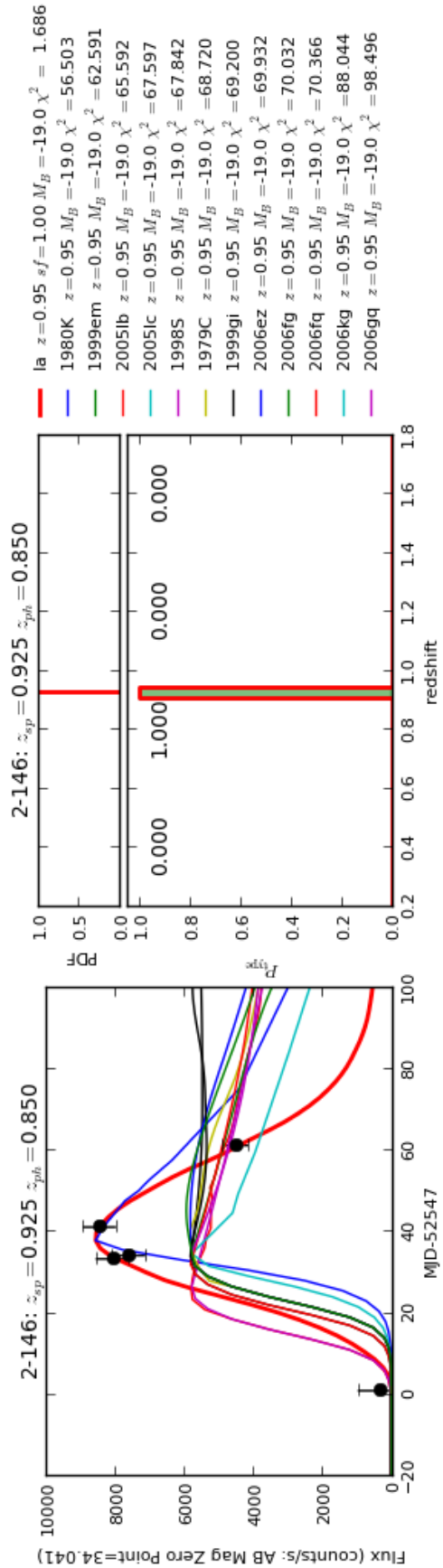
Ia z=0.95 sf=1.00 M_B=-19.0 χ^2= 1.686
1980K z=0.95 M_B=-19.0 χ^2=56.503
1999em z=0.95 M_B=-19.0 χ^2=62.591
2005lb z=0.95 M_B=-19.0 χ^2=65.592
2005lc z=0.95 M_B=-19.0 χ^2=67.597
1998S z=0.95 M_B=-19.0 χ^2=67.842
1979C z=0.95 M_B=-19.0 χ^2=68.720
1999gi z=0.95 M_B=-19.0 χ^2=69.200
2006ez z=0.95 M_B=-19.0 χ^2=69.932
2006fg z=0.95 M_B=-19.0 χ^2=70.032
2006fq z=0.95 M_B=-19.0 χ^2=70.366
2006kg z=0.95 M_B=-19.0 χ^2=88.044
2006gq z=0.95 M_B=-19.0 χ^2=98.496
2-146: z_{sp}=0.925 z_{ph}=0.850
PDF
P_{type}
redshift
0.000
1.000
0.000
0.000
2-146: z_{sp}=0.925 z_{ph}=0.850
MJD-52547
Flux (counts/s: AB Mag Zero Point=34.041)

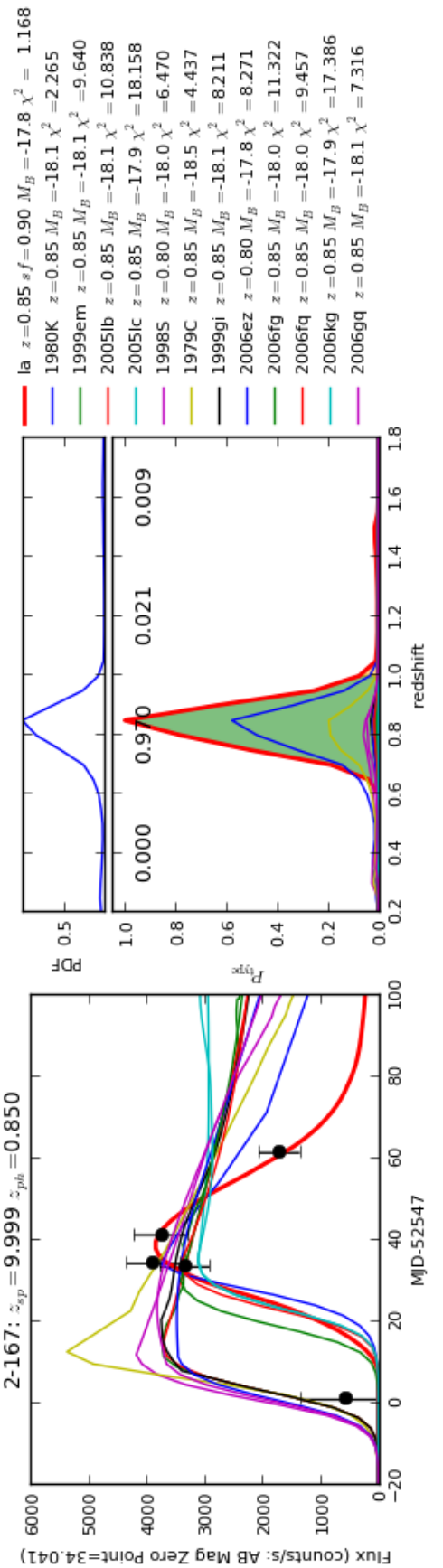
Ia z=0.85 sf=0.90 M_B=-17.8 χ^2= 1.168
1980K z=0.85 M_B=-18.1 χ^2=2.265
1999em z=0.85 M_B=-18.1 χ^2=9.640
2005lb z=0.85 M_B=-18.1 χ^2=10.838
2005lc z=0.85 M_B=-17.9 χ^2=18.158
1998S z=0.80 M_B=-18.0 χ^2=6.470
1979C z=0.85 M_B=-18.5 χ^2=4.437
1999gi z=0.85 M_B=-18.1 χ^2=8.211
2006ez z=0.80 M_B=-17.8 χ^2=8.271
2006fg z=0.85 M_B=-18.0 χ^2=11.322
2006fq z=0.85 M_B=-18.0 χ^2=9.457
2006kg z=0.85 M_B=-17.9 χ^2=17.386
2006gq z=0.85 M_B=-18.1 χ^2=7.316
PDF
P_{type}
redshift
0.000
0.970
0.021
0.009
2-167: z_{sp}=9.999 z_{ph}=0.850
MJD-52547
Flux (counts/s: AB Mag Zero Point=34.041)

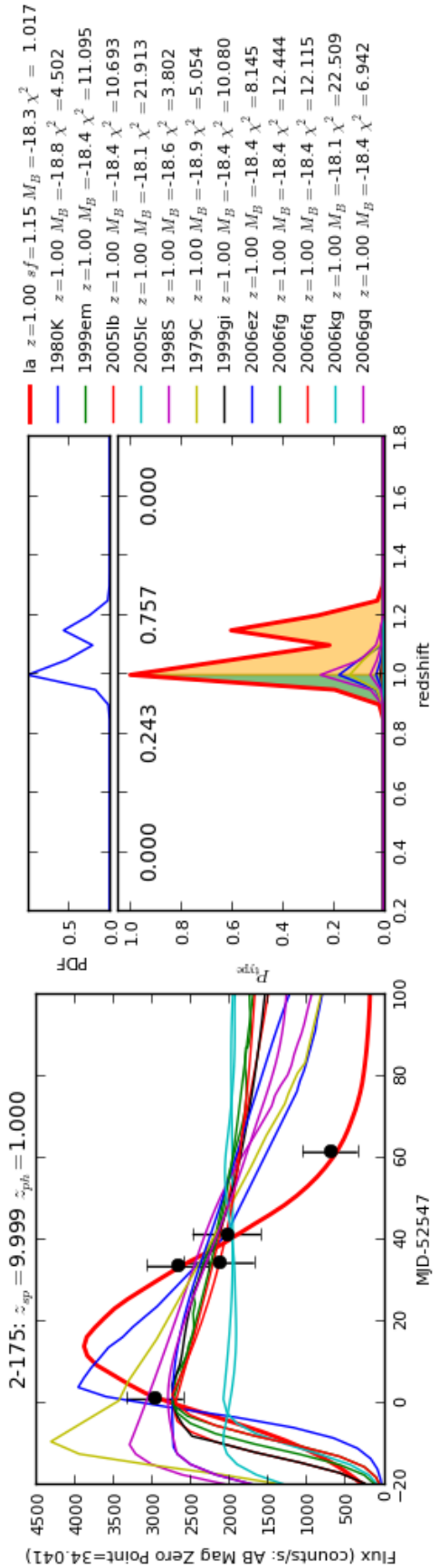
2-175: z_{sp}=9.999 z_{ph}=1.000
Flux (counts/s: AB Mag Zero Point=34.041)
MJD-52547
P_{type}
redshift
PDF
0.000
0.243
0.757
0.000
Ia z=1.00 sf=1.15 M_B=-18.3 χ^2 = 1.017
1980K z=1.00 M_B=-18.8 χ^2=4.502
1999em z=1.00 M_B=-18.4 χ^2=11.095
2005lb z=1.00 M_B=-18.4 χ^2=10.693
2005lc z=1.00 M_B=-18.1 χ^2=21.913
1998S z=1.00 M_B=-18.6 χ^2=3.802
1979C z=1.00 M_B=-18.9 χ^2=5.054
1999gi z=1.00 M_B=-18.4 χ^2=10.080
2006ez z=1.00 M_B=-18.4 χ^2=8.145
2006fg z=1.00 M_B=-18.4 χ^2=12.444
2006fq z=1.00 M_B=-18.4 χ^2=12.115
2006kg z=1.00 M_B=-18.1 χ^2=22.509
2006gq z=1.00 M_B=-18.4 χ^2=6.942

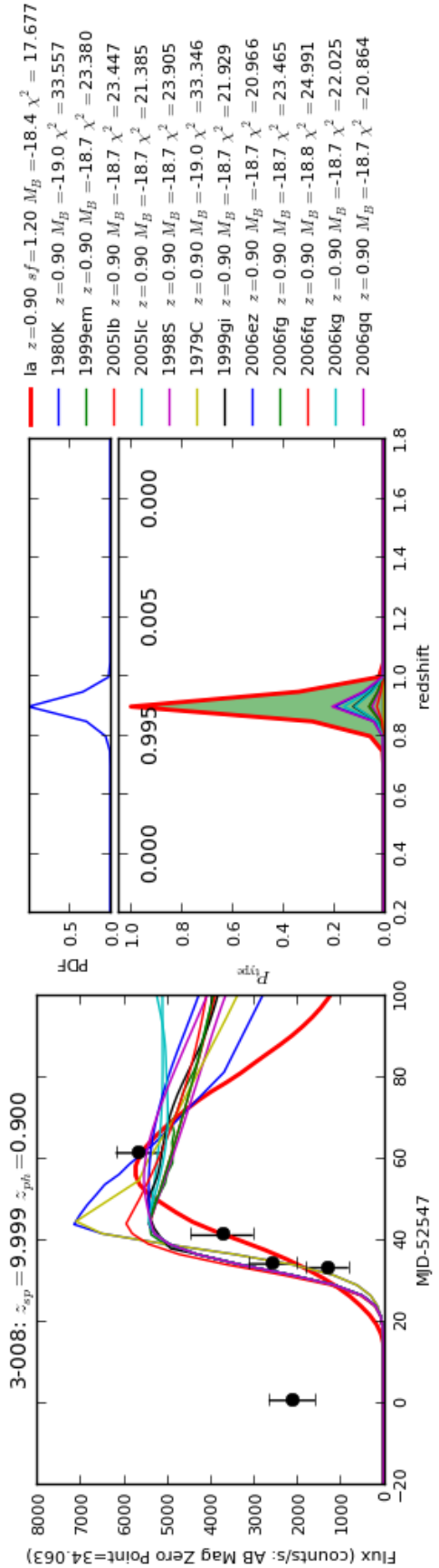
3-008: z_{sp}=9.999 z_{ph}=0.900
Flux (counts/s: AB Mag Zero Point=34.063)
MJD-52547
P_{type}
redshift
PDF
0.000
0.995
0.005
0.000
Ia z=0.90 sf=1.20 M_B=-18.4 χ^2 = 17.677
1980K z=0.90 M_B=-19.0 χ^2=33.557
1999em z=0.90 M_B=-18.7 χ^2=23.380
2005lb z=0.90 M_B=-18.7 χ^2=23.447
2005lc z=0.90 M_B=-18.7 χ^2=21.385
1998S z=0.90 M_B=-18.7 χ^2=23.905
1979C z=0.90 M_B=-19.0 χ^2=33.346
1999gi z=0.90 M_B=-18.7 χ^2=21.929
2006ez z=0.90 M_B=-18.7 χ^2=20.966
2006fg z=0.90 M_B=-18.7 χ^2=23.465
2006fq z=0.90 M_B=-18.8 χ^2=24.991
2006kg z=0.90 M_B=-18.7 χ^2=22.025
2006gq z=0.90 M_B=-18.7 χ^2=20.864

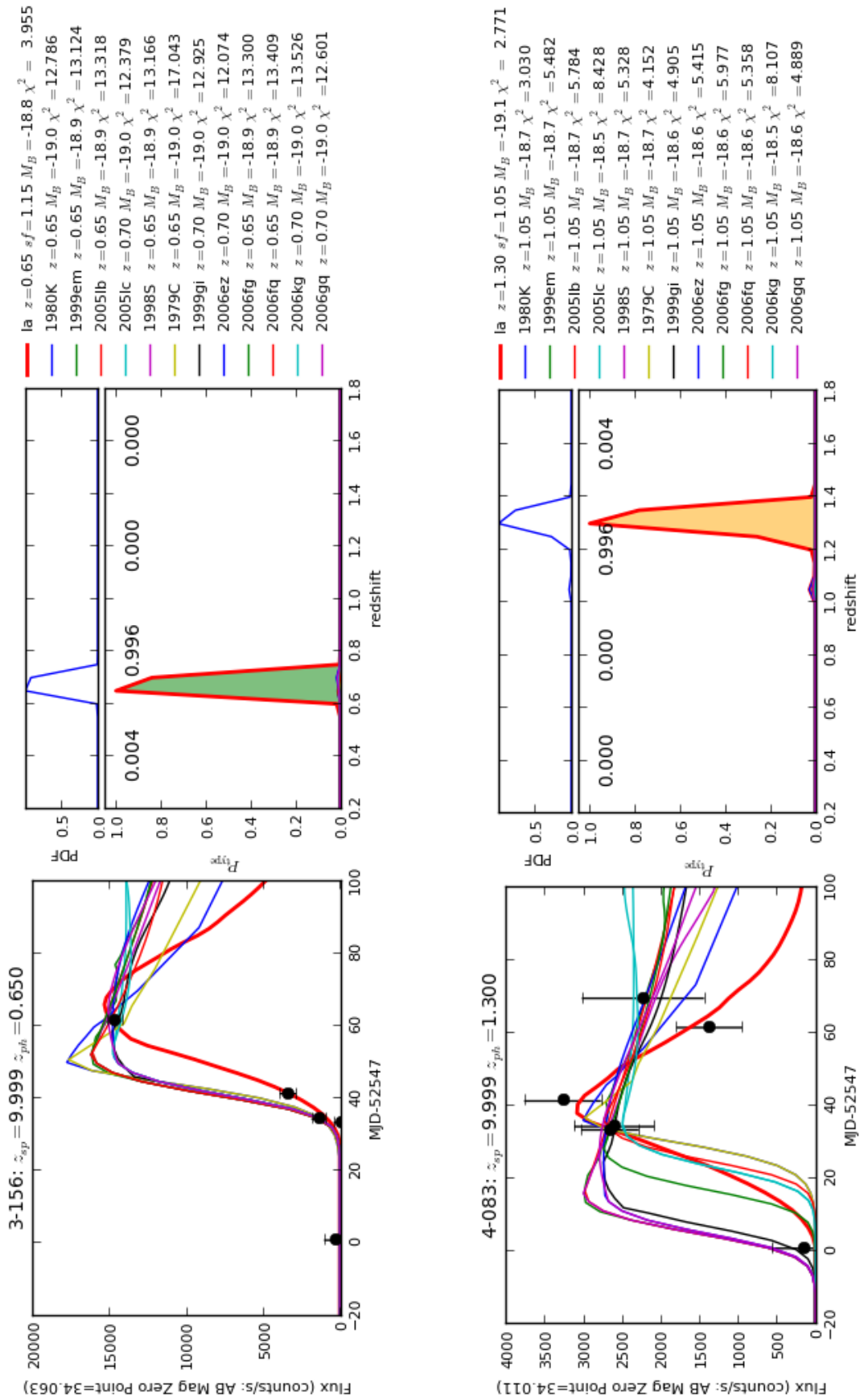
3-156: z_{sp}=9.999 z_{ph}=0.650
4-083: z_{sp}=9.999 z_{ph}=1.300
MJD-52547
redshift
PDF
P_{type}
Flux (counts/s: AB Mag Zero Point=34.063)
Flux (counts/s: AB Mag Zero Point=34.011)
Ia z=0.65 sf=1.15 M_B=-18.8 χ^2= 3.955
1980K z=0.65 M_B=-19.0 χ^2=12.786
1999em z=0.65 M_B=-18.9 χ^2=13.124
2005lb z=0.65 M_B=-18.9 χ^2=13.318
2005lc z=0.70 M_B=-19.0 χ^2=12.379
1998S z=0.65 M_B=-18.9 χ^2=13.166
1979C z=0.65 M_B=-19.0 χ^2=17.043
1999gi z=0.70 M_B=-19.0 χ^2=12.925
2006ez z=0.70 M_B=-19.0 χ^2=12.074
2006fg z=0.65 M_B=-18.9 χ^2=13.300
2006fq z=0.65 M_B=-18.9 χ^2=13.409
2006kg z=0.70 M_B=-19.0 χ^2=13.526
2006gq z=0.70 M_B=-19.0 χ^2=12.601
Ia z=1.30 sf=1.05 M_B=-19.1 χ^2= 2.771
1980K z=1.05 M_B=-18.7 χ^2=3.030
1999em z=1.05 M_B=-18.7 χ^2=5.482
2005lb z=1.05 M_B=-18.7 χ^2=5.784
2005lc z=1.05 M_B=-18.5 χ^2=8.428
1998S z=1.05 M_B=-18.7 χ^2=5.328
1979C z=1.05 M_B=-18.7 χ^2=4.152
1999gi z=1.05 M_B=-18.6 χ^2=4.905
2006ez z=1.05 M_B=-18.6 χ^2=5.415
2006fg z=1.05 M_B=-18.6 χ^2=5.977
2006fq z=1.05 M_B=-18.6 χ^2=5.358
2006kg z=1.05 M_B=-18.5 χ^2=8.107
2006gq z=1.05 M_B=-18.6 χ^2=4.889
0.004
0.996
0.000
0.000
0.000
0.004
0.000
0.996

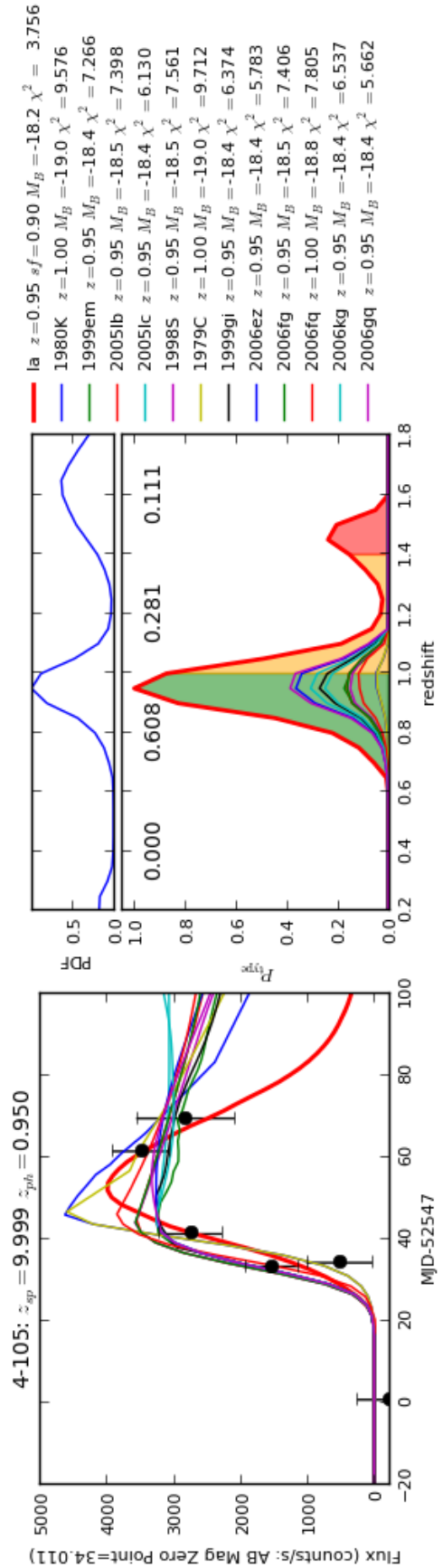
Ia z=0.95 sf=0.90 M_B=-18.2 χ^2= 3.756
1980K z=1.00 M_B=-19.0 χ^2=9.576
1999em z=0.95 M_B=-18.4 χ^2=7.266
2005lb z=0.95 M_B=-18.5 χ^2=7.398
2005lc z=0.95 M_B=-18.4 χ^2=6.130
1998S z=0.95 M_B=-18.5 χ^2=7.561
1979C z=1.00 M_B=-19.0 χ^2=9.712
1999gi z=0.95 M_B=-18.4 χ^2=6.374
2006ez z=0.95 M_B=-18.4 χ^2=5.783
2006fg z=0.95 M_B=-18.5 χ^2=7.406
2006fq z=1.00 M_B=-18.8 χ^2=7.805
2006kg z=0.95 M_B=-18.4 χ^2=6.537
2006gq z=0.95 M_B=-18.4 χ^2=5.662
4-105: z_{sp}=9.999 z_{ph}=0.950
Flux (counts/s: AB Mag Zero Point=34.011)
MJD-52547
P_{type}
0.000
0.608
0.281
0.111
redshift
PDF

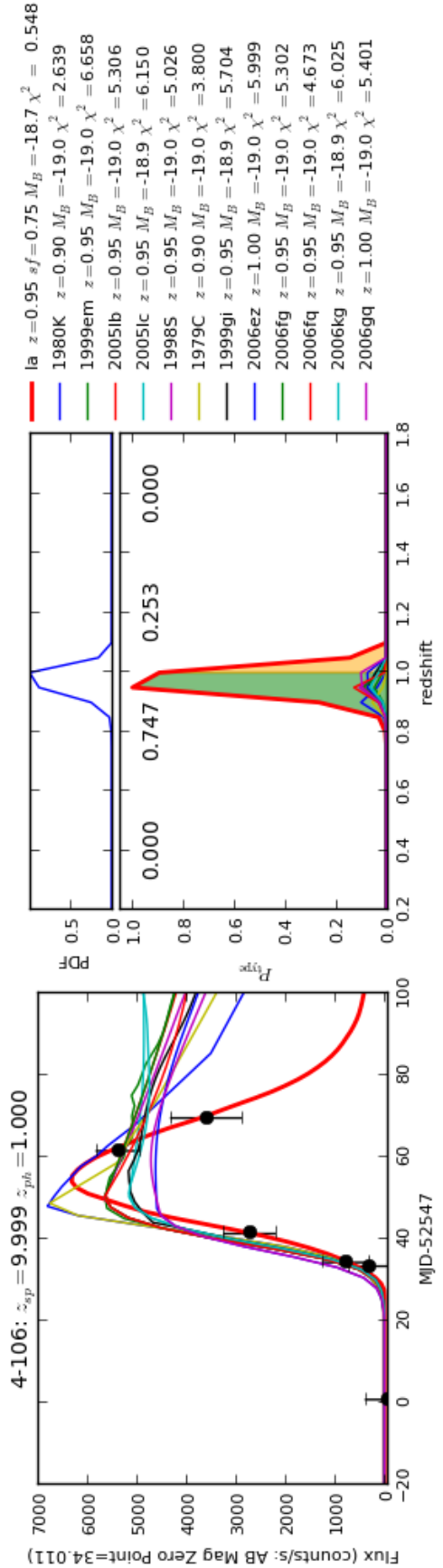
Ia z=0.95 sf=0.75 M_B=-18.7 χ^2= 0.548
1980K z=0.90 M_B=-19.0 χ^2=2.639
1999em z=0.95 M_B=-19.0 χ^2=6.658
2005lb z=0.95 M_B=-19.0 χ^2=5.306
2005lc z=0.95 M_B=-18.9 χ^2=6.150
1998S z=0.95 M_B=-19.0 χ^2=5.026
1979C z=0.90 M_B=-19.0 χ^2=3.800
1999gi z=0.95 M_B=-18.9 χ^2=5.704
2006ez z=1.00 M_B=-19.0 χ^2=5.999
2006fg z=0.95 M_B=-19.0 χ^2=5.302
2006fq z=0.95 M_B=-19.0 χ^2=4.673
2006kg z=0.95 M_B=-18.9 χ^2=6.025
2006gq z=1.00 M_B=-19.0 χ^2=5.401
4-106: z_{sp}=9.999 z_{ph}=1.000
Flux (counts/s: AB Mag Zero Point=34.011)
MJD-52547
P_{type}
0.000
0.747
0.253
0.000
redshift
PDF

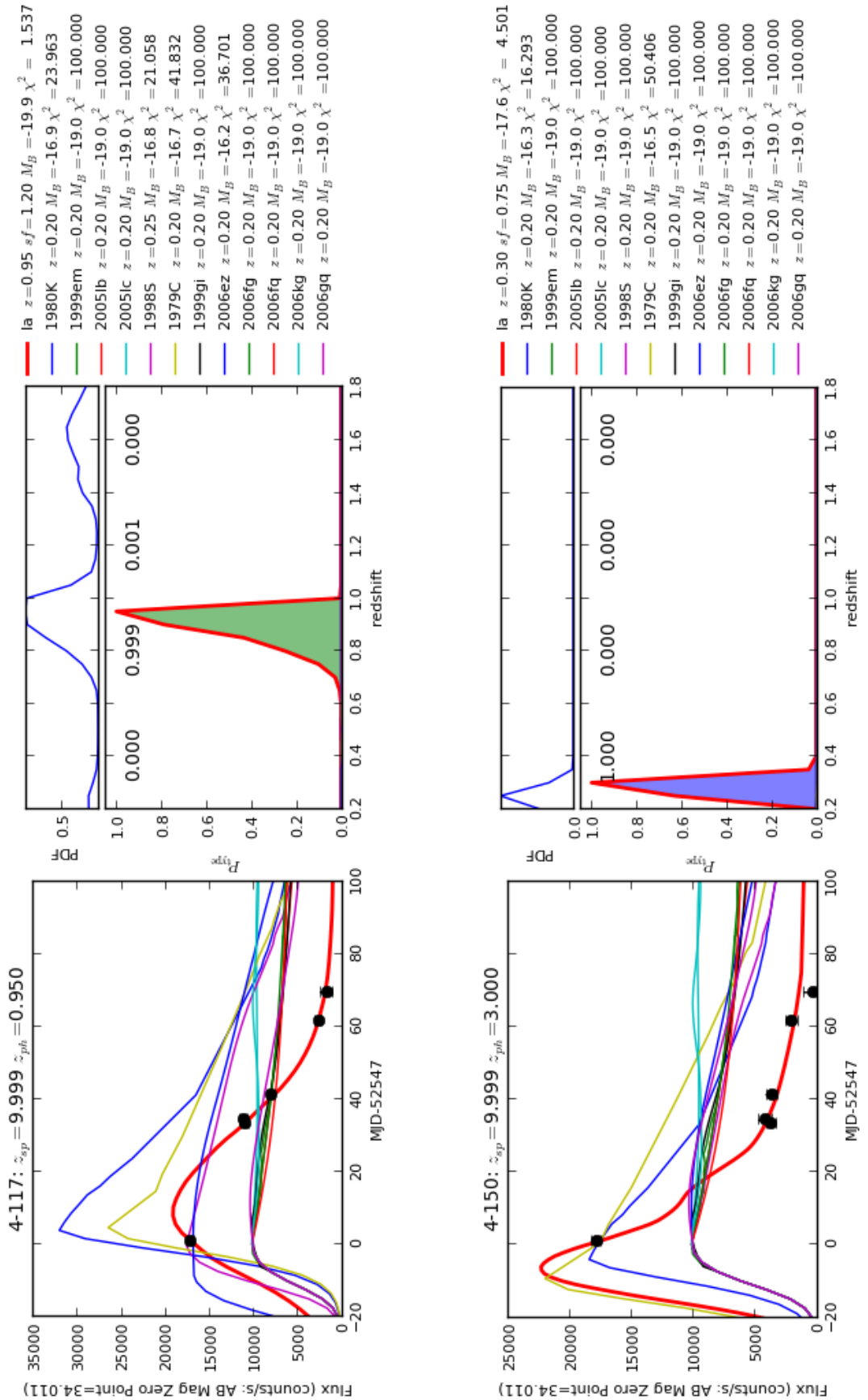
Ia z=0.95 sf=1.20 M_B=-19.9 χ^2= 1.537
1980K z=0.20 M_B=-16.9 χ^2=23.963
1999em z=0.20 M_B=-19.0 χ^2=100.000
2005lb z=0.20 M_B=-19.0 χ^2=100.000
2005lc z=0.20 M_B=-19.0 χ^2=100.000
1998S z=0.25 M_B=-16.8 χ^2=21.058
1979C z=0.20 M_B=-16.7 χ^2=41.832
1999gi z=0.20 M_B=-19.0 χ^2=100.000
2006ez z=0.20 M_B=-16.2 χ^2=36.701
2006fg z=0.20 M_B=-19.0 χ^2=100.000
2006fq z=0.20 M_B=-19.0 χ^2=100.000
2006kg z=0.20 M_B=-19.0 χ^2=100.000
2006gq z=0.20 M_B=-19.0 χ^2=100.000
4-117: z_{sp}=9.999 z_{ph}=0.950
Flux (counts/s: AB Mag Zero Point=34.011)
MJD-52547
P_{type}
redshift
PDF
0.000
0.999
0.001
Ia z=0.30 sf=0.75 M_B=-17.6 χ^2= 4.501
1980K z=0.20 M_B=-16.3 χ^2=16.293
1999em z=0.20 M_B=-19.0 χ^2=100.000
2005lb z=0.20 M_B=-19.0 χ^2=100.000
2005lc z=0.20 M_B=-19.0 χ^2=100.000
1998S z=0.20 M_B=-19.0 χ^2=100.000
1979C z=0.20 M_B=-16.5 χ^2=50.406
1999gi z=0.20 M_B=-19.0 χ^2=100.000
2006ez z=0.20 M_B=-19.0 χ^2=100.000
2006fg z=0.20 M_B=-19.0 χ^2=100.000
2006fq z=0.20 M_B=-19.0 χ^2=100.000
2006kg z=0.20 M_B=-19.0 χ^2=100.000
2006gq z=0.20 M_B=-19.0 χ^2=100.000
4-150: z_{sp}=9.999 z_{ph}=3.000
Flux (counts/s: AB Mag Zero Point=34.011)
MJD-52547
P_{type}
redshift
PDF
1.000
0.000

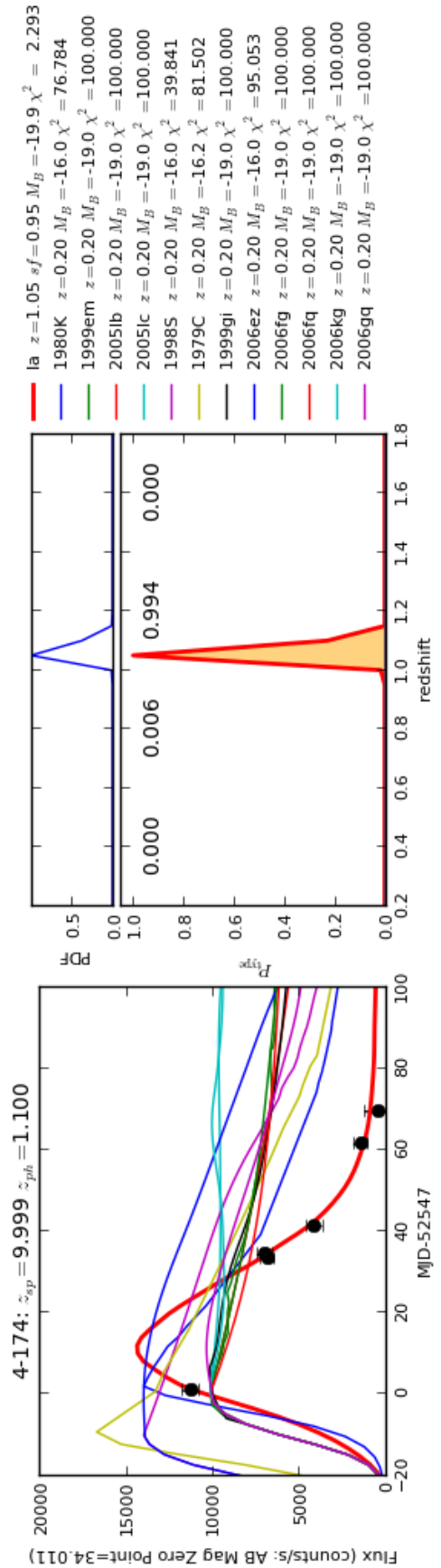
Ia z=1.05 sf=0.95 M_B=-19.9 χ^2 = 2.293
1980K z=0.20 M_B=-16.0 χ^2 =76.784
1999em z=0.20 M_B=-19.0 χ^2 =100.000
2005lb z=0.20 M_B=-19.0 χ^2 =100.000
2005lc z=0.20 M_B=-19.0 χ^2 =100.000
1998S z=0.20 M_B=-16.0 χ^2 =39.841
1979C z=0.20 M_B=-16.2 χ^2 =81.502
1999gi z=0.20 M_B=-19.0 χ^2 =100.000
2006ez z=0.20 M_B=-16.0 χ^2 =95.053
2006fg z=0.20 M_B=-19.0 χ^2 =100.000
2006fq z=0.20 M_B=-19.0 χ^2 =100.000
2006kg z=0.20 M_B=-19.0 χ^2 =100.000
2006gq z=0.20 M_B=-19.0 χ^2 =100.000
4-174: z_{sp}=9.999 z_{ph}=1.100
Flux (counts/s: AB Mag Zero Point=34.011)
MJD-52547
P_{type}
PDF
0.000
0.006
0.994
0.000
redshift

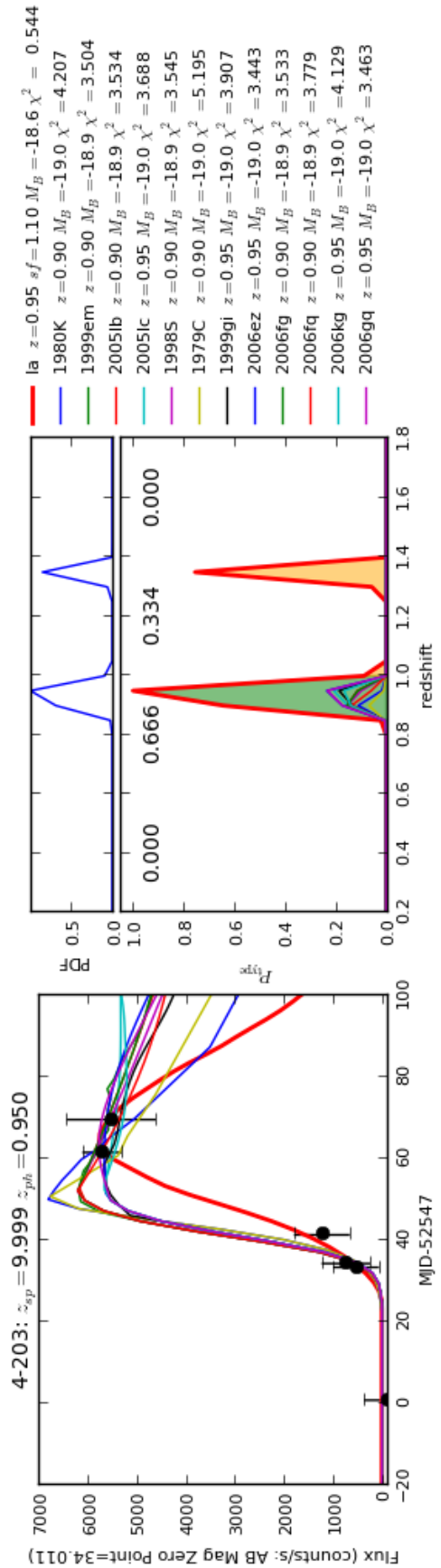
Ia z=0.95 sf=1.10 M_B=-18.6 χ^2 = 0.544
1980K z=0.90 M_B=-19.0 χ^2 =4.207
1999em z=0.90 M_B=-18.9 χ^2 =3.504
2005lb z=0.90 M_B=-18.9 χ^2 =3.534
2005lc z=0.95 M_B=-19.0 χ^2 =3.688
1998S z=0.90 M_B=-18.9 χ^2 =3.545
1979C z=0.90 M_B=-19.0 χ^2 =5.195
1999gi z=0.95 M_B=-19.0 χ^2 =3.907
2006ez z=0.95 M_B=-19.0 χ^2 =3.443
2006fg z=0.90 M_B=-18.9 χ^2 =3.533
2006fq z=0.90 M_B=-18.9 χ^2 =3.779
2006kg z=0.95 M_B=-19.0 χ^2 =4.129
2006gq z=0.95 M_B=-19.0 χ^2 =3.463
4-203: z_{sp}=9.999 z_{ph}=0.950
Flux (counts/s: AB Mag Zero Point=34.011)
MJD-52547
P_{type}
PDF
0.000
0.666
0.334
0.000
redshift

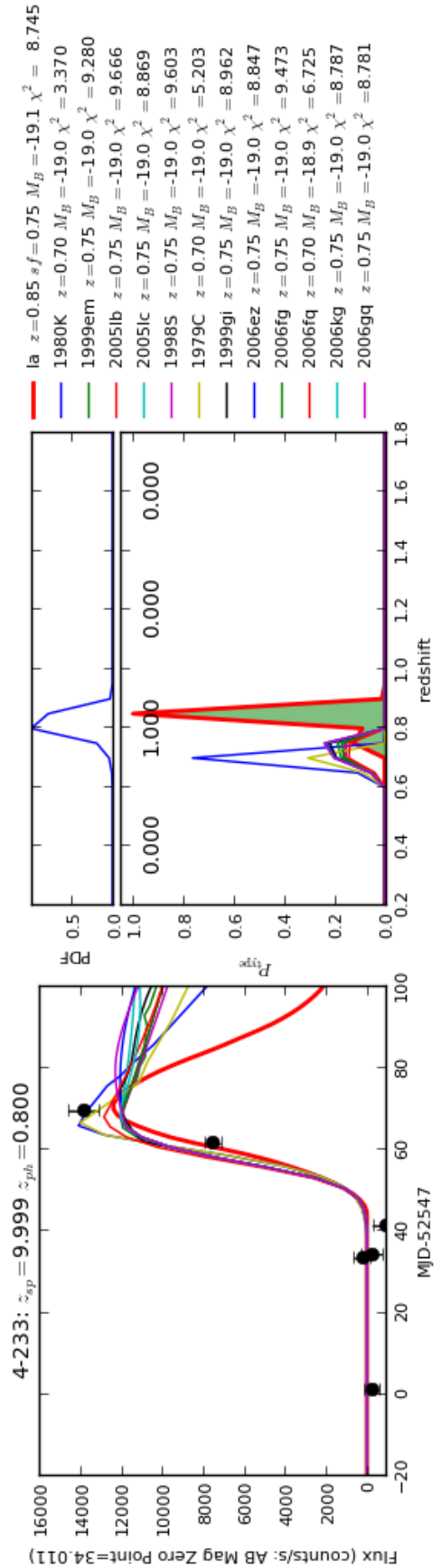
Ia z=0.85 sf=0.75 M_B=-19.1 χ^2 = 8.745
1980K z=0.70 M_B=-19.0 χ^2=3.370
1999em z=0.75 M_B=-19.0 χ^2=9.280
2005lb z=0.75 M_B=-19.0 χ^2=9.666
2005lc z=0.75 M_B=-19.0 χ^2=8.869
1998S z=0.75 M_B=-19.0 χ^2=9.603
1979C z=0.70 M_B=-19.0 χ^2=5.203
1999gi z=0.75 M_B=-19.0 χ^2=8.962
2006ez z=0.75 M_B=-19.0 χ^2=8.847
2006fg z=0.75 M_B=-19.0 χ^2=9.473
2006fq z=0.70 M_B=-18.9 χ^2=6.725
2006kg z=0.75 M_B=-19.0 χ^2=8.787
2006gq z=0.75 M_B=-19.0 χ^2=8.781
4-233: z_{sp}=9.999 z_{ph}=0.800
Flux (counts/s: AB Mag Zero Point=34.011)
MJD-52547
P_{type}
redshift
PDF
0.000
1.000
0.000
0.000
Ia z=0.65 sf=1.00 M_B=-19.3 χ^2 = 14.803
1980K z=0.65 M_B=-19.0 χ^2=72.292
1999em z=0.65 M_B=-19.0 χ^2=74.570
2005lb z=0.65 M_B=-19.0 χ^2=77.214
2005lc z=0.65 M_B=-19.0 χ^2=86.877
1998S z=0.65 M_B=-19.0 χ^2=100.000
1979C z=0.65 M_B=-19.0 χ^2=100.000
1999gi z=0.65 M_B=-19.0 χ^2=100.000
2006ez z=0.65 M_B=-19.0 χ^2=100.000
2006fg z=0.65 M_B=-19.0 χ^2=100.000
2006fq z=0.65 M_B=-19.0 χ^2=100.000
2006kg z=0.65 M_B=-19.0 χ^2=100.000
2006gq z=0.65 M_B=-19.0 χ^2=100.000
5-029: z_{sp}=0.606 z_{ph}=0.550
Flux (counts/s: AB Mag Zero Point=34.079)
MJD-52547
P_{type}
redshift
PDF
0.000
1.000
0.000
0.000

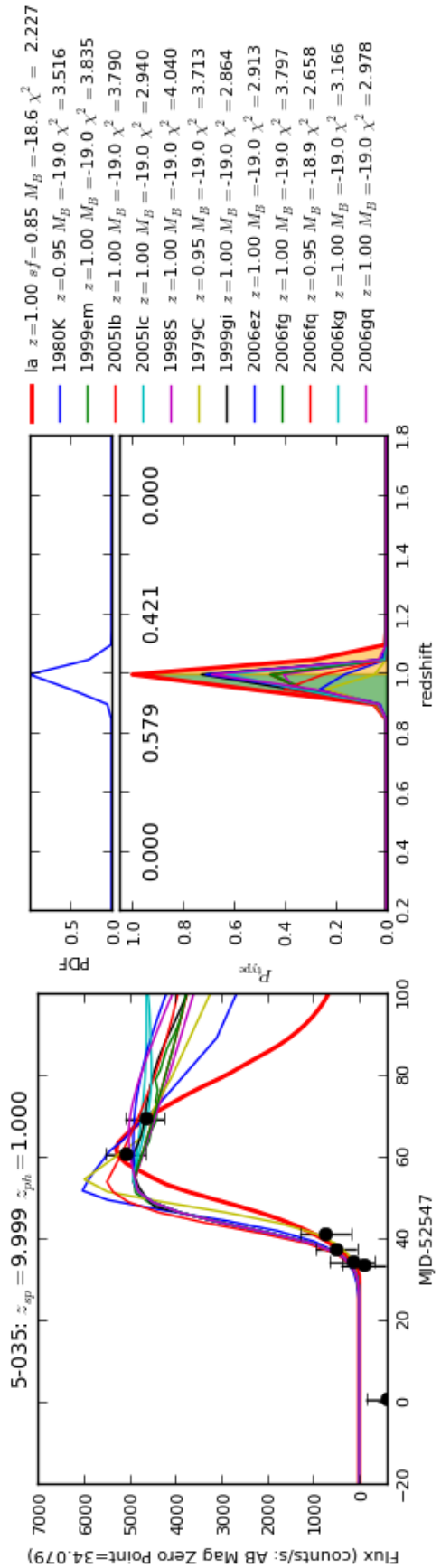
Ia z=1.00 sf=0.85 M_B=-18.6 χ^2= 2.227
1980K z=0.95 M_B=-19.0 χ^2=3.516
1999em z=1.00 M_B=-19.0 χ^2=3.835
2005lb z=1.00 M_B=-19.0 χ^2=3.790
2005lc z=1.00 M_B=-19.0 χ^2=2.940
1998S z=1.00 M_B=-19.0 χ^2=4.040
1979C z=0.95 M_B=-19.0 χ^2=3.713
1999gi z=1.00 M_B=-19.0 χ^2=2.864
2006ez z=1.00 M_B=-19.0 χ^2=2.913
2006fg z=1.00 M_B=-19.0 χ^2=3.797
2006fq z=0.95 M_B=-18.9 χ^2=2.658
2006kg z=1.00 M_B=-19.0 χ^2=3.166
2006gq z=1.00 M_B=-19.0 χ^2=2.978
5-035: z_{sp}=9.999 z_{ph}=1.000
0.000
0.579
0.421
0.000
PDF
P_{type}
redshift
MJD-52547
Flux (counts/s: AB Mag Zero Point=34.079)
Ia z=1.05 sf=0.90 M_B=-19.0 χ^2= 5.596
1980K z=1.05 M_B=-19.0 χ^2=24.683
1999em z=1.05 M_B=-19.0 χ^2=25.873
2005lb z=1.05 M_B=-19.0 χ^2=29.093
2005lc z=1.05 M_B=-19.0 χ^2=32.754
1998S z=1.05 M_B=-19.0 χ^2=33.077
1979C z=1.05 M_B=-19.0 χ^2=38.956
1999gi z=1.05 M_B=-19.0 χ^2=40.990
2006ez z=1.05 M_B=-19.0 χ^2=41.069
2006fg z=1.05 M_B=-19.0 χ^2=43.223
2006fq z=1.05 M_B=-19.0 χ^2=48.879
2006kg z=1.05 M_B=-19.0 χ^2=82.714
2006gq z=1.05 M_B=-19.0 χ^2=87.665
5-049: z_{sp}=1.094 z_{ph}=1.000
0.000
0.000
1.000
0.000
PDF
P_{type}
redshift
MJD-52547
Flux (counts/s: AB Mag Zero Point=34.079)

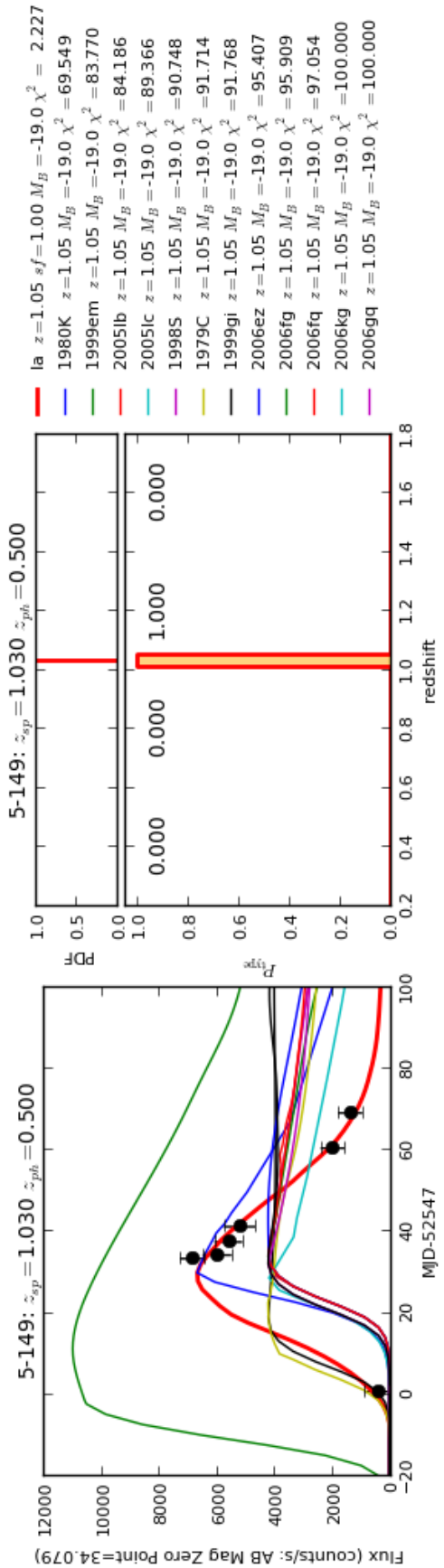
Ia z=1.05 sf=1.00 M_B=-19.0 χ^2 = 2.227
1980K z=1.05 M_B=-19.0 χ^2=69.549
1999em z=1.05 M_B=-19.0 χ^2=83.770
2005lb z=1.05 M_B=-19.0 χ^2=84.186
2005lc z=1.05 M_B=-19.0 χ^2=89.366
1998S z=1.05 M_B=-19.0 χ^2=90.748
1979C z=1.05 M_B=-19.0 χ^2=91.714
1999gi z=1.05 M_B=-19.0 χ^2=91.768
2006ez z=1.05 M_B=-19.0 χ^2=95.407
2006fg z=1.05 M_B=-19.0 χ^2=95.909
2006fq z=1.05 M_B=-19.0 χ^2=97.054
2006kg z=1.05 M_B=-19.0 χ^2=100.000
2006gq z=1.05 M_B=-19.0 χ^2=100.000
5-149: z_{sp}=1.030 z_{ph}=0.500
PDF
0.000
1.000
0.000
0.000
redshift
P_{type}
5-149: z_{sp}=1.030 z_{ph}=0.500
MJD-52547
Flux (counts/s: AB Mag Zero Point=34.079)

Bibliography

[Alard & Lupton 1998] C. Alard and R. H. Lupton. *A Method for Optimal Image Subtraction.* The Astrophysical Journal, vol. 503, page 325, August 1998.

[Alard 2000] C. Alard. *Image subtraction using a space-varying kernel.* Astronomy & Astrophysics Supplement Series, vol. 144, pages 363–370, June 2000.

[Aldering et al. 2006] G. Aldering, P. Antilogus, S. Bailey, C. Baltay, A. Bauer, N. Blanc, S. Bongard, Y. Copin, E. Gangler, S. Gilles, R. Kessler, D. Kocevski, B. C. Lee, S. Loken, P. Nugent, R. Pain, E. Pécontal, R. Pereira, S. Perlmutter, D. Rabinowitz, G. Rigaudier, R. Scalzo, G. Smadja, R. C. Thomas, L. Wang, B. A. Weaver and Nearby Supernova Factory. *Nearby Supernova Factory Observations of SN 2005gj: Another Type Ia Supernova in a Massive Circumstellar Envelope.* The Astrophysical Journal, vol. 650, pages 510–527, October 2006.

[Amanullah et al. 2010] R. Amanullah, C. Lidman, D. Rubin, G. Aldering, P. Astier, K. Barbary, M. S. Burns, A. Conley, K. S. Dawson, S. E. Deustua, M. Doi, S. Fabbro, L. Faccioli, H. K. Fakhouri, G. Folatelli, A. S. Fruchter, H. Furusawa, G. Garavini, G. Goldhaber, A. Goobar, D. E. Groom, I. Hook, D. A. Howell, N. Kashikawa, A. G. Kim, R. A. Knop, M. Kowalski, E. Linder, J. Meyers, T. Morokuma, S. Nobili, J. Nordin, P. E. Nugent, L. Östman, R. Pain, N. Panagia, S. Perlmutter, J. Raux, P. Ruiz-Lapuente, A. L. Spadafora, M. Strovink, N. Suzuki, L. Wang, W. M. Wood-Vasey, N. Yasuda and T. Supernova Cosmology Project. *Spectra and Hubble Space Telescope Light Curves of Six Type Ia Supernovae at* $0.511 \leq z \leq 1.12$ *and the Union2 Compilation.* The Astrophysical Journal, vol. 716, pages 712–738, June 2010.

[Arnett et al. 1985] W. D. Arnett, D. Branch and J. C. Wheeler. *Hubble's constant and exploding carbon-oxygen white dwarf models for Type I supernovae.* Nature, vol. 314, page 337, March 1985.

[Arnett 1982] W. D. Arnett. *Type I supernovae. I - Analytic solutions for the early part of the light curve.* The Astrophysical Journal, vol. 253, pages 785–797, February 1982.

[Arnouts et al. 1999] S. Arnouts, S. Cristiani, L. Moscardini, S. Matarrese, F. Lucchin, A. Fontana and E. Giallongo. *Measuring and modelling the redshift evolution of clustering: the Hubble Deep Field North.* Monthly Notices of the Royal Astronomical Society, vol. 310, pages 540–556, December 1999.

[Astier et al. 2006] P. Astier, J. Guy, N. Regnault, R. Pain, E. Aubourg, D. Balam, S. Basa, R. G. Carlberg, S. Fabbro, D. Fouchez, I. M. Hook, D. A. Howell, H. Lafoux,

J. D. Neill, N. Palanque-Delabrouille, K. Perrett, C. J. Pritchet, J. Rich, M. Sullivan, R. Taillet, G. Aldering, P. Antilogus, V. Arsenijevic, C. Balland, S. Baumont, J. Bronder, H. Courtois, R. S. Ellis, M. Filiol, A. C. Gonçalves, A. Goobar, D. Guide, D. Hardin, V. Lusset, C. Lidman, R. McMahon, M. Mouchet, A. Mourao, S. Perlmutter, P. Ripoche, C. Tao and N. Walton. *The Supernova Legacy Survey: measurement of Ω_M, Ω_λ and w from the first year data set.* Astronomy & Astrophysics, vol. 447, pages 31–48, February 2006.

[Baade & Zwicky 1934] W. Baade and F. Zwicky. *On Super-novae.* Proceedings of the National Academy of Science, vol. 20, pages 254–259, May 1934.

[Badenes & Maoz 2012] C. Badenes and D. Maoz. *The Merger Rate of Binary White Dwarfs in the Galactic Disk.* The Astrophysical Journal Letters, vol. 749, page L11, April 2012.

[Bailey et al. 2009] S. Bailey, G. Aldering, P. Antilogus, C. Aragon, C. Baltay, S. Bongard, C. Buton, M. Childress, N. Chotard, Y. Copin, E. Gangler, S. Loken, P. Nugent, R. Pain, E. Pecontal, R. Pereira, S. Perlmutter, D. Rabinowitz, G. Rigaudier, K. Runge, R. Scalzo, G. Smadja, H. Swift, C. Tao, R. C. Thomas, C. Wu and Nearby Supernova Factory. *Using spectral flux ratios to standardize SN Ia luminosities.* Astronomy & Astrophysics, vol. 500, pages L17–L20, June 2009.

[Barbary et al. 2012] K. Barbary, G. Aldering, R. Amanullah, M. Brodwin, N. Connolly, K. S. Dawson, M. Doi, P. Eisenhardt, L. Faccioli, V. Fadeyev, H. K. Fakhouri, A. S. Fruchter, D. G. Gilbank, M. D. Gladders, G. Goldhaber, A. Goobar, T. Hattori, E. Hsiao, X. Huang, Y. Ihara, N. Kashikawa, B. Koester, K. Konishi, M. Kowalski, C. Lidman, L. Lubin, J. Meyers, T. Morokuma, T. Oda, N. Panagia, S. Perlmutter, M. Postman, P. Ripoche, P. Rosati, D. Rubin, D. J. Schlegel, A. L. Spadafora, S. A. Stanford, M. Strovink, N. Suzuki, N. Takanashi, K. Tokita, N. Yasuda and Supernova Cosmology Project. *The Hubble Space Telescope Cluster Supernova Survey. VI. The Volumetric Type Ia Supernova Rate.* The Astrophysical Journal, vol. 745, page 31, January 2012.

[Barbon et al. 1979] R. Barbon, F. Ciatti and L. Rosino. *Photometric properties of type II supernovae.* Astronomy & Astrophysics, vol. 72, pages 287–292, February 1979.

[Bazin et al. 2009] G. Bazin, N. Palanque-Delabrouille, J. Rich, V. Ruhlmann-Kleider, E. Aubourg, L. Le Guillou, P. Astier, C. Balland, S. Basa, R. G. Carlberg, A. Conley, D. Fouchez, J. Guy, D. Hardin, I. M. Hook, D. A. Howell, R. Pain, K. Perrett, C. J. Pritchet, N. Regnault, M. Sullivan, P. Antilogus, V. Arsenijevic, S. Baumont, S. Fabbro, J. Le Du, C. Lidman, M. Mouchet, A. Mourão and E. S. Walker. *The core-collapse rate from the Supernova Legacy Survey.* Astronomy & Astrophysics, vol. 499, pages 653–660, June 2009.

[Benetti et al. 2006] S. Benetti, E. Cappellaro, M. Turatto, S. Taubenberger, A. Harutyunyan and S. Valenti. *Supernova 2002ic: The Collapse of a Stripped-Envelope, Massive Star*

in a Dense Medium? The Astrophysical Journal Letters, vol. 653, pages L129–L132, December 2006.

[Blondin et al. 2009] S. Blondin, J. L. Prieto, F. Patat, P. Challis, M. Hicken, R. P. Kirshner, T. Matheson and M. Modjaz. *A Second Case of Variable Na I D Lines in a Highly Reddened Type Ia Supernova.* The Astrophysical Journal, vol. 693, pages 207–215, March 2009.

[Blondin et al. 2011] S. Blondin, K. S. Mandel and R. P. Kirshner. *Do spectra improve distance measurements of Type Ia supernovae?* Astronomy & Astrophysics, vol. 526, page A81, February 2011.

[Bloom et al. 2012] J. S. Bloom, D. Kasen, K. J. Shen, P. E. Nugent, N. R. Butler, M. L. Graham, D. A. Howell, U. Kolb, S. Holmes, C. A. Haswell, V. Burwitz, J. Rodriguez and M. Sullivan. *A Compact Degenerate Primary-star Progenitor of SN 2011fe.* The Astrophysical Journal Letters, vol. 744, page L17, January 2012.

[Boissier & Prantzos 2009] S. Boissier and N. Prantzos. *Relative frequencies of supernovae types: dependence on host galaxy magnitude, galactocentric radius, and local metallicity.* Astronomy & Astrophysics, vol. 503, pages 137–150, August 2009.

[Botticella et al. 2008] M. T. Botticella, M. Riello, E. Cappellaro, S. Benetti, G. Altavilla, A. Pastorello, M. Turatto, L. Greggio, F. Patat, S. Valenti, L. Zampieri, A. Harutyunyan, G. Pignata and S. Taubenberger. *Supernova rates from the Southern inTermediate Redshift ESO Supernova Search (STRESS).* Astronomy & Astrophysics, vol. 479, pages 49–66, February 2008.

[Botticella et al. 2012] M. T. Botticella, S. J. Smartt, R. C. Kennicutt, E. Cappellaro, M. Sereno and J. C. Lee. *A comparison between star formation rate diagnostics and rate of core collapse supernovae within 11 Mpc.* Astronomy & Astrophysics, vol. 537, page A132, January 2012.

[Brahe 1573] T. Brahe. Tychonis Brahe Astronomiae instauratae progymnasmata, quorum haec prima pars de restitutione motuum SOLIS et lunae stellarumque inerrantium tractat, et praeterea de admiranda nova stella anno 1572 exorta luculenter agit. 1573.

[Branch & Tammann 1992] D. Branch and G. A. Tammann. *Type IA supernovae as standard candles.* Annual Review of Astronomy and Astrophysics, vol. 30, pages 359–389, 1992.

[Branch et al. 1993] D. Branch, A. Fisher and P. Nugent. *On the relative frequencies of spectroscopically normal and peculiar type IA supernovae.* The Astronomical Journal, vol. 106, pages 2383–2391, December 1993.

[Branch 1998] D. Branch. *Type IA Supernovae and the Hubble Constant.* Annual Review of Astronomy and Astrophysics, vol. 36, pages 17–56, 1998.

[Brown et al. 2012] P. J. Brown, K. S. Dawson, M. de Pasquale, C. Gronwall, S. Holland, S. Immler, P. Kuin, P. Mazzali, P. Milne, S. Oates and M. Siegel. *A Swift Look*

at SN 2011fe: The Earliest Ultraviolet Observations of a Type Ia Supernova. The Astrophysical Journal, vol. 753, page 22, July 2012.

[Buta 1982] R. J. Buta. *Photometric observations of the bright Type II supernova 1980K in NGC 6946.* Publications of the Astronomical Society of the Pacific, vol. 94, pages 578–585, June 1982.

[Cappellaro et al. 1999] E. Cappellaro, R. Evans and M. Turatto. *A new determination of supernova rates and a comparison with indicators for galactic star formation.* Astronomy & Astrophysics, vol. 351, pages 459–466, November 1999.

[Cappellaro et al. 2005] E. Cappellaro, M. Riello, G. Altavilla, M. T. Botticella, S. Benetti, A. Clocchiatti, J. I. Danziger, P. Mazzali, A. Pastorello, F. Patat, M. Salvo, M. Turatto and S. Valenti. *Death rate of massive stars at redshift* $\tilde{0}.3$. Astronomy & Astrophysics, vol. 430, pages 83–93, January 2005.

[Chandrasekhar 1931] S. Chandrasekhar. *The Maximum Mass of Ideal White Dwarfs.* The Astrophysical Journal, vol. 74, page 81, July 1931.

[Chevalier 1982] R. A. Chevalier. *Self-similar solutions for the interaction of stellar ejecta with an external medium.* The Astrophysical Journal, vol. 258, pages 790–797, July 1982.

[Chevalier 1998] R. A. Chevalier. *Synchrotron Self-Absorption in Radio Supernovae.* The Astrophysical Journal, vol. 499, page 810, May 1998.

[Chomiuk et al. 2012] L. Chomiuk, A. M. Soderberg, M. Moe, R. A. Chevalier, M. P. Rupen, C. Badenes, R. Margutti, C. Fransson, W.-f. Fong and J. A. Dittmann. *EVLA Observations Constrain the Environment and Progenitor System of Type Ia Supernova 2011fe.* The Astrophysical Journal, vol. 750, page 164, May 2012.

[Chugai & Yungelson 2004] N. N. Chugai and L. R. Yungelson. *Type-Ia Supernovae in Dense Circumstellar Gas.* Astronomy Letters, vol. 30, pages 65–72, February 2004.

[Colgate & McKee 1969] S. A. Colgate and C. McKee. *Early Supernova Luminosity.* The Astrophysical Journal, vol. 157, page 623, August 1969.

[Conley et al. 2008] A. Conley, M. Sullivan, E. Y. Hsiao, J. Guy, P. Astier, D. Balam, C. Balland, S. Basa, R. G. Carlberg, D. Fouchez, D. Hardin, D. A. Howell, I. M. Hook, R. Pain, K. Perrett, C. J. Pritchet and N. Regnault. *SiFTO: An Empirical Method for Fitting SN Ia Light Curves.* The Astrophysical Journal, vol. 681, pages 482–498, July 2008.

[Dahlen et al. 2004] T. Dahlen, L.-G. Strolger, A. G. Riess, B. Mobasher, R.-R. Chary, C. J. Conselice, H. C. Ferguson, A. S. Fruchter, M. Giavalisco, M. Livio, P. Madau, N. Panagia and J. L. Tonry. *High-Redshift Supernova Rates.* The Astrophysical Journal, vol. 613, pages 189–199, September 2004.

[Dahlen et al. 2008] T. Dahlen, L.-G. Strolger and A. G. Riess. *The Extended HST Supernova Survey: The Rate of SNe Ia at $z \geq 1.4$ Remains Low.* The Astrophysical Journal, vol. 681, pages 462–469, July 2008.

[Dahlen et al. 2012] T. Dahlen, L.-G. Strolger, A. G. Riess, S. Mattila, E. Kankare and B. Mobasher. *The Extended Hubble Space Telescope Supernova Survey: The Rate of Core Collapse Supernovae to z ˜ 1.* The Astrophysical Journal, vol. 757, page 70, September 2012.

[D'Andrea et al. 2010] C. B. D'Andrea, M. Sako, B. Dilday, J. A. Frieman, J. Holtzman, R. Kessler, K. Konishi, D. P. Schneider, J. Sollerman, J. C. Wheeler, N. Yasuda, D. Cinabro, S. Jha, R. C. Nichol, H. Lampeitl, M. Smith, D. W. Atlee, B. Bassett, F. J. Castander, A. Goobar, R. Miquel, J. Nordin, L. Östman, J. L. Prieto, R. Quimby, A. G. Riess and M. Stritzinger. *Type II-P Supernovae from the SDSS-II Supernova Survey and the Standardized Candle Method.* The Astrophysical Journal, vol. 708, pages 661–674, January 2010.

[de Vaucouleurs et al. 1981] G. de Vaucouleurs, A. de Vaucouleurs, R. Buta, H. D. Ables and A. V. Hewitt. *The bright supernova 1979c in M100.* Publications of the Astronomical Society of the Pacific, vol. 93, pages 36–44, February 1981.

[della Valle & Livio 1996] M. della Valle and M. Livio. *On the Frequency of Occurrence of Recurrent Novae and Their Role as Type IA Supernova Progenitors.* The Astrophysical Journal, vol. 473, page 240, December 1996.

[Di Stefano et al. 2011] R. Di Stefano, R. Voss and J. S. W. Claeys. *Spin-up/Spin-down Models for Type Ia Supernovae.* The Astrophysical Journal Letters, vol. 738, page L1, September 2011.

[Di Stefano 2010] R. Di Stefano. *The Progenitors of Type Ia Supernovae. I. Are they Supersoft Sources?* The Astrophysical Journal, vol. 712, pages 728–733, March 2010.

[Dilday et al. 2008] B. Dilday, R. Kessler, J. A. Frieman, J. Holtzman, J. Marriner, G. Miknaitis, R. C. Nichol, R. Romani, M. Sako, B. Bassett, A. Becker, D. Cinabro, F. DeJongh, D. L. Depoy, M. Doi, P. M. Garnavich, C. J. Hogan, S. Jha, K. Konishi, H. Lampeitl, J. L. Marshall, D. McGinnis, J. L. Prieto, A. G. Riess, M. W. Richmond, D. P. Schneider, M. Smith, N. Takanashi, K. Tokita, K. van der Heyden, N. Yasuda, C. Zheng, J. Barentine, H. Brewington, C. Choi, A. Crotts, J. Dembicky, M. Harvanek, M. Im, W. Ketzeback, S. J. Kleinman, J. Krzesiński, D. C. Long, E. Malanushenko, V. Malanushenko, R. J. McMillan, A. Nitta, K. Pan, G. Saurage, S. A. Snedden, S. Watters, J. C. Wheeler and D. York. *A Measurement of the Rate of Type Ia Supernovae at Redshift z ˜ 0.1 from the First Season of the SDSS-II Supernova Survey.* The Astrophysical Journal, vol. 682, pages 262–282, July 2008.

[Dilday et al. 2010] B. Dilday, B. Bassett, A. Becker, R. Bender, F. Castander, D. Cinabro, J. A. Frieman, L. Galbany, P. Garnavich, A. Goobar, U. Hopp, Y. Ihara, S. W. Jha, R. Kessler, H. Lampeitl, J. Marriner, R. Miquel, M. Mollá, R. C. Nichol, J. Nordin,

A. G. Riess, M. Sako, D. P. Schneider, M. Smith, J. Sollerman, J. C. Wheeler, L. Östman, D. Bizyaev, H. Brewington, E. Malanushenko, V. Malanushenko, D. Oravetz, K. Pan, A. Simmons and S. Snedden. *A Measurement of the Rate of Type Ia Supernovae in Galaxy Clusters from the SDSS-II Supernova Survey.* The Astrophysical Journal, vol. 715, pages 1021–1035, June 2010.

[Dilday et al. 2012] B. Dilday, D. A. Howell, S. B. Cenko, J. M. Silverman, P. E. Nugent, M. Sullivan, S. Ben-Ami, L. Bildsten, M. Bolte, M. Endl, A. V. Filippenko, O. Gnat, A. Horesh, E. Hsiao, M. M. Kasliwal, D. Kirkman, K. Maguire, G. W. Marcy, K. Moore, Y. Pan, J. T. Parrent, P. Podsiadlowski, R. M. Quimby, A. Sternberg, N. Suzuki, D. R. Tytler, D. Xu, J. S. Bloom, A. Gal-Yam, I. M. Hook, S. R. Kulkarni, N. M. Law, E. O. Ofek, D. Polishook and D. Poznanski. *PTF 11kx: A Type Ia Supernova with a Symbiotic Nova Progenitor.* Science, vol. 337, pages 942–, August 2012.

[Doggett & Branch 1985] J. B. Doggett and D. Branch. *A comparative study of supernova light curves.* The Astronomical Journal, vol. 90, pages 2303–2311, November 1985.

[Edwards et al. 2012] Z. I. Edwards, A. Pagnotta and B. E. Schaefer. *The Progenitor of the Type Ia Supernova that Created SNR 0519-69.0 in the Large Magellanic Cloud.* The Astrophysical Journal Letters, vol. 747, page L19, March 2012.

[Elias-Rosa et al. 2006] N. Elias-Rosa, S. Benetti, E. Cappellaro, M. Turatto, P. A. Mazzali, F. Patat, W. P. S. Meikle, M. Stehle, A. Pastorello, G. Pignata, R. Kotak, A. Harutyunyan, G. Altavilla, H. Navasardyan, Y. Qiu, M. Salvo and W. Hillebrandt. *Anomalous extinction behaviour towards the Type Ia SN 2003cg.* Monthly Notices of the Royal Astronomical Society, vol. 369, pages 1880–1900, July 2006.

[Elias-Rosa et al. 2008] N. Elias-Rosa, S. Benetti, M. Turatto, E. Cappellaro, S. Valenti, A. A. Arkharov, J. E. Beckman, A. di Paola, M. Dolci, A. V. Filippenko, R. J. Foley, K. Krisciunas, V. M. Larionov, W. Li, W. P. S. Meikle, A. Pastorello, G. Valentini and W. Hillebrandt. *SN 2002cv: a heavily obscured Type Ia supernova.* Monthly Notices of the Royal Astronomical Society, vol. 384, pages 107–122, February 2008.

[Ellis et al. 2008] R. S. Ellis, M. Sullivan, P. E. Nugent, D. A. Howell, A. Gal-Yam, P. Astier, D. Balam, C. Balland, S. Basa, R. G. Carlberg, A. Conley, D. Fouchez, J. Guy, D. Hardin, I. Hook, R. Pain, K. Perrett, C. J. Pritchet and N. Regnault. *Verifying the Cosmological Utility of Type Ia Supernovae: Implications of a Dispersion in the Ultraviolet Spectra.* The Astrophysical Journal, vol. 674, pages 51–69, February 2008.

[Elmhamdi et al. 2003] A. Elmhamdi, I. J. Danziger, N. Chugai, A. Pastorello, M. Turatto, E. Cappellaro, G. Altavilla, S. Benetti, F. Patat and M. Salvo. *Photometry and spectroscopy of the Type IIP SN 1999em from outburst to dust formation.* Monthly Notices of the Royal Astronomical Society, vol. 338, pages 939–956, February 2003.

[Fassia et al. 2000] A. Fassia, W. P. S. Meikle, W. D. Vacca, S. N. Kemp, N. A. Walton, D. L. Pollacco, S. Smartt, A. Oscoz, A. Aragón-Salamanca, S. Bennett, T. G. Hawarden,

A. Alonso, D. Alcalde, A. Pedrosa, J. Telting, M. J. Arevalo, H. J. Deeg, F. Garzón, A. Gómez-Roldán, G. Gómez, C. Gutiérrez, S. López, M. Rozas, M. Serra-Ricart and M. R. Zapatero-Osorio. *Optical and infrared photometry of the Type IIn SN 1998S: days 11-146.* Monthly Notices of the Royal Astronomical Society, vol. 318, pages 1093–1104, November 2000.

[Filippenko 1997] A. V. Filippenko. *Optical Spectra of Supernovae.* Annual Review of Astronomy and Astrophysics, vol. 35, pages 309–355, 1997.

[Fioc & Rocca-Volmerange 1997] M. Fioc and B. Rocca-Volmerange. *PEGASE: a UV to NIR spectral evolution model of galaxies. Application to the calibration of bright galaxy counts.* Astronomy & Astrophysics, vol. 326, pages 950–962, October 1997.

[Fioc & Rocca-Volmerange 1999] M. Fioc and B. Rocca-Volmerange. *A statistical study of nearby galaxies. I. NIR growth curves and optical-to-NIR colors as a function of type, luminosity and inclination.* Astronomy & Astrophysics, vol. 351, pages 869–882, November 1999.

[Folatelli et al. 2010] G. Folatelli, M. M. Phillips, C. R. Burns, C. Contreras, M. Hamuy, W. L. Freedman, S. E. Persson, M. Stritzinger, N. B. Suntzeff, K. Krisciunas, L. Boldt, S. González, W. Krzeminski, N. Morrell, M. Roth, F. Salgado, B. F. Madore, D. Murphy, P. Wyatt, W. Li, A. V. Filippenko and N. Miller. *The Carnegie Supernova Project: Analysis of the First Sample of Low-Redshift Type-Ia Supernovae.* The Astronomical Journal, vol. 139, pages 120–144, January 2010.

[Foley et al. 2009] R. J. Foley, R. Chornock, A. V. Filippenko, M. Ganeshalingam, R. P. Kirshner, W. Li, S. B. Cenko, P. J. Challis, A. S. Friedman, M. Modjaz, J. M. Silverman and W. M. Wood-Vasey. *SN 2008ha: An Extremely Low Luminosity and Exceptionally Low Energy Supernova.* The Astronomical Journal, vol. 138, pages 376–391, August 2009.

[Foley et al. 2010] R. J. Foley, P. J. Brown, A. Rest, P. J. Challis, R. P. Kirshner and W. M. Wood-Vasey. *Early- and Late-Time Observations of SN 2008ha: Additional Constraints for the Progenitor and Explosion.* The Astrophysical Journal Letters, vol. 708, pages L61–L65, January 2010.

[Foley et al. 2012] R. J. Foley, J. D. Simon, C. R. Burns, A. Gal-Yam, M. Hamuy, R. P. Kirshner, N. I. Morrell, M. M. Phillips, G. A. Shields and A. Sternberg. *Linking Type Ia Supernova Progenitors and Their Resulting Explosions.* The Astrophysical Journal, vol. 752, page 101, June 2012.

[Foley et al. 2013] R. J. Foley, P. J. Challis, R. Chornock, M. Ganeshalingam, W. Li, G. H. Marion, N. I. Morrell, G. Pignata, M. D. Stritzinger, J. M. Silverman, X. Wang, J. P. Anderson, A. V. Filippenko, W. L. Freedman, M. Hamuy, S. W. Jha, R. P. Kirshner, C. McCully, S. E. Persson, M. M. Phillips, D. E. Reichart and A. M. Soderberg. *Type Iax Supernovae: A New Class of Stellar Explosion.* The Astrophysical Journal, vol. 767, page 57, April 2013.

[Fransson et al. 2005] C. Fransson, P. M. Challis, R. A. Chevalier, A. V. Filippenko, R. P. Kirshner, C. Kozma, D. C. Leonard, T. Matheson, E. Baron, P. Garnavich, S. Jha, B. Leibundgut, P. Lundqvist, C. S. J. Pun, L. Wang and J. C. Wheeler. *Hubble Space Telescope and Ground-based Observations of SN 1993J and SN 1998S: CNO Processing in the Progenitors.* The Astrophysical Journal, vol. 622, pages 991–1007, April 2005.

[Frieman et al. 2008] J. A. Frieman, B. Bassett, A. Becker, C. Choi, D. Cinabro, F. DeJongh, D. L. Depoy, B. Dilday, M. Doi, P. M. Garnavich, C. J. Hogan, J. Holtzman, M. Im, S. Jha, R. Kessler, K. Konishi, H. Lampeitl, J. Marriner, J. L. Marshall, D. McGinnis, G. Miknaitis, R. C. Nichol, J. L. Prieto, A. G. Riess, M. W. Richmond, R. Romani, M. Sako, D. P. Schneider, M. Smith, N. Takanashi, K. Tokita, K. van der Heyden, N. Yasuda, C. Zheng, J. Adelman-McCarthy, J. Annis, R. J. Assef, J. Barentine, R. Bender, R. D. Blandford, W. N. Boroski, M. Bremer, H. Brewington, C. A. Collins, A. Crotts, J. Dembicky, J. Eastman, A. Edge, E. Edmondson, E. Elson, M. E. Eyler, A. V. Filippenko, R. J. Foley, S. Frank, A. Goobar, T. Gueth, J. E. Gunn, M. Harvanek, U. Hopp, Y. Ihara, Ž. Ivezić, S. Kahn, J. Kaplan, S. Kent, W. Ketzeback, S. J. Kleinman, W. Kollatschny, R. G. Kron, J. Krzesiński, D. Lamenti, G. Leloudas, H. Lin, D. C. Long, J. Lucey, R. H. Lupton, E. Malanushenko, V. Malanushenko, R. J. McMillan, J. Mendez, C. W. Morgan, T. Morokuma, A. Nitta, L. Ostman, K. Pan, C. M. Rockosi, A. K. Romer, P. Ruiz-Lapuente, G. Saurage, K. Schlesinger, S. A. Snedden, J. Sollerman, C. Stoughton, M. Stritzinger, M. Subba Rao, D. Tucker, P. Vaisanen, L. C. Watson, S. Watters, J. C. Wheeler, B. Yanny and D. York. *The Sloan Digital Sky Survey-II Supernova Survey: Technical Summary.* The Astronomical Journal, vol. 135, pages 338–347, January 2008.

[Furusawa et al. 2008] H. Furusawa, G. Kosugi, M. Akiyama, T. Takata, K. Sekiguchi, I. Tanaka, I. Iwata, M. Kajisawa, N. Yasuda, M. Doi, M. Ouchi, C. Simpson, K. Shimasaku, T. Yamada, J. Furusawa, T. Morokuma, C. M. Ishida, K. Aoki, T. Fuse, M. Imanishi, M. Iye, H. Karoji, N. Kobayashi, T. Kodama, Y. Komiyama, Y. Maeda, S. Miyazaki, Y. Mizumoto, F. Nakata, J. Noumaru, R. Ogasawara, S. Okamura, T. Saito, T. Sasaki, Y. Ueda and M. Yoshida. *The Subaru/XMM-Newton Deep Survey (SXDS). II. Optical Imaging and Photometric Catalogs.* The Astrophysical Journal Supplement Series, vol. 176, pages 1–18, May 2008.

[Gallagher et al. 2008] J. S. Gallagher, P. M. Garnavich, N. Caldwell, R. P. Kirshner, S. W. Jha, W. Li, M. Ganeshalingam and A. V. Filippenko. *Supernovae in Early-Type Galaxies: Directly Connecting Age and Metallicity with Type Ia Luminosity.* The Astrophysical Journal, vol. 685, pages 752–766, October 2008.

[Geier et al. 2007] S. Geier, S. Nesslinger, U. Heber, N. Przybilla, R. Napiwotzki and R.-P. Kudritzki. *The hot subdwarf B + white dwarf binary KPD 1930+2752. A supernova type Ia progenitor candidate.* Astronomy & Astrophysics, vol. 464, pages 299–307, March 2007.

[Gilfanov & Bogdán 2010] M. Gilfanov and Á. Bogdán. *An upper limit on the contribution of*

accreting white dwarfs to the typeIa supernova rate. Nature, vol. 463, pages 924–925, February 2010.

[González Hernández et al. 2009] J. I. González Hernández, P. Ruiz-Lapuente, A. V. Filippenko, R. J. Foley, A. Gal-Yam and J. D. Simon. *The Chemical Abundances of Tycho G in Supernova Remnant 1572.* The Astrophysical Journal, vol. 691, pages 1–15, January 2009.

[González Hernández et al. 2012] J. I. González Hernández, P. Ruiz-Lapuente, H. M. Tabernero, D. Montes, R. Canal, J. Méndez and L. R. Bedin. *No surviving evolved companions of the progenitor of SN1006.* Nature, vol. 489, pages 533–536, September 2012.

[Graur & Maoz 2013] O. Graur and D. Maoz. *Discovery of 90 Type Ia supernovae among 700 000 Sloan spectra: the Type Ia supernova rate versus galaxy mass and star formation rate at redshift 0.1.* Monthly Notices of the Royal Astronomical Society, vol. 430, pages 1746–1763, April 2013.

[Graur et al. 2011] O. Graur, D. Poznanski, D. Maoz, N. Yasuda, T. Totani, M. Fukugita, A. V. Filippenko, R. J. Foley, J. M. Silverman, A. Gal-Yam, A. Horesh and B. T. Jannuzi. *Supernovae in the Subaru Deep Field: the rate and delay-time distribution of Type Ia supernovae out to redshift 2.* Monthly Notices of the Royal Astronomical Society, vol. 417, pages 916–940, October 2011.

[Graur et al. 2013] O. Graur, S. A. Rodney, D. Maoz, A. G. Riess, S. W. Jha, M. Postman, T. Dahlen, T. W.-S. Holoien, C. McCully, B. Patel, L.-G. Strolger, N. Benitez, D. Coe, S. Jouvel, E. Medezinski, A. Molino, M. Nonino, L. Bradley, A. Koekemoer, I. Balestra, S. Blondin, S. B. Cenko, K. I. Clubb, M. E. Dickinson, A. V. Filippenko, T. F. Frederiksen, P. Garnavich, J. Hjorth, D. O. Jones, B. Leibundgut, T. Matheson, B. Mobasher, P. Rosati, J. M. Silverman, V. U, K. Jedruszczuk, C. Li, K. Lin, M. Mirmelstein, J. Neustadt, A. Ovadia and E. H. Rogers. *Type-Ia Supernova Rates to Redshift 2.4 from CLASH: the Cluster Lensing And Supernova survey with Hubble.* ArXiv e-prints, October 2013.

[Guy et al. 2007] J. Guy, P. Astier, S. Baumont, D. Hardin, R. Pain, N. Regnault, S. Basa, R. G. Carlberg, A. Conley, S. Fabbro, D. Fouchez, I. M. Hook, D. A. Howell, K. Perrett, C. J. Pritchet, J. Rich, M. Sullivan, P. Antilogus, E. Aubourg, G. Bazin, J. Bronder, M. Filiol, N. Palanque-Delabrouille, P. Ripoche and V. Ruhlmann-Kleider. *SALT2: using distant supernovae to improve the use of type Ia supernovae as distance indicators.* Astronomy & Astrophysics, vol. 466, pages 11–21, April 2007.

[Hachinger et al. 2012] S. Hachinger, P. A. Mazzali, S. Taubenberger, M. Fink, R. Pakmor, W. Hillebrandt and I. R. Seitenzahl. *Spectral modelling of the 'super-Chandrasekhar' Type Ia SN 2009dc - testing a 2 $M_{\odot}$ white dwarf explosion model and alternatives.* Monthly Notices of the Royal Astronomical Society, vol. 427, pages 2057–2078, December 2012.

[Hachisu & Kato 2001] I. Hachisu and M. Kato. *Recurrent Novae as a Progenitor System of Type Ia Supernovae. I. RS Ophiuchi Subclass: Systems with a Red Giant Companion.* The Astrophysical Journal, vol. 558, pages 323–350, September 2001.

[Hachisu & Kato 2012] I. Hachisu and M. Kato. *A Extremely Massive White Dwarf of the Symbiotic Classical Nova V407 Cyg as Suggested by the RS Oph and U Sco Models.* Baltic Astronomy, vol. 21, pages 68–75, 2012.

[Hachisu et al. 1996] I. Hachisu, M. Kato and K. Nomoto. *A New Model for Progenitor Systems of Type IA Supernovae.* The Astrophysical Journal Letters, vol. 470, page L97, October 1996.

[Hachisu et al. 1999a] I. Hachisu, M. Kato and K. Nomoto. *A Wide Symbiotic Channel to Type IA Supernovae.* The Astrophysical Journal, vol. 522, pages 487–503, September 1999.

[Hachisu et al. 1999b] I. Hachisu, M. Kato, K. Nomoto and H. Umeda. *A New Evolutionary Path to Type IA Supernovae: A Helium-rich Supersoft X-Ray Source Channel.* The Astrophysical Journal, vol. 519, pages 314–323, July 1999.

[Hachisu et al. 2008] I. Hachisu, M. Kato and K. Nomoto. *The Delay-Time Distribution of Type Ia Supernovae and the Single-Degenerate Model.* The Astrophysical Journal Letters, vol. 683, pages L127–L130, August 2008.

[Hamuy et al. 1996] M. Hamuy, M. M. Phillips, N. B. Suntzeff, R. A. Schommer, J. Maza and R. Aviles. *The Absolute Luminosities of the Calan/Tololo Type IA Supernovae.* The Astronomical Journal, vol. 112, page 2391, December 1996.

[Hamuy et al. 2003] M. Hamuy, M. Phillips, N. Suntzeff and J. Maza. *Supernova 2002ic.* International Astronomical Union Circular, vol. 8151, page 2, June 2003.

[Han & Podsiadlowski 2006] Z. Han and P. Podsiadlowski. *A single-degenerate model for the progenitor of the Type Ia supernova 2002ic.* Monthly Notices of the Royal Astronomical Society, vol. 368, pages 1095–1100, May 2006.

[Hancock et al. 2011] P. J. Hancock, B. M. Gaensler and T. Murphy. *Visibility Stacking in the Quest for Type Ia Supernova Radio Emission.* The Astrophysical Journal Letters, vol. 735, page L35, July 2011.

[Hatano et al. 1998] K. Hatano, D. Branch and J. Deaton. *Extinction and Radial Distribution of Supernova Properties in Their Parent Galaxies.* The Astrophysical Journal, vol. 502, page 177, July 1998.

[Hicken et al. 2009] M. Hicken, W. M. Wood-Vasey, S. Blondin, P. Challis, S. Jha, P. L. Kelly, A. Rest and R. P. Kirshner. *Improved Dark Energy Constraints from ˜100 New CfA Supernova Type Ia Light Curves.* The Astrophysical Journal, vol. 700, pages 1097–1140, August 2009.

[Hillebrandt & Niemeyer 2000] W. Hillebrandt and J. C. Niemeyer. *Type IA Supernova Explosion Models.* Annual Review of Astronomy and Astrophysics, vol. 38, pages 191–230, 2000.

[Hillebrandt et al. 2013] W. Hillebrandt, M. Kromer, F. K. Röpke and A. J. Ruiter. *Towards an understanding of Type Ia supernovae from a synthesis of theory and observations.* Frontiers of Physics, vol. 8, pages 116–143, April 2013.

[Holwerda 2008] B. W. Holwerda. *Host galaxy extinction of Type Ia supernovae: co-evolution of interstellar medium structure and the extinction law with star formation.* Monthly Notices of the Royal Astronomical Society, vol. 386, pages 475–480, May 2008.

[Hopkins & Beacom 2006] A. M. Hopkins and J. F. Beacom. *On the Normalization of the Cosmic Star Formation History.* The Astrophysical Journal, vol. 651, pages 142–154, November 2006.

[Horesh et al. 2008] A. Horesh, D. Poznanski, E. O. Ofek and D. Maoz. *The rate of Type Ia supernovae at z ˜ 0.2 from SDSS-I overlapping fields.* Monthly Notices of the Royal Astronomical Society, vol. 389, pages 1871–1880, October 2008.

[Horesh et al. 2012] A. Horesh, S. R. Kulkarni, D. B. Fox, J. Carpenter, M. M. Kasliwal, E. O. Ofek, R. Quimby, A. Gal-Yam, S. B. Cenko, A. G. de Bruyn, A. Kamble, R. A. M. J. Wijers, A. J. van der Horst, C. Kouveliotou, P. Podsiadlowski, M. Sullivan, K. Maguire, D. A. Howell, P. E. Nugent, N. Gehrels, N. M. Law, D. Poznanski and M. Shara. *Early Radio and X-Ray Observations of the Youngest nearby Type Ia Supernova PTF 11kly (SN 2011fe).* The Astrophysical Journal, vol. 746, page 21, February 2012.

[Horiuchi et al. 2011] S. Horiuchi, J. F. Beacom, C. S. Kochanek, J. L. Prieto, K. Z. Stanek and T. A. Thompson. *The Cosmic Core-collapse Supernova Rate Does Not Match the Massive-star Formation Rate.* The Astrophysical Journal, vol. 738, page 154, September 2011.

[Howell et al. 2007] D. A. Howell, M. Sullivan, A. Conley and R. Carlberg. *Predicted and Observed Evolution in the Mean Properties of Type Ia Supernovae with Redshift.* The Astrophysical Journal Letters, vol. 667, pages L37–L40, September 2007.

[Howell et al. 2009] D. A. Howell, M. Sullivan, E. F. Brown, A. Conley, D. Le Borgne, E. Y. Hsiao, P. Astier, D. Balam, C. Balland, S. Basa, R. G. Carlberg, D. Fouchez, J. Guy, D. Hardin, I. M. Hook, R. Pain, K. Perrett, C. J. Pritchet, N. Regnault, S. Baumont, J. LeDu, C. Lidman, S. Perlmutter, N. Suzuki, E. S. Walker and J. C. Wheeler. *The Effect of Progenitor Age and Metallicity on Luminosity and ^{56}Ni Yield in Type Ia Supernovae.* The Astrophysical Journal, vol. 691, pages 661–671, January 2009.

[Howell 2001] D. A. Howell. *The Progenitors of Subluminous Type Ia Supernovae.* The Astrophysical Journal Letters, vol. 554, pages L193–L196, June 2001.

[Howell 2011] D. A. Howell. *Type Ia supernovae as stellar endpoints and cosmological tools.* Nature Communications, vol. 2, June 2011.

[Hoyle & Fowler 1960] F. Hoyle and W. A. Fowler. *Nucleosynthesis in Supernovae.* The Astrophysical Journal, vol. 132, page 565, November 1960.

[Hsiao et al. 2007] E. Y. Hsiao, A. Conley, D. A. Howell, M. Sullivan, C. J. Pritchet, R. G. Carlberg, P. E. Nugent and M. M. Phillips. *K-Corrections and Spectral Templates of Type Ia Supernovae.* The Astrophysical Journal, vol. 663, pages 1187–1200, July 2007.

[Hughes et al. 2007] J. P. Hughes, N. Chugai, R. Chevalier, P. Lundqvist and E. Schlegel. *Chandra Observations of Type Ia Supernovae: Upper Limits to the X-Ray Flux of SN 2002bo, SN 2002ic, SN 2005gj, and SN 2005ke.* The Astrophysical Journal, vol. 670, pages 1260–1274, December 2007.

[Iben & Tutukov 1984] I. Iben Jr. and A. V. Tutukov. *Supernovae of type I as end products of the evolution of binaries with components of moderate initial mass (M not greater than about 9 solar masses).* The Astrophysical Journal Supplement Series, vol. 54, pages 335–372, February 1984.

[Iben et al. 1987] I. Iben Jr., K. Nomoto, A. Tornambe and A. V. Tutukov. *On interacting helium star-white dwarf pairs as supernova precursors.* The Astrophysical Journal, vol. 317, pages 717–723, June 1987.

[Ihara et al. 2007] Y. Ihara, J. Ozaki, M. Doi, T. Shigeyama, N. Kashikawa, K. Komiyama and T. Hattori. *Searching for a Companion Star of Tycho's Type Ia Supernova with Optical Spectroscopic Observations.* Publications of the Astronomical Society of Japan, vol. 59, pages 811–826, August 2007.

[Ilbert et al. 2006] O. Ilbert, S. Arnouts, H. J. McCracken, M. Bolzonella, E. Bertin, O. Le Fèvre, Y. Mellier, G. Zamorani, R. Pellò, A. Iovino, L. Tresse, V. Le Brun, D. Bottini, B. Garilli, D. Maccagni, J. P. Picat, R. Scaramella, M. Scodeggio, G. Vettolani, A. Zanichelli, C. Adami, S. Bardelli, A. Cappi, S. Charlot, P. Ciliegi, T. Contini, O. Cucciati, S. Foucaud, P. Franzetti, I. Gavignaud, L. Guzzo, B. Marano, C. Marinoni, A. Mazure, B. Meneux, R. Merighi, S. Paltani, A. Pollo, L. Pozzetti, M. Radovich, E. Zucca, M. Bondi, A. Bongiorno, G. Busarello, S. de La Torre, L. Gregorini, F. Lamareille, G. Mathez, P. Merluzzi, V. Ripepi, D. Rizzo and D. Vergani. *Accurate photometric redshifts for the CFHT legacy survey calibrated using the VIMOS VLT deep survey.* Astronomy & Astrophysics, vol. 457, pages 841–856, October 2006.

[Jha et al. 2007] S. Jha, A. G. Riess and R. P. Kirshner. *Improved Distances to Type Ia Supernovae with Multicolor Light-Curve Shapes: MLCS2k2.* The Astrophysical Journal, vol. 659, pages 122–148, April 2007.

[Justham 2011] S. Justham. *Single-degenerate Type Ia Supernovae Without Hydrogen Contamination.* The Astrophysical Journal Letters, vol. 730, page L34, April 2011.

[Kasen 2006] D. Kasen. *Secondary Maximum in the Near-Infrared Light Curves of Type Ia Supernovae.* The Astrophysical Journal, vol. 649, pages 939–953, October 2006.

[Kato & Hachisu 2012] M. Kato and I. Hachisu. *Recurrent novae as progenitors of Type Ia supernovae.* Bulletin of the Astronomical Society of India, vol. 40, page 393, September 2012.

[Kepler 1606] J. Kepler. De Stella nova in pede serpentarii. 1606.

[Kerzendorf et al. 2009] W. E. Kerzendorf, B. P. Schmidt, M. Asplund, K. Nomoto, P. Podsiadlowski, A. Frebel, R. A. Fesen and D. Yong. *Subaru High-Resolution Spectroscopy of Star G in the Tycho Supernova Remnant.* The Astrophysical Journal, vol. 701, pages 1665–1672, August 2009.

[Kerzendorf et al. 2012] W. E. Kerzendorf, B. P. Schmidt, J. B. Laird, P. Podsiadlowski and M. S. Bessell. *Hunting for the Progenitor of SN 1006: High-resolution Spectroscopic Search with the FLAMES Instrument.* The Astrophysical Journal, vol. 759, page 7, November 2012.

[Kerzendorf et al. 2013a] W. E. Kerzendorf, M. Childress, J. Scharwaechter, T. Do and B. P. Schmidt. *A reconnaissance of the possible donor stars to the Kepler supernova.* ArXiv e-prints, September 2013.

[Kerzendorf et al. 2013b] W. E. Kerzendorf, D. Yong, B. P. Schmidt, J. D. Simon, C. S. Jeffery, J. Anderson, P. Podsiadlowski, A. Gal-Yam, J. M. Silverman, A. V. Filippenko, K. Nomoto, S. J. Murphy, M. S. Bessell, K. A. Venn and R. J. Foley. *A High-resolution Spectroscopic Search for the Remaining Donor for Tycho's Supernova.* The Astrophysical Journal, vol. 774, page 99, September 2013.

[Kessler et al. 2009a] R. Kessler, A. C. Becker, D. Cinabro, J. Vanderplas, J. A. Frieman, J. Marriner, T. M. Davis, B. Dilday, J. Holtzman, S. W. Jha, H. Lampeitl, M. Sako, M. Smith, C. Zheng, R. C. Nichol, B. Bassett, R. Bender, D. L. Depoy, M. Doi, E. Elson, A. V. Filippenko, R. J. Foley, P. M. Garnavich, U. Hopp, Y. Ihara, W. Ketzeback, W. Kollatschny, K. Konishi, J. L. Marshall, R. J. McMillan, G. Miknaitis, T. Morokuma, E. Mörtsell, K. Pan, J. L. Prieto, M. W. Richmond, A. G. Riess, R. Romani, D. P. Schneider, J. Sollerman, N. Takanashi, K. Tokita, K. van der Heyden, J. C. Wheeler, N. Yasuda and D. York. *First-Year Sloan Digital Sky Survey-II Supernova Results: Hubble Diagram and Cosmological Parameters.* The Astrophysical Journal Supplement Series, vol. 185, pages 32–84, November 2009.

[Kessler et al. 2009b] R. Kessler, J. P. Bernstein, D. Cinabro, B. Dilday, J. A. Frieman, S. Jha, S. Kuhlmann, G. Miknaitis, M. Sako, M. Taylor and J. Vanderplas. *SNANA: A Public Software Package for Supernova Analysis.* Publications of the Astronomical Society of the Pacific, vol. 121, pages 1028–1035, September 2009.

[Kessler et al. 2010] R. Kessler, B. Bassett, P. Belov, V. Bhatnagar, H. Campbell, A. Conley, J. A. Frieman, A. Glazov, S. González-Gaitán, R. Hlozek, S. Jha, S. Kuhlmann, M. Kunz, H. Lampeitl, A. Mahabal, J. Newling, R. C. Nichol, D. Parkinson, N. S. Philip, D. Poznanski, J. W. Richards, S. A. Rodney, M. Sako, D. P. Schneider,

M. Smith, M. Stritzinger and M. Varughese. *Results from the Supernova Photometric Classification Challenge.* Publications of the Astronomical Society of the Pacific, vol. 122, pages 1415–1431, December 2010.

[Knop et al. 2003] R. A. Knop, G. Aldering, R. Amanullah, P. Astier, G. Blanc, M. S. Burns, A. Conley, S. E. Deustua, M. Doi, R. Ellis, S. Fabbro, G. Folatelli, A. S. Fruchter, G. Garavini, S. Garmond, K. Garton, R. Gibbons, G. Goldhaber, A. Goobar, D. E. Groom, D. Hardin, I. Hook, D. A. Howell, A. G. Kim, B. C. Lee, C. Lidman, J. Mendez, S. Nobili, P. E. Nugent, R. Pain, N. Panagia, C. R. Pennypacker, S. Perlmutter, R. Quimby, J. Raux, N. Regnault, P. Ruiz-Lapuente, G. Sainton, B. Schaefer, K. Schahmaneche, E. Smith, A. L. Spadafora, V. Stanishev, M. Sullivan, N. A. Walton, L. Wang, W. M. Wood-Vasey and N. Yasuda. *New Constraints on Ω_M, Ω_λ, and w from an Independent Set of 11 High-Redshift Supernovae Observed with the Hubble Space Telescope.* The Astrophysical Journal, vol. 598, pages 102–137, November 2003.

[Koester et al. 2005] D. Koester, K. Rollenhagen, R. Napiwotzki, B. Voss, N. Christlieb, D. Homeier and D. Reimers. *Metal traces in white dwarfs of the SPY (ESO Supernova Ia Progenitor Survey) sample.* Astronomy & Astrophysics, vol. 432, pages 1025–1032, March 2005.

[Kovetz & Prialnik 1994] A. Kovetz and D. Prialnik. *Accretion onto a 1.4 solar mass white dwarf: Classical nova, recurrent nova, or supernova?* The Astrophysical Journal, vol. 424, pages 319–332, March 1994.

[Kowalski et al. 2008] M. Kowalski, D. Rubin, G. Aldering, R. J. Agostinho, A. Amadon, R. Amanullah, C. Balland, K. Barbary, G. Blanc, P. J. Challis, A. Conley, N. V. Connolly, R. Covarrubias, K. S. Dawson, S. E. Deustua, R. Ellis, S. Fabbro, V. Fadeyev, X. Fan, B. Farris, G. Folatelli, B. L. Frye, G. Garavini, E. L. Gates, L. Germany, G. Goldhaber, B. Goldman, A. Goobar, D. E. Groom, J. Haissinski, D. Hardin, I. Hook, S. Kent, A. G. Kim, R. A. Knop, C. Lidman, E. V. Linder, J. Mendez, J. Meyers, G. J. Miller, M. Moniez, A. M. Mourão, H. Newberg, S. Nobili, P. E. Nugent, R. Pain, O. Perdereau, S. Perlmutter, M. M. Phillips, V. Prasad, R. Quimby, N. Regnault, J. Rich, E. P. Rubenstein, P. Ruiz-Lapuente, F. D. Santos, B. E. Schaefer, R. A. Schommer, R. C. Smith, A. M. Soderberg, A. L. Spadafora, L.-G. Strolger, M. Strovink, N. B. Suntzeff, N. Suzuki, R. C. Thomas, N. A. Walton, L. Wang, W. M. Wood-Vasey, J. L. Yun and Supernova Cosmology Project. *Improved Cosmological Constraints from New, Old, and Combined Supernova Data Sets.* The Astrophysical Journal, vol. 686, pages 749–778, October 2008.

[Krisciunas et al. 2004] K. Krisciunas, M. M. Phillips and N. B. Suntzeff. *Hubble Diagrams of Type Ia Supernovae in the Near-Infrared.* The Astrophysical Journal Letters, vol. 602, pages L81–L84, February 2004.

[Krisciunas et al. 2006] K. Krisciunas, J. L. Prieto, P. M. Garnavich, J.-L. G. Riley, A. Rest, C. Stubbs and R. McMillan. *Photometry of the Type Ia Supernovae 1999cc, 1999cl, and 2000cf.* The Astronomical Journal, vol. 131, pages 1639–1647, March 2006.

[Krisciunas et al. 2007] K. Krisciunas, P. M. Garnavich, V. Stanishev, N. B. Suntzeff, J. L. Prieto, J. Espinoza, D. Gonzalez, M. E. Salvo, N. Elias de la Rosa, S. J. Smartt, J. R. Maund and R.-P. Kudritzki. *The Type Ia Supernova 2004S, a Clone of SN 2001el, and the Optimal Photometric Bands for Extinction Estimation.* The Astronomical Journal, vol. 133, pages 58–72, January 2007.

[Lentz et al. 2001] E. J. Lentz, E. Baron, P. Lundqvist, D. Branch, P. H. Hauschildt, C. Fransson, P. Garnavich, N. Bastian, A. V. Filippenko, R. P. Kirshner, P. M. Challis, S. Jha, B. Leibundgut, R. McCray, E. Michael, N. Panagia, M. M. Phillips, C. S. J. Pun, B. Schmidt, G. Sonneborn, N. B. Suntzeff, L. Wang and J. C. Wheeler. *Analysis of Type IIn SN 1998S: Effects of Circumstellar Interaction on Observed Spectra.* The Astrophysical Journal, vol. 547, pages 406–411, January 2001.

[Leonard et al. 2002] D. C. Leonard, A. V. Filippenko, W. Li, T. Matheson, R. P. Kirshner, R. Chornock, S. D. Van Dyk, P. Berlind, M. L. Calkins, P. M. Challis, P. M. Garnavich, S. Jha and A. Mahdavi. *A Study of the Type II-Plateau Supernova 1999gi and the Distance to its Host Galaxy, NGC 3184.* The Astronomical Journal, vol. 124, pages 2490–2505, November 2002.

[Leonard 2007] D. C. Leonard. *Constraining the Type Ia Supernova Progenitor: The Search for Hydrogen in Nebular Spectra.* The Astrophysical Journal, vol. 670, pages 1275–1282, December 2007.

[Li et al. 2003] W. Li, A. V. Filippenko, R. Chornock, E. Berger, P. Berlind, M. L. Calkins, P. Challis, C. Fassnacht, S. Jha, R. P. Kirshner, T. Matheson, W. L. W. Sargent, R. A. Simcoe, G. H. Smith and G. Squires. *SN 2002cx: The Most Peculiar Known Type Ia Supernova.* Publications of the Astronomical Society of the Pacific, vol. 115, pages 453–473, April 2003.

[Li et al. 2011a] W. Li, R. Chornock, J. Leaman, A. V. Filippenko, D. Poznanski, X. Wang, M. Ganeshalingam and F. Mannucci. *Nearby supernova rates from the Lick Observatory Supernova Search - III. The rate-size relation, and the rates as a function of galaxy Hubble type and colour.* Monthly Notices of the Royal Astronomical Society, vol. 412, pages 1473–1507, April 2011.

[Li et al. 2011b] W. Li, J. Leaman, R. Chornock, A. V. Filippenko, D. Poznanski, M. Ganeshalingam, X. Wang, M. Modjaz, S. Jha, R. J. Foley and N. Smith. *Nearby supernova rates from the Lick Observatory Supernova Search - II. The observed luminosity functions and fractions of supernovae in a complete sample.* Monthly Notices of the Royal Astronomical Society, vol. 412, pages 1441–1472, April 2011.

[Lidman et al. 2005] C. Lidman, D. A. Howell, G. Folatelli, G. Garavini, S. Nobili, G. Aldering, R. Amanullah, P. Antilogus, P. Astier, G. Blanc, M. S. Burns, A. Conley, S. E. Deustua, M. Doi, R. Ellis, S. Fabbro, V. Fadeyev, R. Gibbons, G. Goldhaber, A. Goobar, D. E. Groom, I. Hook, N. Kashikawa, A. G. Kim, R. A. Knop, B. C. Lee, J. Mendez, T. Morokuma, K. Motohara, P. E. Nugent, R. Pain, S. Perlmutter, V. Prasad, R. Quimby, J. Raux, N. Regnault, P. Ruiz-Lapuente, G. Sainton, B. E.

Schaefer, K. Schahmaneche, E. Smith, A. L. Spadafora, V. Stanishev, N. A. Walton, L. Wang, W. M. Wood-Vasey, N. Yasuda and Supernova Cosmology Project. *Spectroscopic confirmation of high-redshift supernovae with the ESO VLT.* Astronomy & Astrophysics, vol. 430, pages 843–851, February 2005.

[Livio & Truran 1992] M. Livio and J. W. Truran. *Type I supernovae and accretion-induced collapses from cataclysmic variables?* The Astrophysical Journal, vol. 389, pages 695–703, April 1992.

[Lonsdale et al. 2004] C. Lonsdale, M. d. C. Polletta, J. Surace, D. Shupe, F. Fang, C. K. Xu, H. E. Smith, B. Siana, M. Rowan-Robinson, T. Babbedge, S. Oliver, F. Pozzi, P. Davoodi, F. Owen, D. Padgett, D. Frayer, T. Jarrett, F. Masci, J. O'Linger, T. Conrow, D. Farrah, G. Morrison, N. Gautier, A. Franceschini, S. Berta, I. Perez-Fournon, E. Hatziminaoglou, A. Afonso-Luis, H. Dole, G. Stacey, S. Serjeant, M. Pierre, M. Griffin and R. Puetter. *First Insights into the Spitzer Wide-Area Infrared Extragalactic Legacy Survey (SWIRE) Galaxy Populations.* The Astrophysical Journal Supplement Series, vol. 154, pages 54–59, September 2004.

[Lundqvist et al. 2013] P. Lundqvist, S. Mattila, J. Sollerman, C. Kozma, E. Baron, N. L. J. Cox, C. Fransson, B. Leibundgut and J. Spyromilio. *Hydrogen and helium in the spectra of Type Ia supernovae.* Monthly Notices of the Royal Astronomical Society, vol. 435, pages 329–345, October 2013.

[Magnelli et al. 2009] B. Magnelli, D. Elbaz, R. R. Chary, M. Dickinson, D. Le Borgne, D. T. Frayer and C. N. A. Willmer. *The* $0.4 \leq z \leq 1.3$ *star formation history of the Universe as viewed in the far-infrared.* Astronomy & Astrophysics, vol. 496, pages 57–75, March 2009.

[Maguire et al. 2013] K. Maguire, M. Sullivan, F. Patat, A. Gal-Yam, I. M. Hook, S. Dhawan, D. A. Howell, P. Mazzali, P. E. Nugent, Y.-C. Pan, P. Podsiadlowski, J. D. Simon, A. Sternberg, S. Valenti, C. Baltay, D. Bersier, N. Blagorodnova, T.-W. Chen, N. Ellman, U. Feindt, F. Förster, M. Fraser, S. González-Gaitán, M. L. Graham, C. Gutiérrez, S. Hachinger, E. Hadjiyska, C. Inserra, C. Knapic, R. R. Laher, G. Leloudas, S. Margheim, R. McKinnon, M. Molinaro, N. Morrell, E. O. Ofek, D. Rabinowitz, A. Rest, D. Sand, R. Smareglia, S. J. Smartt, F. Taddia, E. S. Walker, N. A. Walton and D. R. Young. *A statistical analysis of circumstellar material in Type Ia supernovae.* Monthly Notices of the Royal Astronomical Society, vol. 436, pages 222–240, November 2013.

[Mannucci et al. 2005] F. Mannucci, M. Della Valle, N. Panagia, E. Cappellaro, G. Cresci, R. Maiolino, A. Petrosian and M. Turatto. *The supernova rate per unit mass.* Astronomy & Astrophysics, vol. 433, pages 807–814, April 2005.

[Mannucci et al. 2006] F. Mannucci, M. Della Valle and N. Panagia. *Two populations of progenitors for Type Ia supernovae?* Monthly Notices of the Royal Astronomical Society, vol. 370, pages 773–783, August 2006.

[Mannucci et al. 2007] F. Mannucci, M. Della Valle and N. Panagia. *How many supernovae are we missing at high redshift?* Monthly Notices of the Royal Astronomical Society, vol. 377, pages 1229–1235, May 2007.

[Maoz & Badenes 2010] D. Maoz and C. Badenes. *The supernova rate and delay time distribution in the Magellanic Clouds.* Monthly Notices of the Royal Astronomical Society, vol. 407, pages 1314–1327, September 2010.

[Maoz & Mannucci 2012] D. Maoz and F. Mannucci. *Type-Ia Supernova Rates and the Progenitor Problem: A Review.* Publications of the Astronomical Society of Australia, vol. 29, pages 447–465, January 2012.

[Maoz et al. 2011] D. Maoz, F. Mannucci, W. Li, A. V. Filippenko, M. Della Valle and N. Panagia. *Nearby supernova rates from the Lick Observatory Supernova Search - IV. A recovery method for the delay-time distribution.* Monthly Notices of the Royal Astronomical Society, vol. 412, pages 1508–1521, April 2011.

[Maoz et al. 2012a] D. Maoz, C. Badenes and S. J. Bickerton. *Characterizing the Galactic White Dwarf Binary Population with Sparsely Sampled Radial Velocity Data.* The Astrophysical Journal, vol. 751, page 143, June 2012.

[Maoz et al. 2012b] D. Maoz, F. Mannucci and T. D. Brandt. *The delay-time distribution of Type Ia supernovae from Sloan II.* Monthly Notices of the Royal Astronomical Society, vol. 426, pages 3282–3294, November 2012.

[Maoz et al. 2013] D. Maoz, F. Mannucci and G. Nelemans. *Observational clues to the progenitors of Type-Ia supernovae.* ArXiv e-prints, December 2013.

[Margutti et al. 2012] R. Margutti, A. M. Soderberg, L. Chomiuk, R. Chevalier, K. Hurley, D. Milisavljevic, R. J. Foley, J. P. Hughes, P. Slane, C. Fransson, M. Moe, S. Barthelmy, W. Boynton, M. Briggs, V. Connaughton, E. Costa, J. Cummings, E. Del Monte, H. Enos, C. Fellows, M. Feroci, Y. Fukazawa, N. Gehrels, J. Goldsten, D. Golovin, Y. Hanabata, K. Harshman, H. Krimm, M. L. Litvak, K. Makishima, M. Marisaldi, I. G. Mitrofanov, T. Murakami, M. Ohno, D. M. Palmer, A. B. Sanin, R. Starr, D. Svinkin, T. Takahashi, M. Tashiro, Y. Terada and K. Yamaoka. *Inverse Compton X-Ray Emission from Supernovae with Compact Progenitors: Application to SN2011fe.* The Astrophysical Journal, vol. 751, page 134, June 2012.

[Marietta et al. 2000] E. Marietta, A. Burrows and B. Fryxell. *Type IA Supernova Explosions in Binary Systems: The Impact on the Secondary Star and Its Consequences.* The Astrophysical Journal Supplement Series, vol. 128, pages 615–650, June 2000.

[Mattila et al. 2005] S. Mattila, P. Lundqvist, J. Sollerman, C. Kozma, E. Baron, C. Fransson, B. Leibundgut and K. Nomoto. *Early and late time VLT spectroscopy of SN 2001el - progenitor constraints for a type Ia supernova.* Astronomy & Astrophysics, vol. 443, pages 649–662, November 2005.

[Mattila et al. 2012] S. Mattila, T. Dahlen, A. Efstathiou, E. Kankare, J. Melinder, A. Alonso-Herrero, M. Á. Pérez-Torres, S. Ryder, P. Väisänen and G. Östlin. *Core-collapse Supernovae Missed by Optical Surveys.* The Astrophysical Journal, vol. 756, page 111, September 2012.

[McClelland et al. 2010] C. M. McClelland, P. M. Garnavich, L. Galbany, R. Miquel, R. J. Foley, A. V. Filippenko, B. Bassett, J. C. Wheeler, A. Goobar, S. W. Jha, M. Sako, J. A. Frieman, J. Sollerman, J. Vinko and D. P. Schneider. *The Subluminous Supernova 2007qd: A Missing Link in a Family of Low-luminosity Type Ia Supernovae.* The Astrophysical Journal, vol. 720, pages 704–716, September 2010.

[McMillan 2011] P. J. McMillan. *Mass models of the Milky Way.* Monthly Notices of the Royal Astronomical Society, vol. 414, pages 2446–2457, July 2011.

[Melinder et al. 2012] J. Melinder, T. Dahlen, L. Mencía Trinchant, G. Östlin, S. Mattila, J. Sollerman, C. Fransson, M. Hayes, E. Kankare and S. Nasoudi-Shoar. *The rate of supernovae at redshift 0.1-1.0. The Stockholm VIMOS Supernova Survey III.* Astronomy & Astrophysics, vol. 545, page A96, September 2012.

[Minkowski 1941] R. Minkowski. *Spectra of Supernovae.* Publications of the Astronomical Society of the Pacific, vol. 53, page 224, August 1941.

[Minkowski 1964] R. Minkowski. *Supernovae and Supernova Remnants.* Annual Review of Astronomy and Astrophysics, vol. 2, page 247, 1964.

[Miyaji et al. 1980] S. Miyaji, K. Nomoto, K. Yokoi and D. Sugimoto. *Supernova Triggered by Electron Captures.* Publications of the Astronomical Society of Japan, vol. 32, page 303, 1980.

[Miyazaki et al. 2002] S. Miyazaki, Y. Komiyama, M. Sekiguchi, S. Okamura, M. Doi, H. Furusawa, M. Hamabe, K. Imi, M. Kimura, F. Nakata, N. Okada, M. Ouchi, K. Shimasaku, M. Yagi and N. Yasuda. *Subaru Prime Focus Camera – Suprime-Cam.* Publications of the Astronomical Society of Japan, vol. 54, pages 833–853, December 2002.

[Moriya 2013] J. T. Moriya. *Supernova Interacting with Circumstellar Media.* PhD thesis, The University of Tokyo, 2013.

[Morokuma et al. 2008] T. Morokuma, M. Doi, N. Yasuda, M. Akiyama, K. Sekiguchi, H. Furusawa, Y. Ueda, T. Totani, T. Oda, T. Nagao, N. Kashikawa, T. Murayama, M. Ouchi, M. G. Watson, M. W. Richmond, C. Lidman, S. Perlmutter, A. L. Spadafora, G. Aldering, L. Wang, I. M. Hook and R. A. Knop. *The Subaru/XMM-Newton Deep Survey (SXDS). V. Optically Faint Variable Object Survey.* The Astrophysical Journal, vol. 676, pages 163–183, March 2008.

[Morokuma et al. 2010] T. Morokuma, K. Tokita, C. Lidman, M. Doi, N. Yasuda, G. Aldering, R. Amanullah, K. Barbary, K. Dawson, V. Fadeyev, H. K. Fakhouri, G. Goldhaber, A. Goobar, T. Hattori, J. Hayano, I. M. Hook, D. A. Howell, H. Furusawa,

Y. Ihara, N. Kashikawa, R. A. Knop, K. Konishi, J. Meyers, T. Oda, R. Pain, S. Perlmutter, D. Rubin, A. L. Spadafora, N. Suzuki, N. Takanashi, T. Totani, H. Utsunomiya and L. Wang. *Subaru FOCAS Spectroscopic Observations of High-Redshift Supernovae.* Publications of the Astronomical Society of Japan, vol. 62, pages 19–, February 2010.

[Napiwotzki et al. 2004] R. Napiwotzki, C. A. Karl, T. Lisker, U. Heber, N. Christlieb, D. Reimers, G. Nelemans and D. Homeier. *Close binary EHB stars from SPY.* Astrophysics and Space Science, vol. 291, pages 321–328, June 2004.

[Neill et al. 2006] J. D. Neill, M. Sullivan, D. Balam, C. J. Pritchet, D. A. Howell, K. Perrett, P. Astier, E. Aubourg, S. Basa, R. G. Carlberg, A. Conley, S. Fabbro, D. Fouchez, J. Guy, I. Hook, R. Pain, N. Palanque-Delabrouille, N. Regnault, J. Rich, R. Taillet, G. Aldering, P. Antilogus, V. Arsenijevic, C. Balland, S. Baumont, J. Bronder, R. S. Ellis, M. Filiol, A. C. Gonçalves, D. Hardin, M. Kowalski, C. Lidman, V. Lusset, M. Mouchet, A. Mourao, S. Perlmutter, P. Ripoche, D. Schlegel and C. Tao. *The Type Ia Supernova Rate at z˜0.5 from the Supernova Legacy Survey.* The Astronomical Journal, vol. 132, pages 1126–1145, September 2006.

[Nelemans et al. 2001] G. Nelemans, L. R. Yungelson and S. F. Portegies Zwart. *The gravitational wave signal from the Galactic disk population of binaries containing two compact objects.* Astronomy & Astrophysics, vol. 375, pages 890–898, September 2001.

[Nelemans et al. 2005] G. Nelemans, R. Napiwotzki, C. Karl, T. R. Marsh, B. Voss, G. Roelofs, R. G. Izzard, M. Montgomery, T. Reerink, N. Christlieb and D. Reimers. *Binaries discovered by the SPYproject. IV. Five single-lined DA double white dwarfs.* Astronomy & Astrophysics, vol. 440, pages 1087–1095, September 2005.

[Nelemans et al. 2013] G. Nelemans, S. Toonen and M. Bours. *Theoretical Delay Time Distributions.* In R. Di Stefano, M. Orio and M. Moe, editeurs, IAU Symposium, volume 281 of *IAU Symposium*, pages 225–231, January 2013.

[Nelson et al. 2012] T. Nelson, D. Donato, K. Mukai, J. Sokoloski and L. Chomiuk. *X-Ray Emission from an Asymmetric Blast Wave and a Massive White Dwarf in the Gamma-Ray Emitting Nova V407 Cyg.* The Astrophysical Journal, vol. 748, page 43, March 2012.

[Nobili & Goobar 2008] S. Nobili and A. Goobar. *The colour-lightcurve shape relation of type Ia supernovae and the reddening law.* Astronomy & Astrophysics, vol. 487, pages 19–31, August 2008.

[Nomoto et al. 1997] K. Nomoto, K. Iwamoto and N. Kishimoto. *Type Ia supernovae: their origin and possible applications in cosmology.* Science, vol. 276, pages 1378–1382, 1997.

[Nomoto 1982] K. Nomoto. *Accreting white dwarf models for type I supernovae. I - Presupernova evolution and triggering mechanisms.* The Astrophysical Journal, vol. 253, pages 798–810, February 1982.

[Nomoto 1987] K. Nomoto. *Evolution of 8-10 solar mass stars toward electron capture supernovae. II - Collapse of an O + NE + MG core.* The Astrophysical Journal, vol. 322, pages 206–214, November 1987.

[Nugent et al. 2002] P. Nugent, A. Kim and S. Perlmutter. *K-Corrections and Extinction Corrections for Type Ia Supernovae.* Publications of the Astronomical Society of the Pacific, vol. 114, pages 803–819, August 2002.

[Nugent et al. 2011] P. E. Nugent, M. Sullivan, S. B. Cenko, R. C. Thomas, D. Kasen, D. A. Howell, D. Bersier, J. S. Bloom, S. R. Kulkarni, M. T. Kandrashoff, A. V. Filippenko, J. M. Silverman, G. W. Marcy, A. W. Howard, H. T. Isaacson, K. Maguire, N. Suzuki, J. E. Tarlton, Y.-C. Pan, L. Bildsten, B. J. Fulton, J. T. Parrent, D. Sand, P. Podsiadlowski, F. B. Bianco, B. Dilday, M. L. Graham, J. Lyman, P. James, M. M. Kasliwal, N. M. Law, R. M. Quimby, I. M. Hook, E. S. Walker, P. Mazzali, E. Pian, E. O. Ofek, A. Gal-Yam and D. Poznanski. *Supernova SN 2011fe from an exploding carbon-oxygen white dwarf star.* Nature, vol. 480, pages 344–347, December 2011.

[Paczynski 1985] B. Paczynski. *Evolution of cataclysmic binaries.* In D. Q. Lamb and J. Patterson, editeurs, Cataclysmic Variables and Low-Mass X-ray Binaries, volume 113 of *Astrophysics and Space Science Library*, pages 1–12, 1985.

[Pain et al. 2002] R. Pain, S. Fabbro, M. Sullivan, R. S. Ellis, G. Aldering, P. Astier, S. E. Deustua, A. S. Fruchter, G. Goldhaber, A. Goobar, D. E. Groom, D. Hardin, I. M. Hook, D. A. Howell, M. J. Irwin, A. G. Kim, M. Y. Kim, R. A. Knop, J. C. Lee, C. Lidman, R. G. McMahon, P. E. Nugent, N. Panagia, C. R. Pennypacker, S. Perlmutter, P. Ruiz-Lapuente, K. Schahmaneche, B. Schaefer and N. A. Walton. *The Distant Type Ia Supernova Rate.* The Astrophysical Journal, vol. 577, pages 120–132, September 2002.

[Pan et al. 2013] K.-C. Pan, P. M. Ricker and R. E. Taam. *Evolution of Post-impact Remnant Helium Stars in Type Ia Supernova Remnants within the Single-degenerate Scenario.* The Astrophysical Journal, vol. 773, page 49, August 2013.

[Panagia et al. 2006] N. Panagia, S. D. Van Dyk, K. W. Weiler, R. A. Sramek, C. J. Stockdale and K. P. Murata. *A Search for Radio Emission from Type Ia Supernovae.* The Astrophysical Journal, vol. 646, pages 369–377, July 2006.

[Patat et al. 2007] F. Patat, S. Benetti, S. Justham, P. A. Mazzali, L. Pasquini, E. Cappellaro, M. Della Valle, P. -Podsiadlowski, M. Turatto, A. Gal-Yam and J. D. Simon. *Upper limit for circumstellar gas around the type Ia SN 2000cx.* Astronomy & Astrophysics, vol. 474, pages 931–936, November 2007.

[Pérez-Montero et al. 2007] E. Pérez-Montero, G. F. Hägele, T. Contini and Á. I. Díaz. *Neon and argon optical emission lines in ionized gaseous nebulae: implications and applications.* Monthly Notices of the Royal Astronomical Society, vol. 381, pages 125–135, October 2007.

[Perlmutter et al. 1997] S. Perlmutter, S. Gabi, G. Goldhaber, A. Goobar, D. E. Groom, I. M. Hook, A. G. Kim, M. Y. Kim, J. C. Lee, R. Pain, C. R. Pennypacker, I. A. Small, R. S. Ellis, R. G. McMahon, B. J. Boyle, P. S. Bunclark, D. Carter, M. J. Irwin, K. Glazebrook, H. J. M. Newberg, A. V. Filippenko, T. Matheson, M. Dopita, W. J. Couch and Supernova Cosmology Project. *Measurements of the Cosmological Parameters Omega and Lambda from the First Seven Supernovae at Z $\geq$= 0.35.* The Astrophysical Journal, vol. 483, page 565, July 1997.

[Perlmutter et al. 1999] S. Perlmutter, G. Aldering, G. Goldhaber, R. A. Knop, P. Nugent, P. G. Castro, S. Deustua, S. Fabbro, A. Goobar, D. E. Groom, I. M. Hook, A. G. Kim, M. Y. Kim, J. C. Lee, N. J. Nunes, R. Pain, C. R. Pennypacker, R. Quimby, C. Lidman, R. S. Ellis, M. Irwin, R. G. McMahon, P. Ruiz-Lapuente, N. Walton, B. Schaefer, B. J. Boyle, A. V. Filippenko, T. Matheson, A. S. Fruchter, N. Panagia, H. J. M. Newberg, W. J. Couch and Supernova Cosmology Project. *Measurements of Omega and Lambda from 42 High-Redshift Supernovae.* The Astrophysical Journal, vol. 517, pages 565–586, June 1999.

[Perrett et al. 2012] K. Perrett, M. Sullivan, A. Conley, S. González-Gaitán, R. Carlberg, D. Fouchez, P. Ripoche, J. D. Neill, P. Astier, D. Balam, C. Balland, S. Basa, J. Guy, D. Hardin, I. M. Hook, D. A. Howell, R. Pain, N. Palanque-Delabrouille, C. Pritchet, N. Regnault, J. Rich, V. Ruhlmann-Kleider, S. Baumont, C. Lidman, S. Perlmutter and E. S. Walker. *Evolution in the Volumetric Type Ia Supernova Rate from the Supernova Legacy Survey.* The Astronomical Journal, vol. 144, page 59, August 2012.

[Phillips et al. 2007] M. M. Phillips, W. Li, J. A. Frieman, S. I. Blinnikov, D. DePoy, J. L. Prieto, P. Milne, C. Contreras, G. Folatelli, N. Morrell, M. Hamuy, N. B. Suntzeff, M. Roth, S. González, W. Krzeminski, A. V. Filippenko, W. L. Freedman, R. Chornock, S. Jha, B. F. Madore, S. E. Persson, C. R. Burns, P. Wyatt, D. Murphy, R. J. Foley, M. Ganeshalingam, F. J. D. Serduke, K. Krisciunas, B. Bassett, A. Becker, B. Dilday, J. Eastman, P. M. Garnavich, J. Holtzman, R. Kessler, H. Lampeitl, J. Marriner, S. Frank, J. L. Marshall, G. Miknaitis, M. Sako, D. P. Schneider, K. van der Heyden and N. Yasuda. *The Peculiar SN 2005hk: Do Some Type Ia Supernovae Explode as Deflagrations?1,.* Publications of the Astronomical Society of the Pacific, vol. 119, pages 360–387, April 2007.

[Phillips et al. 2013] M. M. Phillips, J. D. Simon, N. Morrell, C. R. Burns, N. L. J. Cox, R. J. Foley, A. I. Karakas, F. Patat, A. Sternberg, R. E. Williams, A. Gal-Yam, E. Y. Hsiao, D. C. Leonard, S. E. Persson, M. Stritzinger, I. B. Thompson, A. Campillay, C. Contreras, G. Folatelli, W. L. Freedman, M. Hamuy, M. Roth, G. A. Shields, N. B. Suntzeff, L. Chomiuk, I. I. Ivans, B. F. Madore, B. E. Penprase, D. Perley, G. Pignata, G. Preston and A. M. Soderberg. *On the Source of the Dust Extinction in Type Ia Supernovae and the Discovery of Anomalously Strong Na I Absorption.* The Astrophysical Journal, vol. 779, page 38, December 2013.

[Phillips 1993] M. M. Phillips. *The absolute magnitudes of Type IA supernovae.* The Astrophysical Journal Letters, vol. 413, pages L105–L108, August 1993.

[Poludnenko et al. 2011] A. Y. Poludnenko, T. A. Gardiner and E. S. Oran. *Spontaneous Transition of Turbulent Flames to Detonations in Unconfined Media.* Physical Review Letters, vol. 107, no. 5, page 054501, July 2011.

[Poznanski et al. 2007a] D. Poznanski, D. Maoz and A. Gal-Yam. *Bayesian Single-Epoch Photometric Classification of Supernovae.* The Astronomical Journal, vol. 134, pages 1285–1297, September 2007.

[Poznanski et al. 2007b] D. Poznanski, D. Maoz, N. Yasuda, R. J. Foley, M. Doi, A. V. Filippenko, M. Fukugita, A. Gal-Yam, B. T. Jannuzi, T. Morokuma, T. Oda, H. Schweiker, K. Sharon, J. M. Silverman and T. Totani. *Supernovae in the Subaru Deep Field: an initial sample and Type Ia rate out to redshift 1.6.* Monthly Notices of the Royal Astronomical Society, vol. 382, pages 1169–1186, December 2007.

[Prialnik 1986] D. Prialnik. *The evolution of a classical nova model through a complete cycle.* The Astrophysical Journal, vol. 310, pages 222–237, November 1986.

[Prieto et al. 2005] J. Prieto, P. Garnavich, D. Depoy, J. Marshall, J. Eastman and S. Frank. *Supernova 2005gj.* International Astronomical Union Circular, vol. 8633, page 1, November 2005.

[Quimby et al. 2007] R. M. Quimby, G. Aldering, J. C. Wheeler, P. Höflich, C. W. Akerlof and E. S. Rykoff. *SN 2005ap: A Most Brilliant Explosion.* The Astrophysical Journal Letters, vol. 668, pages L99–L102, October 2007.

[Raskin & Kasen 2013] C. Raskin and D. Kasen. *Tidal Tail Ejection as a Signature of Type Ia Supernovae from White Dwarf Mergers.* The Astrophysical Journal, vol. 772, page 1, July 2013.

[Richardson et al. 2002] D. Richardson, D. Branch, D. Casebeer, J. Millard, R. C. Thomas and E. Baron. *A Comparative Study of the Absolute Magnitude Distributions of Supernovae.* The Astronomical Journal, vol. 123, pages 745–752, February 2002.

[Richardson et al. 2006] D. Richardson, D. Branch and E. Baron. *Absolute Magnitude Distributions and Light Curves of Stripped-Envelope Supernovae.* The Astronomical Journal, vol. 131, pages 2233–2244, April 2006.

[Riello & Patat 2005] M. Riello and F. Patat. *Extinction correction for Type Ia supernova rates - I. The model.* Monthly Notices of the Royal Astronomical Society, vol. 362, pages 671–680, September 2005.

[Riess et al. 1998] A. G. Riess, A. V. Filippenko, P. Challis, A. Clocchiatti, A. Diercks, P. M. Garnavich, R. L. Gilliland, C. J. Hogan, S. Jha, R. P. Kirshner, B. Leibundgut, M. M. Phillips, D. Reiss, B. P. Schmidt, R. A. Schommer, R. C. Smith, J. Spyromilio, C. Stubbs, N. B. Suntzeff and J. Tonry. *Observational Evidence from Supernovae for an Accelerating Universe and a Cosmological Constant.* The Astronomical Journal, vol. 116, pages 1009–1038, September 1998.

[Riess et al. 2007] A. G. Riess, L.-G. Strolger, S. Casertano, H. C. Ferguson, B. Mobasher, B. Gold, P. J. Challis, A. V. Filippenko, S. Jha, W. Li, J. Tonry, R. Foley, R. P. Kirshner, M. Dickinson, E. MacDonald, D. Eisenstein, M. Livio, J. Younger, C. Xu, T. Dahlén and D. Stern. *New Hubble Space Telescope Discoveries of Type Ia Supernovae at z≥ = 1: Narrowing Constraints on the Early Behavior of Dark Energy.* The Astrophysical Journal, vol. 659, pages 98–121, April 2007.

[Rodney & Tonry 2010] S. A. Rodney and J. L. Tonry. *Revised Supernova Rates from the IfA Deep Survey.* The Astrophysical Journal, vol. 723, pages 47–53, November 2010.

[Rola et al. 1997] C. S. Rola, E. Terlevich and R. J. Terlevich. *New diagnostic methods for emission-line galaxies in deep surveys.* Monthly Notices of the Royal Astronomical Society, vol. 289, pages 419–427, August 1997.

[Röpke 2007] F. K. Röpke. *Flame-driven Deflagration-to-Detonation Transitions in Type Ia Supernovae?* The Astrophysical Journal, vol. 668, pages 1103–1108, October 2007.

[Ruiter et al. 2009] A. J. Ruiter, K. Belczynski and C. Fryer. *Rates and Delay Times of Type Ia Supernovae.* The Astrophysical Journal, vol. 699, pages 2026–2036, July 2009.

[Ruiz-Lapuente et al. 2004] P. Ruiz-Lapuente, F. Comeron, J. Méndez, R. Canal, S. J. Smartt, A. V. Filippenko, R. L. Kurucz, R. Chornock, R. J. Foley, V. Stanishev and R. Ibata. *The binary progenitor of Tycho Brahe's 1572 supernova.* Nature, vol. 431, pages 1069–1072, October 2004.

[Russell & Immler 2012] B. R. Russell and S. Immler. *Swift X-Ray Upper Limits on Type Ia Supernova Environments.* The Astrophysical Journal Letters, vol. 748, page L29, April 2012.

[Sahman et al. 2013] D. I. Sahman, V. S. Dhillon, T. R. Marsh, S. Moll, T. D. Thoroughgood, C. A. Watson and S. P. Littlefair. *CI Aql: a Type Ia supernova progenitor?* Monthly Notices of the Royal Astronomical Society, vol. 433, pages 1588–1598, August 2013.

[Saio & Nomoto 1985] H. Saio and K. Nomoto. *Evolution of a merging pair of C + O white dwarfs to form a single neutron star.* Astronomy & Astrophysics, vol. 150, pages L21–L23, September 1985.

[Sako et al. 2008] M. Sako, B. Bassett, A. Becker, D. Cinabro, F. DeJongh, D. L. Depoy, B. Dilday, M. Doi, J. A. Frieman, P. M. Garnavich, C. J. Hogan, J. Holtzman, S. Jha, R. Kessler, K. Konishi, H. Lampeitl, J. Marriner, G. Miknaitis, R. C. Nichol, J. L. Prieto, A. G. Riess, M. W. Richmond, R. Romani, D. P. Schneider, M. Smith, M. Subba Rao, N. Takanashi, K. Tokita, K. van der Heyden, N. Yasuda, C. Zheng, J. Barentine, H. Brewington, C. Choi, J. Dembicky, M. Harnavek, Y. Ihara, M. Im, W. Ketzeback, S. J. Kleinman, J. Krzesiński, D. C. Long, E. Malanushenko, V. Malanushenko, R. J. McMillan, T. Morokuma, A. Nitta, K. Pan, G. Saurage and S. A. Snedden. *The Sloan Digital Sky Survey-II Supernova Survey: Search Algorithm and Follow-Up Observations.* The Astronomical Journal, vol. 135, pages 348–373, January 2008.

[Sako et al. 2011] M. Sako, B. Bassett, B. Connolly, B. Dilday, H. Cambell, J. A. Frieman, L. Gladney, R. Kessler, H. Lampeitl, J. Marriner, R. Miquel, R. C. Nichol, D. P. Schneider, M. Smith and J. Sollerman. *Photometric Type Ia Supernova Candidates from the Three-year SDSS-II SN Survey Data.* The Astrophysical Journal, vol. 738, page 162, September 2011.

[Scalo 1986] J. M. Scalo. *The stellar initial mass function.* Fundamentals of Cosmic Physics, vol. 11, pages 1–278, May 1986.

[Schaefer & Pagnotta 2012] B. E. Schaefer and A. Pagnotta. *An absence of ex-companion stars in the type Ia supernova remnant SNR 0509-67.5.* Nature, vol. 481, pages 164–166, January 2012.

[Schaefer 2010] B. E. Schaefer. *Comprehensive Photometric Histories of All Known Galactic Recurrent Novae.* The Astrophysical Journal Supplement Series, vol. 187, pages 275–373, April 2010.

[Schaefer 2013] B. E. Schaefer. *The Recurrent Nova U Scorpii Blew Off A Century Worth Of Accreted Material During Its 2010 Eruption, So It Will Not Become A Type Ia Supernova.* In American Astronomical Society Meeting Abstracts, volume 221 of *American Astronomical Society Meeting Abstracts*, page 233.06, January 2013.

[Sekiguchi & SXDS Team 2004] K. Sekiguchi and SXDS Team. *Subaru/XMM-Newton Deep Survey (SXDS).* In American Astronomical Society Meeting Abstracts, volume 36 of *Bulletin of the American Astronomical Society*, page 1478, December 2004.

[Shappee et al. 2013] B. J. Shappee, K. Z. Stanek, R. W. Pogge and P. M. Garnavich. *No Stripped Hydrogen in the Nebular Spectra of Nearby Type Ia Supernova 2011fe.* The Astrophysical Journal Letters, vol. 762, page L5, January 2013.

[Shen et al. 2013] K. J. Shen, J. Guillochon and R. J. Foley. *Circumstellar Absorption in Double Detonation Type Ia Supernovae.* The Astrophysical Journal Letters, vol. 770, page L35, June 2013.

[Silverman et al. 2013] J. M. Silverman, P. E. Nugent, A. Gal-Yam, M. Sullivan, D. A. Howell, A. V. Filippenko, Y.-C. Pan, S. B. Cenko and I. M. Hook. *Late-time Spectral Observations of the Strongly Interacting Type Ia Supernova PTF11kx.* The Astrophysical Journal, vol. 772, page 125, August 2013.

[Simon et al. 2009] J. D. Simon, A. Gal-Yam, O. Gnat, R. M. Quimby, M. Ganeshalingam, J. M. Silverman, S. Blondin, W. Li, A. V. Filippenko, J. C. Wheeler, R. P. Kirshner, F. Patat, P. Nugent, R. J. Foley, S. S. Vogt, R. P. Butler, K. M. G. Peek, E. Rosolowsky, G. J. Herczeg, D. N. Sauer and P. A. Mazzali. *Variable Sodium Absorption in a Low-extinction Type Ia Supernova.* The Astrophysical Journal, vol. 702, pages 1157–1170, September 2009.

[Smartt et al. 2009] S. J. Smartt, J. J. Eldridge, R. M. Crockett and J. R. Maund. *The death of massive stars - I. Observational constraints on the progenitors of Type II-P supernovae.* Monthly Notices of the Royal Astronomical Society, vol. 395, pages 1409–1437, May 2009.

[Solheim & Yungelson 2005] J.-E. Solheim and L. R. Yungelson. *The White Dwarfs in AM CVn Systems – Candidates for SN Ia?* In D. Koester and S. Moehler, editeurs, 14th European Workshop on White Dwarfs, volume 334 of *Astronomical Society of the Pacific Conference Series*, page 387, July 2005.

[Starrfield et al. 1985] S. Starrfield, W. M. Sparks and J. W. Truran. *Recurrent novae as a consequence of the accretion of solar material onto a 1.38 solar mass white dwarf.* The Astrophysical Journal, vol. 291, pages 136–146, April 1985.

[Starrfield et al. 1988] S. Starrfield, W. M. Sparks and G. Shaviv. *A model for the 1987 outburst of the recurrent nova U Scorpii.* The Astrophysical Journal Letters, vol. 325, pages L35–L38, February 1988.

[Stephenson & Green 2002] F. R. Stephenson and D. A. Green. *Historical supernovae and their remnants.* Historical supernovae and their remnants, by F. Richard Stephenson and David A. Green. International series in astronomy and astrophysics, vol. 5. Oxford: Clarendon Press, 2002, ISBN 0198507666, vol. 5, 2002.

[Sternberg et al. 2011] A. Sternberg, A. Gal-Yam, J. D. Simon, D. C. Leonard, R. M. Quimby, M. M. Phillips, N. Morrell, I. B. Thompson, I. Ivans, J. L. Marshall, A. V. Filippenko, G. W. Marcy, J. S. Bloom, F. Patat, R. J. Foley, D. Yong, B. E. Penprase, D. J. Beeler, C. Allende Prieto and G. S. Stringfellow. *Circumstellar Material in Type Ia Supernovae via Sodium Absorption Features.* Science, vol. 333, pages 856–, August 2011.

[Stritzinger et al. 2010] M. Stritzinger, C. R. Burns, M. M. Phillips, G. Folatelli, K. Krisciunas, S. Kattner, S. E. Persson, L. Boldt, A. Campillay, C. Contreras, W. Krzeminski, N. Morrell, F. Salgado, W. L. Freedman, M. Hamuy, B. F. Madore, M. Roth and N. B. Suntzeff. *The Distance to NGC 1316 (Fornax A) from Observations of Four Type Ia Supernovae.* The Astronomical Journal, vol. 140, pages 2036–2051, December 2010.

[Stritzinger et al. 2013] M. D. Stritzinger, E. Hsiao, S. Valenti, F. Taddia, T. J. Rivera-Thorsen, G. Leloudas, K. Maeda, A. Pastorello, M. M. Phillips, G. Pignata, E. Baron, C. R. Burns, C. Contreras, G. Folatelli, M. Hamuy, P. Hoeflich, N. Morrell, J. L. Prieto, S. Benetti, A. Campillay, J. B. Haislip, A. P. LaClutze, J. P. Moore and D. E. Reichart. *Optical and Near-IR Observations of the Faint and Fast 2008ha-like Supernova 2010ae.* ArXiv e-prints, November 2013.

[Sullivan et al. 2006] M. Sullivan, D. Le Borgne, C. J. Pritchet, A. Hodsman, J. D. Neill, D. A. Howell, R. G. Carlberg, P. Astier, E. Aubourg, D. Balam, S. Basa, A. Conley, S. Fabbro, D. Fouchez, J. Guy, I. Hook, R. Pain, N. Palanque-Delabrouille, K. Perrett,

N. Regnault, J. Rich, R. Taillet, S. Baumont, J. Bronder, R. S. Ellis, M. Filiol, V. Lusset, S. Perlmutter, P. Ripoche and C. Tao. *Rates and Properties of Type Ia Supernovae as a Function of Mass and Star Formation in Their Host Galaxies.* The Astrophysical Journal, vol. 648, pages 868–883, September 2006.

[Sullivan et al. 2010] M. Sullivan, A. Conley, D. A. Howell, J. D. Neill, P. Astier, C. Balland, S. Basa, R. G. Carlberg, D. Fouchez, J. Guy, D. Hardin, I. M. Hook, R. Pain, N. Palanque-Delabrouille, K. M. Perrett, C. J. Pritchet, N. Regnault, J. Rich, V. Ruhlmann-Kleider, S. Baumont, E. Hsiao, T. Kronborg, C. Lidman, S. Perlmutter and E. S. Walker. *The dependence of Type Ia Supernovae luminosities on their host galaxies.* Monthly Notices of the Royal Astronomical Society, vol. 406, pages 782–802, August 2010.

[Sullivan et al. 2011] M. Sullivan, J. Guy, A. Conley, N. Regnault, P. Astier, C. Balland, S. Basa, R. G. Carlberg, D. Fouchez, D. Hardin, I. M. Hook, D. A. Howell, R. Pain, N. Palanque-Delabrouille, K. M. Perrett, C. J. Pritchet, J. Rich, V. Ruhlmann-Kleider, D. Balam, S. Baumont, R. S. Ellis, S. Fabbro, H. K. Fakhouri, N. Fourmanoit, S. González-Gaitán, M. L. Graham, M. J. Hudson, E. Hsiao, T. Kronborg, C. Lidman, A. M. Mourao, J. D. Neill, S. Perlmutter, P. Ripoche, N. Suzuki and E. S. Walker. *SNLS3: Constraints on Dark Energy Combining the Supernova Legacy Survey Three-year Data with Other Probes.* The Astrophysical Journal, vol. 737, page 102, August 2011.

[Suzuki et al. 2012] N. Suzuki, D. Rubin, C. Lidman, G. Aldering, R. Amanullah, K. Barbary, L. F. Barrientos, J. Botyanszki, M. Brodwin, N. Connolly, K. S. Dawson, A. Dey, M. Doi, M. Donahue, S. Deustua, P. Eisenhardt, E. Ellingson, L. Faccioli, V. Fadeyev, H. K. Fakhouri, A. S. Fruchter, D. G. Gilbank, M. D. Gladders, G. Goldhaber, A. H. Gonzalez, A. Goobar, A. Gude, T. Hattori, H. Hoekstra, E. Hsiao, X. Huang, Y. Ihara, M. J. Jee, D. Johnston, N. Kashikawa, B. Koester, K. Konishi, M. Kowalski, E. V. Linder, L. Lubin, J. Melbourne, J. Meyers, T. Morokuma, F. Munshi, C. Mullis, T. Oda, N. Panagia, S. Perlmutter, M. Postman, T. Pritchard, J. Rhodes, P. Ripoche, P. Rosati, D. J. Schlegel, A. Spadafora, S. A. Stanford, V. Stanishev, D. Stern, M. Strovink, N. Takanashi, K. Tokita, M. Wagner, L. Wang, N. Yasuda, H. K. C. Yee and T. Supernova Cosmology Project. *The Hubble Space Telescope Cluster Supernova Survey. V. Improving the Dark-energy Constraints above $z \geq 1$ and Building an Early-type-hosted Supernova Sample.* The Astrophysical Journal, vol. 746, page 85, February 2012.

[Takanashi et al. 2008] N. Takanashi, M. Doi and N. Yasuda. *Light-curve studies of nearby Type Ia supernovae with a Multiband Stretch method.* Monthly Notices of the Royal Astronomical Society, vol. 389, pages 1577–1592, October 2008.

[Tanaka et al. 2010] M. Tanaka, K. S. Kawabata, M. Yamanaka, K. Maeda, T. Hattori, K. Aoki, K. Nomoto, M. Iye, T. Sasaki, P. A. Mazzali and E. Pian. *Spectropolarimetry of Extremely Luminous Type Ia Supernova 2009dc: Nearly Spherical Explosion of Super-Chandrasekhar Mass White Dwarf.* The Astrophysical Journal, vol. 714, pages 1209–1216, May 2010.

[Taubenberger et al. 2008] S. Taubenberger, S. Hachinger, G. Pignata, P. A. Mazzali, C. Contreras, S. Valenti, A. Pastorello, N. Elias-Rosa, O. Bärnbantner, H. Barwig, S. Benetti, M. Dolci, J. Fliri, G. Folatelli, W. L. Freedman, S. Gonzalez, M. Hamuy, W. Krzeminski, N. Morrell, H. Navasardyan, S. E. Persson, M. M. Phillips, C. Ries, M. Roth, N. B. Suntzeff, M. Turatto and W. Hillebrandt. *The underluminous Type Ia supernova 2005bl and the class of objects similar to SN 1991bg.* Monthly Notices of the Royal Astronomical Society, vol. 385, pages 75–96, March 2008.

[Taubenberger et al. 2011] S. Taubenberger, S. Benetti, M. Childress, R. Pakmor, S. Hachinger, P. A. Mazzali, V. Stanishev, N. Elias-Rosa, I. Agnoletto, F. Bufano, M. Ergon, A. Harutyunyan, C. Inserra, E. Kankare, M. Kromer, H. Navasardyan, J. Nicolas, A. Pastorello, E. Prosperi, F. Salgado, J. Sollerman, M. Stritzinger, M. Turatto, S. Valenti and W. Hillebrandt. *High luminosity, slow ejecta and persistent carbon lines: SN 2009dc challenges thermonuclear explosion scenarios.* Monthly Notices of the Royal Astronomical Society, vol. 412, pages 2735–2762, April 2011.

[Thoroughgood et al. 2001] T. D. Thoroughgood, V. S. Dhillon, S. P. Littlefair, T. R. Marsh and D. A. Smith. *The mass of the white dwarf in the recurrent nova U Scorpii.* Monthly Notices of the Royal Astronomical Society, vol. 327, pages 1323–1333, November 2001.

[Timmes et al. 2003] F. X. Timmes, E. F. Brown and J. W. Truran. *On Variations in the Peak Luminosity of Type Ia Supernovae.* The Astrophysical Journal Letters, vol. 590, pages L83–L86, June 2003.

[Tonry et al. 2003] J. L. Tonry, B. P. Schmidt, B. Barris, P. Candia, P. Challis, A. Clocchiatti, A. L. Coil, A. V. Filippenko, P. Garnavich, C. Hogan, S. T. Holland, S. Jha, R. P. Kirshner, K. Krisciunas, B. Leibundgut, W. Li, T. Matheson, M. M. Phillips, A. G. Riess, R. Schommer, R. C. Smith, J. Sollerman, J. Spyromilio, C. W. Stubbs and N. B. Suntzeff. *Cosmological Results from High-z Supernovae.* The Astrophysical Journal, vol. 594, pages 1–24, September 2003.

[Toonen et al. 2012] S. Toonen, G. Nelemans and S. Portegies Zwart. *Supernova Type Ia progenitors from merging double white dwarfs. Using a new population synthesis model.* Astronomy & Astrophysics, vol. 546, page A70, October 2012.

[Totani et al. 2008] T. Totani, T. Morokuma, T. Oda, M. Doi and N. Yasuda. *Delay Time Distribution Measurement of Type Ia Supernovae by the Subaru/XMM-Newton Deep Survey and Implications for the Progenitor.* Publications of the Astronomical Society of Japan, vol. 60, pages 1327–, December 2008.

[Trundle et al. 2008] C. Trundle, R. Kotak, J. S. Vink and W. P. S. Meikle. *SN 2005 gj: evidence for LBV supernovae progenitors?* Astronomy & Astrophysics, vol. 483, pages L47–L50, June 2008.

[Truran et al. 1967] J. W. Truran, W. D. Arnett and A. G. W. Cameron. *Nucleosynthesis in supernova shock waves.* Canadian Journal of Physics, vol. 45, page 2315, 1967.

[Tutukov & Yungelson 1979] A. V. Tutukov and L. R. Yungelson. *On the influence of emission of gravitational waves on the evolution of low-mass close binary stars.* Acta Astronomica, vol. 29, pages 665–680, 1979.

[Ueda et al. 2008] Y. Ueda, M. G. Watson, I. M. Stewart, M. Akiyama, A. D. Schwope, G. Lamer, J. Ebrero, F. J. Carrera, K. Sekiguchi, T. Yamada, C. Simpson, G. Hasinger and S. Mateos. *The Subaru/XMM-Newton Deep Survey (SXDS). III. X-Ray Data.* The Astrophysical Journal Supplement Series, vol. 179, pages 124–141, November 2008.

[van Kerkwijk et al. 2010] M. H. van Kerkwijk, P. Chang and S. Justham. *Sub-Chandrasekhar White Dwarf Mergers as the Progenitors of Type Ia Supernovae.* The Astrophysical Journal Letters, vol. 722, pages L157–L161, October 2010.

[Wang et al. 2006] L. Wang, M. Strovink, A. Conley, G. Goldhaber, M. Kowalski, S. Perlmutter and J. Siegrist. *Nonlinear Decline-Rate Dependence and Intrinsic Variation of Type Ia Supernova Luminosities.* The Astrophysical Journal, vol. 641, pages 50–69, April 2006.

[Wang et al. 2009a] B. Wang, X. Chen, X. Meng and Z. Han. *Evolving to Type Ia Supernovae with Short Delay Times.* The Astrophysical Journal, vol. 701, pages 1540–1546, August 2009.

[Wang et al. 2009b] X. Wang, A. V. Filippenko, M. Ganeshalingam, W. Li, J. M. Silverman, L. Wang, R. Chornock, R. J. Foley, E. L. Gates, B. Macomber, F. J. D. Serduke, T. N. Steele and D. S. Wong. *Improved Distances to Type Ia Supernovae with Two Spectroscopic Subclasses.* The Astrophysical Journal Letters, vol. 699, pages L139–L143, July 2009.

[Warren et al. 2007] S. J. Warren, N. C. Hambly, S. Dye, O. Almaini, N. J. G. Cross, A. C. Edge, S. Foucaud, P. C. Hewett, S. T. Hodgkin, M. J. Irwin, R. F. Jameson, A. Lawrence, P. W. Lucas, A. J. Adamson, R. M. Bandyopadhyay, J. Bryant, R. S. Collins, C. J. Davis, J. S. Dunlop, J. P. Emerson, D. W. Evans, E. A. Gonzales-Solares, P. Hirst, M. J. Jarvis, T. R. Kendall, T. H. Kerr, S. K. Leggett, J. R. Lewis, R. G. Mann, R. J. McLure, R. G. McMahon, D. J. Mortlock, M. G. Rawlings, M. A. Read, M. Riello, C. Simpson, D. J. B. Smith, E. T. W. Sutorius, T. A. Targett and W. P. Varricatt. *The United Kingdom Infrared Telescope Infrared Deep Sky Survey First Data Release.* Monthly Notices of the Royal Astronomical Society, vol. 375, pages 213–226, February 2007.

[Webbink 1984] R. F. Webbink. *Double white dwarfs as progenitors of R Coronae Borealis stars and Type I supernovae.* The Astrophysical Journal, vol. 277, pages 355–360, February 1984.

[Whelan & Iben 1973] J. Whelan and I. Iben Jr. *Binaries and Supernovae of Type I.* The Astrophysical Journal, vol. 186, pages 1007–1014, December 1973.

[Wood-Vasey & Sokoloski 2006] W. M. Wood-Vasey and J. L. Sokoloski. *Novae as a Mechanism for Producing Cavities around the Progenitors of SN 2002ic and Other Type Ia Supernovae.* The Astrophysical Journal Letters, vol. 645, pages L53–L56, July 2006.

[Wood-Vasey et al. 2007] W. M. Wood-Vasey, G. Miknaitis, C. W. Stubbs, S. Jha, A. G. Riess, P. M. Garnavich, R. P. Kirshner, C. Aguilera, A. C. Becker, J. W. Blackman, S. Blondin, P. Challis, A. Clocchiatti, A. Conley, R. Covarrubias, T. M. Davis, A. V. Filippenko, R. J. Foley, A. Garg, M. Hicken, K. Krisciunas, B. Leibundgut, W. Li, T. Matheson, A. Miceli, G. Narayan, G. Pignata, J. L. Prieto, A. Rest, M. E. Salvo, B. P. Schmidt, R. C. Smith, J. Sollerman, J. Spyromilio, J. L. Tonry, N. B. Suntzeff and A. Zenteno. *Observational Constraints on the Nature of Dark Energy: First Cosmological Results from the ESSENCE Supernova Survey.* The Astrophysical Journal, vol. 666, pages 694–715, September 2007.

[Wood-Vasey et al. 2008] W. M. Wood-Vasey, A. S. Friedman, J. S. Bloom, M. Hicken, M. Modjaz, R. P. Kirshner, D. L. Starr, C. H. Blake, E. E. Falco, A. H. Szentgyorgyi, P. Challis, S. Blondin, K. S. Mandel and A. Rest. *Type Ia Supernovae Are Good Standard Candles in the Near Infrared: Evidence from PAIRITEL.* The Astrophysical Journal, vol. 689, pages 377–390, December 2008.

[Woosley et al. 1987] S. E. Woosley, P. A. Pinto, P. G. Martin and T. A. Weaver. *Supernova 1987A in the Large Magellanic Cloud - The explosion of an approximately 20 solar mass star which has experienced mass loss?* The Astrophysical Journal, vol. 318, pages 664–673, July 1987.

[Woosley et al. 2009] S. E. Woosley, A. R. Kerstein, V. Sankaran, A. J. Aspden and F. K. Röpke. *Type Ia Supernovae: Calculations of Turbulent Flames Using the Linear Eddy Model.* The Astrophysical Journal, vol. 704, pages 255–273, October 2009.

[Woosley 2007] S. E. Woosley. *Type Ia Supernovae: Burning and Detonation in the Distributed Regime.* The Astrophysical Journal, vol. 668, pages 1109–1117, October 2007.

[Yamanaka et al. 2009] M. Yamanaka, K. S. Kawabata, K. Kinugasa, M. Tanaka, A. Imada, K. Maeda, K. Nomoto, A. Arai, S. Chiyonobu, Y. Fukazawa, O. Hashimoto, S. Honda, Y. Ikejiri, R. Itoh, Y. Kamata, N. Kawai, T. Komatsu, K. Konishi, D. Kuroda, H. Miyamoto, S. Miyazaki, O. Nagae, H. Nakaya, T. Ohsugi, T. Omodaka, N. Sakai, M. Sasada, M. Suzuki, H. Taguchi, H. Takahashi, H. Tanaka, M. Uemura, T. Yamashita, K. Yanagisawa and M. Yoshida. *Early Phase Observations of Extremely Luminous Type Ia Supernova 2009dc.* The Astrophysical Journal Letters, vol. 707, pages L118–L122, December 2009.

[Yasuda & Fukugita 2010] N. Yasuda and M. Fukugita. *Luminosity Functions of Type Ia Supernovae and Their Host Galaxies from the Sloan Digital Sky Survey.* The Astronomical Journal, vol. 139, pages 39–52, January 2010.

[Yoon et al. 2010] S.-C. Yoon, S. E. Woosley and N. Langer. *Type Ib/c Supernovae in Binary Systems. I. Evolution and Properties of the Progenitor Stars.* The Astrophysical Journal, vol. 725, pages 940–954, December 2010.

[Zhao et al. 2006] F.-Y. Zhao, R. G. Strom and S.-Y. Jiang. *The Guest Star of AD185 must have been a Supernova*. Chinese Journal of Astronomy and Astrophysics, vol. 6, pages 635–640, October 2006.

[Zheng et al. 2013] W. Zheng, J. M. Silverman, A. V. Filippenko, D. Kasen, P. E. Nugent, M. Graham, X. Wang, S. Valenti, F. Ciabattari, P. L. Kelly, O. D. Fox, I. Shivvers, K. I. Clubb, S. B. Cenko, D. Balam, D. A. Howell, E. Hsiao, W. Li, G. H. Marion, D. Sand, J. Vinko, J. C. Wheeler and J. Zhang. *The Very Young Type Ia Supernova 2013dy: Discovery, and Strong Carbon Absorption in Early-time Spectra*. The Astrophysical Journal Letters, vol. 778, page L15, November 2013.